Effect of electromagnetic fields in the activation of indigenous strains of the cocoa bean during controlled fermentation

(*Efecto de los campos electromagnéticos en la activación de cepas autóctonas del grano de cacao durante la fermentación controlada)*

Escuela Politécnica Nacional

Tania María Guzmán Armenteros

Quito, Ecuador

2023

Escuela Politécnica Nacional

Philosophy Doctor in Food Science and Technology

Effect of electromagnetic fields in the activation of indigenous strains of the cocoa bean during controlled fermentation

Presented by: Tania María Guzmán Armenteros

Supervised by: Jenny Cumandá Ruales Najera, Ph.D.

A dissertation submitted to Escuela Politécnica Nacional in partial fulfillment of the requirements for the degree of Doctor (Ph.D.) of the Department of Food Science and Biotechnology, Av. Ladrón de Guevara E11–253, Quito, Ecuador

Autor: Tania María Guzmán Armenteros

tania.guzman@epn.edu.ec

Director: Jenny Cumandá Ruales Najera

jenny.ruales@epn.edu.ec

Oral examination date Examination committee:

Nombre, PhD.

Universidad,

President

Nombre, PhD.

Universidad,

Secretar,

Reviewer 1

Nombre, PhD Mauricio Mosquera,

Universidad, Escuela Politécnica Nacional.

Reviewer 2

Nombre, PhD. Mary Casa

Universidad, Escuela Politécnica Nacional.

Reviewer 3

Nombre, PhD. Pedro Maldonado

Universidad, Escuela Politécnica Nacional.

Reviewer 4

Nombre, PhD. Juan Manuel Cevallos

Universidad, Escuela Politécnica del Litoral

Reviewer 5

Nombre, PhD. Marco Lazo

Universidad, Universidad del Azuay

Effect of electromagnetic fields in the activation of indigenous strains of the cocoa bean during controlled fermentation

Thesis

ISBN

Sponsor

Cooperation

Escuela Politécnica Nacional, Departamento de Ciencia de Alimentos y Biotecnología, Quito, Ecuador.

Centro de Investigación de Alimentos, CIAL, Universidad UTE, EC 170527, Quito, Ecuador;

Universidad Central del Ecuador (UCE), Facultad de Ciencias Médicas, Carrera de Medicina, Campus El Dorado, Quito, Ecuador

Centro de Investigaciones Aplicadas a Polímeros, Escuela Politécnica Nacional, Quito, Ecuador. Laboratorio de Nuevos Materiales, Escuela Politécnica Nacional, Quito, Ecuador.

Laboratorio de Reología, Dirección de Ciencias, Instituto de Investigaciones para la industria de los alimentos (IIIA). La Habana. Cuba

Laboratorio de Microbiología, Dirección de Ciencias, Instituto de Investigaciones para la industria de los alimentos (IIIA). La Habana. Cuba

Laboratorio de Evaluación sensorial, Dirección de Ciencias, Instituto de Investigaciones para la industria de los alimentos (IIIA). La Habana. Cuba

Dedication

Make a moving thesis dedication to God

I would like to express my deepest gratitude and dedicate this thesis to God, the source of all wisdom and understanding. Throughout this journey of knowledge and discovery, I have been humbled by the wonders of the universe and the complexities of the subject. I acknowledge that every insight gained, every breakthrough achieved, and every challenge overcome has been made possible by God's grace and guidance. I am immensely grateful for His unwavering presence, strength, and inspiration that have sustained me in moments of doubt and propelled me forward. May this work be a testament to His greatness and a humble offering of my efforts? To God, I dedicate this thesis with heartfelt appreciation and profound reverence

Acknowledgment

I would like to express my sincerest gratitude to Dr. Jenny Ruales for her invaluable support and unwavering interest throughout the entire journey of this thesis. Her guidance and expertise have been instrumental in shaping the direction of my research and nurturing my academic growth. Additionally, I extend my heartfelt appreciation to José Villacis for his significant contributions and unwavering assistance, which have greatly enriched this work.

I would also like to extend my thanks to Santiago Guerra and Dr. Luis Ramos for their exceptional collaboration. His insights and contributions have greatly enhanced the quality and depth of this research.

Furthermore, I am grateful to my fellow students, Paulina, Jessenia, Veronica, Nelly, and Diego, for their invaluable support and camaraderie throughout this academic endeavor. Their encouragement, shared experiences, and collaborative spirit have been instrumental in overcoming challenges and fostering a conducive learning environment.

Lastly, I would like to express my deepest appreciation to all the individuals, including friends, family, and mentors, who have supported and believed in me throughout this journey. Their unwavering support, encouragement, and belief in my abilities has been a constant source of motivation and inspiration.

I am truly grateful for the collective contributions and support of these individuals, as they have played an integral role in the successful completion of this thesis.

Tabla de contenido

List of papers

Guzmán–Armenteros, T. M., Ramos–Guerrero, L. A., Guerra, L. S., & Ruales, J. (2023). Optimization of cacao beans fermentation by native species and electromagnetic fields. *Heliyon*, 9(4). *https://doi.org/10.1016/j.heliyon.2023.e15065*

Guzmán–Armenteros, T. M., Ruales, J., Villacís–Chiriboga, J., & Guerra, L. S. (2023). Experimental Prototype of Electromagnetic Emissions for Biotechnological Research: Monitoring Cocoa Bean Fermentation Parameters. *Foods*, *12(13)*, *2539*. *https://doi.org/10.3390/foods12132539*

Guzmán–Armenteros, T. M., Villacís–Chiriboga, J., Guerra, L. S., & Ruales, J. (2023). Electromagnetic fields effects on microbial growth in cocoa fermentation: a controlled experimental approach using established growth models. *Heliyon*, (Research manuscript submitted to Journal)

Guzmán–Armenteros, T. M., J., Guerra, L. S., & Ruales, J. (2023). Cocoa Mucilage as a Novel Culture Medium: Unveiling its Potential for Microbial Growth and Biotechnological Applications. *Comprehensive Reviews in Food Science and Food Safety (CRFSFS)*. (Research manuscript submitted to Journal)

Guzmán–Armenteros, T. M., Cuesta, C., Bravo, J., Sinche, M., Vera, E., Vargas, P., Ciobota, V., Ortega, F., Montalvo, G., Proaño, A., Echeverría, A., & Ramos–Guerrero, L. (2023). Raman spectroscopic and sensory evaluation of Ecuadorian cocoa liquor prepared with gamma–irradiated and induced electromagnetic field fermentation cocoa beans. *Foods*. (Research manuscript submitted to Journal)

Guzmán–Armenteros, T. M., J., Guerra, L. S., & Ruales, J. (2023). Magnetic Field Effects on Biological Systems: A Comprehensive Analysis on Cocoa Bean Fermentation (Preparation manuscript to be sent to Journal)

Summary of the thesis

CCN–51 cocoa from the Ecuadorian coastal region is a high–yielding variety, resistant to pests and with intense notes of cocoa flavor. However, due to the lack of control during the fermentation of the grain, this variety usually has high notes of acidity and bitterness. The combined use of starter cultures and emerging technologies such as electromagnetic fields (EMF) can be important alternatives to improve grain quality, since both techniques have been widely used to improve fermentation processes. Therefore, on the proposed basis, this study aims to 1) To design and validate electromagnetic field equipment for cocoa bean fermentation under controlled conditions, 2) To analyze the influence of the electromagnetic field generation process (density and exposure time) on the fermentation process, evaluating the characteristics of the fermented grain and the dry almond. 3) To Characterize chemical, thermal, microstructure properties of the cocoa paste obtained, 4) To determine the effect of electromagnetic fields on the kinetic and growth parameters of crops, and 5) To evaluate the effect of electromagnetic fields on bacterial cultures, based on their metabolic, genomic and cell microstructure characteristics, under simulated conditions

A Helmholtz–type oscillating magnetic field (OMF) electromagnetic emission prototype with a usable area for biotechnological studies was built and validated. The control of the EMF measurements was performed with a Hall effect sensor with a digital signal connection (Arduino nano) and data output to a PC using LabVIEW software. The fermentation process of the cocoa bean variety CCN–51 exposed to four levels of OMF density for 60 min (0, 5, 40, 80 mT/60 min) and using native cultures was evaluated. Different variables of the grain fermentation process were evaluated for six days.

The electromagnetic emissions equipment was tested in terms of linearity, accuracy, precision, repeatability, reliability, and robustness, demonstrating its validity under working conditions. Subsequently, the impact of OMF density levels (0, 5, 40, and 80 mT/60 min) on the fermentation process, kernel characteristics, and dry almond properties was analyzed using native cultures. Throughout the six–day controlled fermentation process, various factors including pH, temperature, humidity, growth variables, and metagenomics of microbial groups were evaluated, and their influence on grain yield and sensory quality. An additional analysis was carried out by subjecting the fermented cocoa beans of the CCN–51 and National varieties to gamma radiation and then analyzing them using Raman.

The metagenomics and growth profiles of the microbial species exhibited variations according to EMF exposure. The changes observed in the fermentation process were attributed to alterations in gene expression and metabolic activity of the microbial species present. Notably, different microbial genera responded differently to EMF conditions, directly influencing fermentation performance and the resulting sensory characteristics of cocoa beans. Lower EMF densities showed positive effects

on the sensory profile, while higher densities produced contrasting results. This emphasized the importance of optimizing EMF parameters to achieve optimal cocoa bean fermentation results.

Raman's analysis revealed that the strongest signals in the spectra corresponded to the lipid components of the samples. Regarding the sensory evaluation, the cocoa beans showed a wide range of attributes, including floral, fruity, almond, sour, bitter, astringent, intensely aromatic and earthy flavors. The intensity of these attributes varied depending on the dose of gamma radiation applied and the variety of cocoa.

Resumen de la tesis

El cacao CCN–51 de la región costera ecuatoriana es una variedad de alto rendimiento, resistente a plagas y con intensas notas de sabor a cacao. Sin embargo, debido a la falta de control durante la fermentación del grano, esta variedad suele tener notas altas de acidez y amargor. El uso combinado de cultivos iniciadores y tecnologías emergentes como los campos electromagnéticos (EMF) pueden ser alternativas importantes para mejorar la calidad del grano, ya que ambas técnicas han sido ampliamente utilizadas para mejorar los procesos de fermentación. Por lo tanto, sobre la base propuesta, este estudio tiene como objetivo 1) Diseñar y validar equipos de campos electromagnéticos para la fermentación de granos de cacao en condiciones controladas, 2) Analizar la influencia del proceso de generación de campos electromagnéticos (densidad y tiempo de exposición) en el proceso de fermentación, evaluando las características del grano fermentado y la almendra seca. 3) Caracterizar las propiedades químicas, térmicas, microestructurales de la pasta de cacao obtenida, 4) Determinar el efecto de los campos electromagnéticos en la cinética y parámetros de crecimiento de los cultivos, y 5) Evaluar el efecto de los campos electromagnéticos en cultivos bacterianos, con base en sus características metabólicas, genómicas y de microestructura celular, en condiciones simuladas.

Se construyó y validó un prototipo de emisión electromagnética de campo magnético oscilante (OMF) tipo Helmholtz con un área utilizable para estudios biotecnológicos. El control de las mediciones de EMF se realizó con un sensor de efecto Hall con conexión de señal digital (Arduino nano) y salida de datos a una PC usando el software LabVIEW. Se evaluó el proceso de fermentación del grano de cacao variedad CCN–51 expuesto a cuatro niveles de densidad OMF por 60 min (0, 5, 40, 80 mT/60 min) y utilizando cultivos nativos. Se evaluaron diferentes variables del proceso de fermentación del grano durante seis días.

El equipo de emisiones electromagnéticas fue probado en términos de linealidad, exactitud, precisión, repetibilidad, confiabilidad y robustez, demostrando su validez en condiciones de trabajo. Posteriormente, se analizó el impacto de los niveles de densidad de OMF (0, 5, 40 y 80 mT/60 min) en el proceso de fermentación, las características del grano y las propiedades de la almendra seca

utilizando cultivos nativos. A lo largo del proceso de fermentación controlada de seis días, se evaluaron varios factores, incluidos el pH, la temperatura, la humedad, las variables de crecimiento y la metagenómica de los grupos microbianos y su influencia en el rendimiento del grano y la calidad sensorial. Se realizó un análisis adicional sometiendo los granos de cacao fermentados de las variedades CCN–51 y Nacional a radiación gamma y luego analizándolos mediante RAMAN.

La metagenómica y los perfiles de crecimiento de las especies microbianas exhibieron variaciones según la exposición a los CEM. Los cambios observados en el proceso de fermentación se atribuyeron a alteraciones en la expresión génica y actividad metabólica de las especies microbianas presentes. En particular, diferentes géneros microbianos respondieron de manera diferente a las condiciones de EMF, lo que influyó directamente en el rendimiento de la fermentación y las características sensoriales resultantes de los granos de cacao. Las densidades más bajas de EMF mostraron efectos positivos en el perfil sensorial, mientras que las densidades más altas produjeron resultados contrastantes. Esto enfatizó la importancia de optimizar los parámetros EMF para lograr resultados óptimos de fermentación del grano de cacao.

El análisis de Raman reveló que las señales más fuertes en los espectros correspondían a los componentes lipídicos de las muestras. En cuanto a la evaluación sensorial, los granos de cacao mostraron una amplia gama de atributos, incluyendo sabores florales, afrutados, almendrados, ácidos, amargos, astringentes, intensamente aromáticos y terrosos. La intensidad de estos atributos varió según la dosis de radiación gamma aplicada y la variedad de cacao.

Research framework

The Theobroma CCN–51 cocoa variety has become popular due to its high yield and resistance to pests. However, it is often associated with pronounced sourness and astringency, posing a challenge for market acceptance and consumer preference. Conventional fermentation methods have had limited success in reducing these off–flavors. Furthermore, conventional fermentation methods have had limited success in reducing these off–flavors.

To address this problem, innovative techniques such as electromagnetic fields (EMF) and starter cultures have been explored to control the fermentation process effectively. While previous studies have focused on improving cocoa fermentation using starter cultures, the potential of using electromagnetic fields (EMF) to enhance cocoa fermentation remains relatively unexplored. Consequently, there is a research gap that requires investigation of the potential synergistic effects of electromagnetic fields and starter cultures on CCN–51 cocoa fermentation to address its quality challenges.

This thesis holds significant implications for the cocoa industry, specifically in addressing the challenges associated with the strongly acidic and astringent flavor notes of the CCN–51 cocoa variety. Combining electromagnetic fields with appropriate starter cultures, this novel and effective approach aims to control fermentation, leading to improved flavor profiles and overall enhanced quality of CCN–51 cocoa. The results of this research will have practical applications for cocoa producers, processors, and manufacturers. This approach will ensure the production of premium quality cocoa with desirable flavor attributes.

The research will involve carefully designed fermentation experiments using CCN–51 cocoa beans. It will incorporate different electromagnetic field strengths (ranging from 5 to 80 mT) and exposure durations (ranging from 10 to 60 minutes). Indigenous starter cultures will also be employed. The fermentation process will be monitored using the main process variables to detect changes in microbial dynamics, metabolic pathways, and flavor development using advanced analytical techniques. Sensory evaluations, including assessments by a trained panel, will be conducted to evaluate the sensory attributes and acceptability of both the resulting cocoa beans and the cocoa paste.

General objective

Evaluate the effect of electromagnetic fields on cocoa fermentation CCN–51 under controlled conditions

Specific objectives

To design and validate electromagnetic field equipment for cocoa bean fermentation under controlled conditions.

To analyze the influence of the electromagnetic field generation process (density and exposure time) on the fermentation process, evaluating the characteristics of the fermented grain and the dry almond.

To characterize cocoa paste obtained based on its thermal properties, chemical composition, and microstructure.

To determine the effect of electromagnetic fields on the kinetic and growth parameters of crops.

To evaluate the effect of electromagnetic fields on bacterial cultures based on their metabolic, genomic, and cell microstructure characteristics under simulated conditions.

Chapter 1

Magnetic Fields on Biological Systems: A Comprehensive Analysis on Cocoa Bean Fermentation

Tania María Guzmán–Armenteros[1], Jenny Ruales[1], and Luis Santiago Guerra[2]

[1] Department of Food Science and Biotechnology, Escuela Politécnica Nacional, P.O. Box 17–01–2759, Quito, Ecuador; tania.guzman@epn.edu.ec; (T.M.G.–A) jenny.ruales@epn.edu.ec

[2] Carrera de Medicina, Facultad de Ciencias Médicas, Universidad Central del Ecuador, P.O. Box 17–12–759, Quito, Ecuador; lsguerrap@uce.edu.ec

*Corresponding author: tania.guzman@epn.edu.ec

Abstract

The influence of magnetic fields on biological systems, including fermentation processes and cocoa bean fermentation, is a multifaceted area of study. Mechanisms such as magnetosensitivity, protein conformational changes, cellular biophysical properties, ROS production and gene expression, and epigenetic modifications have been identified to explain how magnetic fields affect microorganisms and cellular processes. These mechanisms can lead to alterations in enzyme activity, protein stability, cell signaling, intercellular communication, and oxidative stress. In the context of cocoa fermentation, electromagnetic field offers a potential means to enhance the sensory attributes of chocolate by modulating microbial metabolism and optimizing flavor and aroma development. This area of study offers possibilities for innovation and the creation of premium chocolate products. In this review, these aspects will be explored synthetically and illustratively.

1. Introduction

In recent times, there has been substantial progress in studying the connection between electromagnetic fields (EMFs) and biological systems, with a particular emphasis on fermentation processes [1,2]. The influence of magnetic fields on various biological entities has been well–established, leading researchers to adopt a dual perspective to gain a comprehensive understanding of this phenomenon. On the one hand, studies have concentrated on the direct effects of EMFs on biological entities, delving into the molecular and cellular mechanisms governing their response and adaptation to magnetic fields [2–4]. On the other hand, researchers have recognized the importance of considering the broader environmental context in which these fermentation processes unfold, encompassing the complex interplay between magnetic fields, microorganisms, and their surrounding ecosystems [3].

Studies examining the direct effects of EMFs on biological entities have revealed intriguing insights into the ways in which magnetic fields can influence cellular behavior and functionality [4–8]. These investigations have explored the cellular responses to magnetic fields at various levels, ranging from changes in gene expression and protein synthesis to alterations in metabolic pathways and signaling cascades [1–5]. By dissecting these intricate mechanisms, researchers aim to elucidate how magnetic fields can either stimulate or inhibit biological systems, uncovering the underlying factors that contribute to such diverse outcomes.

Simultaneously, researchers have recognized the significance of the environment in shaping the impact of magnetic fields on fermentation processes. The surrounding environment encompasses not only the physical conditions, but also the microbial communities and interactions that occur within the fermentation milieu. It is within this intricate web of interactions that the effects of magnetic fields manifest, as they intertwine with the complex dynamics of microbial metabolism, nutrient availability, and ecological factors [3–8]. Understanding the interplay between magnetic fields and the fermentation environment is crucial for comprehending the holistic picture of how microorganisms respond and adapt to these magnetic stimuli.

While the direct effects of EMFs and the role of the surrounding environment in fermentation processes have been the subject of investigation, researchers are also venturing into uncharted territories to explore additional dimensions. These encompass investigating the enduring impacts of magnetic field exposure on microbial populations, exploring potential synergistic or antagonistic effects of combined environmental factors, and understanding the role of magnetic fields in influencing the evolution and adaptation of microorganisms in fermentation systems [7–10]. By broadening the scope of inquiry, researchers can uncover novel insights into the complexities of EMF–microorganism interactions, ultimately paving the way for innovative applications in biotechnology, agriculture, and environmental remediation.

To unravel the intricate relationship between magnetic fields and fermentation processes, a multidisciplinary approach is crucial. Collaborations between experts in microbiology, biochemistry, biophysics, and environmental science can facilitate a comprehensive exploration of the diverse mechanisms and phenomena at play. By incorporating advanced experimental techniques, such as high–resolution imaging, omics technologies, and mathematical modeling, a deeper understanding of the fundamental principles governing the impact of magnetic fields on microorganisms and their fermentation activities can be achieved [10–14].

In summary, the impact of electromagnetic fields on biological systems, especially in fermentation processes, has become a global focal point of global research. Scientists are delving into the direct effects of EMFs on biological entities and investigating their relationship with the surrounding environment, leading to a gradual understanding of this phenomenon. However, the field remains

ripe with opportunities for further exploration, requiring interdisciplinary collaboration and cutting–edge methodologies. As the knowledge base expands, the potential applications of harnessing magnetic fields in biotechnology, agriculture, and environmental sustainability are poised to revolutionize these fields, driving innovation and progress in the years to come.

2. EMFs and Biological Systems: Unveiling Effects, Practical Applications, and Environmental Preservation

Emerging research has shed light on the remarkable ability of electromagnetic fields (EMFs) to exert both stimulating and inhibitory effects on a wide range of biological systems [4–19]. These effects extend beyond the realm of microorganisms and encompass diverse organisms such as plants, fruits, and even human and animal cells [6–10]. The intricate interplay between electromagnetic fields and cellular processes has captivated scientists, as it holds immense potential for various practical applications across multiple domains.

The impact of electromagnetic fields is particularly remarkable in the domain of plant growth and development. Research has shown that precise application of EMFs can lead to accelerated seed germination, improved root growth, and higher crop yield [6, 19–20]. By carefully adjusting the electromagnetic stimulation parameters, scientists have effectively utilized these effects to enhance agricultural practices, promoting sustainable and efficient food production. Additionally, the focused use of electromagnetic fields has shown promising outcomes in enhancing the post–harvest preservation and quality of fruits, prolonging their shelf life, and reducing spoilage [7].

Microorganisms, including bacteria, yeast, and fungi, also exhibit fascinating responses to electromagnetic fields. Research has illuminated how controlled exposure to specific EMFs can modulate microbial growth rates, metabolic activity, and enzymatic processes [8]. This newfound understanding has paved the way for novel applications in biotechnology and industrial processes. For instance, electromagnetic field–mediated stimulation of microbial metabolism has been harnessed to optimize the production of valuable metabolites such as enzymes, biofuels, and pharmaceutical compounds [13,19–20]. Furthermore, the utilization of electromagnetic fields has revolutionized the process of remediating contaminated environments. Through harnessing the natural abilities of microorganisms, electromagnetic field–assisted bioremediation methods effectively break down pollutants in soil, water, and air, providing a sustainable approach to environmental protection [14–16]. Table 1 offers a brief summary of the effects and practical applications of electromagnetic fields, showcasing their potential across various fields and underscoring the importance of responsible and evidence–based implementation.

Table 1. EMF effect in different biological systems, including microorganisms, plants, fruits, human cells, and industrial production.

Biological Systems	Effects and Applications	References
Microorganisms	– Modulation of microbial growth rates, metabolic activity, and enzymatic processes. – Microbial metabolism for valuable metabolites' production, biotechnology, and industrial processes – Electromagnetic field–assisted bioremediation techniques for efficient pollutant degradation.	[11], 12–14] [12], 15] [3]
Plants and Fruits	– Accelerated seed germination and enhanced root growth – Increased crop yield and improved agricultural practices. – Post–harvest preservation and quality enhancement of fruits. – Extension of fruit shelf life and reduction of spoilage.	[2], [6]: [7]
Human Cells and Therapy	– Promotion of tissue regeneration and wound healing. – Alleviation of pain and inflammation. – Non–invasive and targeted therapies as alternatives to traditional treatment modalities.	[16, 30, 48, 61]
Industrial Production	– Optimization of fermentation processes for cost–effective and sustainable production of commodities. – Enhancement of efficiency and yield in various industrial fermentation processes.	[18], [17]
Environmental Preservation	– Remediation of contaminated sites through electromagnetic field–assisted bioremediation techniques. – Mitigation of the harmful effects of pollutants in soil, water, and air. – Preservation of ecological integrity and natural habitats.	[13], [14], [15].

The potential of electromagnetic fields extends beyond organismal and cellular levels, encompassing diverse practical applications that benefit human health, production processes, and environmental preservation. In the realm of medical therapy, electromagnetic fields have shown promise in promoting tissue regeneration, accelerating wound healing, and alleviating pain and inflammation [17]. Non–invasive and targeted electromagnetic field–based therapies offer an alternative to traditional treatment modalities, providing patients with enhanced comfort and improved outcomes.

Industrial production processes have also witnessed the transformative impact of electromagnetic fields. By optimizing process parameters and leveraging the effects of EMFs on microbial growth and metabolism, industries can enhance the efficiency and yield of various fermentation processes, leading to cost–effective and sustainable production of commodities ranging from food and beverages to biopharmaceuticals [18, 19–20]. Furthermore, electromagnetic fields play a vital role

in environmental protection efforts. They can be employed to remediate contaminated sites, mitigate the harmful effects of pollutants, and preserve the ecological integrity of natural habitats [19].

However, while the potential benefits of electromagnetic fields are substantial, it is crucial to ensure their responsible and controlled application. Safeguarding natural integrity and minimizing any potential adverse effects is of utmost importance. Therefore, extensive research is necessary to comprehend the intricate relationship between electromagnetic fields and biological systems, enabling the formulation of evidence–based guidelines and protocols for their practical application.

Despite substantial advances in this domain, there remains a conspicuous absence of universally standardized specified ranges of electromagnetic fields capable of causing measurable effects in biological systems. This gap between empirical progress underscores a complex interplay of factors that contribute to the current situation. Achieving a universally applicable EMF standard requires a level of precision and robustness that considers this inherent variability in various biological contexts.

Addressing this challenge requires a comprehensive and multidisciplinary approach that combines scientific rigor, technological adaptation, and ethical prudence. table 2 provides some general examples of EMF parameters commonly studied in research up to that time. It should be noted that the specific frequencies, densities, and exposure times used in the studies can vary widely depending on the specific objectives and conditions of each experiment.

The diverse impacts of EMF on biological systems encompass microorganisms, plants, and human cells. The ability of electromagnetic fields to stimulate or inhibit cellular processes has paved the way for diverse practical applications, ranging from medical therapy and industrial production to environmental protection [20–24]. However, additional research is necessary to gain a comprehensive understanding of the underlying mechanisms and to optimize the implementation of electromagnetic field–based approaches, all while ensuring the preservation of natural integrity. By harnessing the power of electromagnetic fields, we have the potential to revolutionize various fields and drive innovation toward sustainable and efficient solutions for society and the environment

Table 2. General examples of commonly studied EMF parameters by categories

Category	Frequency (Hz)	Field Density (mT)	Exposure Time	e.g. & Cite
Plants	Frequencies commonly used in plant studies range from extremely low frequency (ELF) to radiofrequency (RF) ranges. ELF frequencies typically fall within the range of 1 Hz to 300 Hz, while RF frequencies can range from kHz to GHz.	Field densities can also vary greatly, and they are usually measured in millitesla (mT) for ELF fields. The typical densities used in plant studies can range from a few mT (0.1) to around 100 mT.	Exposure times in plant studies can span from a few minutes to several days or even weeks. Short–term exposures of a few hours are common, but some studies involve longer–term exposures of 24 hours or more.	Type: Triticum sppFrequency: ELF (50–60 Hz) Density: 10mT, 15mT Exposure Time: 10min,15min (4) Hussain 2020
Animals	Frequencies used in animal studies can span a wide range, from extremely low frequencies (ELF) to radio frequencies. Frequencies commonly investigated include 50 Hz, 60 Hz, 900 MHz, 2.45 GHz, and others.	Field densities are often measured in millitesla (mT) or microtesla (μT) for ELF fields. Depending on the study, the field densities may range from fractions of a μT to several mT.	Exposure times in animal studies can vary widely based on the research objectives. Short–term exposures can be as brief as a few hours, while long–term studies might extend over several weeks or even months. Common exposure durations include 24 hours, 48 hours, 7 days, and longer.	Type: Rat brain Frequency: ELF (50–60 Hz) Density: 4.3mT, 12.9mT Exposure Time:21 days (8) Yakir–Blumkin 2020
Humans	Frequencies used in human studies encompass a wide range, from extremely low frequencies (ELF) to radio frequencies. Frequencies commonly investigated include 50 Hz, 60 Hz, 900 MHz, 2.45 GHz, and others.	Field densities are often measured in millitesla (mT) or microtesla (μT) for ELF fields. For radio frequency EMFs, specific absorption rate (SAR) is used, measured in watts per kilogram (W/kg). The densities can vary significantly, from fractions of a μT to several mT for ELF fields and SAR values ranging from a few milliwatts per kilogram (mW/kg) to higher values for radio frequency fields.	Exposure times in human studies can also vary widely based on research objectives and safety considerations. Short–term exposures can be as brief as a few minutes to an hour, while longer–term studies might extend over several hours. Common exposure durations include 15 minutes, 30 minutes, and 1 hour for short–term studies, and up to 24 hours for longer–term studies.	Type: NHDF (normal human dermal fibroblasts) cell line Frequency: ELF (50–60 Hz) Density: 0,65 T Exposure Time: 24h (56) Kimsa–Dudek 2021
Fermentation Processes	Studies have investigated a wide range of frequencies in fermentation processes. Frequencies in the extremely low–frequency (ELF) range (around 50–60 Hz) have been explored, likely due to their potential biological effects and ease of generation.	Field densities can vary significantly based on the type of fermentation process and the specific objectives of the study. For ELF fields, densities might range from a fraction of a microtesla (μT) to several μT	Exposure times for fermentation process studies can also vary. Short–term exposures might last from minutes to hours, while longer–term studies could extend over the course of the fermentation process, which can range from several hours to days or even weeks.	Type: Bioethanol production by S. cerevisiae Frequency: ELF (50–60 Hz) Density: 10 mT Exposure Time: 2h (11) Andrade 2021
Microorganisms	Frequencies commonly explored include extremely low frequencies (ELF) in the range of 50 Hz and 60 Hz, as well as radio frequencies in the microwave range, such as 900 MHz and 2.45 GHz.	Densities can vary greatly, ranging from fractions of a μT to several T for ELF fields,	Exposure times for microorganism studies can vary based on the research objectives. Short–term exposures might last from a few minutes to several hours, while longer–term studies could extend over multiple hours or even days. Common exposure durations include 15 minutes, 30 minutes, 1 hour, and up to 24 hours.	Type: Airborne fungal Frequency: ELF (50–60 Hz) Density: 5mT Exposure Time: 2h (14) Anaya 2021

3. EMFs in Biological Systems: Unveiling Mechanisms

Magnetic fields exert their influence on biological systems through various mechanisms. These mechanisms involve magnetosensitivity, electromagnetic induction, protein conformational changes, ROS production, gene expression and epigenetic modifications, cellular biophysical properties, and neural activity. Understanding these diverse mechanisms is crucial for unraveling the intricate interactions between magnetic fields and biological systems and exploring their potential applications in various fields, including biomedicine, neuroscience, and biotechnology (Table 3).

Table 3. EMF's interaction mechanisms with biological systems. Every mechanism illustrates the diverse impacts of magnetic fields on biological systems, highlighting their importance across various fields of research and application. The table offers a succinct summary of each mechanism and its practical implications.

Mechanism	Description	Examples and Implications	References
Magnetosensitivity	Organisms are equipped with magnetosensitive structures that enable them to sense and react to magnetic fields. These structures enable orientation, navigation, and detection of magnetic field changes.	– Magnetite crystals or protein complexes act as magnetic sensors. – Organisms can orient themselves and detect changes in magnetic fields.	[24] [25], [24]
Electromagnetic Induction	Magnetic fields induce electric currents in tissues and conductive fluids, influencing cellular processes. Induced currents affect ion transport, cell signaling, and regulation of physiological processes. Localized heat generation influences metabolic activities and cellular functions.	Influences ion transport across cell membranes – Affects cell signaling and physiological regulation – Generates localized heat within tissues.	[31] [37] [40]
Changes in Protein Conformation	Magnetic fields cause conformational changes in proteins, leading to modifications in their structure and function. Interaction between magnetic fields and paramagnetic centers in proteins leads to modifications in enzyme activity, ligand binding, and protein stability.	– Alters enzyme activity, ligand binding, and protein stability – Impacts metabolic pathways, signal transduction, and gene expression.	[42] [55], [56]
Reactive Oxygen Species (ROS) Production	Biological systems experience modulation of reactive oxygen species (ROS) generation due to magnetic fields. ROS play	– Modulates the production of ROS molecules. – Influences cellular homeostasis and	[48] [10], [50]

Mechanism	Description	Examples and Implications	References
	pivotal roles in cell signaling and oxidative stress. Magnetic fields influence electron transfer processes and enzymatic activities responsible for ROS generation and elimination.	physiological processes.	
Gene Expression and Epigenetic Modifications	Magnetic fields influence gene expression and epigenetic modifications, regulating cellular functions. They modulate the expression of specific genes, leading to changes in cellular functions and phenotypic traits. Magnetic fields also impact epigenetic modifications such as DNA	– Modulates gene expression patterns and cellular functions. – Leads to long–term changes in cell behavior and phenotypic traits.	[53], [55] [65], [67]

3.1. Magnetosensitivity

The observation of magnetosensitivity in specific organisms provides an intriguing glimpse into the impact of magnetic fields on biological systems. Organisms possessing magnetosensitive structures, such as magnetite crystals or protein complexes, have a distinct capability to perceive and react to magnetic fields in their surroundings. [25]. These structures, often found in specialized cells or tissues, serve as magnetic sensors, allowing organisms to perceive the Earth's magnetic field and harness it for various biological purposes [25–28].

The mechanisms underlying magnetosensitivity are still the subject of ongoing investigation, yet current understanding suggests that the interaction between magnetic fields and specialized biomolecules within cells plays a pivotal role. In organisms with magnetite–based magnetosensors, it is proposed that the alignment of magnetite crystals, influenced by the magnetic field, generates mechanical or chemical signals that are transduced into cellular responses [26, 27]. The complex interaction between the magnetic field and internal biomolecular processes allows organisms to navigate during migration, orient themselves with respect to magnetic field lines, and potentially perceive alterations in magnetic field intensity and orientation [29, 30].

Fascinatingly, magnetosensitivity extends beyond organisms engaged in long–distance migrations, such as birds or sea turtles. It has been observed in a diverse array of organisms, including bacteria, insects, fish, and even mammals [30–32]. In certain cases, magnetosensitivity has been linked to particular behaviors, like homing, or predator avoidance. In other instances, it seems to play a role in regulating physiological processes, such as the migration of neuronal cells during development or the alignment of certain tissues during morphogenesis [33–35].

While the exact mechanisms of magnetosensitivity are still being elucidated, several hypotheses have been proposed. These include the involvement of magneto–receptive proteins, such as cytochromes, which can undergo conformational changes in response to magnetic fields and potentially trigger downstream cellular signaling pathways [25–28,33]. Another hypothesis suggests the role of ion channels, which may be influenced by magnetic fields and modulate neural activity or cellular responses. Additionally, the presence of magnetosensitive bacteria in symbiotic relationships with higher organism's raises intriguing possibilities for the transfer of magnetic information across species boundaries [27, 30–33].

Underlying molecular mechanisms hold great potential for diverse fields of study. It not only sheds light on the remarkable sensory capabilities of organisms but also offers inspiration for the development of bioinspired technologies, such as biomagnetic sensors or navigational systems. Moreover, as we unravel the underlying mechanisms of magnetosensitivity, we enhance our comprehension of the intricate interconnections between magnetic fields and biological systems. This deepens our insight into the complex dynamics that influence life on Earth.

3.2. Protein conformational

Protein conformational alterations provide an intriguing pathway through which magnetic fields exert their impact on biological systems, contributing to a deeper comprehension of the complex relationship between electromagnetic forces and cellular mechanisms. Although the exact mechanisms through which magnetic fields induce conformational changes in proteins are still being investigated, recent evidence indicates that this phenomenon is likely a result of the interaction between magnetic fields and paramagnetic centers found within protein structures [25–27].

Paramagnetic centers, such as metal ions or organic radicals, possess unpaired electrons that render them sensitive to magnetic fields. When exposed to a magnetic field, these paramagnetic centers can experience alterations in their electronic spin configurations, leading to subtle rearrangements of the surrounding protein structure [13, 25]. These conformational changes can manifest as shifts in the relative positions of amino acid residues, alterations in secondary structure elements, or modifications in the overall folding of the protein [13, 25–27, 31].

The consequences of protein conformational changes induced by magnetic fields can be far–reaching. One notable impact is the modulation of enzyme activity. Magnetic field–induced conformational alterations can either enhance or inhibit enzymatic catalysis by affecting the active site geometry, substrate binding affinity, or accessibility of critical residues involved in catalytic reactions [13, 31]. Such modifications in enzyme activity can significantly influence metabolic pathways, including those involved in energy production, biosynthesis, and cellular signaling [25–

27].

Furthermore, ligand binding processes can be influenced by magnetic field–induced protein conformational changes [26]. The binding affinity and specificity of proteins for ligands, such as small molecules, ions, or even other proteins, can be modulated by alterations in the protein structure. Magnetic fields have the potential to impact the binding site architecture, electrostatic interactions, and hydrophobic characteristics, thereby influencing the recognition and binding of ligands to their protein targets [25, 27]. This can have implications for diverse biological processes, including signal transduction, cellular communication, and regulation of gene expression [13].

In addition to enzyme activity and ligand binding, magnetic field–induced protein conformational changes can affect overall protein stability. Alterations in protein folding patterns and structural dynamics can render proteins more susceptible to denaturation or aggregation [27,31]. Conversely, magnetic fields can promote the stabilization of protein structures, enhancing their resistance to environmental stresses and maintaining their functional integrity [13].

While the study of magnetic field–induced protein conformational changes is still in its infancy, it holds great promise for applications in various fields. Gaining insight into and utilizing these phenomena could lead to the advancement of creative approaches in biotechnology, drug design, and therapeutic interventions. By modulating protein conformation through controlled magnetic fields, it may be possible to optimize enzyme activity, design novel ligand–binding interfaces, or stabilize proteins for industrial or biomedical applications [13, 31].

The ability of magnetic fields to induce conformational changes in proteins offers a fascinating insight into the influence of electromagnetic forces on biological systems. This mechanism, mediated through the interaction between magnetic fields and paramagnetic centers within proteins, holds the potential to modulate enzyme activity, ligand binding, and protein stability, thereby impacting fundamental cellular processes. Further exploration of these intricate mechanisms will deepen our understanding of the interplay between magnetic fields and proteins, opening doors to novel applications and advancements in various scientific disciplines.

3.3. Cellular Biophysical Properties

Beyond the molecular level, magnetic fields have a profound impact on biological systems, encompassing the biophysical properties of cells. This reveals a captivating realm of cellular responses and interactions [32–34]. Through their interaction with cellular components, magnetic fields can modulate various biophysical properties, such as membrane fluidity, ion channel activities, and cytoskeleton dynamics, ultimately shaping the behavior and functions of cells [33].

One notable consequence of magnetic fields is their influence on membrane fluidity. The cell membrane, consisting of lipids and proteins, plays a crucial role as an interface between the cell and its surroundings. Studies have shown that magnetic fields can affect the organization and dynamics of membrane components, leading to changes in the fluidity and permeability of the cell membrane [34–36]. These changes in membrane properties can have consequences for cellular processes such as membrane protein function, membrane receptor signaling, and the transport of molecules across the membrane [35].

Furthermore, magnetic fields have demonstrated their ability to influence ion channel activities, which are vital for cellular communication and signaling. Ion channels, as membrane proteins, control the movement of ions in and out of cells, thereby impacting electrical signaling and cellular balance [36–38]. Magnetic fields can influence the opening and closing of ion channels, potentially altering ion fluxes and intracellular ion concentrations. These modifications in ion channel activities can have significant effects on cellular excitability, electrical signaling, and the overall balance of ion concentrations within cells [37].

Magnetic fields also impact another aspect of cellular biophysics, which is the cytoskeleton. The cytoskeleton is a complex network of filaments that plays a crucial role in providing structural support and regulating cellular shape, motility, and mechanical properties [38–40]. Magnetic fields can interact with cytoskeleton elements, including microtubules, actin filaments, and intermediate filaments, leading to changes in their organization and dynamics [40–42]. These alterations in cytoskeleton architecture can impact cellular morphology, mechanical properties, and intracellular transport processes. For example, EMF has been found to cause cytoskeleton reorganization and influence cell migration, proliferation, and differentiation [40].

The effects of EMF on cellular biophysical properties have implications for various cellular functions and processes. They can influence intercellular communication, as changes in membrane fluidity and ion channel activities can alter the transmission of signals between cells [40–42]. Furthermore, modifications in cytoskeleton dynamics can impact cellular adhesion, tissue development, and mechanical properties, influencing cell–cell interactions and tissue organization [40].

Understanding the mechanisms by which magnetic fields modulate cellular biophysical properties is a dynamic area of research. It involves investigating the interaction between magnetic fields and specific cellular components, elucidating the signaling pathways and molecular mechanisms involved, and exploring the functional consequences of the cellular and tissue levels. The insights gained from these studies have the potential to contribute to diverse fields, including regenerative medicine, tissue engineering, and the development of novel therapeutic approaches.

Magnetic fields exert their influence on biological systems by impacting cellular biophysical properties. The modulation of membrane fluidity, ion channel activities, and cytoskeleton dynamics represents a fascinating avenue through which magnetic fields shape cellular behavior and functions. Further exploration of these mechanisms will deepen our understanding of the magnetic fields and cellular biophysics connections, paving the way for innovative applications in biomedicine and biotechnology.

3.4. Reactive Oxygen Species (ROS)

The generation of Reactive Oxygen Species (ROS) stands as an intriguing dimension of how EMF impacts biological systems, unveiling the complex interaction between EMF and cellular redox mechanisms. ROS, such as superoxide radicals (O_2•–), hydrogen peroxide (H_2O_2), and hydroxyl radicals (•OH), are highly reactive molecules that serve as signaling molecules and mediators of oxidative stress within cells [43–45].

Scientific research has focused on examining the impact of magnetic fields on ROS production, providing insights into the underlying mechanisms and potential implications for cellular homeostasis [42]. Several studies have provided evidence of magnetic field–induced modulation of ROS generation, offering insights into the intricate relationship between magnetic fields and cellular redox signaling [44].

One mechanism by which magnetic fields can influence ROS production is through their direct effect on electron transfer processes. Magnetic fields can alter the dynamics of electron flow within cells, affecting redox reactions and the production of ROS as byproducts [44–46]. The interaction between magnetic fields and electron transport chains, such as those found in mitochondria and chloroplasts, can result in changes in electron leakage and subsequent ROS generation [47]. The modulation of electron transfer processes by magnetic fields may cause fluctuations in ROS levels, thereby influencing cellular redox signaling and oxidative stress responses [48].

Additionally, magnetic fields can influence the enzymatic activities responsible for generating and scavenging ROS [48–49]. Enzymes like NADPH oxidase and superoxide dismutases have essential roles in ROS production and detoxification within cells [50]. Studies have demonstrated that magnetic fields can regulate the activity and expression of these enzymes, thereby impacting the equilibrium between ROS generation and removal [44]. The changes in enzymatic activities caused by magnetic fields can significantly affect cellular redox homeostasis and fine–tune oxidative stress responses.

Alterations in ROS levels triggered by magnetic fields can influence a range of physiological

processes. ROS play crucial roles as signaling molecules, participating in cellular functions like immune responses, differentiation, cell proliferation, and apoptosis [44,45]. Modulation of ROS production by magnetic fields can thus have downstream effects on these cellular processes, potentially influencing cell fate decisions, tissue development, and overall organismal health [47, 48].

Furthermore, exposure to magnetic fields can lead to dysregulation of ROS levels, inducing oxidative stress that involves an imbalance between the production of reactive oxygen species (ROS) and the antioxidant defense mechanisms [45, 46]. Excessive ROS levels can result in oxidative damage to cellular components like DNA, proteins, and lipids, leading to a range of medical conditions, including neurodegenerative diseases, cancer, and aging. On the other hand, insufficient ROS levels can disrupt normal redox signaling and hinder cellular functions [43–45].

Understanding the mechanisms by which magnetic fields modulate ROS production is an active area of research. Investigations aim to elucidate the specific molecular pathways and cellular targets involved, as well as the dose– and time–dependent effects of magnetic field exposure on ROS dynamics [48, 49]. This knowledge will add to the overall comprehension of the complex interaction between magnetic fields and cellular redox processes, opening possibilities for devising approaches to utilize the positive impacts of magnetic fields while also addressing any potential negative effects [50].

Magnetic fields have the capacity to modulate ROS production within biological systems, thereby influencing cellular redox signaling and oxidative stress responses. The direct effects on electron transfer processes and the modulation of enzymatic activities involved in ROS generation and scavenging represent key mechanisms by which magnetic fields exert their influence. Understanding these mechanisms and their implications for cellular homeostasis and physiological processes will enhance our knowledge of the multifaceted interactions between magnetic fields and cellular redox biology, opening up new avenues for therapeutic interventions and the development of innovative approaches in biomedicine.

3.5. Gene expression and epigenetic modifications

Gene expression and epigenetic modifications represent fascinating avenues through which magnetic fields can exert their influence on biological systems, transcending conventional understanding and delving into the intricate regulatory mechanisms that shape cellular function and phenotype. Research has unveiled the capacity of magnetic fields to modulate gene expression and contribute to epigenetic modifications, shedding light on their potential to shape cellular behavior and long–term cellular outcomes [52–53].

According to several studies [54–56], it has been established that EMF has the capacity to affect the expression of certain genes, indicating its direct influence on cellular functions. These effects may arise from the interaction between magnetic fields and intracellular signaling pathways, transcription factors, and regulatory elements within the genome [51, 52]. According to research studies [55], magnetic fields have demonstrated the ability to influence the transcriptional activity of genes that play a role in a wide range of biological processes, such as cellular growth, differentiation, metabolism, and immune responses. The modulation of gene expression by magnetic fields can result in alterations in cellular behavior, impacting the overall physiology and functionality of biological systems [57].

Apart from their influence on gene expression, magnetic fields have also been associated with the modulation of epigenetic modifications [58, 59]. These epigenetic mechanisms, including histone modifications and DNA methylation, play essential roles in governing gene expression patterns and maintaining cellular identity [58, 59]. Emerging evidence suggests that magnetic fields can influence these epigenetic marks, potentially leading to long–lasting changes in gene expression profiles [60]. Magnetic fields may affect the accessibility of DNA to transcriptional machinery and the establishment of specific epigenetic states [60–63]. The modulation of epigenetic modifications by magnetic fields can have profound implications for cellular development, differentiation, and disease progression.

Understanding the underlying mechanisms through which magnetic fields influence gene expression and epigenetic modifications is an active area of research. Investigations aim to elucidate the signaling pathways, transcriptional regulators, and epigenetic modifiers involved in mediating the effects of EMF on these processes [54, 56]. Moreover, the interplay between magnetic fields and other environmental factors, like chemical cues, temperature, and light, is being explored to unravel the complex interactions that shape gene expression and epigenetic landscapes [59, 61].

The influence of EMF on gene regulation and epigenetic modifications has far–reaching implications for various fields of study. In biomedicine, understanding how magnetic fields can modulate gene expression programs holds promise for therapeutic applications, including the development of novel approaches for targeted gene regulation and gene therapy [58–60]. Furthermore, the ability of magnetic fields to influence epigenetic marks opens up avenues for interventions aimed at reprogramming cellular behavior and restoring aberrant epigenetic states associated with diseases.

Beyond biomedicine, the impact of magnetic fields on gene expression and epigenetic modifications has broader implications for fields such as agriculture and environmental science [6, 62]. Manipulating gene expression patterns through EMF exposure could potentially enhance crop traits,

improve stress tolerance, and optimize yield. Additionally, the ability of magnetic fields to modulate epigenetic modifications could offer new strategies for environmental remediation, such as targeted epigenetic reprogramming to mitigate the effects of pollutants or promote ecological restoration.

In conclusion, magnetic fields have the potential to influence gene expression and epigenetic modifications, unraveling the intricate regulatory mechanisms that shape cellular behavior and phenotype. The modulation of gene expression patterns and epigenetic landscapes by magnetic fields opens up new avenues for therapeutic interventions, agricultural advancements, and environmental applications. Further research is needed to unravel the underlying molecular mechanisms and establish the dose– and context–dependent effects of EMF exposure on gene and epigenetic modifications. By deepening our understanding of these complex interactions, we can harness the potential of magnetic fields to reshape cellular function and drive transformative advancements in diverse scientific fields.

3.6. Electromagnetic induction

Electromagnetic induction is a phenomenon that, represents a captivating mechanism through which magnetic fields exert their influence on biological systems. It involves the generation of electric currents within conductive tissues and fluids, giving rise to a multitude of effects that impact cellular processes in intriguing ways [32, 63].

One notable effect of electromagnetic induction is its ability to modulate ion transport across cell membranes. The induced currents can perturb the delicate balance of ion concentrations, disrupting cellular electrochemical gradients and influencing cell signaling pathways [41, 49]. By altering ion transport, electromagnetic induction can regulate a wide range of physiological processes, such as nerve hormone secretion, impulse transmission, and muscle contraction [65]. This interconnection between magnetic fields and ion dynamics underscores the sophisticated nature of cellular responses to magnetic stimuli.

Moreover, electromagnetic induction can result in the generation of localized heat within tissues. As electric currents flow through conductive fluids or tissues, resistive heating occurs, leading to temperature increases in specific regions [50, 56]. This localized heating can have profound consequences for cellular metabolism and function [66]. Elevated temperatures may accelerate enzymatic reactions, affect protein folding and stability, and impact overall cellular physiology [55]. Consequently, the thermal effects of electromagnetic induction contribute to the complex interplay between magnetic fields and cellular activities.

The interrelations between electromagnetic induction and cellular processes holds implications for

diverse areas of research and applications. In the field of medicine, understanding the effects of electromagnetic induction on ion transport and thermal dynamics can guide the development of innovative therapeutic strategies [68]. Electromagnetic induction–based therapies, such as magnetic hyperthermia for cancer treatment, utilize the localized heating effect to selectively target and destroy tumor cells [69]. Furthermore, the modulation of ion transport through electromagnetic induction has potential implications for neuromodulation techniques and the treatment of various neurological disorders.

Beyond medical applications, the influence of electromagnetic induction on cellular processes has relevance in fields such as bioengineering and environmental sciences. In bioengineering, knowledge of electromagnetic induction can aid in the design of biocompatible materials and devices that interact with biological systems [70]. Understanding the effects of induced currents on ion transport and cellular functions is crucial for developing safe and effective biomedical implants and prosthetics [71]. In the field of environmental sciences, the importance of electromagnetic induction becomes evident when examining the effects of anthropogenic electromagnetic fields on wildlife and ecosystems. The effects of induced currents on organisms, such as migratory patterns or behavior, necessitate further exploration to ensure the preservation of ecological integrity.

Electromagnetic induction represents a captivating mechanism through which magnetic fields influence biological systems. By inducing electric currents and eliciting various effects such as modulating ion transport and generating localized heat, electromagnetic induction contributes to the interrelation’s between magnetic fields and cellular processes [67–70]. These effects have wide–ranging implications for medical therapies, bioengineering applications, and environmental studies [65–68]. Further research is needed to unravel the specific molecular and cellular mechanisms involved in electromagnetic induction, paving the way for innovative advancements in multiple scientific domains.

4. Unraveling the Complexities of Electromagnetic Field–Microorganism Interactions in Fermentation Processes

Expanding the horizons of inquiry, researchers are venturing into unexplored realms to unravel additional dimensions surrounding the interplay of electromagnetic fields (EMFs) and fermentation processes. While investigations have addressed the direct effects of EMFs and the influence of the surrounding environment, there is a growing recognition of the need to delve deeper into these phenomena. Researchers are now turning their attention to long–term effects, exploring the sustained impact of magnetic field exposure on microbial populations within fermentation systems [11–15]. Through in–depth analysis of microorganisms' dynamic responses and long–term adaptations, a deeper comprehension of the intricate interactions between EMFs and microbial

communities can be attained.

Furthermore, the combined effects of multiple environmental factors alongside magnetic fields represent another intriguing avenue of exploration [11]. The fermentation milieu is a complex ecosystem characterized by the interplay of various physical and chemical parameters, including temperature, pH, nutrient availability, and oxygen levels. Researchers are now investigating the potential synergistic or antagonistic interactions between these factors and EMFs [7,56,58]. Understanding the combined effects of magnetic fields with other environmental variables can shed light on how microorganisms respond, adapt, and optimize their metabolic activities in the presence of multiple stimuli [11]. This comprehensive approach offers a more practical depiction of the fermentation environment and opens up avenues for devising strategies to improve process efficiency and product quality.

Moreover, researchers are delving into the role of EMF in shaping the evolution and adaptation of microorganisms within fermentation systems [58]. The application of EMFs can induce selective pressures on microbial populations, potentially leading to genetic and phenotypic changes over time [12]. By investigating the mechanisms by which magnetic fields influence microbial evolution, researchers can uncover novel insights into the adaptive capabilities of microorganisms and their potential for biotechnological applications [14, 15]. Understanding how magnetic fields shape microbial traits and behaviors opens up avenues for harnessing and manipulating these phenomena to optimize fermentation processes and develop innovative biotechnological solutions.

Expanding the scope of inquiry beyond the obvious allows researchers to uncover new frontiers in the realm of EMF–microorganism interactions. The knowledge gained from these endeavors holds great potential for applications in various fields. In biotechnology, gaining a deeper comprehension of the intricacies of EMF–microorganism interactions can pave the way for the development of innovative fermentation strategies to produce high–value compounds, such as biofuels [15], pharmaceuticals [14], and biopolymers [7, 13]. In agriculture, insights into the interplay between magnetic fields and microbial populations can lead to innovative approaches for enhancing crop productivity and nutrient uptake [56]. Furthermore, in environmental remediation, understanding the role of magnetic fields in shaping microbial communities can inform the development of sustainable strategies for bioremediation and the removal of pollutants from water, soil, and air [12–15].

Researchers are venturing beyond the established boundaries to explore new dimensions in the field of EMF–microorganism interactions in fermentation processes. By investigating the long–term effects of EMF exposure, the combined effects of multiple environmental factors, and its role in microbial evolution, researchers are pushing the frontiers of knowledge. The insights gained from

these endeavors have the potential to revolutionize biotechnology, agriculture, and environmental remediation, paving the way for innovative and sustainable applications in the future.

5. EMFs in Fermentation Processes: Unveiling the Interplay with the Surrounding Environment and Microbial Dynamics

Concurrently, researchers have garnered a deep appreciation for the paramount importance of the fermentation environment in shaping the influence of EMF on the intricate processes at play. The surrounding environment encompasses a myriad of factors, including the physical conditions, the intricate microbial communities, and the dynamic interactions within the fermentation milieu. Within this intricate web of interactions, the EMF effect manifests and intertwines with the complex dynamics of microbial metabolism, nutrient availability, and ecological factors, culminating in a remarkable interplay that determines the response and adaptation of microorganisms to these magnetic stimuli [3–6].

The physical conditions existing in the fermentation environment, encompassing temperature, pH, humidity, and oxygen availability, provide the basis for the intricate interaction between magnetic fields and microorganisms [14, 18–22]. The cited research indicates that these pathological conditions significantly impact metabolic pathways, enzymatic activities, and growth kinetics of microorganisms involved in the fermentation process. Magnetic fields, acting in concert with these physical factors, exert a regulatory influence on the metabolic processes and cellular behaviors of microorganisms, leading to alterations in their fermentation efficiency and product profiles [20]. Moreover, the presence of magnetic fields can modulate the physical properties of the fermentation environment itself, including the mixing and mass transfer phenomena, further influencing the overall performance of the fermentation process [5–8].

The fermentation milieu is a dynamic ecosystem teeming with diverse microbial communities that intricately interact with one another. Within this microbial tapestry, magnetic fields exert a discernible impact on the composition, diversity, and dynamics of the microbial populations. Magnetic fields can influence the selection and succession of microbial species, shaping the microbial consortia responsible for fermentation [5–7]. Microorganisms, in turn, respond to the presence of magnetic fields through complex communication mechanisms, such as quorum sensing and intercellular signaling, further modulating their physiological and metabolic activities [20–22]. Understanding the connections between magnetic fields and the complex microbial communities within the fermentation environment is of paramount importance for unraveling the mechanisms underpinning microbial interactions, community dynamics, and the overall stability and robustness of the fermentation process [10, 11, 14].

Moreover, the availability and accessibility of nutrients significantly influence the performance of fermentation processes. The presence of magnetic fields can influence the transport and uptake of nutrients by microorganisms, thereby impacting their metabolic activity, growth rates, and product formation. Magnetic fields can alter the solubility and diffusion characteristics of nutrients, affecting their bioavailability in the microbial cells [9–11]. Furthermore, magnetic fields can induce changes in the cellular membrane properties, including permeability and electrochemical gradients, influencing the transport processes involved in nutrient acquisition and waste product expulsion [15,16–18]. Unraveling the relations between magnetic fields and nutrient dynamics within the fermentation environment provides crucial insights into the factors governing microbial growth, metabolism, and overall process performance.

Ecological factors, encompassing interactions with non–microbial components of the fermentation environment, further contribute to the complexity of the magnetic field–microorganism interplay. For instance, magnetic fields interact with both organic and inorganic compounds present in the fermentation milieu, influencing their chemical reactivity, stability, and availability to microorganisms (Figure 1) [1–6]. Furthermore, the presence of magnetic fields can impact the interactions between microorganisms and their symbiotic or competing counterparts, affecting their growth rates, cooperative behaviors, and ecological niche establishment [4–6, 23, 24]. Understanding the connections between magnetic fields and the ecological factors within the fermentation environment allows for a comprehensive comprehension of the regulatory mechanisms and dynamics that govern microbial communities, their functions, and their impact on the overall fermentation process [20–24].

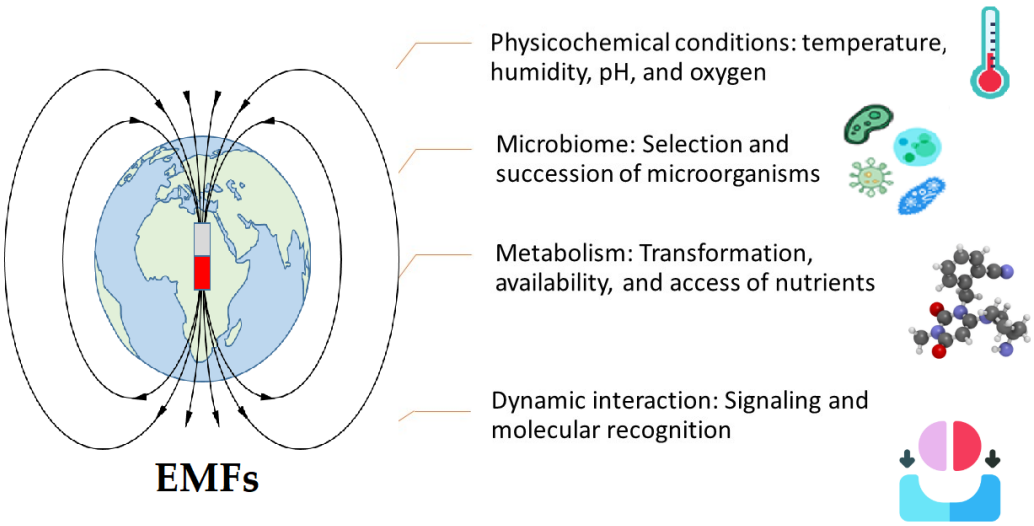

Figure 1. EMFs interactions with the surrounding environment

The significance of the fermentation environment in shaping the impact of magnetic fields on

fermentation processes cannot be overstated. The interplay between magnetic fields and the physical conditions, microbial communities, and ecological factors within the fermentation milieu orchestrate a complex symphony of interactions that govern the response and adaptation of microorganisms to these magnetic stimuli. Unraveling the intricacies of this interplay holds.

6. Cocoa Bean Fermentation: Microbial Interactions, Metabolic Dynamics, and Physical Transformations

The fermentation of cocoa beans emerges as an exemplary and highly reproducible biological system that offers valuable insights into the interplay between microorganisms and their surrounding environment. This intricate process involves a diverse array of microbial species, functioning as an interconnected ecosystem that operates high on various environmental factors crucial for its successful progression [71–75]. Factors like oxygen tension, temperature, humidity, and pH are essential in influencing the fermentation environment during cocoa pulp fermentation. The dynamic interaction among these factors is intricately regulated by the metabolic activity of the microbial species involved [76–78].

The cocoa bean ecosystem's native microorganisms undergo a natural selection process, gradually colonizing the pulp according to their distinct metabolic capabilities [75–77]. This selective colonization results in the establishment of a specialized microbial consortium that exhibits synergistic interactions and concerted metabolic activities [71–73]. The metabolic potential of these microorganisms dictates their ability to thrive within the cocoa pulp environment, thereby contributing to the overall fermentation process [77–79]. The metabolic activities of the microorganisms involve the degradation of intricate organic compounds found in cocoa pulp, resulting in the generation of a plethora of metabolic byproducts that contribute to the development of distinctive flavors, aromas, and chemical transformations within cocoa beans [81].

Microbial metabolism within the cocoa bean fermentation process induces both external and internal physical changes in the beans themselves [73–75]. Externally, the fermentation process triggers visible alterations in the appearance and texture of the beans [74]. These changes can include modifications in color, size, and surface characteristics, as well as the development of specific patterns or markings [76]. Internally, microbial metabolism gives rise to a series of biochemical transformations that impact the composition and properties of the cocoa beans [73, 74]. This includes the conversion of complex carbohydrates into simpler sugars, the breakdown of proteins, the generation of volatile compounds, and the synthesis of bioactive compounds, all of which play a significant role in shaping the distinct sensory attributes and quality characteristics of the final cocoa product [76, 78].

The fermentation of cocoa beans provides a valuable model system for investigating microbial–plant interactions and the dynamics of complex microbial communities. It provides researchers with a well–defined and reproducible system to investigate the interplay between microorganisms and their environment [78–81]. By examining the mechanisms governing microbial colonization, metabolic activities, and the resulting physical changes in the cocoa beans, researchers can gain more profound insights into the intricate processes underlying fermentation [72, 73]. Furthermore, the knowledge acquired from studying cocoa bean fermentation can be extrapolated to other fermentation systems, providing a more comprehensive insight into the dynamics of microbial ecosystems and their influence on the ultimate product quality.

The complexities of microbial metabolism and the physical changes induced by fermentation in cocoa beans have wide–ranging implications. The knowledge gained from studying this functional and reproducible biological system can be harnessed for various applications. In the field of food science, it can inform strategies for optimizing fermentation processes, improving product consistency, and enhancing the development of desirable sensory attributes in cocoa–based products [73, 74]. Moreover, the understanding of cocoa bean fermentation can contribute to the formulation of sustainable practices and interventions that support the conservation and cultivation of the crucial microbial biodiversity involved in this process [78, 79]. Overall, the study of cocoa bean fermentation contributes to both scientific advancements and practical applications, underscoring its significance as a model system for understanding and harnessing microbial–driven fermentation processes.

7. Exploring the Influence of EMF on Cocoa Fermentation

The influence of magnetic fields on cocoa fermentation is an emerging area of research that holds exciting possibilities that go beyond the apparent scope of the effects. While the direct influence of EMF on cocoa fermentation is still being explored, preliminary evidence suggests that magnetic fields can potentially modulate microbial activities, metabolic pathways, and overall fermentation dynamics [17, 83]. By understanding and taking advantage of the interaction between magnetic fields and cocoa fermentation, new avenues for process optimization, quality improvement, and sustainability can be sought.

In the realm of cocoa fermentation, the intricate process of transforming cocoa beans into chocolate involves a complex interaction of microbial species that function as a tight–knit ecosystem [72–74]. These microorganisms, comprising bacteria and yeasts, have a significant impact on the fermentation process as they metabolize the sugars found in the cocoa pulp, resulting in the production of diverse bioactive compounds [76, 78]. Through natural selection, specific microbial species gradually colonize the cacao pulp, establishing a dynamic and diverse community driven by

their unique metabolic capabilities [79, 80].

The metabolic activity of these microorganisms during cocoa fermentation induces significant physical transformations within the cocoa bean itself. This metabolism–driven transformation is responsible for the formation of distinct flavor precursors and aromatic compounds, which significantly influence the sensory characteristics of chocolate. These changes include the breakdown of complex carbohydrates, the release of volatile compounds, and the synthesis of active flavor molecules. The duration and conditions of fermentation directly influence the final sensory attributes and the quality of the resulting chocolate product.

In recent studies, researchers have investigated the potential influence of electromagnetic fields (EMF) on the microbial ecosystem during cocoa fermentation [17, 83, 84]. Electromagnetic fields have shown promise in positively influencing the sensory quality of chocolate by enhancing certain desirable characteristics [17]. By applying controlled magnetic fields, microbial metabolism, enzymatic activities and the production of key bioactive compounds could be modulated. These changes can lead to improvements in flavor development, aroma complexity, and overall sensory attributes of the final chocolate product [17].

Electromagnetic fields can indirectly affect the fermentation environment by influencing nutrient and ion transport, optimizing the availability of essential components for microbial growth and metabolism [37, 39]. Another potential mechanism through which magnetic fields can influence cocoa fermentation is by affecting microbial populations and their behavior [12–14].

In the context of cocoa fermentation, recent research has indicated that EMF can alter microbial growth rates [83]. Consequently, when the colonization of specific microbial species occurs, the general fermentation kinetics and metabolic byproduct profiles are affected. Therefore, it is plausible that magnetic fields could alter the enzyme profiles of cocoa fermenting microorganisms, which could lead to variations in the production of key metabolites and flavor precursors. The metabolic changes observed during cocoa fermentation can potentially provide opportunities to customize the sensory characteristics and quality attributes of cocoa–based products.

Another aspect to consider is the potential interaction between EMF and the physical transformations that occur during cocoa fermentation. Magnetic fields have been shown to impact physical properties like surface tension, viscosity, and crystallization behavior in various systems [42, 47]. In the context of cocoa fermentation, magnetic fields could potentially influence the formation and stability of cocoa butter crystals, which are crucial for the desired texture and mouthfeel of chocolate products. Exploring the interaction between magnetic fields and physical transformations during cocoa fermentation can provide insights into how magnetic fields can shape

the structural properties of cocoa beans to improve the overall chocolate product quality [84].

Also, magnetic fields can have indirect effects on cocoa fermentation by influencing surrounding environmental conditions. By interacting with environmental factors, such as temperature, oxygen availability, and pH, which are known to significantly influence fermentation processes [82]. Understanding how magnetic fields interact with these environmental parameters may provide a more holistic view of their impact on cocoa fermentation. This knowledge can guide the development of strategies to optimize fermentation conditions, promote desirable microbial activities, and ultimately improve the fermentation process efficiency.

The potential of electromagnetic fields to improve the sensory quality of chocolate through the specific modulation of cocoa fermentation presents an exciting avenue for research and application. However, more studies are needed to better understand the precise mechanisms by which electromagnetic fields influence the microbial ecosystem and to establish the optimal conditions for their application in cocoa fermentation.

8. Conclusions

Understanding the mechanisms underlying the influence of EMF on fermentation processes and microorganisms is essential to understanding their holistic effects. It covers several aspects, such as magneto sensitivity, protein conformational changes, cellular biophysical properties, ROS production, and gene expression and epigenetic modifications. This knowledge can pave the way for innovative applications in biotechnology, agriculture, and environmental remediation.

Magnetic field effects on fermentation processes, microorganisms, and cocoa bean fermentation encompasses a wide range of mechanisms and their impacts on cellular processes and microbial dynamics. By unraveling these complex interactions, researchers can discover new knowledge and potential applications in various scientific fields such as cocoa bean fermentation.

Declarations

Author contribution statement

The author worked on the development and the writing of this article.

Funding statement

No applicable

Data availability statement

Data is available on request.

Declaration of Interests statement

The author declares no conflict of interest.

Additional information

Supplementary information is not available for this paper.

Acknowledgments

The author would like to thanks to the collaboration of the Center for Applied Electromagnetism of the Universidad de Oriente and the Institute of Research for the Food Industry

References

1. Carbonell, M. V., Flórez, M., Martínez, E., & Álvarez, J. (2017). Aportaciones sobre el campo magnético: historia e influencia en sistemas biológicos. Intropica: Revista del Instituto de Investigaciones Tropicales, 12(2), 143–159. http://doi.org/10.21676/23897864.228

2. Sarraf, M., Kataria, S., Taimourya, H., Santos, L. O., Menegatti, R. D., Jain, M., & Liu, S. (2020). Magnetic field (MF) applications in plants: An overview. Plants, 9(9), 1139. https://doi.org/10.3390/plants9091139

3. Qu, M., Chen, J., Huang, Q., Chen, J., Xu, Y., Luo, J., & Zheng, Y. (2018). Bioremediation of hexavalent chromium contaminated soil by a bioleaching system with weak magnetic fields. International Biodeterioration & Biodegradation, 128, 41–47.https://doi.org/10.1016/j.ibiod.201608022

4. Miñano, H. L. A., Silva, A. C. D. S., Souto, S., & Costa, E. J. X. (2020). Magnetic fields in food processing perspectives, applications and action models. Processes, 8(7), 814. https://doi.org/103390/pr8070814

5. Ercan, I., Tombuloglu, H., Alqahtani, N., Alotaibi, B., Bamhrez, M., Alshumrani, R., Ozcelik, S., & Kayed, T. S. (2022). Magnetic field effects on the magnetic properties, germination, chlorophyll fluorescence, and nutrient content of barley (*Hordeum vulgare L.*). Plant Physiology and Biochemistry, 170, 36–48. https://doi.org/https://doi.org/10.1016/j.plaphy.2021.11.033

6. El–Zawily, A. E. S., Meleha, M., El–Sawy, M., El–Attar, E. H., Bayoumi, Y., & Alshaal, T. (2019). Application of magnetic field improves growth, yield and fruit quality of tomato irrigated alternatively by fresh and agricultural drainage water. Ecotoxicology and environmental safety, 181, 248–254. https://doi.org/10.1016/jecoenv2019.06.018

7. Khokhlova, G., Abashina, T., Belova, N., Panchelyuga, V., Petrov, A., Abreu, F., & Vainshtein, M. (2018). Effects of combined magnetic fields on bacteria Rhodospirillum rubrum VKM B-1621. Bioelectromagnetics, 39(6), 485–490. https://doi.org/10.1002/bem.22130

8. Chen, L., Ye, A., Liu, X., Lu, J., Xie, Q., Guo, Y. & Sun, W. (2021). Combined effect of co–exposure to di (2–ethylhexyl) phthalates and 50–Hz magnetic–fields on promoting human amniotic cells proliferation. Ecotoxicology, and Environmental Safety, 224, 112704. https://doi.org/10.1016/j.ecoenv.2021.112704

9. Yakir–Blumkin, M. B., Loboda, Y., Schächter, L. & Finberg, J. P. (2020). Static Magnetic Field Exposure In Vivo Enhances the Generation of New Doublecortin–expressing Cells in the Sub–ventricular Zone and Neocortex of Adult Rats. Neuroscience, 425, 217–234. https://doi.org/10.1016/j.neuroscience.2019.11.005

10. Maziarz, A., Kocan, B., Bester, M., Budzik, S., Cholewa, M., Ochiya, T., & Banas, A. (2016). How electromagnetic fields can influence adult stem cells: positive and negative impacts. *Stem cell research & therapy*, 7(1), 1–12. https://doi.org/10.1186/s13287–016–0312–5

11. Lu, H., Wang, X., Hu, S., Han, T., He, S., Zhang, G. & Lin, X. (2020). Bioeffect of static magnetic field on photosynthetic bacteria: Evaluation of bioresources production and wastewater treatment efficiency. *Water Environment Research*, 92(8), 1131–1141. https://doi.org/10.1002/wer.1308

12. Andrade, C. M., Cogo, A. J., Perez, V. H., dos Santos, N. F., Okorokova–Façanha, A. L., Justo, O. R., & Façanha, A. R. (2021). Increases of bioethanol productivity by *S. cerevisiae* in unconventional bioreactor under ELF–magnetic field: New advances in the biophysical mechanism elucidation on yeasts. *Renewable Energy*, 169, 836–842. https://doi.org/10.1016/j.renene.2021.01.074

13. Mansouri, A., Abbes, C. & Landoulsi, A. (2017). Combined intervention of static magnetic field and growth rate of Microbacterium maritypicum CB7 for Benzo (a) Pyrene biodegradation. *Microbial Pathogenesis*, 113, 40–44. https://doi.org/10.1016/j.micpath.2017.10.008

14. Tan, L., Mu, G., Shao, Y., Ning, S. & Shi, S. (2020). Combined enhancement effects of static magnetic field (SMF) and a yeast Candida tropicalis SYF-1 on continuous treatment of Acid Red B by activated sludge under hypersaline conditions. *Journal of Chemical Technology and Biotechnology*, 95(3), 840–849. https://doi.org/10.1002/jctb.6274

15. Anaya, M., Gámez–Espinosa, E., Valdés, O., Guzmán, T., & Borrego, S. (2021). Effect of the oscillating magnetic field on airborne fungal. *Archives of Microbiology*, 203, 2139–2145. https://doi.org/10.1007/s00203–021–02193–x

16. Hajizadeh Maleki, M., Ghanbarvand, M. A., Kazemi, A., Roshangar, L., & Tamadon, A. M. (2021). Effect of electromagnetic field on the proliferation and differentiation potential of mesenchymal stem cells: a systematic review. *Stem Cell Research & Therapy*, 12(1), 1–14. https://doi.org/10.1186/s13287–021–02237–8

17. Guzmán–Armenteros, T. M., Ramos–Guerrero, L. A., Guerra, L. S. & Ruales, J. (2023).

Optimization of cacao beans fermentation by native species and electromagnetic fields. *Heliyon*, 9(4). https://doi.org/10.1016/j.heliyon.2023.e15065

18. Hamedani, B. G., Goliaei, B., Shariatpanahi, S. P., & Nezamtaheri, M. (2022). An overview of the biological effects of extremely low frequency electromagnetic fields combined with ionizing radiation. *Progress in Biophysics and Molecular Biology*, 172, 50–59. https://doi.org/10.1016/j.pbiomolbio.2022.04.008

19. Noble, B. B., Todorova, N., & Yarovsky, I. (2022). Electromagnetic bioeffects: a multiscale molecular simulation perspective. *Physical Chemistry Chemical Physics*, 24(11), 6327–6348. https://doi.org/10.1039/D1CP05510K

20. Peng, W. Y., Li, K. J., Xie, Y. Z., Ma, J. G., & Lu, X. Y. (2020). Development of a TEM–cell–integrated CO2 incubator for cell–based transient electromagnetic field bioeffect study. *Electromagnetic Biology and Medicine*, 39(4), 290–297. https://doi.org/10.1080/15368378.2020.1793170

21. Murase, Masatoshi. (2008). Environmental pollution and health: an interdisciplinary study of the bioeffects of electromagnetic fields. SANSAI: An Environmental Journal for the Global Community 3: 1–35. https://core.ac.uk/reader/39239020

22. Bevelhimer, M. S., Cada, G. F., Fortner, A. M., Schweizer, P. E., & Riemer, K. (2013). Behavioral responses of representative freshwater fish species to electromagnetic fields. *Transactions of the American Fisheries Society*, 142(3), 802–813. https://doi.org/10.1080/00028487.2013.778901

23. Zadeh–Haghighi, Hadi, and Christoph Simon. (2022). Magnetic field effects in biology from the perspective of the radical pair mechanism. *Journal of the Royal Society Interface,* 19(193), 20220325. https://doi.org/10.1098/rsif.2022.0325

24. Clites, B. L., & Pierce, J. T. (2017). Identifying cellular and molecular mechanisms for magnetosensation. *Annual review of neuroscience*, 40, 231–250. https://doi.org/10.1146/annurev–neuro–072116–031312

25. Zhang, X., Yarema, K., & Xu, A. (2017). Molecular Mechanisms for Electromagnetic Field Biosensing BT– Biological Effects of Static Magnetic Fields (X. Zhang, K. Yarema, & A. Xu (eds.); pp. 51–79). Springer Singapore. https://doi.org/10.1007/978–981–10–3579–1_3

26. Jacob, J. J., & Suthindhiran, K. (2016). Magnetotactic bacteria and magnetosomes–Scope and challenges. *Materials Science and Engineering*: C, 68, 919–928.

https://doi.org/10.1016/j.msec.2016.07.049

27. Yan, L., Zhang, S., Chen, P., Liu, H., Yin, H., & Li, H. (2012). Magnetotactic bacteria, magnetosomes and their application. *Microbiological Research*, 167(9), 507–519. https://doi.org/10.1016/j.micres.2012.04.002

28. Gandarias, L., Jefremovas, E. M., Gandia, D., Marcano, L., Martínez–Martínez, V., Ramos–Cabrer, P., Chevrier, D. M., Valencia, S., Fernández Barquín, L., Fdez–Gubieda, M. L., Alonso, J., García–Prieto, A., & Muela, A. (2023). Incorporation of Tb and Gd improves the diagnostic functionality of magnetotactic bacteria. *Materials Today Bio*, 20, 100680. https://doi.org/10.1016/j.mtbio.2023.100680

29. Tan, Shi Ming, Muhammad Hafiz Ismail, and Bin Cao. (2021). Biodiversity of magnetotactic bacteria in the tropical marine environment of Singapore revealed by metagenomic analysis. *Environmental Research* 194: 110714. https://doi.org/10.1016/j.envres.2021.110714

30. Alphandéry, E. (2020). Applications of magnetotactic bacteria and magnetosome for cancer treatment: a review emphasizing on practical and mechanistic aspects. Drug Discovery Today 25(8), 1444–1452. https://doi.org/10.1016/j.drudis.2020.06.010

31. Zablotskii, V., Polyakova, T., & Dejneka, A. (2022). Effects of High Magnetic Fields on the Diffusion of Biologically Active Molecules. Cells, 11(1), 81. https://doi.org/10.3390/cells11010081

32. Stanley, Sarah A., and Jeffrey M. Friedman. (2019). Electromagnetic regulation of cell activity. Cold Spring Harbor Perspectives in Medicine 9.5 https://doi.org/10.1101/cshperspect.a034322

33. Binhi, V. N., & Rubin, A. B. (2022). Theoretical Concepts in Magnetobiology after 40 Years of Research. Cells, 11(2), 274. https://doi.org/10.3390/cells11020274

34. Chen, C., Chen, L., Wang, P., Wu, L. F., & Song, T. (2017). Magnetically–induced elimination of *Staphylococcus aureus* by magnetotactic bacteria under a swing magnetic field. *Nanomedicine: Nanotechnology, Biology and Medicine* 13.2, 363–370. https://doi.org/10.1016/j.nano.2016.08.021

35. Xing, W., Hu, H., Zhang, Y., Zhao, D., Wang, W., Pan, H., & Yan, L. (2020). Magnetotactic bacteria diversity of and magnetism contribution to sediment in Wudalianchi volcanic barrier lakes, *NE China. Science of The Total Environment* 718, 137348. https://doi.org/10.1016/j.scitotenv.2020.137348

36. Yan, Lei, and Weijia Xing. 2018. Methods to study magnetotactic bacteria and magnetosomes. *Methods in Microbiology*. Vol. 45. Academic Press, 357–386. https://doi.org/10.1016/bs.mim.2018.05.003

37. Wu, H., Li, C., Masood, M., Zhang, Z., Zou, G., Xu, X., Wang, L., Zhao, G., Yu, S., Zhu, P., Wang, B., Qin, D., & Liu, J. (2022). Static Magnetic Fields Regulate T–Type Calcium Ion Channels and Mediate Mesenchymal Stem Cells Proliferation. *Cells*, 11(15), 2460. https://doi.org/10.3390/cells11152460

38. Zablotskii, V., Polyakova, T., Lunov, O., & Dejneka, A. (2016). How a High–Gradient Magnetic Field Could Affect Cell Life. Scientific Reports, 6(1), 1–13. https://doi.org/10.1038/srep37407

39. Miyakoshi, J. (2005). Effects of static magnetic fields at the cellular level. *Progress in biophysics and molecular biology*, 87(2–3), 213–223. https://doi.org/10.1016/j.pbiomolbio.2004.08.008

40. Stanley, S. A., & Friedman, J. M. (2019). Electromagnetic Regulation of Cell Activity. Cold Spring Harbor Perspectives in Medicine, 9(5). https://doi.org/10.1101/cshperspect.a034322

41. Mocanu–Dobranici, A. E., Costache, M., & Dinescu, S. (2023). Insights into the Molecular Mechanisms Regulating Cell Behavior in Response to Magnetic Materials and Magnetic Stimulation in Stem Cell (Neurogenic) Differentiation. *International Journal of Molecular Sciences*, 24(3), 2028. https://doi.org/10.3390/ijms24032028

42. Wu, X., Du, J., Song, W., Cao, M., Chen, S., & Xia, R. (2018). Weak power frequency magnetic fields induce microtubule cytoskeleton reorganization depending on the epidermal growth factor receptor and the calcium related signaling. *PloS one*, *13*(10), e0205569. https://doi.org/10.1371/journal.pone.0205569

43. Binhi, V. N. (2023). Statistical Amplification of the Effects of Weak Magnetic Fields in Cellular Translation. *Cells*, 12(5), 724. https://doi.org/10.3390/cells12050724

44. Wang, H., & Zhang, X. (2017). Magnetic fields and reactive oxygen species. International *Journal of Molecular Sciences*, 18(10), 2175. https://doi.org/10.3390/ijms18102175

45. Zablotskii, V., Polyakova, T., & Dejneka, A. (2022). Effects of High Magnetic Fields on the Diffusion of Biologically Active Molecules. *Cells*, 11(1), 81. https://doi.org/10.3390/cells11010081

46. Feng, C., Yu, B., Song, C., Wang, J., Zhang, L., Ji, X., Wang, Y., Fang, Y., Liao, Z., Wei, M.,

& Zhang, X. (2022). Static Magnetic Fields Reduce Oxidative Stress to Improve Wound Healing and Alleviate Diabetic Complications. *Cells*, 11(3), 443. https://doi.org/10.3390/cells11030443

47. Usselman, R. J., Hill, I., Singel, D. J., & Martino, C. F. (2014). Spin biochemistry modulates reactive oxygen species (ROS) production by radio frequency magnetic fields. *PloS one*, 9(3), e93065. https://doi.org/10.1371/journal.pone.0093065

48. Sharpe, M. A., Baskin, D. S., Pichumani, K., Ijare, O. B., & Helekar, S. A. (2021). Rotating magnetic fields inhibit mitochondrial respiration, promote oxidative stress and produce loss of mitochondrial integrity in cancer cells. *Frontiers in Oncology*, 11, 768758. https://doi.org/10.3389/fonc.2021.768758

49. Zadeh–Haghighi, H., & Simon, C. (2022). Magnetic field effects in biology from the perspective of the radical pair mechanism. *Journal of the Royal Society Interface*, 19(193), 20220325. https://doi.org/10.48550/arXiv.2204.09147

50. Mocanu–Dobranici, A. E., Costache, M., & Dinescu, S. (2023). Insights into the Molecular Mechanisms Regulating Cell Behavior in Response to Magnetic Materials and Magnetic Stimulation in Stem Cell (Neurogenic) Differentiation. *International Journal of Molecular Sciences*, 24(3), 2028. https://doi.org/10.3390/ijms24032028

51. Giorgi, G., & Del Re, B. (2021). Epigenetic dysregulation in various types of cells exposed to extremely low–frequency magnetic fields. *Cell and Tissue Research*, 386(1), 1–15. https://doi.org/10.1007/s00441–021–03489–6

52. Consales, C., Cirotti, C., Filomeni, G., Panatta, M., Butera, A., Merla, C., & Benassi, B. (2018). Fifty–hertz magnetic field affects the epigenetic modulation of the miR–34b/c in neuronal cells. *Molecular Neurobiology*, 55, 5698–5714. https://doi.org/10.1007/s12035–017–0791–0

53. Dhiman, S. K., & Galland, P. (2018). Effects of weak static magnetic fields on the gene expression of seedlings of Arabidopsis thaliana. *Journal of plant physiology*, 231, 9–18. https://doi.org/10.1016/j.jplph.2018.08.016

54. Binninger, D. M., & Ungvichian, V. (1997). Effects of 60 Hz AC magnetic fields on gene expression following exposure over multiple cell generations using Saccharomyces cerevisiae. *Bioelectrochemistry and bioenergetics*, 43(1), 83–89. https://doi.org/10.1016/S0302–4598(96)05180–X

55. Ortner, V., Kaspar, C., Halter, C., Töllner, L., Mykhaylyk, O., Walzer, J., ... & Czerny, T. (2012). Magnetic field–controlled gene expression in encapsulated cells. *Journal of controlled release*, 158(3), 424–432. https://doi.org/10.1016/j.jconrel.2011.12.006

56. Zhou, H., Xuanyuan, X., Lv, X., Wang, J., Feng, K., Chen, C., ... & Xing, D. (2023). Mechanisms of magnetic sensing and regulating extracellular electron transfer of electroactive bacteria under magnetic fields. *Science of The Total Environment*, 165104. https://doi.org/10.1016/j.scitotenv.2023.165104

57. Kimsa–Dudek, M., Synowiec–Wojtarowicz, A., Krawczyk, A., Kruszniewska–Rajs, C., & Gola, J. (2021). A static magnetic field changes the expression profile of the transforming growth factor β family genes in human cells that have been treated with fluoride ions. *Cytokine*, 143, 155537. https://doi.org/10.1016/j.cyto.2021.155537

58. Rashidieh, B., Ansari, A. M., Behdani, M., Darvishi, B., & Habibi–Anbouhi, M. (2022). Extremely low frequency magnetic field enhances expression of a specific recombinant protein in bacterial host. *Analytical Biochemistry*, 652, 114745. https://doi.org/10.1016/j.ab.2022.114745

59. Harrison, G. H., Balcer–Kubiczek, E. K., Shi, Z. M., Zhang, Y. F., McCready, W. A., & Davis, C. C. (1997). Kinetics of gene expression following exposure to 60 Hz, 2 mT magnetic fields in three human cell lines. *Bioelectrochemistry and bioenergetics*, 43(1), 1–6. https://doi.org/10.1016/S0302–4598(97)00034–2

60. Czyz, J., Nikolova, T., Schuderer, J., Kuster, N., & Wobus, A. M. (2004). Non–thermal effects of power–line magnetic fields (50 Hz) on gene expression levels of pluripotent embryonic stem cells the role of tumour suppressor p53. *Mutation Research/Genetic Toxicology and Environmental Mutagenesis*, 557(1), 63–74. https://doi.org/10.1016/j.mrgentox.2003.09.011

61. Wang, J., & Shang, P. (2022). Static magnetic field: A potential tool of controlling stem cells fates for stem cell therapy in osteoporosis. *Progress in Biophysics and Molecular Biology*. https://doi.org/10.1016/j.pbiomolbio.2022.12.007

62. Moritsuka, N., Matsuoka, K., Katsura, K., Sano, S., & Yanai, J. (2021). Laboratory and field measurement of magnetic susceptibility of Japanese agricultural soils for rapid soil assessment. *Geoderma*, 393, 115013. https://doi.org/10.1016/j.geoderma.2021.115013

63. Frey, A. H. (1993). Electromagnetic field interactions with biological systems 1. *The FASEB journal*, 7(2), 272–281. https://doi.org/10.1096/fasebj.7.2.8440406

64. Härtel, H. (2018). Electromagnetic induction: An alternative for teaching and understanding. *European Journal of Physics Education*, 9(2), 1–13. https://doi.org/10.20308/ejpe.v9i2.210

65. Everett, M. E., & Chave, A. D. (2019). On the physical principles underlying electromagnetic induction. Geophysics, 84(5), W21–W32. https://doi.org/10.1190/geo2018–0232.1

66. Lu, L., Jia, Y., Xu, Y., Ge, M., Yang, L., & Zhan, X. (2019). Energy dependence on modes of electric activities of neuron driven by different external mixed signals under electromagnetic induction. *Science China Technological Sciences*, 62, 427–440. https://doi.org/10.1007/s11431–017–9217–x

67. Wu, F., Gu, H., & Li, Y. (2019). Inhibitory electromagnetic induction current induces enhancement instead of reduction of neural bursting activities. Communications in Nonlinear Science and Numerical Simulation, 79, 104924. https://doi.org/10.1209/0295–5075/81/60002

68. Ma, J., Wu, F., Hayat, T., Zhou, P., & Tang, J. (2017). Electromagnetic induction and radiation–induced abnormality of wave propagation in excitable media. Physica A: Statistical Mechanics and its Applications, 486, 508–516. https://doi.org/10.1016/j.physa.2017.05.075

69. Kitaori, A., Kanazawa, N., Yokouchi, T., Kagawa, F., Nagaosa, N., & Tokura, Y. (2021). Emergent electromagnetic induction beyond room temperature. Proceedings of the National Academy of Sciences, 118(33), e2105422118. https://doi.org/10.1073/pnas.2105422118

70. Megateli, S., & Krea, M. (2018). Enhancement of total phenolic and flavonoids extraction from Rosmarinus officinalis L using electromagnetic induction heating (EMIH) process. Physiology and Molecular Biology of Plants, 24(5), 889–897. https://doi.org/10.1007/s12298–018–0585–5

71. Biehl, B., Nyanga, L. K., & Kebe, I. (2018). Diversity of lactic acid bacteria and yeasts during spontaneous fermentation of cocoa beans. *Food Research International*, 107, 565–574. https://doi.org/10.1016/j.foodres.2018.03.066

72. Afoakwa, E. O., Kongor, J. E., Takrama, J. F., & Budu, A. S. (2012). Changes in acidification, sugars, and mineral composition of cocoa pulp during fermentation of pulp pre–conditioned cocoa (*Theobroma cacao*) beans. *International Journal of Food Science & Technology*, 47(12), 2510–2517. https://doi.org/10.1111/j.1365–2621.2012.03125.x

73. Camu, N., De Winter, T., Verbrugghe, K., Cleenwerck, I., Vandamme, P., Takrama, J. S., & Vancanneyt, M. (2013). Dynamics and biodiversity of populations of lactic acid bacteria and acetic acid bacteria involved in spontaneous heap fermentation of cocoa beans in Ghana.

Applied and Environmental Microbiology, 79(22), 7699–7710. https://doi.org/10.1128/AEM.02393–13

74. Sánchez–Moreno, P., Ramos, L., & Nevárez–Moorillón, G. V. (2020). Changes in cocoa bean chemical composition during fermentation: Effect of temperature and inoculation with cocoa pulp–acidifying bacteria. *Food Research International*, 128, 108800. https://doi.org/10.1016/j.foodres.2019.108800

75. Adomako, M. A., Takrama, J. F., & Oldham, J. H. (2020). The impact of lactic acid bacteria (LAB) fermentation on the quality of Ghanaian cocoa beans. *International Journal of Food Science and Technology*, 55(2), 680–687. https://doi.org/10.1111/ijfs.14218

76. Agyirifo, D. S., Wamalwa, M., Otwe, E. P., Galyuon, I., Runo, S., Takrama, J., & Ngeranwa, J. (2019) Metagenomics analysis of cocoa bean fermentation microbiome identifying species diversity and putative functional capabilities. *Heliyon*, 5(7). https://doi.org/10.1016/j.heliyon.2019.e02170

77. Figueroa–Hernández, C., Mota–Gutierrez, J., Ferrocino, I., Hernández–Estrada, Z. J., González–Ríos, O., Cocolin, L., & Suárez–Quiroz, M. L. (2019). The challenges and perspectives of the selection of starter cultures for fermented cocoa beans. International *Journal of Food Microbiology*, 301, 41–50. https://doi.org/10.1016/j.ijfoodmicro.2019.05.002

78. Samaniego, I., Espín, S., Quiroz, J., Rosales, C., Carrillo, W., Mena, P., & García–Viguera, C. (2021). Effect of the growing area on the fat content and the fatty acid composition of Ecuadorian cocoa beans. *International Journal of Food Sciences and Nutrition*, 72(7), 901–911. https://doi.org/10.1080/09637486.2021.1884204

79. Illeghems, K., Papalexandratou, Z., De Vuyst, L., & Weckx, S. (2018). Impact of post–harvest processing on the natural microbiota and flavor of cocoa beans. *Current Opinion in Food Science*, 22, 1–7. https://doi.org/10.1016/j.cofs.2018.01.003

80. Camu, N., De Winter, T., Addo, S. K., Takrama, J. F., Bernaert, H., De Vuyst, L., & Vuyst, L. D. (2018). Fermentation of cocoa beans: influence of microbial activities and polyphenol concentrations on the flavour of chocolate. *Journal of the Science of Food and Agriculture*, 98(5), 1754–1763. https://doi.org/10.1002/jsfa.8642

81. Dzah, C. S., Amoa–Awua, W. K., Appiah, F., & Quao, J. (2020). Identification of microorganisms associated with Ghanaian cocoa bean fermentation and their potential for bioflocculant production. *Journal of Food Science and Technology*, 57(3), 903–915.

https://doi.org/10.1007/s13197–019–04172

82. Guzmán–Armenteros, T. M., Ruales, J., Villacís–Chiriboga, J., & Guerra, L. S. Experimental Prototype of Electromagnetic Emissions for Biotechnological Research: Monitoring Cocoa Bean Fermentation Parameters. *Foods* 12.13 (2023): 2539. https://doi.org/10.3390/foods12132539

83. Guzmán–Armenteros, T. M., Ramos–Guerrero, L. A., Guerra, L. S., Weckx, S., & Ruales, J. (2023). Optimization of cacao beans fermentation by native species and electromagnetic fields. *Heliyon*, 9(4). https://doi.org/10.1016/j.heliyon.2023.e15065

84. Bektiarso, S., Prastowo, S. H. B., Prihandono, T., & Handayani, R. D. (2020). Optimizing lactobacillus growth in the fermentation process of artificial civet coffee using extremely–low frequency (ELF) magnetic field. In Journal of Physics: Conference Series (1465(1):012010). IOP Publishing. https://doi.org/10.1088/1742–6596/1465/1/012010

Chapter 2

Experimental Prototype of Electromagnetic Emissions for Biotechnological research: Monitoring Cocoa Bean Fermentation Parameters

Tania María Guzmán–Armenteros [1], Jenny Ruales [1]*, José Villacís–Chiriboga [1] and Luis Santiago Guerra [2]

[1] Department of Food Science and Biotechnology, Escuela Politécnica Nacional, P.O. Box 17–01–2759, Quito, Ecuador; tania.guzman@epn.edu.ec; (T.M.G.–A) jenny.ruales@epn.edu.ec; (J.R.);jo–se.villacis@epn.edu.ec; (J.V.–C.)

[2] Carrera de Medicina, Facultad de Ciencias Médicas, Universidad Central del Ecuador, P.O. Box 17–12–759, Quito, Ecuador; lsguerrap@uce.edu.ec

* Corresponding author: jenny.ruales@epn.edu.ec

Abstract

A Helmholtz–type electromagnetic emission device, which uses an oscillating magnetic field (OMF), with potential applications in biotechnological research, was built and validated. The coils were connected to an alternating current (AC) generator to generate a 0.5 to 110 mT field at their center. OMF measurements were performed with a Hall effect sensor with a digital signal connection (Arduino nano) and data output to a PC using LabVIEW v2017SP1 software. The fermentation process of the cocoa bean variety CCN–51, exposed to four levels of OMF density for 60 min (0, 5, 40, and 80 mT/60 min), was analyzed. Different variables of the grain fermentation process were evaluated over six days. The ANOVA test probed the device's linearity, accuracy, precision, repeatability, reliability, and robustness. Moreover, CCN–51 cocoa beans' EMF–exposure effect was evaluated under different OMF densities for 60 min. The results show the validity of the equipment under working conditions and the impact of EMF (electromagnetic fields) on the yield, deformation, and pH of cocoa beans. Thus, we concluded that the operation of the prototype is valid for use in biotechnological studies.

Keywords: monitoring; Helmholtz coil; magnetic field; Hall effect sensor; Arduino nano; validation

1. Introduction

The effects of EMFs (electromagnetic fields) on biological systems have been the subject of extensive research, including their impact on fermentation processes [1,2]. It is known that many biological systems are affected by the presence of a magnetic field, and this process can be approached from a double perspective: firstly, through an analysis of the direct action of the EMF study [2] and secondly in the surrounding environment [3].

Recent research indicates that electromagnetic fields can stimulate or inhibit different biological systems [1–18], such as the growth of plants [13], fruits [14], and microorganisms [15]. Similarly, they affect cells in the human [16] and animal [17] body by stimulating or inhibiting different cellular processes [18]. Several of these cellular properties have been used to improve health [4], obtain metabolites of industrial interest [5], and remove contaminants from soil [6], water [7], and air [8]. In this sense, electromagnetic fields offer a sustainable and non–invasive solution with different practical applications such as medical therapy [9], production processes [10], and environmental protection [11], maintaining natural integrity [3].

Therefore, three fundamental criteria must be considered when conducting an EMF investigation. The first is to unify evidence–based research criteria, following a single and coherent trend. The second is to ensure experimental validity to obtain reproducible results while maintaining the uniformity of electromagnetic field measurements in the work area [19]. The third is to select a biological system that can rapidly reproduce the validity of observable effects [20,21]. Thus, observable physical changes in EMF measurements can be appreciated and adjusted in mathematical models that condition their intrinsic behavior [20]. A clear example is the Helmholtz coil system used for sensor validation, which generates a uniform magnetic field inside the coils and reduces the variability around their axes [22]. These systems are simple and convenient to validate different measurement systems, and with specialized programs, their behavior can be easily monitored [23].

Fermentation is a process in which microorganisms convert organic compounds into simpler compounds, such as alcohol or lactic acid, without oxygen [24]. The efficiency of fermentation processes is affected by various factors, such as temperature, pH, humidity, nutrient availability, and the presence of inhibitors or antimicrobial agents [24–26]. Recently, researchers have begun to investigate the potential impact of EMFs on fermentative processes. Although the role and influence of the magnetic field in this process are undeniable, there are many aspects to consider about its effects [12], which still need to be sufficiently understood [4–7,12–18].

On the other hand, one of the most functional and spontaneous biological systems that at the same time is reproducible is the fermentation of the cocoa bean. This process involves several microbial

species [27] that act as a single ecosystem regulated by different environmental factors, such as humidity, pH, oxygen tension, and temperature [26]. These factors, in turn, are modulated by the metabolic activity of the microbial species that ferment the pulp [27]. The native microorganisms of the grain are naturally selected [28] and gradually colonize the pulp based on their metabolic potential [28,29]. Thus, the microbial metabolism produces notable external and internal physical changes in the bean [11].

Studies on the kinetic behavior and synergy of microbial populations during fermentation indicate the susceptibility of this process to environmental factors that often lead to poor fermentation, irreversibly reflected in the structural transformations of the cocoa bean [30]. These changes can be easily controlled using a simple temperature, humidity, pH, and Brix–monitoring device. Since variations in measurement procedures are one of the primary sources of bias in EMF studies, cocoa bean fermentation is an ideal study system to observe magnetic field effects on fermentation parameters. This research aims to validate an experimental prototype that generates low–frequency electromagnetic fields by monitoring CCN–51 cocoa bean fermentation.

To achieve the objective of the investigation, three essential stages were followed. The prototype and the digital signal connection system were designed in the initial step. Subsequently, in the second stage, the prototype underwent a rigorous validation of precision, reproducibility, and robustness against a gold standard for determining its ability to generate the expected electromagnetic emissions. Finally, the third stage consisted of evaluating the biological effects by monitoring key variables that characterize the fermentation process of CCN–51 cocoa beans. This comprehensive analysis examined the associations between the observed electromagnetic emissions and the identified variables.

This research study offers important information on the design, validation, and impact of electromagnetic emissions on cocoa beans. The results have substantial potential to improve the biotech and agricultural sectors by exploring novel approaches that improve cocoa production, contributing to the development of the chocolate industry.

2. Materials and Methods

2.1. Select Prototype Elements

In the selection of the aspects of the experimental prototype of electromagnetic emissions, Equation (1), the weighted factor method of the multi–criteria decision analysis (MCDA) was used [31]:

$$P_i = \sum_{k=n}^{i} . W_K * S_{ki} \quad (1)$$

Where P_i is the score of choice, W_k is the weighting of factor k, and Sk is the rating given to factor k in option n.

Five *k* factors (generation, electrical control, emission, and presentation of signals or data) were analyzed using expert criteria with three alternatives or components of each system or factor for selecting the elements according to their highest *P*. The number of loops in each coil, the magnetic field density, and the current that circulates through the coils were determined by Biot Savart law [32] (Equation (2)) to obtain field density readings of 0.5 to 110 mT.

$$B = \frac{8\mu_0 IN}{5\sqrt{5} \cdot a} \quad (2)$$

where I, is the current in each coil, N is the number of turns in each, B is the density of the magnetic field generated by N loops on the x–axis, and a is the mean radius of the coil.

At the same time, the values of these variables corroborated by measuring instruments were obtained. In electrical measurements, a digital multimeter (UT56 LCD, UNI–T, China) was used, and ± (0.5%) of alternating current was used. The generated temperature was controlled with a digital thermometer (DeltaTrak 11050, California, USA) (±0.1 °C) considering normative guidelines for electrical safety in assembling mechanical, electrical, and electronic elements.

2.1.1. Generation System and Electrical Support

In the design of the coils, materials such as plastic and wood were considered (*P* = 90%). Plastic was chosen for its insulating properties, while wood was selected for its mechanical support and stability. These materials were found to be suitable for the coil design due to their availability, cost–effectiveness, and compatibility with the desired performance of the system.

To power the electromagnetic emission system, an alternating current (AC) generator was chosen (*P* = 72%). The AC generator can deliver a sinusoidal waveform with a variable amplitude ranging from 0 to 100 V, operating at a frequency of 60 Hz. This specific waveform allowed the Helmholtz coils to generate a magnetic field with a density ranging from 0.55 to 110 mT, facilitating the desired experimental conditions for the study [33] (Figure 1).

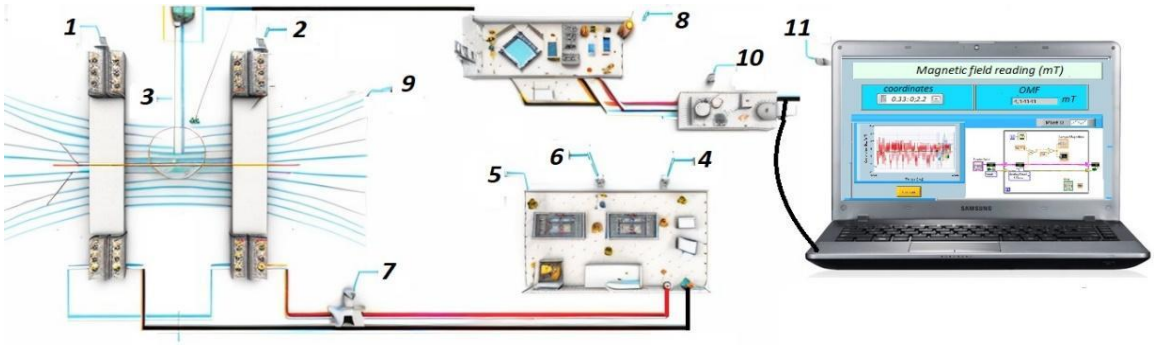

Figure 1. EMF system. (1) Coil 1 (2); coil 2; (3) magnetic sensor (Hall effect Tesla meter); (4) variable voltage source; (5) voltage indicator; (6) current indicator; (7) ammeter; (8) Arduino nano; (9) magnetic field flux lines; (10) sensor module; (11) LabVIEW data output signal on the PC.

The selection of the monoaxial Helmholtz matrix configuration, the careful design of the coils, and the choice of appropriate materials ensured a controlled and uniform magnetic field within the experimental setup. This configuration and the AC generator with the specified waveform parameters enabled the researchers to precisely investigate the effects of electromagnetic emissions on the cocoa beans' fermentation process.

2.1.2. Data Acquisition and Monitoring System

The selection of the high–precision Hall effect sensor (MLX92242, Melexis Co. Lcd, Tessenderlo, Belgium) (±100 mT) (P = 84.24%) was based on its ability to accurately measure the magnetic field strength, specifically the OMF (olfactory magnetic field). This sensor provides a wide measurement range and offers precise and reliable data for the electromagnetic emissions under investigation [34].

The Arduino nano board (Arduino LLC, China) (P = 92.02%) was chosen for signal acquisition. It functioned as the interface between the Hall effect sensor and the data processing system. The Arduino nano board was connected to the PC using an Ethernet cable, establishing a reliable and efficient data transfer and control connection [35].

The acquired data were visualized and analyzed, with the LabVIEW 2017 software (P = 90.23%) employed as a data presentation tool [36]. LabVIEW is a well–established software platform capable of acquiring, processing, and displaying scientific data. The software provides a user–friendly interface to observe and analyze the electromagnetic emission data captured by the Hall effect sensor and Arduino nano board. The data collected during the experiments were stored in a local file, ensuring data integrity and accessibility for further analysis [37, 38] (Figure 1).

Low–cost, open–source boards such as the Arduino nano provide a cost–effective alternative combining advanced measurement and data acquisition capabilities. The Arduino nano offers high–

quality experiments at a low cost, enabling researchers to conduct their studies without budget constraints [39]. The compatibility between the Arduino nano and LabVIEW 2017 software justifies their selection as hardware and software components. LabVIEW is a recognized software platform known for its reliability in scientific data analysis. It provides a comprehensive interface for acquiring, analyzing, and visualizing data, making it suitable for presenting the collected data and ensuring efficient data analysis.

2.2. Electrical Validation of the Prototype

2.2.1. Linearity Measurements

The linearity of the measurements was evaluated by Student's *t*–test (n–2 degrees of freedom, $\alpha = 0.05$) and linear regression (least squares method) with a 95% confidence level [19,36] to corroborate the relationship between the input and output signal. The relationship between OMF oscillating magnetic field density OMF readings was determined using the MLX92242 mark Hall effect sensor (SEH) for the prototype and One–Tesla meter (PT2026, Ltd. GST, Japan) (accuracy 10 ppb) as the "Gold standard" [34] (Figure S2 in supplementary material). Linearity was also evaluated with the hypothesis test for slope (b) and intercept (a) and the significance of the coefficients based on their standard errors (Ho: $b = 0$; Hi: $b \neq 0$; Ho: $a = 0$; Hi: $a \neq 0$) [36,40].

The linearity reveals adequate regression and proportionality in the measurements, and the linear model obtained is unaffected by systematic errors [36,38,40]. The response factors are similar, showing adequate precision of the measurements and the SEH reliability of the responses about the GEs (Table 1).

Table 1. ANOVA for field densities and regression coefficients of the linear model; *t*–test, for the slope of the model, (slope: $b = 0.904$, null hypothesis: $b = 0$, alternative hypothesis: $b \neq 0$); the probability of being $b = 0$ is low (*p*–value = 0.000); for the intercept ($a = 1.641$), the value with a low probability of being is $a = 0$ (*p*–value = 0.000), (slope $\neq 0$; intercept $\neq 0$). The value of the intraclass correlation coefficient is (ICC = 0.994).

Fountain	**Sum of Squares**	**Gl**	**Middle Square**	**F–Reason**	***p*–Value**
Model	50,596.5	1	50,596.5	25,844.27	0.00
Residue	164.451	84	1.95775		
Total (Corr.)	58,444.5	84			
Parameter	Least Squares Dear	Standard Error	Statistical T	*p*–value	
Intercept(a)	1.641	0.287	5.708	0.0000	
Slope(b)	0.904	0.005	160.762	0.0000	
Correlation Coefficient (r)	R–Square	Standard error of the set.	Average absolute error	CCI	
0.998	0.996	1.39	1.13	0.994	

2.2.2. Precision, Reproducibility, and Robustness Measurements

Precision was determined by OMF density measurements from the center of the Helmholtz coil to its edges in the workspace (p, α, z) according to the RS (response surface) design of experiments in the Design Expert v.13 programs (see Section 2.5 and Table S2). The value of the measurements of OMF density was obtained by repeating this test under the same conditions by different analysts, days, and temperatures to different OMF densities (Table S2). In each experiment, the mean, standard deviation, and variance of each response were obtained from the current variations in the coils (R1(5 mT), R2(42 mT), and R3(80 mT)) (Table S3).

2.2.3. Simulation and Validation of the Prototype

In the simulation, the magnetic field around the radial coordinates (ρ, α) starting from the center to the distant points of the axis (z) was calculated (Table S3). From the polynomial equations of the models, three response surface graphs were obtained that describe the behavior of the field density in the work area [22]. The field density remains constant in this area and decreases as we move away from the central point (Table S3). The COMSOL Multiphysics 6.0 program obtained this same behavior profile, where the exact coordinates were simultaneously simulated [41] (Figure 3).

The analysis of variance (ANOVA) conducted on the OMF density at different intensities (R1, R2, and R3) revealed statistically significant differences in the radial coordinates of the prototype, with a confidence level of 95.0%. The model F value for all responses was found to be significant, indicating that the model adequately explains the observed variations in the OMF density (Table S3). Additionally, for the optimization, three random coordinates were selected and tested in the obtained polynomial equations, and simultaneously, the OMF density readings were obtained in the exact coordinates in RI, R2, and R3. Each OMF density measurement was replicated seven times at the selected coordinates (Table S4). The average observations of each confirmation experiment (experimental coordinates) were within the prediction interval, which confirms the validity of the models obtained (Table S4).

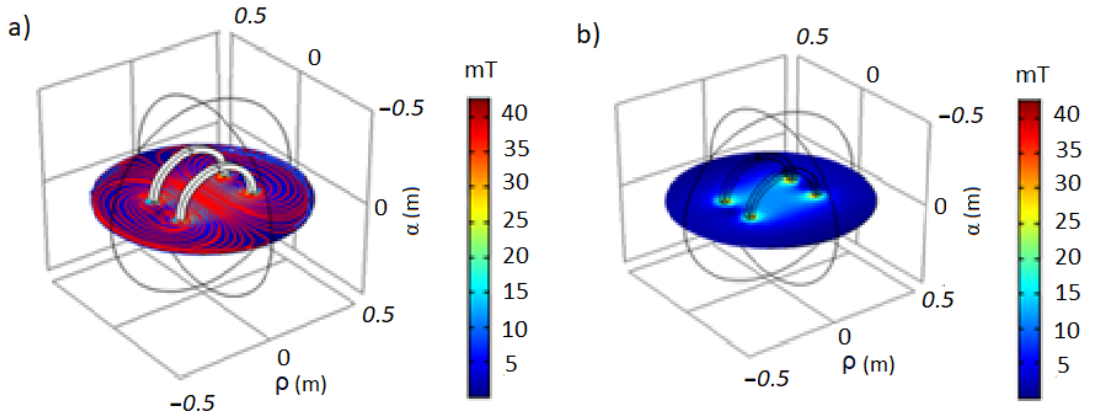

Figure 3. Flux density vs. distance spectra cross–section simulation in COMSOL Multiphysics (radial axis: ρ, α; axial axis: z): (**a**) 5 mT and (**b**) 42 mT.

2.3. Experimental Processing

2.3.1. Beans Processing

The cocoa pods of CCN51 cocoa beans obtained from local producers in the province of Santo Domingo, Ecuador, were disinfected in a 3% sodium hypochlorite solution for one hour. Subsequently, they were washed and manually opened under aseptic conditions to keep the grains clean and free of impurities or defects. Three kilograms of grains were placed in 5 L plastic fermentation boxes with ventral and lateral openings to facilitate the exudation of the beans [42] (Figure 4).

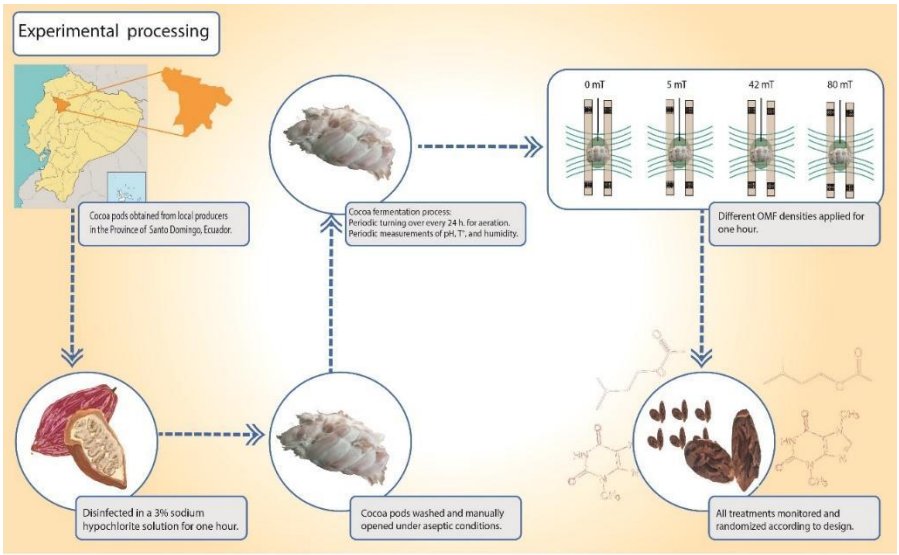

Figure 4. Schematic drawing of the experimental procedure for cocoa beans.

2.3.2. Cocoa Fermentation Process

The fermentation process was carried out under controlled environmental temperature and humidity. The samples were placed in an orderly manner (according to the design described below) in the fermentation chamber and turned over periodically (every 24 h) to facilitate aeration [31,41]. During the periodic measurements of pH, temperature, and humidity, aseptic measures were always sought, and the measurement time was reduced to avoid interfering with the experiment results (Figure 4).

2.3.3. OMF Expositions Process

Eight hours after fermentation, each experimental unit was placed in the center of the Helmholtz coils and subjected to different OMF densities for one hour according to the experimental design (0 mT, 5 mT, 42 mT, and 80 mT). The samples were placed vertically and close to the center of both rings, maintaining adequate separation between them. All treatments were properly monitored and randomized according to design (Figures 4 and 5).

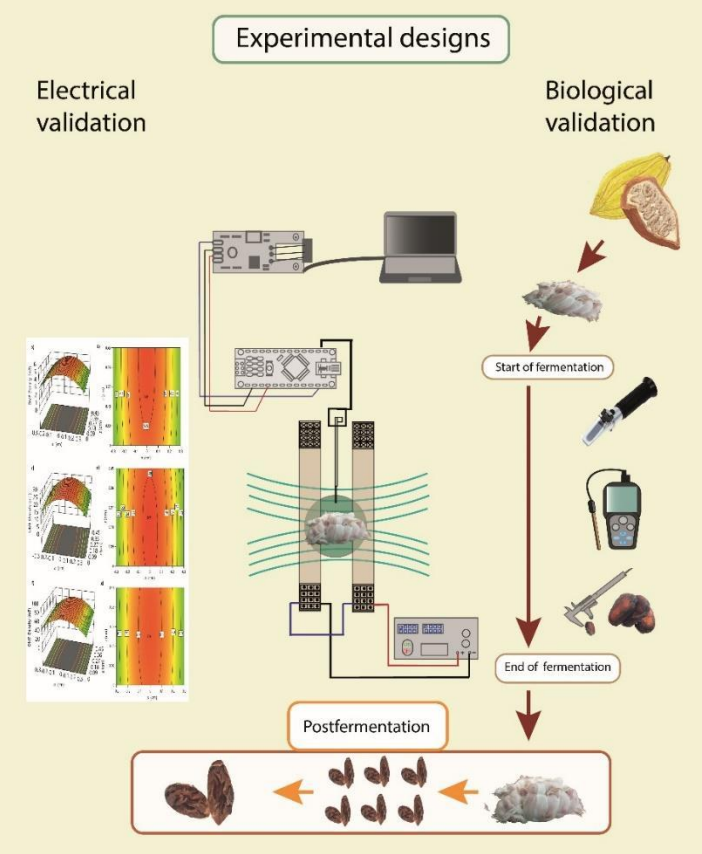

Figure 5. Schematic drawing of experimental designs. Electrical and biological validations in Design Expert software v13.

2.4. Monitoring Variables of the Process

2.4.1. Continuous Variables

During the fermentation process, the CCN51 cocoa beans' weight measurements were recorded with the digital balance brand SF–400 with a capacity of 10,000 g (±0.1 g), and the size of the beans was determined using the digital caliper (Vernier, Oregon, USA) (±0.01 mm). The pH, temperature, humidity, and Brix indices were determined in the mucilaginous pulp. The Brix concentration was measured using a digital refractometer (96801, HANNA Instruments, Woonsocket, USA) (±0.2%); the pH temperature and humidity by using a grain monitoring instrument kit (BlueLab Instruments, New Zealand) (±0.01 °C). For each experimental unit, three measurements (edges and center) were taken, with the average of each measure considered as the final value. All instruments were previously calibrated (Figure 5).

2.4.2. Proportional Variables

At the end of the fermentation process, the cocoa beans were classified according to their degree of fermentation into well–fermented (Bw), moderately fermented (Bm), poorly fermented (Bp), and contaminated (Bc) using the cutting technique [41,42]. Bw was characterized by brown or reddish–brown cotyledons accompanied by well–open veins. Bm contained partially striated cotyledons with purple stripes on the edges; Bp comprised deep purple cotyledons, and Bc included unfermented black or gray cotyledons severely damaged by biological contamination [43–45]. This classification gave rise to the fermentation degree (Equation 3).

$$Fd = \frac{B(i)}{Bt} \times 100 \quad (3)$$

Where B represents beans' average value; (i) is the classification beans; Bt represents total beans.

Weight and size measurements were used to determine different proportional process variables, such as the rate of grain weight loss (W_l) (Equation (4)) and deformation rate (D_r) (Equation (5)). The spectrometry determined the fermentation index through the absorbance ratio at 460 nm and 530 nm (Equation (6)) [45,46].

$$W_l = \frac{Wo - Wf}{Wo} \times 100 \quad (4)$$

$$D_r = \frac{\frac{Xo}{Yo} - \frac{Xf}{Yf}}{\frac{Xo}{Yo}} \times 100 \quad (5)$$

$$F_r = \frac{Bx}{By} \quad (6)$$

where W represents the mean value of the weight of the beans (Equation (4)); Xo is the mean bean initial length value, Yo is the mean initial bean width value, Xf is the mean bean final length value, Yf is the mean bean final width value (Equation (5)), Bx represents the bean reading at 460 nm, and By represents the bean reading at 530 nm (Equation (6)).

2.4.3. Microbial Analysis

Microbial viability was determined using ISO 6887 [47]. Ten grams of cocoa beans contained in 100 mL of sterile dilution of buffered peptone water (MERCK) were shaken vigorously for 10 min to obtain a uniform sample; the sample was filtered and serially diluted in the same water, then plated on selective media WL Nutrient agar to yeast; MRS agar to LAB; and glucose acetate agar (GAA) to AAB; and incubated for 48 h at 30 °C (all media came from Merck KGaA, Darmstadt, Germany) [25]. The microbial concentrations were calculated as the logarithm of the colony–forming units per gram (CFU g^{-1}) by counting the number of colonies on the agar plates and multiplying it by the corresponding dilution factor according to the following Equation (Equation (7)) [48].

$$N = log(\frac{\sum_{n=i}^{j} Cl}{Vi \times p \times d}) \quad (7)$$

Where n represents replicas, i represents the subset of n; j represents a total of replicas, Cl represents the total number of colonies; V represents the inoculum volume, p represents the number of plates counted, and d represents minor dilution.

2.5. Experimental Design

A complete multifactorial design was carried out with a confidence level of 95%, and three repetitions for 48 experimental runs were designed in the Design Expert v.13.0.5.0 program. The factors were the OMF density (mT) and fermentation time (h). Four levels of OMF density were

established (0, 5, 42, and 80 mT/60 min) as well as eight fermentation times in hours from (0, 24, 48, 72, 96, 120, 144, and 168 h). The effects were evaluated using the response variables of different growth parameters (Figures 4 and 5).

The continuous variables, namely pH, temperature, humidity, and viability, were monitored during the seven days of fermentation and analyzed with ANOVA, and the proportions variables were analyzed by Poisson regression (Figures 4 and 5).

3. Results and Discussion

3.1. Prototype Validation Results

3.1.1. Electrical Validation

The spatial simulations of the electromagnetic field (EMF) carried out in this study, as shown in Figure 6a–c yielded valuable information on the prototype's performance. The results indicate that the magnetic flux density (B) readings at the center of the coils remained consistently stable across all tested scenarios (Figures 3 and 6**).** This consistency is supported by the equations describing the density decline as a distance function, as shown in table S3. This confirms the remarkable stability, precision (Figure 6a, b), reproducibility (Figure 6c, d), and robustness (Figure 6e, f) of the prototype (Figure 1). The linearity of the magnetic field within the coils, as seen in table 1, further supports these findings (Figure S2).

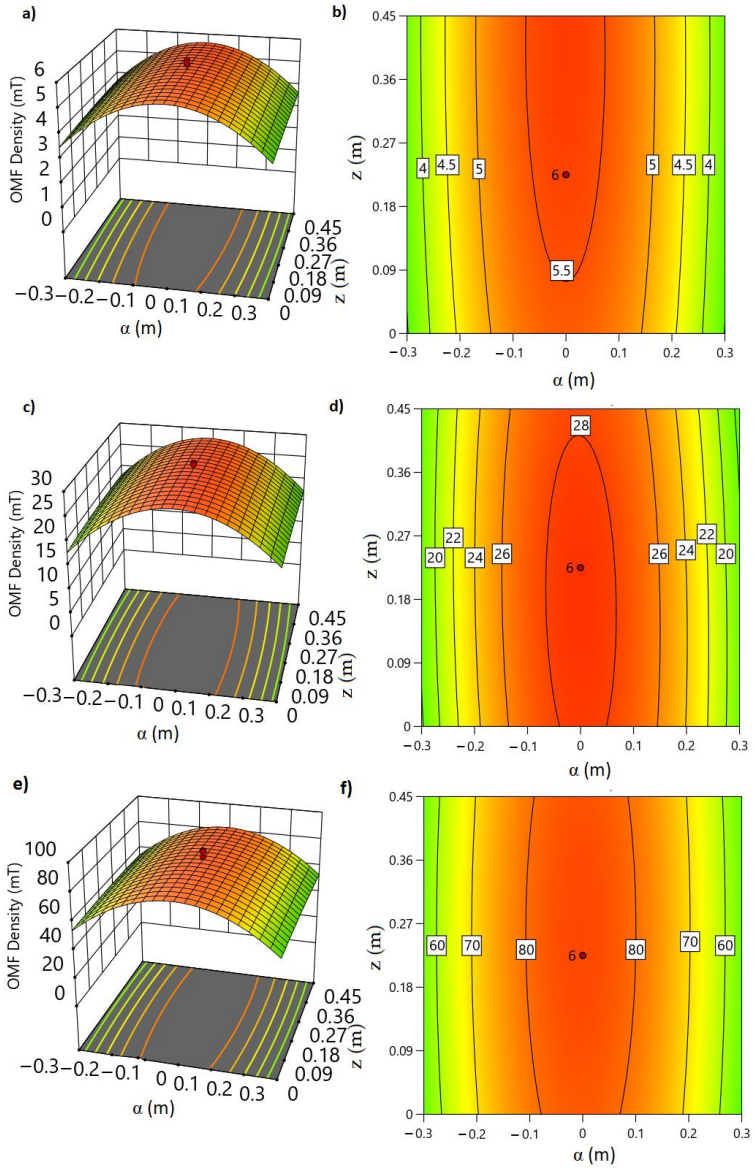

Figure 6. Response surface (RS) and contour graphs (CG). Modeling of the OMF density in the workspace as a function of days (a, b), analysis (c, d), and temperature (e, f). RS: vertical axes, OMF density; horizontal axes, α, and z; CG: vertical axes, α; horizontal axes, z; contour line, OMF density. ρ maintained in 0 values.

Maintaining a stable and predictable nature of the electromagnetic emissions generated by the prototype is crucial to guarantee its reliability and efficiency. This aspect is particularly significant when studying the effects of electromagnetic emissions on biotechnological systems such as cocoa beans. Previous studies emphasize the importance of stability and predictability in electromagnetic fields for precise and controlled experiments in various biotechnological applications [19–23].

The observed consistency in the magnetic field within the coils can be attributed to the design, precise location, and controlled current flow through the coils. Other researchers have also emphasized the importance of filtering the signal and using adequate material to maintain a uniform and stable magnetic field in Helmholtz coil configurations [21–23].

The uniformity of the magnetic field within the Helmholtz coils could be improved by implementing a polygonal coil design. Polygonal configurations strategically distribute coils, minimizing variations in magnetic field strength in the work area. This modification has the potential to improve the overall homogeneity of the field as well as the accuracy and robustness of the prototype [22,23].

It is advisable to recalculate the coil dimensions for a larger work area based on the desired radius. Increasing the coil dimensions proportionally to the desired working area ensures that the electromagnetic emissions cover a wider spatial range while maintaining the desired level of field uniformity. This adjustment allows the prototype to accommodate a larger footprint without compromising its optimal performance characteristics.

Numerous studies have shown that non–uniform magnetic fields can introduce variations in the response of biological systems, affecting the results of controlled biotechnological experiments [1–18]. By addressing non–uniformity through polygonal coil designs and dimension adjustments, the understanding and applicability of electromagnetic technologies in various biotechnology studies can be advanced [21–23]. These findings provide a solid foundation for the practical implementation of the prototype in studying the effects of electromagnetic emissions on cocoa beans. Thus, the stable and predictable nature of the electromagnetic emissions generated by the prototype makes it possible to assess their impact on the cocoa bean fermentation process accurately.

3.1.2. Behavior of Process Parameters

The ANOVA models for the temperature, pH, humidity, and Brix responses demonstrate their significant nature, as indicated by their respective F–values of 94.26, 41.34, 38.69, and 74.56. The probability of obtaining such large F–values solely due to noise is exceptionally low, at 0.01%. These findings confirm the robust significance of the models in explaining the observed variations in the responses. The *p*–values for the model terms A, B, and AB being less than 0.0500 in all four

models indicate their significant contribution to the respective responses (see Table S5 in the Supplemental Material).

During the fermentation of cocoa beans, the temperature and pH values of the beans were monitored and found to increase gradually, reaching their maximum values between 72 and 93 h (Figure 7b). Subsequently, the temperature and pH values decreased at the end of the fermentation period (168 h) (Figure 7 a, b). Among the different OMF density treatments, the highest temperature values (51 °C) were observed at 5 mT and 42 mT, while the lowest temperature value (34 °C) was recorded at 80 mT (Figure 7a).

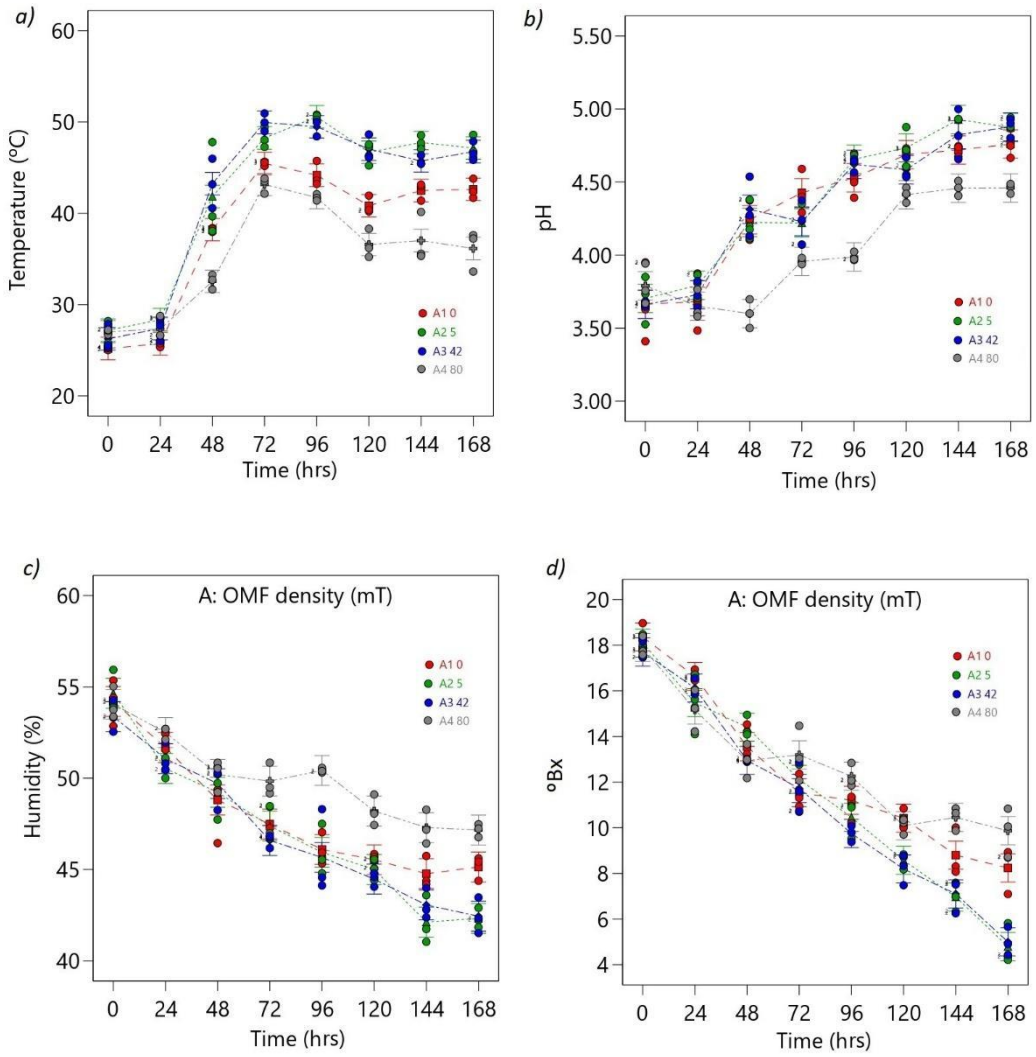

Figure 7 ANOVA interaction plots. Continuous responses: (a) temperature, (b) pH, (c) humidity, and (d) Brix. The ordinal factor, time, is displayed continuously, and the nominal OMF density factor (A) is presented discreetly as separate lines (A1: 0 mT red line, A2: 5 mT green line, A3: 40 mT blue line, A4: 80 mT gray line). The dots represent the values that the response variable takes around the mean; the midpoint of the bar represents the mean value; overlapping bar lines between levels indicate $p > 0.05$; no overlap of bar lines between levels indicates $p < 0.05$.

The temperature values during final fermentation were significantly different ($p < 0.05$) between the control and the OMF density treatments (0:43 °C, 5 mT:48 °C, 42 mT:48 °C, and 80 mT:36 °C) (Figure 7a). The maximum pH value (pH = 5) was recorded at 5 mT after 144 h, while the minimum pH value was observed at 80 mT after 48 h, with significant differences ($p < 0.05$) between the latter treatment and the rest of the treatments, including the control (Figure 7b). These results indicate that the OMF density treatments significantly impacted the temperature and pH levels during cocoa bean fermentation.

The moisture and Brix content gradually decreased, reaching minimum values at the end of the process, as depicted in Figure 7c, d. The highest Brix and moisture contents were recorded at 80 mT (Brix = 11Bx, Hr = 47%), whereas the lowest Brix and moisture contents were observed at 5 mT and 42 mT (Brix = 4Bx, Hr = 42%), with significant differences when compared to the control (Brix = 8, Hr = 45%) (Figure 7c, d).

The OMF density treatments significantly impacted the temperature, pH, moisture, and Brix content of cocoa beans during fermentation. The highest temperature values were observed at 5 mT and 42 mT, while the lowest was recorded at 80 mT. The highest Brix and moisture content was observed at 80 mT, and the lowest was recorded at 5 mT and 42 mT. These results indicate that the OMF density treatments significantly affect these variables during the fermentation of cocoa beans.

The optimum pH range for cocoa bean fermentation was found to be between 4.5 and 5.5, which favored the growth of lactic acid bacteria and the production of desirable flavor compounds [30]. In conclusion, the pH behavior during cocoa bean fermentation is a complex process that varies based on the cocoa variety, fermentation stage, and microbial activity. Additionally, it can be influenced by the pre–conditioning of the pulp, biochemical constituents, and polyphenolic constituents during fermentation [26,30,47,48].

Various scientific articles have discussed the alterations in pH that occur during cocoa fermentation [26,47,48]. In one such study, Mulono et al. [49], reported that the pH of cocoa beans increased from an initial pH of 4.4 to a maximum of 6.4 after 72 h of fermentation. However, after 96 h of fermentation, the pH decreased due to the production of organic acids by lactic acid bacteria. The authors noted that the pH of cocoa beans could vary depending on the microbial community structure and the specific strains of bacteria involved in fermentation.

Afoakwa et al. (2013) [26] also reported a rise in cocoa bean pH during the initial stages of fermentation due to the breakdown of glucose and fructose. However, after 48–72 h, pH levels dropped owing to the production of organic acids such as acetic and lactic acid by lactic acid bacteria. In a subsequent study in 2014, the same authors measured pH changes during cocoa

fermentation and observed a decrease in pH levels after the first and second days of fermentation, with pH values declining from 6 to 3 and 4 at the end of the process due to the production of organic acids by lactic acid bacteria [50], which was in line with other studies [30,48]. Several authors emphasize the impact of the structure of microbial communities and specific bacterial strains on the pH of the cocoa bean, indicating that if the pH becomes too acidic too soon (pH < 4.5), there will be a final reduction in flavor precursors and a final product that is too acidic [25,27].

Herrera–Rocha et al. [51] conducted a study to examine the influence of temperature on the quality of cocoa bean fermentation and its impact on various selected physicochemical characteristics. They determined that a temperature range of 45–50 °C was optimal for cocoa bean fermentation, resulting in desirable flavor compounds and reduced levels of undesirable flavor compounds. Cortez et al. [52] found that cocoa fermentation leads to temperatures exceeding 45 °C. This increase in temperature triggers the activation of native enzymes and the denaturation of proteins, resulting in a notable impact on the development of flavor during cocoa fermentation. Furthermore, this research revealed that the increase in temperature is closely related to the formation of the key aroma molecules responsible for improving the sensory profile and overall quality of cocoa beans.

In cocoa fermentation, Brix degrees can be used to monitor the conversion of sugars into organic acids and alcohol by microorganisms during the fermentation process [49,50]. Velásquez–Reyes et al. [53] studied differences between different cocoa bean varieties of the profile of volatile and non–volatile compounds in the process from fermentation to liquor. The authors found that Brix levels decreased during fermentation due to the metabolic activity of microorganisms involved in the process. Hernandez et al. [54] studied the physicochemical and microbiological dynamics of the fermentation of CCN51 cocoa material in three stages of maturity and demonstrated that microorganisms present in certain states were more effective in metabolizing sugars compared to those in other states. In the same way, it is evident that a gradual decrease in the degrees with the advance of fermentation is due to the consumption of sugars by microorganisms.

In their research, Camu et al. [25] explored the effects of both fermentation and drying processes on the microbial communities associated with cocoa beans. They found that Brix levels increased during fermentation and peaked around days 3–4 before decreasing during drying, likely due to the loss of water and sugars in the beans and the consumption of sugars by microorganisms during fermentation.

Overall, these studies highlight the critical role of temperature, pH, Brix, and humidity in microbial growth during cocoa bean fermentation. The optimal levels of these parameters may vary depending on the specific microbial strains and environmental conditions during fermentation. Thus, the results suggest that EMFs could indirectly affect cocoa bean physicochemical parameters.

3.1.3. Bean Weight and Fermentation Rate Behavior

ANOVA results for the Wi, Fi, and Di responses demonstrate the significance of the models. The F–values for Wi, Fi, and Di are 77.37, 31.60, and 9.59, respectively. These high F–values indicate the models' strong significance, with only a 0.01% probability that the observed F–values are due to noise alone. The A, B, and AB terms have a significant effect on the respective response variables (see Table S6 in the Supplemental Material).

The weight loss of cocoa beans during fermentation increased over time and stabilized between 96 and 168 h, with the highest rates observed as shown in Figure 8a. The 80 mT treatment showed the lowest Wi rates (Wi = 9%), with significant differences between the control (Wi = 16%) and the rest of the treatments (5 mT: Wi = 16%, 42 mT: Wi = 14%) (Figure 8a).

Cocoa beans' Fi increased until stable maximum values were reached between 120 and 168 h (Figure 8b). At the final fermentations, the highest Fi value was observed at 5 mT (Fi = 2.5%), with significant differences compared to the control and the rest of the treatments (42 mT: Fi = 2%, 80 mT: Fi = 1.8%). Conversely, the lowest Fi values were obtained at 80 mT (Fi = 1.5%) at 144 h, with the same statistically significant differences ($p < 0.05$) (Figure 8b).

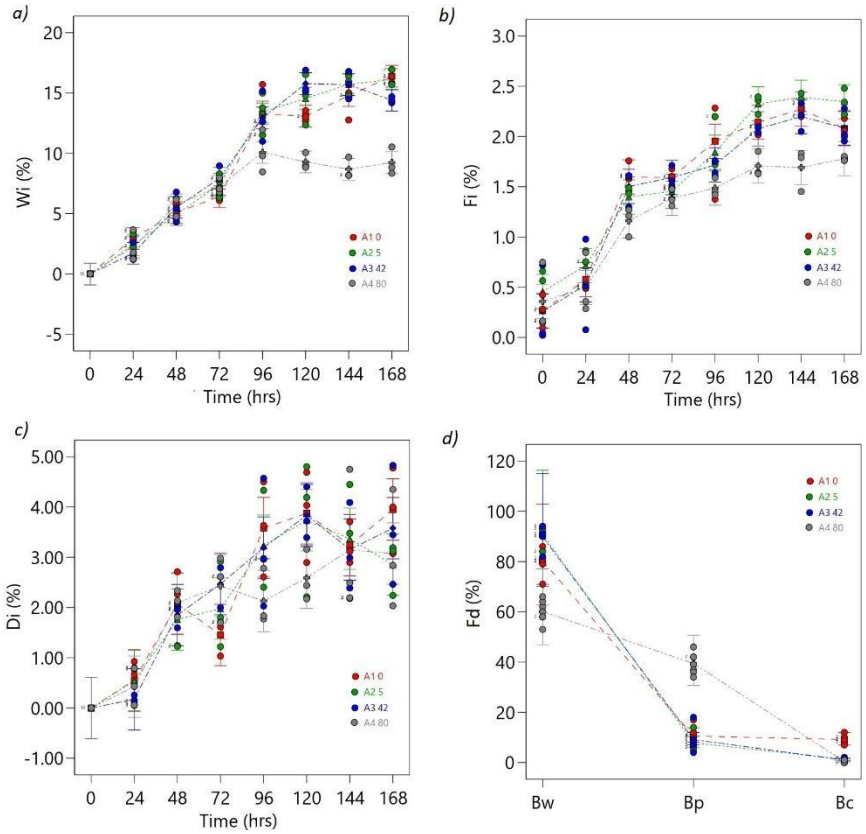

Figure 8. ANOVA interaction plots. Proportional responses: (a) Wi, (b) Fi, (c) Di, and (d) Fd. The ordinal factor, time, is displayed continuously, and the nominal OMF density factor (A) is presented discreetly as separate lines (A1: 0 mT red line, A2: 5 mT green line, A3: 40 mT blue line, A4: 80 mT gray line). The dots represent the values that the response variable takes around the mean; the midpoint of the bar represents the mean value; overlapping bar lines between levels indicate $p > 0.05$; no overlap of bar lines between levels indicates $p < 0.05$.

The deformation of cocoa beans increased over time and exhibited the highest standard deviation compared to other variables (Figure 8c). In the final stages of fermentation, the 42 mT treatment had the highest Di rates (Di = 4.83%), whereas the 80 mT treatment had the lowest (Di = 2.03%), with no significant difference ($p > 0.05$) observed between the control and the other treatments. At the end of fermentation, the values for the treatments and controls were nearly identical (Figure 8c).

The highest Bw rates (dependent on coloration) were observed at 5 mT (Fd = 94%), with the lowest rates recorded at 80 mT (Fd = 53%). These differences were significant ($p < 0.05$) compared to the control (Fd = 80%), as shown in Figure 8d. Furthermore, the highest rates of Bp were observed at 80 mT (Fd = 46%), with significant differences between the control (Fd = 10.5%) and the other treatments (5 mT: Fd = 4%, 45 mT: Fd = 7%) (Figure 8d). Additionally, the control treatment exhibited significantly ($p < 0.05$) higher rates of contaminated grains (Fd = 12%) compared to the other treatments (5 mT: Fd = 1%, 45 mT: Fd = 1%, 80 mT: Fd = 0%) at the end of fermentation (Figure 8d).

These results indicate that the OMF density treatments significantly affect weight loss (Wi) and fermentation index (Fi) as well as fermentation degree (Fd). However, there was no significant difference in the deformation index between the control and other treatments.

Camu et al. [25] documented that the weight loss experienced by cocoa beans during fermentation predominantly originates from the degradation of carbohydrates, proteins, and lipids. Weight loss increases rapidly during the first few days of fermentation, with a typical behavior of 5% to 15%, and then gradually levels off towards the end of the process. Another study by Hernandez–Hernandez et al. [55] reported that weight loss during cocoa fermentation is due to the loss of water and the breakdown of organic matter in the bean. These investigations corroborate the notion that weight loss is an important factor that affects the quality of cocoa beans during fermentation. Still, the exact rate of weight loss and duration of fermentation can depend on several factors, such as the type of cocoa beans, the fermentation method used, and environmental conditions [24,27–30]. Changes in the fermentation rate, color, texture, and flavor of the beans also accompany Wi [19–30].

Camu et al. [27] reported that the fermentation rate of cocoa beans varied depending on the type of microbial community present during fermentation. The authors found that the fermentation rate was higher in the presence of lactic acid bacteria than in the presence of yeasts or acetic acid bacteria. They also noted that the rate of temperature increase was slower in fermentations dominated by lactic acid bacteria, suggesting that these bacteria have a more moderate effect on the fermentation process. This finding is consistent with the idea that the microbial community plays an important role in the fermentation process of cocoa beans. Thus, the presence of lactic acid bacteria can affect the fermentation rate and the temperature increase during fermentation, which can ultimately affect the quality of the cocoa beans.

According to several authors [28–30], during the fermentation process of cocoa beans, the beans undergo deformations due to the rupture of the beans' cell walls and the release of water and sugars from the pulp. The gradual softening of the pulp and the reduction in the size of the bean is attributed to the activity of microorganisms and enzymes, which contribute to the production of flavor precursors and the development of the characteristic flavor of cocoa. Yeasts, acetic acid bacteria, and lactic acid bacteria stimulate enzymatic activity to hydrolyze sugars, organic acids, proteins, and polyphenols in cocoa beans, causing physical and chemical changes in the beans. These changes lead to the deformation of the beans during fermentation [54–57].

In the study conducted by Guéhi et al. [56], it was noted that cocoa subjected to a 4–day fermentation period exhibited a higher percentage of purple beans, reaching approximately 45%. Additionally, the presence of moldy beans was observed to be around 1%, while approximately 10% of the beans

showed signs of discoloration. The formation of brown beans increased from 16% to 50% depending on the fermentation duration and process. Several authors highlight the main changes that determine Fd and the final quality of cocoa that occurs during fermentation given the great number of factors that affect the process including microbial populations [24–30]. Other researchers also found that using a starter culture of LAB resulted in higher fermentation indices and darker bean colors than spontaneous fermentation, indicating that LAB may play an essential role in the fermentation process [24,25].

According to another study by Afoakwa et al. and Saputro et al. [26,55], the fermentation rate of cocoa beans is highest during the first 48 to 72 h. During this time, the temperature of the cocoa mass increases due to microbial activity, suggesting that the initial stages are characterized by a more intense fermentation process, which promotes the development of chocolate flavor. De Vuyst and Weckx as well as Guzmán–Alvarez et al. [28,56] highlighted the role of organic acids, specifically acetic acid and lactic acid, which are produced by microorganisms in the cocoa pulp, in the deformation of cocoa beans during fermentation. The researchers observed that this increase led to a decrease in the size of the beans and a color change, which were indicators of the degree of fermentation and the quality of the beans.

The behavior of Wi, Fi, Di, and Fi is also influenced by microbial activity; consequently, the effect of EMF in variation in these rates may also be conditioned by changes in the growth of microbial groups.

3.1.4. Microbial Group Behavior

The ANOVA models for LAB, AAB, and Y responses exhibit significance, as indicated by the respective F–values and the low probability of obtaining such values due to noise alone. The *p*–values for the model terms A, B, and AB being less than 0.0500 confirm their significance in all three models. These findings strengthen the reliability and validity of the models, indicating that they provide significant results for understanding the relationship between the factors and the observed responses (see Table S7 in the Supplemental Material).

In the control treatment, the concentration of lactic acid bacteria (LABs) reached its maximum point between 24 and 48 h, with values of 5.72 and 5.92 CFU/g, respectively, and decreased to a minimum value of 1.52 CFU/g towards the end of fermentation, corresponding to a reduction of 4.4 log cycle (Figure 9a). In the rest of the treatments, much lower LAB concentration values were obtained, with significant differences compared to the control ($p < 0.05$) (Figure 9a). The lowest LAB values were observed in the 80 mT treatment (1.05 CFU/g), while the highest values were observed in the 5 mT treatment (4.23 CFU/g) at 72 h, with significant differences between treatments ($p < 0.05$) (Figure

9a).

The maximum point of acetic acid bacteria (AAB) was observed in the 5 mT treatment between 96 (7.75 CFU/g) and 120 h (7.96 CFU/g), with significant differences compared to the control (5.69 CFU/g, 5.49 CFU/g) at the same time (Figure 9b). The lowest AAB values were observed in the 80 mT treatment at the final stages of fermentation (2.10 CFU/g), with significant differences compared to the control (4.33 CFU/g) and other treatments (5 mT: 4.35 CFU/g, 42 mT: 5.7 CFU/g) (Figure 9b). The most significant reduction in acetic acid concentration was observed in the 5 mT treatment, with a reduction of 3.4 log cycles (Figure 9b).

During the first 48 h of fermentation, the 5 and 42 mT treatments showed the highest Ys growth rates (7 CFU/g), with significant differences ($p < 0.05$) compared to the control and other treatments (Figure 9c). By the end of fermentation, the concentration of yeasts had reduced to 2.5 CFU log cycle, with the most significant reduction observed in the 80 mT treatment at 4.2 CFU log cycle reduction (Figure 9c).

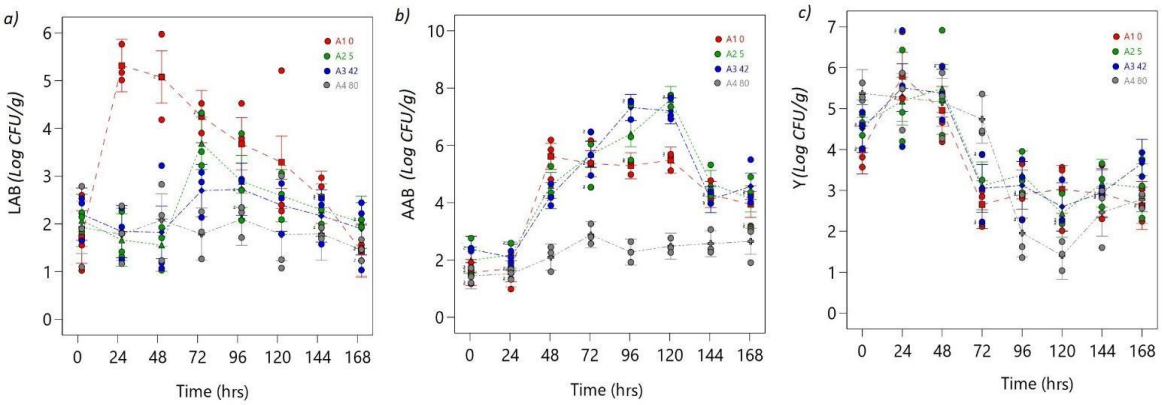

Figure 9. ANOVA interaction plots. Continuous responses: (a) LAB, (b) AAB, and (c) Y. The ordinal factor, time, is displayed continuously, and the nominal OMF density factor (A) is presented as separate lines (A1: 0 mT red line, A2: 5 mT green line, A3: 40 mT blue line, A4: 80 mT gray line). The dots represent the values that the response variable takes around the mean; the midpoint of the bar represents the mean value; overlapping bar lines between levels indicate $p > 0.05$; no overlap of bar lines between levels indicates $p < 0.05$.

The microbial population dynamics during cocoa bean fermentation are highly complex and involve the sequential activation of several microbial populations. Lasting for the first 24 to 36 h, yeasts are the dominant microorganisms, rapidly consuming the sugars in the pulp surrounding the cocoa beans and producing ethanol and carbon dioxide as byproducts. The ethanol produced by yeasts creates an acidic environment that favors the growth of LAB. LAB then dominates the fermentation process and produces lactic acid, which further lowers the pH and inhibits the growth of yeasts. As the fermentation progresses, AAB becomes more active and oxidizes the ethanol produced by yeasts to acetic acid. The acetic acid produced by AAB contributes to the development of the characteristic flavor and aroma of chocolate. However sequential activation of these microbial populations is

influenced by various factors, such as the type of cocoa bean variety, the fermentation conditions, and the presence of other microorganisms [24–28].

The results suggest that the application of magnetic fields during cocoa fermentation affects the growth and population dynamics of yeast, lactic acid bacteria, and acetic acid bacteria. The 5 mT and 42 mT treatments showed the highest yeast growth rates during the first 48 h.

Bubanja et al. [59] investigated the influence of low–frequency magnetic field regions on the respiration and growth of *Saccharomyces. cerevisiae.* The study found statistically significant differences in cumulative oxygen consumption, cumulative carbon dioxide production, and *S. cerevisiae* cell number, which were attributed to the MF–induced stimulation of microbial growth and activity. De Andrade et al. [5] conducted a study to investigate the effect of an extremely low–frequency (ELF) magnetic field on bioethanol productivity by *S. cerevisiae* in an unconventional bioreactor. The study found a 33% increase in bioethanol production, which was consistent with a stimulatory effect of the magnetic fields on plasma membrane H+–ATPase activity. The observed effects were attributed to the EMF–induced enhancement of enzyme activity and regulation of gene expression. Similar studies have shown that applying magnetic fields can positively impact microbial communities by increasing microbial growth, metabolic activity, diversity, and function, improving the efficiency of biotechnological processes such as anaerobic digestion, wastewater treatment, and constructed wetlands [4–7,18].

Zieliński et al. [60] reported increased the microbial diversity and degradation efficiency of organic matter in anaerobic digestion bacteria exposed to a magnetic field. Zaidi et al. [61] found that applying a magnetic field to wastewater treatment systems led to the removal of pollutants, while Ma et al. [62] reported that an external static magnetic field at 14 mT enhances the reduction of antibiotic–resistance genes during pig manure composting.

Hu et al. [63] investigated the impact of a static magnetic field on electron transport and microbial community shifts in the nitritation sequencing batch process. The study found that a static magnetic field can accelerate the start–up of the nitritation process and improve its performance by changing the microbial community structure and improving the HAO activity, the Cyt c content, and ETSA as well as the energy generation of microorganisms. Lyu et al. [64] reported that a magnetic field at 10 mT could increase the abundance and diversity of microbial communities, promoting the secretion of tryptophan and aromatic proteins.

On the other hand, Rakoczy et al. [65] conducted a study to investigate the effect of a ferrofluid and rotating magnetic field (RMF) on the growth rate and metabolic activity of a wine yeast strain. The study found that exposure to RMF resulted in a decrease in yeast cell numbers and inhibited their

metabolic activity. Bayraktar [66] also found that magnetic field treatment at 5 mT for 30 min inhibited the reproduction and enzymatic activity of *S. cerevisiae* [21]. Similarly, in this study, the EMF effect significantly reduced the LAB population in all treatments. Meanwhile, at 80 mT, the lowest growth rates of all the microbial groups compared were produced.

Other studies have demonstrated the ability of magnetic fields to enhance cocoa fermentation. Sudarti et al. [67] reported that exposure to magnetic fields significantly improved cocoa fermentation compared to the control group, as reflected in the reduction of pH and the increase in fermentable sugar content. Similarly, Guzman et al. [10] found that EMF improved the yield and quality of fermented cocoa beans. While there are differences in the methodology used in both studies compared to the other studies reviewed, the conclusive results indicate that electromagnetic fields have a profound impact on microbial metabolism.

Therefore, exposure to magnetic fields could alter the microbial dynamics in cocoa fermentation, which is reflected in a reduction of pH, an increase in the content of fermentable sugars, higher production of acetic acid and ethanol, and possibly better organoleptic characteristics of chocolate. The observed differences in microbial population dynamics suggest that magnetic fields can potentially be used as a tool to manipulate the fermentation process and improve the quality of cocoa products. Moreover, it is noteworthy that the optimal intensity, duration, and other parameters of the magnetic field may vary depending on the specific fermentation process and the microbe being used [58–61].

However, further studies are required to determine the optimal exposure parameters of magnetic fields and to evaluate the long–term effects on the quality of chocolate produced from cocoa beans fermented with magnetic fields. In this sense, the findings of this research suggest that under the conditions of this study, electromagnetic fields influenced microbial populations by inhibiting the growth of LAB and stimulating AAB and yeast, thereby causing a rebound effect in the analyzed process variables.

4. Conclusions

This study successfully developed a prototype to investigate the effects of electromagnetic emissions on bioprocesses, specifically the fermentation of cocoa beans. Magnetic flux density readings remained consistently stable at the center of the coils, demonstrating excellent linearity, reproducibility, and accuracy. These findings provided reliable evidence of the impact of electromagnetic fields on various parameters of the cocoa bean fermentation process.

The observed effects of the electromagnetic field on cocoa bean fermentation can be attributed to EMF–induced growth stimulation, microbial activity, and enzyme activity. However, more research

is needed to fully understand the underlying mechanisms responsible for these effects on cocoa bean microbial populations and their implications for the chocolate industry.

It is widely recognized that the sequential activation of different microbial populations is a critical feature of the fermentation process. Understanding these dynamics is essential to produce high–quality chocolate. Therefore, continuous research on the effects of electromagnetic fields on cocoa bean fermentation will contribute to advancing the knowledge and optimization of chocolate–production processes.

Supplementary Materials: The following supporting information can be downloaded at: www.mdpi.com/xxx/s1, Figure S2: Linearity graph; table S2: Experimental Design; table S3: The ANOVA of the OMF Density at different intensities (R1, R2, and R3); table S4: Confirmation. OMF Density (R1, R2, and R3) in three different working area coordinates; table S5: ANOVA models for Temperature, pH, Humidity, and Brix responses; table S6: The ANOVA for Wi, Fi, and Di responses; table S7: ANOVA models for LAB, AAB, and Y responses.

Authors' Contributions: The authors contributed as follows to this research project. Conceptualization, methodology, validation, and formal analysis; T.M.G.–A., resources, data curation, and writing—original draft, corresponding author; J.R., resources, investigation, supervision, and writing—review and editing; J.V.–C., review and editing; L.S.G., review and editing, visualization, and illustration. All authors have read and agreed to the published version of the manuscript.

Funding: This research received no external funding

Institutional Review Board Statement: Not applicable

Informed Consent Statement: Not applicable

Data Availability Statement: Data is contained within the article or supplementary material.

Acknowledgments: The authors thank Octavio Cordova for his technical support in the OMF device–validation process.

Conflicts of interest: The authors declare no conflict of interest.

References

1. Carbonell, M.V.; Flórez, M.; Martínez, E. & Álvarez, J. Aportaciones sobre el campo magnético: Historia e influencia en sistemas biológicos. *Intropica* **2017**, *12*, 143–159. https://doi.org/10.21676/23897864.2282

2. Lasso–Rivas, N. Efectos positivos del campo magnético en plantas cultivadas. *Intropica* **2019**, *14*, 160–170. https://doi.org/10.21676/23897864.3066

3. Qu, M.; Chen, J.; Huang, Q.; Chen, J.; Xu, Y.; Luo, J.; Wang, K.; Gao, W. & Zheng, Y. Bioremediation of hexavalent chromium contaminated soil by a bioleaching system with weak magnetic fields. *Int. Biodeterior. Biodegrad.* **2018**, *128*, 41–47. https://doi.org/10.1016/j.ibiod.2016.08.022

4. Lu, H.; Wang, X.; Hu, S.; Han, T.; He, S.; Zhang, G.; He, M. & Lin, X. Bioeffect of static magnetic field on photosynthetic bacteria: Evaluation of bioresources production and wastewater treatment efficiency. *Water Environ. Res.* **2020**, *92*, 1131–1141. https://doi.org/10.1002/wer.1308

5. Andrade, C.M.; Cogo, A.J.D.; Perez, V.H.; dos Santos, N.F.; Okorokova–Façanha, A.L.; Justo, O.R. & Façanha, A.R. Increases of bioethanol productivity by *S. cerevisiae* in unconventional bioreactor under ELF–magnetic field: New advances in the biophysical mechanism elucidation on yeasts. *Renew. Energy* **2021**, *169*, 836–842. https://doi.org/10.1016/j.renene.2021.01.074

6. Mansouri, A.; Abbes, C. & Landoulsi, A. Combined intervention of static magnetic field and growth rate of Microbacterium maritypicum CB7 for Benzo(a)Pyrene biodegradation. *Microb. Pathog.* **2017**, *113*, 40–44. https://doi.org/10.1016/j.micpath.2017.10.008

7. Tan, L.; Mu, G.; Shao, Y.; Ning, S. & Shi, S. Combined enhancement effects of static magnetic field (SMF) and a yeast Candida tropicalis SYF–1 on continuous treatment of Acid Red B by activated sludge under hypersaline conditions. *J. Chem. Technol. Biotechnol.* **2020**, *95*, 840–849. https://doi.org/10.1002/jctb.6274

8. Anaya, M.; Gámez–Espinosa, E.; Valdés, O.; Guzmán, T. & Borrego, S. Effect of the oscillating magnetic field on airborne fungal. *Arch. Microbiol.* **2021**, *203*, 2139–2145. https://doi.org/10.1007/s00203–021–02193–x

9. Leone, L.; Podda, M.V. & Grassi, C. Impact of electromagnetic fields on stem cells: Common mechanisms at the crossroad between adult neurogenesis and osteogenesis. *Front. Cell.*

Neurosci. **2015**, *9*, 228. Available online: https://www.frontiersin.org/articles/10.3389/fncel.2015.00228 (accessed on).

10. Guzmán–Armenteros, T.M.; Ramos–Guerrero, L.A.; Guerra, L.S.; Weckx, S. & Ruales, J. Optimization of cacao beans fermentation by native species and electromagnetic fields. *Heliyon* **2023**, *9*, e15065. https://doi.org/10.1016/j.heliyon.2023.e15065

11. Levitt, B.B.; Lai, H.C. & Manville, A.M. Effects of non–ionizing electromagnetic fields on flora and fauna, part 1. Rising ambient EMF levels in the environment. *Rev. Environ. Health* **2022**, *37*, 81–122. https://doi.org/10.1515/reveh–2021–0026

12. Miñano, H.L.; Silva, A.C.; Souto, S. & Costa, E.J. Magnetic Fields in Food Processing Perspectives, Applications and Action Models. *Processes* **2020**, *8*, 814. https://doi.org/10.3390/pr8070814

13. Ercan, I.; Tombuloglu, H.; Alqahtani, N.; Alotaibi, B.; Bamhrez, M.; Alshumrani, R.; Ozcelik, S. & Kayed, T.S. Magnetic field effects on the magnetic properties, germination, chlorophyll fluorescence, and nutrient content of barley *(Hordeum vulgare* L.). *Plant Physiol. Biochem.* **2022**, *170*, 36–48. https://doi.org/10.1016/j.plaphy.2021.11.033

14. El–Shafik El–Zawily, A.; Meleha, M.; El–Sawy, M.; El–Attar, E.–H.; Bayoumi, Y. & Alshaal, T. Application of magnetic field improves growth, yield and fruit quality of tomato irrigated alternatively by fresh and agricultural drainage water. *Ecotoxicol. Environ. Saf.* **2019**, *181*, 248–254. https://doi.org/10.1016/j.ecoenv.2019.06.018

15. Khokhlova, G.; Abashina, T.; Belova, N.; Panchelyuga, V.; Petrov, A.; Abreu, F. & Vainshtein, M. Effects of combined magnetic fields on bacteria Rhodospirillum rubrum VKM B–1621. *Bioelectromagnetics* **2018**, *39*, 485–490. https://doi.org/10.1002/bem.22130

16. Chen, L.; Ye, A.; Liu, X.; Lu, J.; Xie, Q.; Guo, Y. & Sun, W. Combined effect of co–exposure to di (2–ethylhexyl) phthalates and 50–Hz magnetic–fields on promoting human amniotic cells proliferation. *Ecotoxicol. Environ. Saf.* **2021**, *224*, 112704. https://doi.org/10.1016/j.ecoenv.2021.112704

17. Ben Yakir–Blumkin, M.; Loboda, Y.; Schächter, L. & Finberg, J.P.M. Static Magnetic Field Exposure In Vivo Enhances the Generation of New Doublecortin–expressing Cells in the Sub–ventricular Zone and Neocortex of Adult Rats. *Neuroscience* **2020**, *425*, 217–234. https://doi.org/10.1016/j.neuroscience.2019.11.005

18. Pophof, B.; Henschenmacher, B.; Kattnig, D.R.; Kuhne, J.; Vian, A. & Ziegelberger, G.

Biological Effects of Radiofrequency Electromagnetic Fields above 100 MHz on Fauna and Flora: Workshop Report. *Health Phys.* **2023**, *124*, 31–38. Available online: https://journals.lww.com/health–physics/Fulltext/2023/01000/Biological_Effects_of_Radiofrequency.5.aspx (accessed on 12 November 2022).

19. Cifra, M.; Apollonio, F.; Liberti, M.; García–Sánchez, T. & Mir, L.M. Possible molecular and cellular mechanisms at the basis of atmospheric electromagnetic field bioeffects. *Int. J. Biometeorol.* **2021**, *65*, 59–67. https://doi.org/10.1007/s00484–020–01885–1

20. Thomas–Fowlkes, B.; Cifelli, S.; Souza, S.; Visconti, R.; Struck, A.; Weinglass, A. & Wildey, M.J. Cell–Based In Vitro Assay Automation: Balancing Technology and Data Reproducibility/Predictability. *SLAS Technol. Transl. Life Sci. Innov.* **2020**, *25*, 276–285. https://doi.org/10.1177/2472630320902095

21. Grech, C.; Amodeo, M.; Beaumont, A.; Buzio, M.; Capua, V. Di; Giloteaux, D.; Sammut, N. & Wallbank, J.V. Error characterization and calibration of real–time magnetic field measurement systems. *Nucl. Instrum. Methods Phys. Res. Sect. A Accel. Spectrom. Detect. Assoc. Equip.* **2021**, *990*, 164979. https://doi.org/10.1016/j.nima.2020.164979

22. de Melo, C.F.; Araújo, R.L.; Ardjomand, L.M.; Ramos Quoirin, N.S.; Ikeda, M. & Costa, A.A. Calibration of low frequency magnetic field meters using a Helmholtz coil. *Measurement* **2009**, *42*, 1330–1334. https://doi.org/10.1016/j.measurement.2009.04.003

23. Hurtado–Velasco, R. & Gonzalez–Llorente, J. Simulation of the magnetic field generated by square shape Helmholtz coils. *Appl. Math. Model.* **2016**, *40*, 9835–9847. https://doi.org/10.1016/j.apm.2016.06.027

24. Crafack, M.; Keul, H.; Eskildsen, C.E.; Petersen, M.A.; Saerens, S.; Blennow, A.; Skovmand–Larsen, M.; Swiegers, J.H.; Petersen, G.B. & Heimdal, H. Impact of starter cultures and fermentation techniques on the volatile aroma and sensory profile of chocolate. *Food Res. Int.* **2014**, *63*, 306–316. https://doi.org/10.1016/j.foodres.2014.04.032

25. Camu, N.; De Winter, T.; Addo, S.K.; Takrama, J.S.; Bernaert, H. & De Vuyst, L. Fermentation of cocoa beans: Influence of microbial activities and polyphenol concentrations on the flavour of chocolate. *J. Sci. Food Agric.* **2008**, *88*, 2288–2297. https://doi.org/10.1002/jsfa.3349

26. Afoakwa, E.O..; Kongor, J.E..; Takrama, J.F. & Budu, A.S. Changes in acidification, sugars, and mineral composition of cocoa pulp during fermentation of pulp pre–conditioned cocoa

(*Theobroma cacao*) beans. *Int. Food Res. J.* **2013**, *20*, 1215–1222. Available online: www.worldcocoafoundation.org/wp–content/uploads/files_mf/1383600978Afoakwa2013PostHarvestFermentation.pdf (accessed on 12 November 2022).

27. Camu, N.; Tom, D.W.; Kristof, V.; Ilse, C.; Peter, V.; S., T.J.; Marc, V.; Luc, D.V. Dynamics and Biodiversity of Populations of Lactic Acid Bacteria and Acetic Acid Bacteria Involved in Spontaneous Heap Fermentation of Cocoa Beans in Ghana. *Appl. Environ. Microbiol.* **2007**, *73*, 1809–1824. https://doi.org/10.1128/AEM.02189–06.

28. De Vuyst, L. & Weckx, S. The cocoa bean fermentation process: From ecosystem analysis to starter culture development. *J. Appl. Microbiol.* **2016**, *121*, 5–17. https://doi.org/10.1111/jam.13045

29. Guerra, L.S.; Cevallos–Cevallos, J.M.; Weckx, S. & Ruales, J. Traditional Fermented Foods from Ecuador: A Review with a Focus on Microbial Diversity. *Foods* **2022**, *11*, 1854. https://doi.org/10.3390/foods11131854

30. Calvo, A.M.; Botina, B.L.; García, M.C.; Cardona, W.A.; Montenegro, A.C. & Criollo, J. Dynamics of cocoa fermentation and its effect on quality. *Sci. Rep.* **2021**, *11*, 16746. https://doi.org/10.1038/s41598–021–95703–2

31. Odu, G. O. Weighting methods for multi–criteria decision making technique. J. Appl. SCI. Environ. Manag. **2019**, 23, 1449–1457. https://doi.org/10.1080/15732479.2013.795978

32. Gonzalo, F.; Alonso, W.–G. & Quintana, R. The Magnetic Field Generated by Helmholtz Coils and their Applications to Probes Calibration. *Elektron* **2017**, *1*, 91–96. Available online: http://repositoriouba.sisbi.uba.ar/gsdl/cgi–bin/library.cgi?e=d–10000–00—off–0revis—00–2——0–10–0——0——0direct–10——4———0–1l—10–es–Zz–1——20–about——00–3–1–00–00—4——0–0–01–00–0utfZz–8–00&a=d&c=revis&cl=CL1.13&d=elektron–25_oai_oai (accessed on 10 December 2022).

33. Moosavi Nasab, S.D.; Beiranvand, A.; Tale Masouleh, M.; Bahrami, F. & Kalhor, A. Design and development of a multi–axis force sensor based on the hall effect with decouple structure. *Mechatronics* **2022**, *84*, 102766. https://doi.org/10.1016/j.mechatronics.2022.102766

34. Moosavi, S.M. & Ghassabian, S. *Linearity of Calibration Curves for Analytical Methods: A Review of Criteria for Assessment of Method Reliability*; Stauffer, M.T., Ed.; IntechOpen: Rijeka, Croatia, **2018**; Chapter 6. ISBN 978–1–78923–085–7

35. González, I. & Calderón, A.J. Integration of open source hardware Arduino platform in automation systems applied to Smart Grids/Micro–Grids. *Sustain. Energy Technol. Assessments* **2019**, *36*, 100557. https://doi.org/10.1016/j.seta.2019.100557

36. Galea, M.; Bolfarine, H. & Giménez, P. Hypothesis Testing in Functional Comparative Calibration Models. *Commun. Stat.–Theory Methods* **2006**, *35*, 2021–2033. https://doi.org/10.1080/03610920600761980

37. Audrey, D.A.D.; Stanley; Tabaraka, K.S.; Lazaro, A. & Budiharto, W. Monitoring Mung Bean's Growth using Arduino. *Procedia Comput. Sci.* **2021**, *179*, 352–360. https://doi.org/10.1016/j.procs.2021.01.016

38. Patil, A.; Bachute, M. & Kotecha, K. Identification and Classification of the Tea Samples by Using Sensory Mechanism and Arduino UNO. *Inventions* **2021**, *6*, 94. https://doi.org/10.3390/inventions6040094

39. Popa, A.; Hnatiuc, M.; Paun, M.; Geman, O.; Hemanth, D.J.; Dorcea, D.; Son, L.H. & Ghita, S. An Intelligent IoT–Based Food Quality Monitoring Approach Using Low–Cost Sensors. *Symmetry* **2019**, *11*, 374. https://doi.org/10.3390/sym11030374

40. Grégis, F. Assessing accuracy in measurement: The dilemma of safety versus precision in the adjustment of the fundamental physical constants. *Stud. Hist. Philos. Sci.* **2019**, *74*, 42–55. https://doi.org/10.1016/j.shpsa.2018.09.001

41. Kurashkin, S.; Rogova, D.; Tynchenko, V.; Petrenko, V. & Milov, A. Modeling of Product Heating at the Stage of Beam Input in the Process of Electron Beam Welding Using the COMSOL Multiphysics System. In Proceedings of the Software Engineering Perspectives in Intelligent Systems, Online, 14–17 October 2020; Silhavy, R., Silhavy, P., Prokopova, Z., Eds.; Springer International Publishing: Cham, Switzerland, 2020; pp. 905–912

42. Díaz–Muñoz, C.; Van de Voorde, D.; Comasio, A.; Verce, M.; Hernandez, C.E. Weckx, S. & De Vuyst, L. Curing of Cocoa Beans: Fine–Scale Monitoring of the Starter Cultures Applied and Metabolomics of the Fermentation and Drying Steps. *Front. Microbiol.* **2021**, *11*, 616875. Available online: https://www.frontiersin.org/articles/10.3389/fmicb.2020.616875 (accessed on 10 December 2022)

43. Orodoñez–Araque, R.H.; Landines–Vera, E.F.; Urresto–Villegas, J.C. & Caisedo–Jaramillo, C.F. Microorganisms during cocoa fermentation: Systematic review. *Foods Raw Mater*. **2020**, *8*, 155–162. https://doi.org/10.21603/2308–4057–2020–1–155–162

44. Aubain, Y.; N'Zi, C. & Kpalma, K. Cocoa Beans Fermentation Degree Assessment for Quality Control Using Machine Vision and Multiclass SVM Classifier. *Int. J. Innov. Appl. Stud.* **2018**, *24*, 1711–1717. https://hal.science/hal–01986522/ (accessed on 10 December 2022).

45. Sánchez, K.; Bacca, J.; Arévalo–Sánchez, L.; Arguello, H. & Castillo, S. Classification of Cocoa Beans Based on their Level of Fermentation using Spectral Information. *TecnoLógicas* **2021**, *24*, 172–188. https://doi.org/10.22430/22565337.1654

46. León–Roque, N.; Abderrahim, M.; Nuñez–Alejos, L.; Arribas, S.M. & Condezo–Hoyos, L. Prediction of fermentation index of cocoa beans (*Theobroma cacao* L.) based on color measurement and artificial neural networks. *Talanta* **2016**, *161*, 31–39. https://doi.org/10.1016/j.talanta.2016.08.022

47. *ISO 6887–1*; Microbiology of the Food Chain—Preparation of Test Samples, Initial Suspension and Decimal Dilutions for Microbiological Examination—Part 1: General Rules for the Preparation of the Initial Suspension and Decimal Dilutions. ISO: Geneva, Switzerland, **2017**. Available online: https://www.iso.org/standard/63335.html (accessed on 5 January 2023).

48. de Melo Pereira, G.V.; Magalhães, K.T.; de Almeida, E.G.; da Silva Coelho, I. & Schwan, R.F. Spontaneous cocoa bean fermentation carried out in a novel–design stainless steel tank: Influence on the dynamics of microbial populations and physical–chemical properties. *Int. J. Food Microbiol.* **2013**, *161*, 121–133. https://doi.org/10.1016/j.ijfoodmicro.2012.11.018.

49. Mulono, A.; Sutardi; Supriyanto & Harmayani, E. Study on effect of fermentation to the quality parameter of cocoa bean in Indonesia. *Asian J. Dairy Food Res.* **2016**, *35*, 160–163. https://doi.org/10.18805/ajdfr.v35i2.10724.

50. Afoakwa, E.O. Changes in Biochemical and Physico–chemical Qualities during Drying of Pulp Preconditioned and Fermented Cocoa (Theobroma cacao) Beans. *J. Nutr. Health Food Sci.* **2014**, *2*, 1–8. https://doi.org/10.15226/jnhfs.2014.00121

51. Herrera–Rocha, F.; Cala, M.P.; Aguirre Mejía, J.L.; Rodríguez–López, C.M.; Chica, M.J.; Olarte, H.H.; Fernández–Niño, M. & Gonzalez Barrios, A.F. Dissecting fine–flavor cocoa bean fermentation through metabolomics analysis to break down the current metabolic paradigm. *Sci. Rep.* **2021**, *11*, 21904. https://doi.org/10.1038/s41598–021–01427–8

52. Cortez, D.; Quispe–Sanchez, L.; Mestanza, M.; Oliva–Cruz, M.; Yoplac, I.; Torres, C. & Chavez, S.G. Changes in bioactive compounds during fermentation of cocoa (*Theobroma*

cacao) harvested in Amazonas–Peru. *Curr. Res. Food Sci.* **2023**, *6*, 100494. https://doi.org/10.1016/j.crfs.2023.100494

53. Velásquez–Reyes, D.; Rodríguez–Campos, J.; Avendaño–Arrazate, C.; Gschaedler, A.; Alcázar–Valle, M. & Lugo–Cervantes, E. Forastero and Criollo cocoa beans, differences on the profile of volatile and non–volatile compounds in the process from fermentation to liquor. *Heliyon* **2023**, *9*, e15129. https://doi.org/10.1016/j.heliyon.2023.e15129

54. Hernández, M. del P.L.; Núñez, J.C.; Gómez, M.S.H. & Tovar, M.D.L. Physicochemical and microbiological dynamics of the fermentation of the ccn51 cocoa material in three maturity stages. *Rev. Bras. Frutic.* **2019**, *41*, 1–13. https://doi.org/10.1590/0100–29452019010

55. Hernández– Hernández, C.; López–Andrade, P.A.; Ramírez–Guillermo, M.A.; Guerra Ramírez, D. & Caballero Pérez, J.F. Evaluation of different fermentation processes for use by small cocoa growers in mexico. *Food Sci. Nutr.* **2016**, *4*, 690–695. https://doi.org/10.1002/fsn3.333

56. Guéhi, T.S.; Dadie, A.; Koffi, K.; Dabonne, S.; Ban–Koffi, L.; Kedjebo, K. & Nemlin, G. Performance of different fermentation methods and the effect of their duration on the quality of raw cocoa beans. *Int. J. Food Sci. Technol.* **2010**, *45*, 2508–2514. https://doi.org/10.1111/j.1365–2621.2010.02424.x

57. Saputro, D.; Priambodo, D.; Pahlawan, M. & Masithoh, R. Classification of Cocoa Beans Based on Fermentation Level Using PLS–DA Combined with Visible Near–Infrared (VIS–NIR) Spectroscopy. In Proceedings of the 2nd International Conference on Smart and Innovative Agriculture (ICoSIA 2021), Yogyakarta, Indonesia, 3–4 November 2021; Atlantis Press: Amsterdam, The Netherlands, **2022**; pp. 100–106.

58. Guzmán–Alvarez, R.E. & Márquez–Ramos, J.G. *Fermentation of Cocoa Beans*; Laranjo, M., Ed.; IntechOpen: Rijeka, Croatia, **2021**; p. Chapter 7. ISBN 978–1–83968–817–1.

59. Bubanja, I.N.; Lončarević, B.; Lješević, M.; Beškoski, V.; Gojgić–Cvijović, G.; Velikić, Z. & Stanisavljev, D. The influence of low–frequency magnetic field regions on the *Saccharomyces. cerevisiae* respiration and growth. *Chem. Eng. Process. –Process Intensif.* **2019**, *143*, 107593. https://doi.org/10.1016/j.cep.2019.107593

60. Zieliński, M.; Dębowski, M. & Kazimierowicz, J. The Effect of Static Magnetic Field on Methanogenesis in the Anaerobic Digestion of Municipal Sewage Sludge. *Energies* **2021**, *14*, 590. https://doi.org/10.3390/en14030590

61. Zaidi, N.S.; Sohaili, J.; Muda, K. & Sillanpää, M. Magnetic Field Application and its Potential in Water and Wastewater Treatment Systems. *Sep. Purif. Rev.* **2014**, *43*, 206–240. https://doi.org/10.1080/15422119.2013.794148

62. Ma, S.; Liu, H.; Hou, J. & Zhang, J. External static magnetic field potentiates the reduction of antibiotic resistance genes during swine manure composting. *J. Hazard. Mater.* **2023**, *448*, 130882. https://doi.org/10.1016/j.jhazmat.2023.130882

63. Hu, B.; Leng, J.; Quan, J.; Zhang, K.; Wu, P.; Zhao, H.; Wan, C. & Zhao, J. Impact of static magnetic field on electron transport and microbial community shifts in the nitritation sequencing batch reactor. *J. Environ. Chem. Eng.* **2022**, *10*, 108774. https://doi.org/10.1016/j.jece.2022.108774

64. Lyu, W.; Song, Q.; Shi, J.; Wang, H.; Wang, B. & Hu, X. Weak magnetic field affected microbial communities and function in the A/O/A sequencing batch reactors for enhanced aerobic granulation. *Sep. Purif. Technol.* **2021**, *266*, 118537. https://doi.org/10.1016/j.seppur.2021.118537

65. Rakoczy, R.; Konopacki, M. & Fijałkowski, K. The influence of a ferrofluid in the presence of an external rotating magnetic field on the growth rate and cell metabolic activity of a wine yeast strain. *Biochem. Eng. J.* **2016**, *109*, 43–50. https://doi.org/10.1016/j.bej.2016.01.002

66. Bayraktar, V. Magnetic Field Efect on Yeast *Saccharomyces. cerevisiae* activity at Grape Must Fermetation. *Biotechnol. Acta* **2013**, *6*, 125–137. https://doi.org/10.15407/biotech6.01.125

67. Sudarti, S.; Yuli, H.; Sari, A.B.T.; Sumardi, S. & Wahyu, M. Fermentation Process of Dry Cocoa Beans through Extremely Low Frequency (ELF) Magnetic Field Exposure. *J. Penelit. Pendidik. IPA* **2022**, *8*, 584–591. https://doi.org/10.29303/jppipa.v8i2.1356

Suplementary material

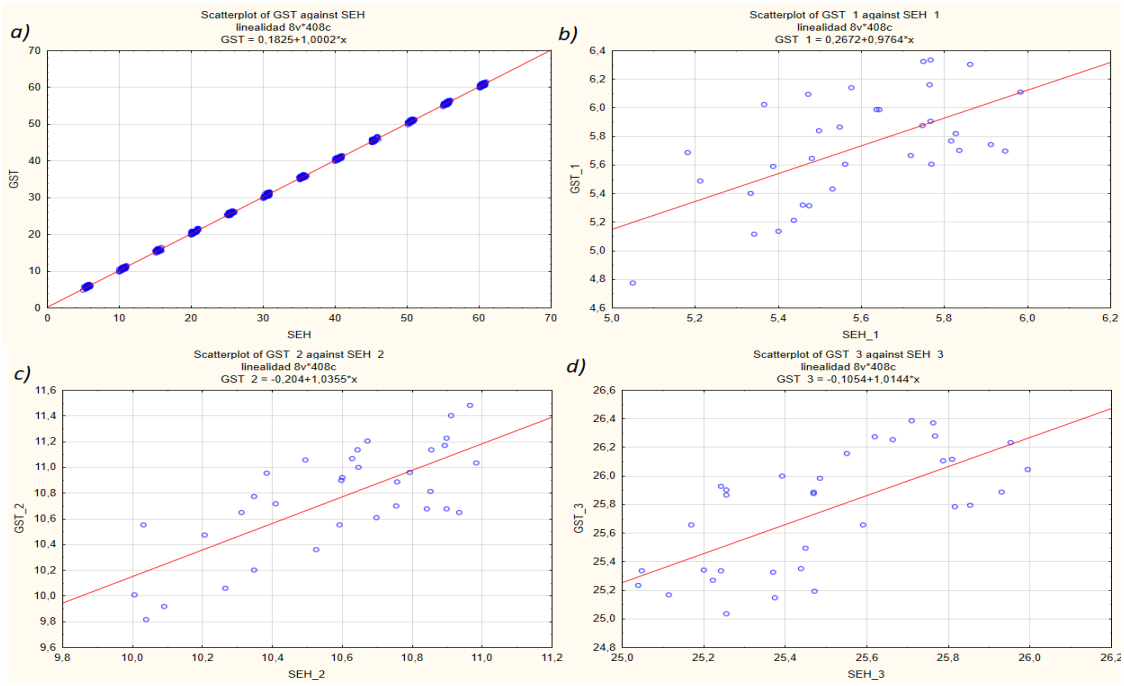

Figure S2 Linearity graph. Vertical axis GST horizontal axis SEH in different OMF density a) cloud of points (4–7mT), b) cloud of points (9–12mT), C) cloud of points (25–27mT)

Table S2. Experimental Design. Factors, levels, and Responses R1 OMF density (6A) levels: analyst1…analyst7; R2 OMF: density (30A) levels: day 1…day 7; R3: OMF density (90A) levels 20, 25, 30, 35, 40, 45, 50

Factor, levels responses	Units	Type	SubType	Minimum	Maximum	Coded Low	Coded High	Mean	Std. Dev.
Radial points ρ	m	Numeric	Continuous	–0.5045	0.5045	–1 ↔ –0.30	+1 ↔ 0.30	0.000	0.2776
Radial points α	m	Numeric	Continuous	–0.5045	0.5045	–1 ↔ –0.30	+1 ↔ 0.30	0.000	0.2776
Axial points Z	m	Numeric	Continuous	–0.1534	0.6034	–1 ↔ 0.00	+1 ↔ 0.45	0.225	0.2082
Levels	–	Categorical	Nominal	Level 1	Level 7	–	–	–	7.00
OMF density (6A)	mT	Numeric	Continuous	0.00078	5.97101	–	–	2.13	2.04
OMF density (30A)	mT	Numeric	Continuous	0.00531	29.9567	–	–	10.76	10.27
OMF density (90A)	mT	Numeric	Continuous	0.00342	89.6288	–	–	31.93	30.15

Table S3 The ANOVA of the OMF Density at different intensities (R1, R2, and R3). There are statistically significant differences in the radial coordinates of the prototype, with a confidence of 95.0%. In all responses, the model F value of the model was significant, and the lack of fit was not significant relative to the pure error. The equations in terms of the coded factors describe the decrease in density as a function of distance

	Model R1					***Model R2***					***Model R1***				
Source	***Sum of Squares***	***df***	***Mean Square***	***F–value***	***p–value***	***Sum of Squares***	***df***	***Mean Square***	***F–value***	***p–value***	***Sum of Squares***	***df***	***Mean Square***	***F–value***	***p–value***
Models	1372.72	33	41.60	537.71	< 0.0001	33856.14	69	490.67	87.63	< 0.0001	2.901E+05	33	8791.88	185.58	< 0.0001
a z	0.5379	1	0.5379	6.95	0.0088	–	–	–	–	–	–	–	–	–	–
p	–	–	–	–	–	–	–	–	–	–	164.67	1	164.67	3.54	164.67
z	–	–	–	–	–	–	–	–	–	–	361.02	1	361.02	7.75	0.0057
A^2	748.32	1	748.32	9673.23	< 0.0001	18180.51	1	18180.51	3246.92	< 0.0001	1.568E+05	1	1.568E+05	3310.49	< 0.0001
B^2	748.30	1	748.30	9672.92	< 0.0001	18826.21	1	18826.21	3362.24	< 0.0001	1.624E+05	1	1.624E+05	3428.70	< 0.0001
C^2	0.6263	1	0.6263	8.10	0.0047	36.53	1	36.53	6.52	0.0112	315.88	1	315.88	6.67	0.0103
Residual	23.36	302	0.0774			1489.42	266	5.60			14307.06	302	47.37		
Lack of Fit	4.04	71	0.0568	0.6795	0.9717	240.19	35	6.86	1.27	0.1547	3512.97	71	49.48	1.06	0.3696
Pure Error	19.33	231	0.0837			1249.22	231	5.41			10794.09	231	46.73		
Cor Total	1396.08	335				35345.56	335				3.044E+05	335			
Equations	R1=79.5189 + –2.5258 * A + 0.820197 * B + 16.313 * C + –315.474 * A^2 + –321.057 * B^2 + –25.1701 * C^2					R2=27.2235 + –0.0341274 * A + 0.419543 * B + 4.67432 * C + –107.411 * A^2 + –109.302 * B^2 + –8.55944 * C^2					R3=81.9151 + –0.757741 * A + 0.246059 * B + 1.12196 * C + –28.3927 * A^2 + –28.8951 * B^2 + –1.27424 * C^2				

Table S4. Confirmation. OMF Density (R1, R2, and R3) in three different working area coordinates. Confidence = 95%

Coord. Analysis (ρ, α, z)	Responses	Predicted Mean	Observed Mean	Std Dev	SE Pred	95% PI low	95% PI high
(0.0, 0.0, 0.27)	R1	5.602	5.457	0.278	0.119	5.367	5.83751
(–0.10,0.18,0.22)	R1	4.606	4.772	0.278	0.121	4.7728	4.84466
(–0.17,–0.14,0.40)	R1	4.454	4.454	0.278	0.124	4.2089	4.70074
(0.0, 0.0, 0.27)	R2	27.86	27.127	2.38	1.023	25.847	29.8753
(–0.17,–0.14,0.40)	R2	22.188	22.188	2.366	1.192	19.841	24.536
(–0.10,0.18,0.22)	R2	23.532	25.951	2.366	1.235	25.951	25.9652
(0.0, 0.0, 0.27)	R3	82.088	79.874	6.823	2.780	76.619	87.5577
(–0.10,0.18,0.22)	R3	69.239	75.027	6.882	2.999	75.027	75.1417
(–0.17,–0.14,0.40)	R3	66.580	66.580	6.882	3.092	60.495	72.6651

Table S5. ANOVA models for Temperature, pH, Humidity, and Brix responses. The models are significant as indicated by their respective F–values of 94.26, 41.34, 38.69, and 74.56. The probability of obtaining such large F–values due to noise is very low (0.01%).

Source	Sum of Squares	df	Mean Square	F–value	p–value	
Temperature model	6666.90	31	215.06	94.26	< 0.0001	significant
A–OMF density	817.54	3	272.51	119.45	< 0.0001	
B–Time	5542.19	7	791.74	347.03	< 0.0001	
AB	307.16	21	14.63	6.41	< 0.0001	
Pure Error	146.01	64	2.28			
Cor Total	6812.91	95				
pH model	18.09	31	0.5836	41.34	< 0.0001	significant
A–OMF density	1.91	3	0.6359	45.04	< 0.0001	
B–Time	14.92	7	2.13	151.00	< 0.0001	
AB	1.26	21	0.0600	4.25	< 0.0001	
Pure Error	0.9036	64	0.0141			
Cor Total	19.00	95				
Humidity model	1207.09	31	38.94	38.69	< 0.0001	significant
A–OMF density	131.32	3	43.77	43.50	< 0.0001	
B–Time	1010.94	7	144.42	143.50	< 0.0001	
AB	64.82	21	3.09	3.07	0.0003	
Pure Error	64.41	64	1.01			
Cor Total	1271.50	95				
Brix model	1315.86	31	42.45	74.56	< 0.0001	significant
A–OMF density	44.80	3	14.93	26.23	< 0.0001	
B–Time	1200.66	7	171.52	301.30	< 0.0001	
AB	70.40	21	3.35	5.89	< 0.0001	
Pure Error	36.43	64	0.5693			
Cor Total	1352.29	95				

The p–values less than 0.0500 for model terms A, B, and AB indicate that they are significant in all four models. Values greater than 0.1000 suggest that model terms are not significant, and their removal may improve the model if there are many insignificant terms.

Table S6. The ANOVA for Wi, Fi, and Di responses. The models for Wi, Fi, and Di are significant. The F–values for Wi, Fi, and Di are 77.37, 31.60, and 9.59, respectively, indicating that the models are highly significant with only a 0.01% chance that the observed F–values are due to noise.

Source	Sum of Squares	df	Mean Square	F–value	p–value	
Wi model	2911.40	31	93.92	77.37	< 0.0001	significant
A–OMF density	125.63	3	41.88	34.50	< 0.0001	
B–Time	2607.83	7	372.55	306.92	< 0.0001	
AB	177.95	21	8.47	6.98	< 0.0001	
Pure Error	77.68	64	1.21			
Cor Total	2989.09	95				
Fi model	42.77	31	1.38	31.60	< 0.0001	significant
A–OMF density	1.78	3	0.5937	13.60	< 0.0001	
B–Time	39.89	7	5.70	130.52	< 0.0001	
AB	1.09	21	0.0521	1.19	0.2870	
Pure Error	2.79	64	0.0437			
Cor Total	45.56	95				
Di model	166.54	31	5.37	9.59	< 0.0001	significant
A–OMF density	1.74	3	0.5803	1.04	0.3827	
B–Time	154.73	7	22.10	39.47	< 0.0001	
AB	10.06	21	0.4792	0.8557	0.6440	
Pure Error	35.84	64	0.5600			
Cor Total	202.38	95				

Source	χ^2	df	p–value
Fd model	3306.74	3	< 0.0001
A–Densidad CMO (mT)	58.69	3	< 0.0001
B–B	3020.86	2	< 0.0001
AB	401.81	6	< 0.0001

The p–values for the model terms A, B, and AB are less than 0.0500 for Wi and Fi, and B is significant for Di, indicating that these terms have a significant effect on the response variable. Poisson Regression (Type III) for Fd. The significant model terms A, B, and AB, with p–values less than 0.0500. Values greater than 0.1000 indicate that the model terms are not significant. The analysis used χ^2 Log Likelihood Ratio p–values. Analysis was performed with a log link and inverse link of exp, using Maximum Likelihood (ML) analysis

Table S7. ANOVA models for LAB, AAB, and Y responses. The models are significant, as indicated by their respective F–values of 6.49, 33.26, and 8.91. The probability of obtaining such large F–values due to noise is very low (0.01%).

Source	Sum of Squares	df	Mean Square	F–value	p–value	
LAB model	90.89	31	2.93	6.49	< 0.0001	significant
A–OMF density	32.91	3	10.97	24.27	< 0.0001	
B–Time	18.02	7	2.57	5.70	< 0.0001	
AB	39.96	21	1.90	4.21	< 0.0001	
Pure Error	28.92	64	0.4519			
Cor Total	119.81	95				
AAB model	320.89	31	10.35	33.26	< 0.0001	significant
A–OMF density	96.80	3	32.27	103.67	< 0.0001	
B–Time	176.00	7	25.14	80.78	< 0.0001	
AB	48.09	21	2.29	7.36	< 0.0001	
Pure Error	19.92	64	0.3112			
Cor Total	340.81	95				
Y model	141.92	31	4.58	8.91	< 0.0001	significant
A–OMF density	1.00	3	0.3346	0.6515	0.5849	
B–Time	119.81	7	17.12	33.32	< 0.0001	
AB	21.11	21	1.01	1.96	0.0211	
Pure Error	32.87	64	0.5136			
Cor Total	174.79	95				

The p–values less than 0.0500 for model terms A, B, and AB indicate that they are significant in all three models. ANOVA Y model terms B and AB are significant. Values greater than 0.1000 suggest that, the three models provide significant results

Chapter 3

Optimization of cacao beans fermentation by native species and electromagnetic fields

Tania María Guzmán–Armenteros[1*], Luis Alejandro Ramos–Guerrero[2], Luis Santiago Guerra[3], and Jenny Ruales[1]

[1]Departamento de Ciencia de Alimentos y Biotecnología (DECAB), Escuela Politécnica Nacional (EPN), Quito, Ecuador; tania.guzman@epn.edu.ec, jenny.ruales@epn.edu.ec

[2]Centro de Investigación de Alimentos, CIAL, Universidad UTE, EC170527 Quito, Ecuador; luis.ramos@ute.edu.ec

[3]Departamento de Patología, Facultad de Ciencias Médicas, Universidad Central del Ecuador (UCE), Capus El Dorado, Quito, Ecuador; lsguerrap@uce.edu.ec

*Corresponding author tania.guzman@epn.edu.ec

Abstract

Acid and bitter notes of the cocoa clone Cacao Castro Naranjal 51 (CCN–51) negatively affect the final quality of the chocolate. Thence, the fermentation process of cocoa beans using native species and electromagnetic fields (EMF) was carried out to evaluate the effect on the yield and quality of CCN–51 cocoa beans. The variables magnetic field density (D), exposure time (T), and inoculum concentration (IC) were optimized through response surface methodology to obtain two statistically validated second–order models, explaining 88.39% and 92.51% of the variability in the yield and quality of the beans, respectively. In the coordinate: 5 mT(D), 22.5 min (T), and 1.6% (CI), yield and bean quality improved to 110% and 120% above the control (without magnetic field). The metagenomic analysis strongly suggested that the changes in the microbial communities favored the aroma profile at low and intermediate field densities (5–42 mT) with high yields and floral, fruity, and nutty notes. Conversely, field densities (80 mT) were evaluated with low yields and undesirable notes of acidity and bitterness. The findings revealed that EMF effectively improves the yield and quality of CCN–51 cocoa beans with future applications in the development and quality of chocolate products.

Keywords: response surface, CCN51, cocoa fermentation, electromagnetic field, ANOVA

1. Introduction

The fact that various microbial species in different conditions and environments are susceptible to being influenced by electromagnetic fields (EMF) is a prominent issue in the scientific community today [1–3]. However, thermal and non–thermal effects can mainly cause these changes. The first is related to the production of heat by cells, and the second is cell growth [4, 5].

It has been seen that the non–thermal effects of the electromagnetic field (EMF) can affect not only microbial growth but also metabolism [6, 7]; however, it has also been shown on several occasions that the metabolic activity induced by EMF is linked to the activation of some areas of DNA [8]. Furthermore, some reports describe that EMF can change many processes in a microorganism, such as increasing antibiotic sensitivity and membrane transport [2, 9], changing morphology [10], biofilm formation [11], and reproduction [12]. These electromagnetic field effects have been found in distinct species of bacteria, both Gram–positive and Gram–negative [9, 13], and in yeast and filamentous fungi [5].

Although these effects cannot be explained totally, cells' response to EMF varies depending on the density, frequency, and exposure time [14]. In addition, it has also been seen that the first concentration of microorganisms and the characteristics of the culture medium are crucial factors that influence the cellular response to EMF [5].

Fermentation of cocoa beans goes through several stages where native microbial species are selected naturally, giving the chocolate its typical organoleptic characteristics [15]. As a result, each variety of cacao plants has distinctive characteristics from the others. The quality of cocoa depends on the first instance of the microbial species' interaction with beans during the fermentative process in that ecosystem [16]. Different microbial groups such as yeasts, lactic acid bacteria, and acetic bacteria that intervene in the fermentation of cocoa beans have been described, among which stand out genera Saccharomyces, Lactobacillus, and Acetobacter [15–17]. However, fermentative processes of the cocoa beans are developed under uncontrolled conditions that produce contamination and decrease the quality of the final product. These damages are irreversible and depend on the type and the growth of the MO naturally selected [18 – 20]. Thus, an effective controlled fermentative process and optimization of parameters like time, temperature, and inoculum concentration are essential.

The Cocoa Castro Naranjal 51 (CCN–51) is considered a cocoa with an intense chocolate flavor, widely productive, resistant, and adaptable to various environmental conditions, however, its acid and; however, have a negative impact on the aroma fine market [21]. Fine aroma studies have proposed several alternatives to improve its sensory profile and mitigate the negative impacts of these important effects on the cocoa market [22]. These alternatives include the control of the fermentative process [23], the introduction of grain pre–drying steps [24], and the use of starter microorganisms

during grain fermentation [25], among the rest [26]. However, research in this field is still in its infancy, and novel alternatives are required to redefine the flavor profile of CCN51. To study the changes induced by OMF in the fermentation process of CCN–51 cocoa beans and optimize this process, a 2^3 factorial design extended to a central composite design (CCD) was carried out to understand the fermentation performance and the quality of the bean of the variety of cocoa beans CCN–51, exposed to OMF of 5 to 80 mT, inoculum concentration of 1 to 2%, and exposure time of 15 to 30 min, in contrast to the non–exposed ones. The procedure was resolved by measuring the grains at the end of fermentation (6–7 days), to estimate the degree of fermentation resulting in each experimental run.

2. Materials and Methods

2.1. Electromagnetic fields (EMF) system

Helmholtz coils designed on a laboratory scale were used to generate the electromagnetic field as described by Hu [26]. This system consisted of two circular coils of 0.205 m in radius and connected in series, running with a variable voltage source at 60 Hz, generating a variable density magnetic field (of 1 to 120 mT). The samples were placed between both coils with a separation of 0.205 m during the magnetic field treatment. To control EMF, a sensor Hall–effect Tesla meter (SS49E) was connected in the middle of the coils. A specialized electronic board (Arduino nano) was used to convert this sensor–emitted signal to a digital signal in the computer [27]. The magnetic field was read in the interface of the Laboratory Virtual Instrument Engineering Workbench (LabVIEW) software version 9.0. (Figure 1).

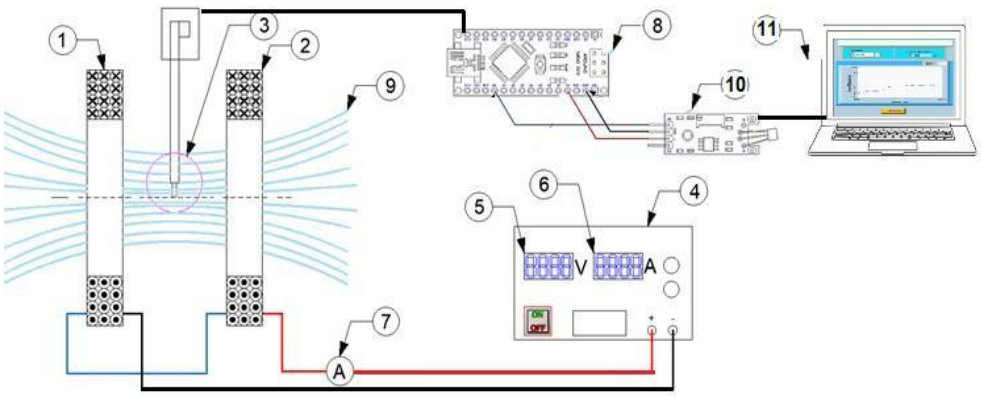

Figure 1. EMF system. (1) Coil 1 (2); Coil 2; (3) Magnetic sensor (Hall–effect Tesla meter); (4) Variable voltage source; (5) Voltage indicator; (6) Current Indicator; (7) Ammeter; (8) Arduino nano; (9) Magnetic field flux lines; (10) Sensor module; (11) PC.

2.2. Cocoa beans processing

2.2.1 Fermentation procedure

The cocoa pods were selected without any defects or damage caused by pests and with a uniform coloration (an indicator of the degree of maturity [28]. The pods obtained were duly packed in polyethylene bags, transported, and stored (7–12 °C) in a cold room until the test (no more than 32 hours). Each pod was adequately treated with sodium hypochlorite at 200 ppm in aseptic procedures for 5 minutes. Then 3 kg of cocoa beans were obtained for each treatment. The experimental units obtained consisted of 3 kg of cocoa beans of the CCN–51 variety ready to ferment. The beans were placed in the fermentation chamber for 168 h, where the temperature (37 °C ± 0.5) and the humidity (85% ± 0.8) of the system were controlled.

2.2.2 Drying and roasting the beans

After fermentation, the obtained beans were placed in different metal meshes, to avoid contact between replicates, inside rotary drying equipment at 60 °C for four hours until reaching a humidity of 10%. Later, in the same equipment, the temperature was raised to 120 °C for 30 minutes for the roasting process. The beans obtained from each experimental unit were sensory evaluated.

2.2.3 Preparation of the inoculum

The natural inoculum was obtained from cocoa pulp CCN–51 previously fermented at 37 °C for 18 hours. For this, the fermented grains were decanted, obtaining a homogeneous suspension of the pulp as inoculum [28 – 30]. This suspension was inoculated by spraying in the fermentation systems at 0.5–2.5% v/v [30]. The same inoculation procedure was performed for each experimental unit.

2.3. Evaluation procedure

2.3.1. Cutting test

The cut test allowed the identification and quantification of the grains. Initially, the fermentation index of each group (described below) was determined according to [31 – 33], and later the different fermentation and contamination rates were calculated. One hundred fermented cocoa beans were cut longitudinally to expose the inner surface of the cotyledon [28, 29, 33]. The beans were classified according to their degree of fermentation into well–fermented (brown or reddish–brown cotyledons, accompanied by well–open streaks), moderately fermented (partially striated cotyledons and purple

stripes on the edges), poorly fermented (cotyledons of intense violet color), and contaminated (cotyledon black or gray) unfermented bean highly damaged by insects and fungi [33 – 35].

2.3.2. Sensorial profile

The pre–dried and roasted cocoa beans were analyzed by a sensory panel composed of seven judges from the National Institute for Agricultural Research (INIAP) of Ecuador, trained in the sensory profile of cocoa. The appropriate protocols for protecting the rights and privacy of all judge's participants were utilized during the execution of the sensory analysis. Sensory attributes (cocoa, floral, fruity, nutty, sweet, bitter, astringent, green, color, odor, texture) were evaluated using a predetermined visual scale for sensory evaluation of cocoa [34, 36]. This scale presents ten measurable points for each attribute, from a minimum sensation of the attribute (1) to a maximum (10). Scores were compared to a reference cocoa bean derived from Ecuadorian cocoa beans [21]. In each sample, three measurements of each attribute were made; according to the criteria evaluated by the panel, the instrument's reliability was measured using Cronbach's alpha coefficient ($\alpha = 0.879$) [37].

2.3.3 Metagenomic analysis

Samples were taken for metagenomic analysis in each experimental run to distinguish the predominant microbial genera during the first 18 hours of fermentation.

2.3.3.1 Cocoa beans sample preparation and DNA extraction

The cocoa beans collected at 18 hours were resuspended in 10 mL of saline solution and vortexed with an average speed of 30 seconds. Subsequently, the almonds were removed, and the obtained solution was centrifuged at 6000 rpm. Next, the obtained pellet was resuspended in 2 mL of 1.5M sorbitol buffer, and this procedure was performed twice. In the last step, the obtained pellet was frozen for 1 hour to later proceed with the DNA extraction protocol [38].

The DNA extraction process began with the cell lysis of the microbial communities. Then, it was carried out using the same extraction protocol used by Florac De Bruyn 2015 [39] for coffee seeds, with some modifications in the proportions of chloroform: phenol: alcohol. Isoamyl (49.5: 49.5: 1) is used to remove proteins. During DNA extraction, the QIAamp genomic DNA Kits were also produced with some modifications and using a DNA affinity column with two ultracentrifugation steps. Finally, for each sample, the concentration and quality of the DNA extraction were measured by spectrophotometry (NanoDrop 2000, brand Thermo Fischer Scientific) [40].

2.3.3.2 Amplification and sequencing of microbial communities

The DNA obtained from the microbial communities was amplified by PCR with specific primers of the 16s rDNA region for the V4 sections in F515 (5'–GTGCCAGCMGCCGCGGTAA–3') and R806 (5'–GGACTACVSGGGTATCTAAT–3') for bacteria [39]. The primers BITS (5'—ACCTGCGGARGGATCA–3') and B58S3(5'– GAGATCCRTTGYTRAAAGTT–3') were also used for the ITS region of fungi and yeasts. PCR products were run on agarose gel under standard conditions. PCR products retained on the gel were cleaned using the Kit Wizard SV gel and PCR cleanup System (Promega) [41]. Sizing of sequences (genomic libraries) was performed using Agencourt AMPure XP PCR for magnetic bead purification (Beckman Coulter). Once purified PCR products >100 bp, DNA concentration, and quality were measured by fluorescence (Qubit 2.0; Thermo Fisher Scientific). The amplified DNA sequences of the microbial communities were sequenced by synthesis using the Illumina MiSeq platform (Illumina, San Diego, California, USA) through the VUB–ULB (Brussels, Belgium) inter–university agreement. Results were obtained in FASTQ format for analysis with bioinformatics tools [40, 42].

2.3.3.3 Sequence analysis and taxonomic assignment

The sequences obtained from the NGS were subjected to quality cleaning with the DADA2 package version 1.6 [32, 33] and performing order and alignment of the sequences for analysis with R language, version 3.6. 3. The sequences obtained by Ilumina for bacteria were compared with the SILVA 16s rRNA databases (HTTP: // www.Arb–silva.de; version 128). For the sequences amplified with the BITS primer (due to their length), less demanding quality filtering was performed, and these unique sequences were taxonomically classified with the UNITE database (http://www.unite.ut.ee; version 8, sh 99) [43, 44]. The relative abundance of metagenomic sequences of the different genera obtained was used to calculate the rates in the groups (LDR, IDR, and HDR) and to determine the Shannon diversity index (H).

2.3.3.4 Biodiversity analysis

A phyloseq object was used to analyze biodiversity, comprising the following files: taxonomic assignment, sequence counter, and test characteristics. The sequences were then grouped by operational taxonomic units (OTU) based on a genus. Next, it was filtered according to a 1E–05 mean read count threshold. Subsequently, the sequencing depth was determined; from this point, found the alpha diversity [45].

2.4. Variable selections

2.4.1. Fermentation yields

Three variables of the fermentation process (Y1, Y2, and Y3) were determined to relate the rates between those exposed and the controls: The total fermentation yield (Equation 1), the best fermentation yield (Equation 2), and the contamination rate (Equation 3). Barrel's criteria (rate greater than or equal to 60%) was used to decide the best rate of fermentation quality [46].

$$Y1 = \frac{(\mathrm{v3} - \mathrm{v4}) * \mathrm{wt}}{(\mathrm{w3} - \mathrm{w4}) * \mathrm{vt}} \times 100 \quad (1)$$

$$Y2 = \frac{(\mathrm{v1}) * \mathrm{wt}}{(\mathrm{w1}) * \mathrm{vt}} \times 100 \quad (2)$$

$$Y3 = \frac{(\mathrm{v4}) * \mathrm{wt}}{(\mathrm{w4}) * \mathrm{vt}} \times 100 \quad (3)$$

Where:

v1 mean values of well–fermented beans exposed

v2 mean values of moderate fermented beans exposed

v3 mean values of fermented beans exposed

v4 mean values of contaminated beans exposed

vt total beans exposed

w1 mean values of well–fermented beans controls

w2 mean values of moderate fermented beans controls

w3 mean values of fermented beans controls

w4 mean values of contaminated beans controls

wt total beans controls

2.4.2. Roasted bean quality

The variable quality of roasted beans (Equation 4) was obtained from the mean of the mean values of each attribute obtained in the sensory test, according to the following formula:

$$Y4 = \frac{(\mathrm{m1} + \mathrm{m2} + \mathrm{m3})}{(\mathrm{n1} + \mathrm{n2} + \mathrm{n3})} \times 100 \quad (4)$$

Where:

m1– mean values of color exposed

m2– mean values of texture exposed

m3– mean values of odor exposed

n1– mean values of color controls

n2– mean values of texture controls

n3– mean values of odor controls

2.5. Statistical procedures for the optimization process

Optimization procedures were performed using experimental design (DOE) in the Design Expert v 13 software (Stat–Ease). A Face–Centered Cube (α = 1) Central Composite Design (CCCFCD) was carried out (Table 1). Consisted of six center points (0, 0) (for lack–of–fit (LoF) test), 18 axial (– 1; + 1) points, and 27 factorial (− 1; + 1) points, making a total of 47 experimental runs performed in random order (Table 1). In the experimental design, three groups are distinguished depending on the density of the magnetic field: LMD (Low Magnetic Density), IMD (Intermediate Magnetic Density Runs), HMD (High Magnetic Density Runs), and three groups are distinguished depending on the starter culture concentration LIC (Low Inoculum Concentration), IIC (Intermediate Inoculum Concentration) and HIC (High Inoculum Concentration Runs).

2.5.1. Experimental limits

Factors and corresponding levels were selected to find which of them and their interactions can significantly affect the fermentation process of cocoa beans CCN51 and how they do it. The MEF density (5–80 mT), time (15–60 min), and inoculum concentration (1–1.5 % v/v) were the limit selected for the design. The established levels of the factors density and time of the MEF were as far

apart as possible to generate a significant difference in the response (Δy); for that, it was proved as a strategy to analyze the entire experimental region delimited by the maximum and minimum range of the electromagnetic device where stable MFE emissions were obtained over time [47]. In the case of inoculum concentration, the percentage ranges (v/v), which do not cause excessive humidity (by exudations) in the fermentation system, were selected [20].

2.5.2. Model fit

Since the responses are proportions that express quantities, second–order polynomial functions were used to fit them. In this sense, the data were also normalized using square root transformations to stabilize the variance and achieve a reasonable and satisfactory fit. [47]. In each case, the adjustment of each Model was verified by the statistical analysis of variance, and it was reduced, neglecting the terms that were not significant ($p < 0.05$). Likewise, each Model tried to find an adequate approximation of the functional relationship between the response variables and factors [48].

2.5.3. Optimization approach

A multi–response optimization approach was carried out to maximize the process variables, using the desirability function provided by the Design Expert optimizer, which is an integral mathematical protocol [47, 48]. In these conditions, a maximum desirability of 70% was obtained in the following factorial coordinate: A, B, C = 5, 22.5, 1.6., The models obtained were evaluated employing experimental replicates in this coordinate to see the agreement between each response's calculated and experimental values (Figure S1) [48]. The theoretical and practical results obtained (Table S2) show an agreement in the observed data mean and calculated predicted mean values, for both responses (Y2 and Y4), with a 95% confidence, which ratifies this Model can be used to navigate in the design space (Table S2).

Table 1. Matrix of actual and coded factors of the CCCFCD. Responses values of the 2^3 factorial design extended to face–centered cube central composite design: fermentative yield (Y2) and bean quality (Y4); three repetitions, 48 experimental runs.

			Actual and coded factors			Responses values					
			A:MEF density	B:Exposure time	C:Inoculum concentration						
		Runs	(mT)	(min)	%(v/v)	$Y2_1$	$Y2_1$	$Y2_1$	$Y4_1$	$Y4_1$	$Y4_1$
ffactorialpoints	LDR	F1	5(–1)	15(–1)	0.5(–1)	87.94	80.43	79.58	111.27	101.07	113.23
		F2	5(–1)	30(+1)	0.5(–1)	92.46	91.84	91.13	101.62	110.38	106.25
		F3	5(–1)	15(–1)	2.5(+1)	95.66	93.02	88.66	102.25	97.62	92.29
		F4	5(–1)	30(+1)	2.5(+1)	100.21	112.01	107.25	67.86	62.45	65.25
	HDR	F5	80(+1)	15(–1)	0,5(–1)	77.49	82.06	89.65	60.61	67.71	60.10
		F6	80(+1)	30(+1)	0.5(–1)	80.93	76.45	80.78	69.26	59.26	60.92
		F7	80(+1)	15(–1)	2.5(+1)	80.92	76.92	82.96	58.20	48.40	50.05
		F8	80(+1)	30(+1)	2.5(+1)	78.12	72.44	70.56	60.86	57.70	51.31
central point		F9*	42.5*(0)	22.5*(0)	1.5*(0)	112.47	109.40	113.43	88.47	83.34	89.49
axial points	IDR	A10	5(–1)	22.5(0)	1.5(0)	120.82	120.70	115.01	105.75	10.62	109.13
		A11	80(+1)	22.5(0)	1.5(0)	104.05	10.26	102.15	54.27	67.96	69.53
		A12	42.5(0)	22.5(0)	2.5(+1)	125.46	120.59	117.04	67.86	62.45	65.25
		A13	42.5(0)	22.5(0)	0.5(–1)	117.12	114.48	115.59	79.86	68.80	77.07
		A14	42.5(0)	30(+1)	1.5(0)	122.18	116.16	124.53	59.10	75.14	62.80
		A15	42.5(0)	15(–1)	1.5(0)	119.16	119.78	116.41	57.36	65.44	79.35
		A16	42.5*(0)	22.5*(0)	1.5*(0)	118.69	124.37	122.05	79.62	78.15	75.71

Replicas (3). runs (48). blocks (2). center points* (6). factorial points (24). and axial points (18). F: factorial points. A: axial points

2.5.4. Design output

The F–values of the Y1 and Y3 model responses were insignificant compared to the noise, and significant terms were not found in the model for these responses. However, the quadratic regression model for fermentative yield (Y2) and bean quality (Y4) were significant ($p < 0.05$) with F–values of 44.79; and 97.10, respectively. Consequently, with a probability of more than 99.99% confidence, it is clear that the studied factors influence the yield and quality of beans [48] (Table S2).

For Y2–response, A, B, C, AB, AC, A^2, B^2, and C^2 are significant model terms. For Y4 responses: A, C, A^2, B^2, and C^2 are significant model terms ($p < 0.05$). The lack of fit F–value in both models is not significant ($p > 0.05$) compared to the pure error, which suggested that in the study region, both models adequately explain the response variations [44, 48] (Table S2).

The Predicted R^2 of 0.84 for Y2 is in reasonable agreement with the adjusted R^2 of 0.88. The same occurs for Y4: Predicted R^2 of 0.90 is in reasonable agreement with the Adjusted R^2 of 0.92. [48]. The coefficients of variation obtained for each response written down (Y2: CV = 3.51 and Y4: CV = 6.82) proved the reliability of the experiments performed. The residual diagnosis reveals no statistical problems [47, 48] (Figure S1).

2.4. Principal Component Analysis (PCA)

To analyze the sensory attributes most affected by the magnetic field, a PCA was performed for each DOE treatment (individuals). The results of the data matrix were processed using the R (version 4.1.3) programming language environment with the help of the Bioconductor packages (version 3.14). In the PCA, the multidimensional data of the quality attributes of the previously standardized cocoa beans (x=0; SD=1) were projected to a reduced dimensional space of n variables [22, 23]. The PC chosen were those with a maximum variance, and the values of each biplot (score) were obtained from a linear combination of the reduced variables [23]. Correlations were also made between other variables to interpret obtained data better.

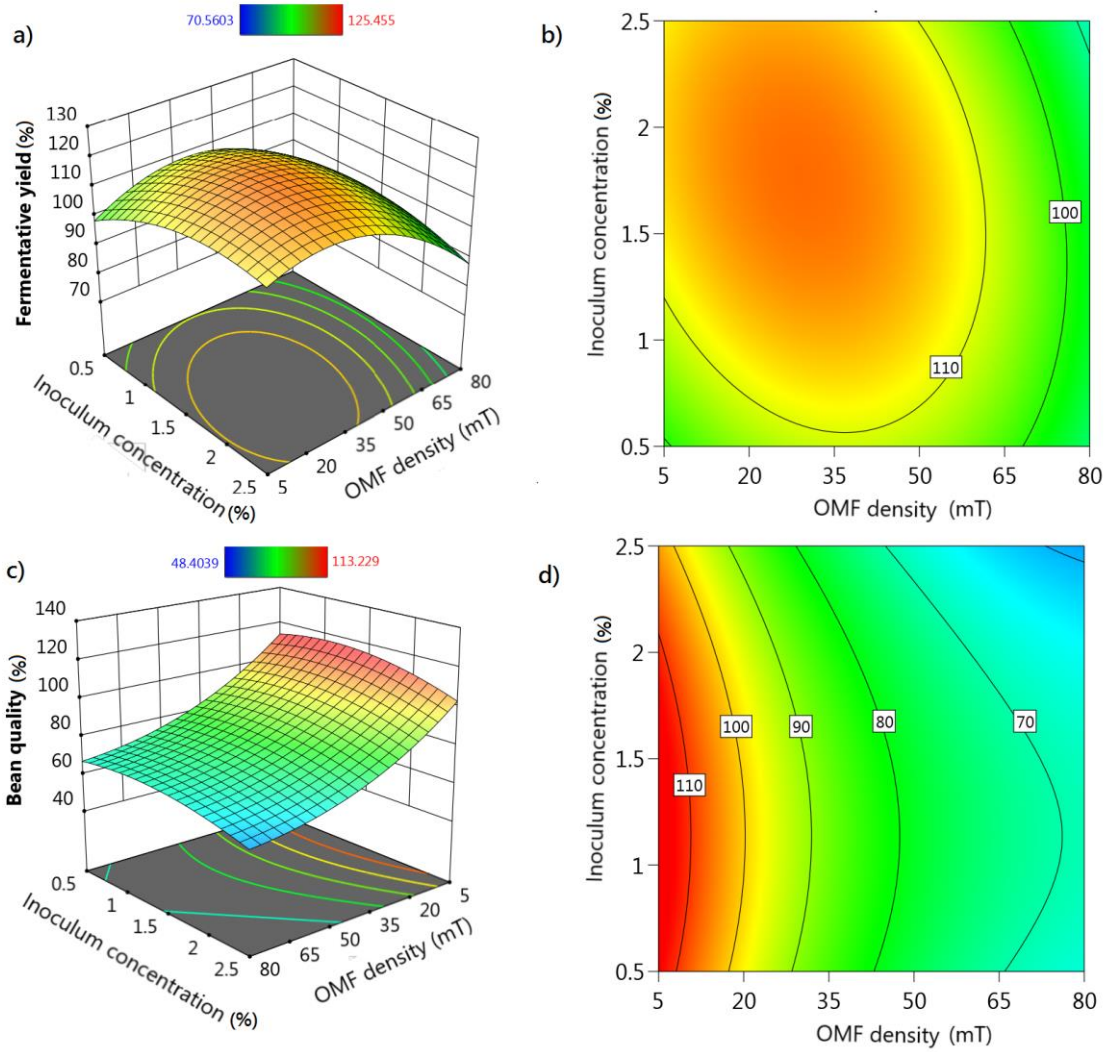

Figure 2. Response–surface (RS) and contour graphs (CG). (a. d) RS: vertical axes: fermentative yield (a) and bean quality(d), horizontal axes: OMF density and Inoculum concentration; (b. d) CG: vertical axes: Inoculum concentrations, horizontal axes: OMF density, contour line: fermentative yield (b) and bean quality (d); Exposure time supported at best levels

3. Results

3.1. SRM results

Response–surface and contour graphs (Figure 2 a, b, c, d) show two curves that obey the quadratic terms of two second–order polynomial equations (1, 2). Polynomial equations reveal that whether the inoculum concentration or exposure time is high or low, the yield (Y2) and quality (Y4) are consistently lower with increasing field density (A). This implies a strong negative effect of OMF on both factors, time and inoculum concentration (C and B).

Consequently, plots show that an increase in OMF density causes a substantial decrease in fermentation yield (Figure 2 a, b) and grain quality (Figure 2 a, c). Conversely, a reduction in OMF density to values close to 5 mT causes an increase in both responses and the ratio between exposed and controls (closer contour lines) (Figure 2 b, d).

The effect of culture concentration and exposure time depends on OMF density values, and better grain quality can be obtained with lower OMF density values (Figure 2 a, b, c, d). In the coordinate: 5 mT(A), 22.5 min (B), and 1.6% (C), yield and bean quality improved to 110% and 120% above the control. However, the graph indicates that at densities below 5 mT, optimum grain quality values could be reached.

$$\text{Sqrt(Y2)} = 10.8528 - 0.370432A + 0.0733862B + 0.102468C - 0.221457AB - 0.21719AC - 0.641664A^2 - 0.270573B^2 - 0.331708C^2 \quad (1)$$

$$\text{Sqrt(Y4)} = 9.04851 - 1.23934A + 0.0241599B - 0.256541C + 0.46818A^2 - 0.581385B^2 - 0.3519C^2 \quad (2)$$

3.2. PCA results

Two principal components (PC1 and PC2) explained 77% and 10% of the total variance of the data set, respectively, where two groups separated by the central axis were distinguished (Figure 3 a). The notes with the highest floral, fruity, and nutty scores perceived by the judges were found in group A, associated with the LDR and IDR. On the contrary, the highest scores in astringency, acidity, green, and bitterness were found in group B, corresponding to HDR (opposite vectors in the biplot graph showing a negative correlation) (Figure 3 a).

In the radial graph (Figure 3 c, d), two sensory profiles are also distinguished and associated with PCA results. LDR and IDR (Figure 3 b) corresponded with group A (Figure 3 a), and HDR (Figure

3 c) corresponded with group B. In summary, the judges perceived a greater intensity of aroma, flavor, and better texture of the bean in LDR and IDR, having a more favorable effect on the quality of the roasted bean (fine flavors) than the HDR scores (unpleasant flavors). This result corresponds with the polynomial equations obtained in DOE, where an increase in field density decreases yield and grain quality while a decrease has the opposite effect.

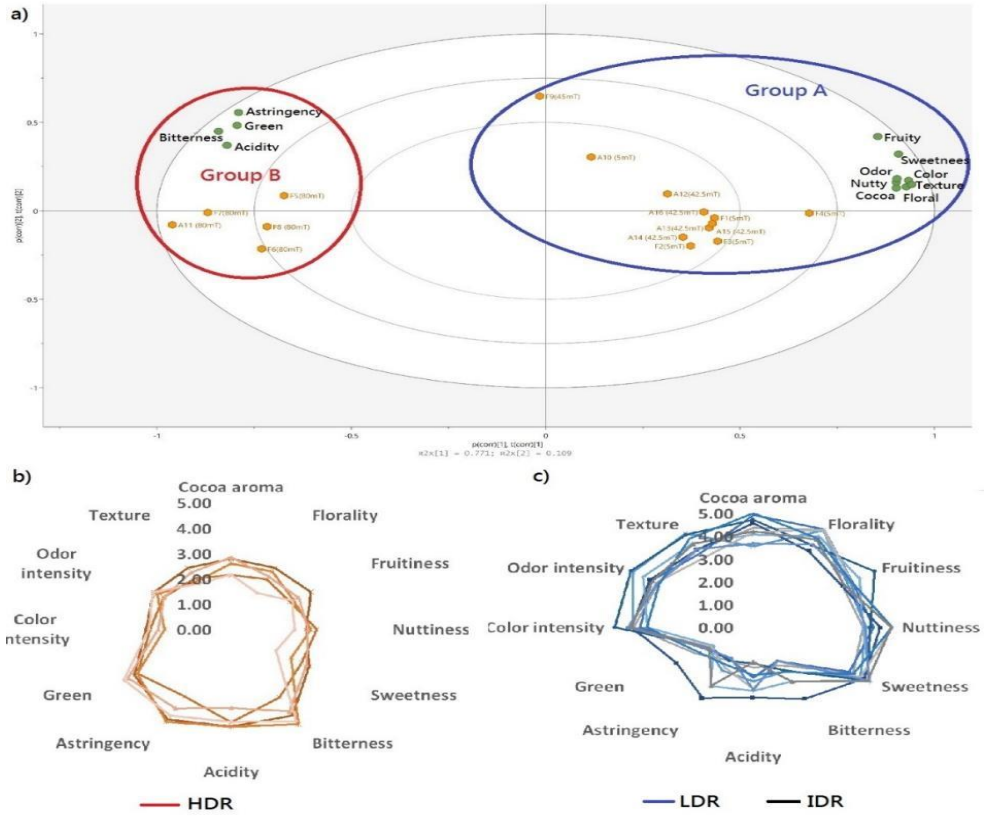

Figure 3. Biplot PCA: a) 2D view (group A: LDR and IDR, group B HDR); Spider plot: b) LDR and IDR scores, c) HDR scores

3.3 Correlations results

In the correlation graph between microbial genera and sensory quality attributes (Figure 4), the following positive correlations stand out: Weisella, Frauteria, and Pichia with flavors cocoa and fruity, Luteibacter with flavors cocoa and floral, Gluconobacter and Luteibacter with cocoa and floral (blue ovals). On the other hand, the negative correlations of the genera Acetobacter, Bacillus, Klebsiella, Isatechia, and Mucor are also remarkable, with the sensory attributes: of florality, fruitiness, nuttiness, and cocoa (red ovals) (Figure 4).

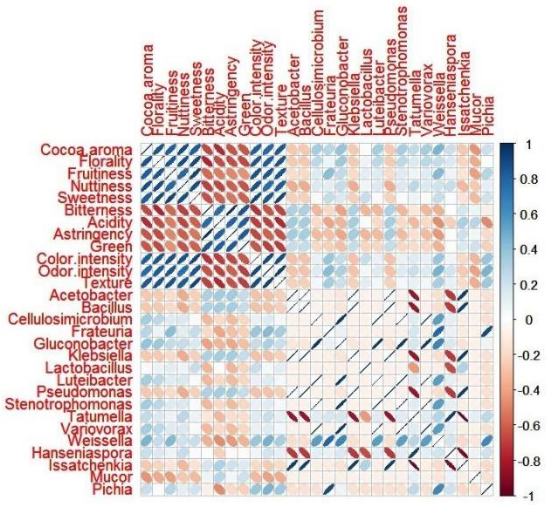

Figure 4. Correlation graph between microbial genera and quality attributes: blue ovals: positive correlation; red ovals: negative correlation; darker ovals: higher correlation

3.4. Metagenomic results

After 24 hours of fermentation, five yeast genera and 13 bacterial genera were identified in the different groups (Figure 5 a, b, c). The highest RAR of these metagenomic sequences corresponded to LDR (39.8%), followed by IDR (32.09%), and finally, HDR (28.03%) (Figure 5 d). Microbial genus greater diversity could also be noted in LDR and IDR.

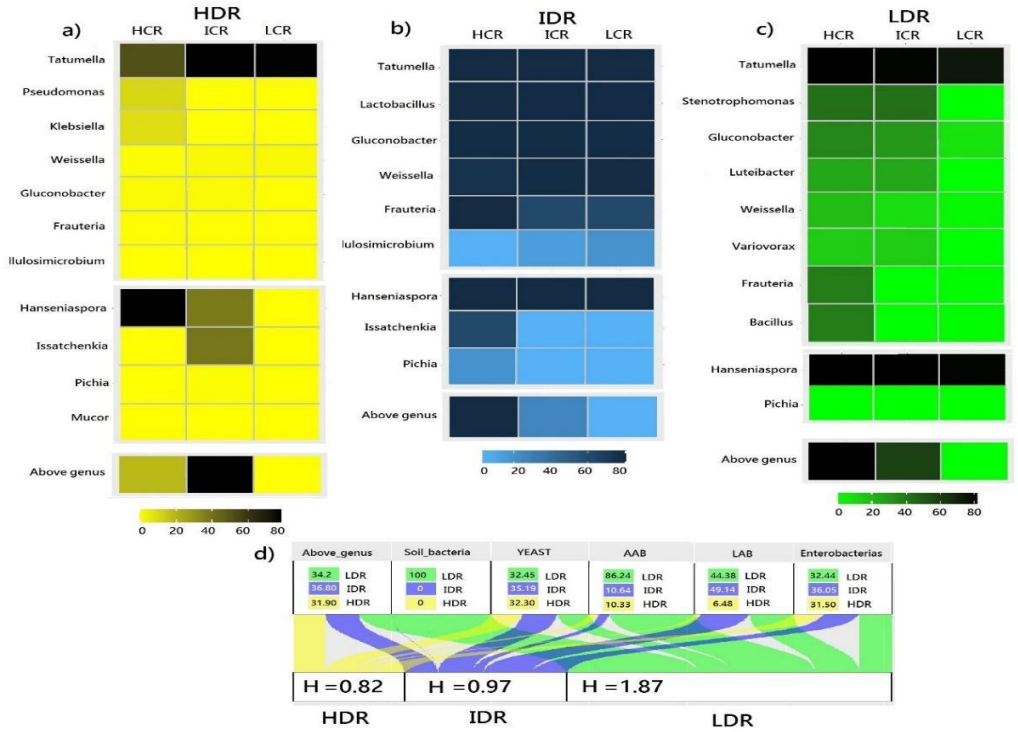

Figure 5. Heatmap of microbial genera by groups. a) Metagenomic sequences of the HDL group: light yellow color represents low RA. a dark color represents high RA; b) IDL group of metagenomic sequences: light blue color represents low RA. a dark color represents high AR; c) LDL group of metagenomic sequences: light green color represents low RA. a dark color represents high RA; d) Alluvial plot: yellow color represents RAR of HDL group; blue color represents RAR of IDL group and. green color represents RAR of LDL group. Shannon's diversity index (H)

The relative abundance (RA) of enterobacteria genus in order of declining was: *Tatumella* (72,83), *Pseudomonas* (22,05), and *Klebsiella* (18,11). *Tatumella* was found in the three groups, but *Pseudomonas* and *Klebsiella* were present exclusively in HDR (Figure 5 a). The highest RAR of enterobacteria metagenomic sequences corresponded to IDR (36.05%), followed by LDR (32.44%), and finally, HDR (31.50%) (Figure 5 d).

Three yeast genera were identified in order of declining abundance: *Hanseniaspora* (93.0), *Issatchenkia* (68.6), and *Pichia* (0.77) (Figure 5 a, b, c). *Hanseniaspora* was present in the three groups together with the genus *Pichia*. However, the genus *Issatchenkia* only occurred in IDR and HDR (Figure 5 a, b). Metagenomic sequences of filamentous fungi of the *Mucor* (2.37) genus were notable in HDR (Figure 5 a), but these sequences did not appear in LDR and IDR (Figure 5 b, c). The yeasts' RAR in order of declining abundance corresponded to IDR (36.8%), LDR (34.2%), and HDR (31.9%) (Figure 5 d). Other sequences above the genus, not identified, were also found. In decreasing order of RAR, they correspond to IDR (36.8%), LDR (33.8%), and HDR (31.9%) (Figure 5 d).

The relative abundance of metagenomic sequences of two LAB genera was highlighted: The *Lactobacillus* (36.49) genus, which was only present in IDR, and *Weissella* (3.95), present in all three groups (Figure 5 a, b, c). The highest RAR of these metagenomic sequences corresponded to IDR (49.14%), followed by LDR (44.38%) and HDR (6.48%) (Figure 5 d).

Two genera of AAB were found: *Gluconobacter* (6.42), present in all three groups, with a higher RA, and *Acetobacter* (0.14), which only occurred in IDR with a lower RA (Figure 5 b). In addition, an increased relative abundance of the *Frauteria* genus was also found, a genus with metabolic characteristics like AAB (Figure 5 b). In these cases, the RAR was as follows: LDR (86.24%), IDR (10.64%), and HDR (10.33%) (Figure 5 d).

Another important finding was the presence of the genus *Bacillus* (20.47), which was also presented exclusively in LDR (Figure 5 c). Other three genera of bacteria soil were also found in decreasing order of abundance: *Stenotrophomonas* (85.71), *Luteibacter* (51.02), and *Variovorax* (28.57), which are not frequent among CFCs but appeared with high RA in LDR (Figure 5 c). Metagenomic sequences of the genus *Cellulosimicrobium* (6.58) in LDR and IDR were also highlighted (Figure 5 b, c). Although, the CFS metagenomic analysis did not previously detect this genus.

4. Discussion

The results suggest that the OMF density had the highest contribution to fermentation quality and performance. In this case, it was successfully implemented to obtain the best conditions that influenced the efficiency of the fermentation process. OMF treatment in CCN–51 cocoa beans fermentation process effectively increased both the fermentative yield and bean quality, implying a satisfactory alternative for the optimization fermentation process of this essential product. A quadratic behavior in the Model of both responses was observed when the OMF changed. This behavior in both models was consistent with the findings of Anaya et al. (2021), who reported that OMF 60 Hz/220 V and 5 mT influences the quadratic behavior of the colony's diameter of various species of fungi [5].

4.1. Changes in sensory profile

Cocoa beans' sensory quality and performance improvement results induced by MEF during cocoa fermentation agree with different processes modulated by electromagnetic fields. Konopacka et al. (2019) [7], and Andrade et al. (2021) [49], found that a rotating magnetic field of 16–18.5 mT by continuous exposure up to 72 hours and a magnetic flux density of 10 mT by 24 hours, respectively, increases the bioethanol production process by *S. cerevisiae*. Boeira et al. point out that a magnetic field of 35 mT exposure between 24 and 40 hours reduces 56.5% nivalenol in alcoholic fermentation by *S. cerevisiae* [50]. Also, Lin et al. demonstrated that the inactivation efficacy of PMF on E. coli

O157:H7 was proportional to the pulse number and intensity of PMF [51]. In contrast, Nakasono et al. report that a 300 mT exposure for 5–24 hours in yeast cultures has no effect [52].

4.2. Microbial ecosystem changes

The higher microbial diversity in LDR and minor diversity in HDR at 24 hours could be explained based on EMF effects on microorganisms. Several authors confirm that EMFs can condition both the stimulation and the inhibition of microbial species, affecting the dynamics of microbial populations in each ecosystem [6 – 14]. For example, Strašák et al. demonstrated that OMF of density 2.7–10 mT, frequency 50 Hz, and time 0–12 minutes reduces the growth of *Escherichia coli* [53]. On the other hand, Novák et al. report that OMF density of 10 mT, frequency 50 Hz, and time of 24 minutes decreased the growth of *S. cerevisiae* [54]. This fact was also corroborated by Bayraktar et al., who also found that OMF density of 5 mT, frequency of 160 Hz, and time of 30 minutes decrease the growth of *S. cerevisiae* [55]. For their part, Gao et al. also found that OMF of density 0.2–1 mT, frequency 50 Hz, and time 4–8 hours increased the growth of *Aspergillus niger* [56].

4.2.1. Effects in enterobacterial communities

In SCFs, the enterobacterial colonizes the early hours and is involved in the pectinolytic degradation of cocoa pulp and the assimilation of citric acid [57]. Recent investigations confirm that *Tatumella* correlated positively with gluconate in the cocoa pulp and with ethyl isovalerate and benzaldehyde in the cocoa beans, which conditions good flavors in the chocolate [58]. However, *Pseudomonas* is a primary colonizer that prolonge the lactic acid phase and limits enzyme activities [59]. In this sense, the high notes of bitterness and acidity in HDR may be related to the development of these genera.

4.2.2. Effects on yeast communities

The genera *Hanseniaspora*, *Issatchenkia,* and *Pichia* have also been reported as predominant in the first hours of FCs due to their active participation in the enzymatic degradation of cocoa pulp. These yeasts have high fermentative activity and condition important flavor precursors in the first hours of the SFC by transforming sugars into aldehydes, esters, and alcohols, compounds related to pleasant notes in the cocoa bean [57, 58]. Recent studies indicate that *Hanseniaspora* and *Pichia* can produce monoterpenes (nerolidol, linalool, geraniol, and citronellol) related to the floral flavor of cocoa beans [59, 60]. The absence of the Saccharomyces genus occasionally isolated from SFCs is also a notable result in this study since most of the SFCs highlight the prevalence of this yeast genus. The Saccharomyces genus is particularly sensitive to MEF and can be stimulated or inhibited at different densities [12, 52, 54]. The relative abundance of these genera in HDR and HDR could also condition the differences in the notes found as a function of the field density.

4.2.3. Effects in LABs communities

LABs are generally considered an important group developed in the anaerobic phase of SFCs and associated with producing cocoa bean flavor and color precursor molecules [60 – 66] by transforming citric acid and pulp sugars into lactic acid, acetic acid, and mannitol [60, 61]. However, no other LAB genera were found, except *Weissella* and *Lactobacillus*. Although several authors highlight the role of the LAB in CFS, others question its relevance in CFS [67]. Another notable result was the low AR of the *Lactobacillus* genus, which was only found in LDR despite being the most abundant genus in SFCs, which is evidence of the inhibitory effect of magnetic fields on some bacterial genera [68].

4.2.4. Effects in AABs communities

In the aerobic phase, AABs are also the most common in SFCs. However, they can also be present from the beginning of fermentation, oxidizing ethanol and lactic acid (produced by yeasts and LABs) to acetic acid [69 – 72]. This process promotes the death of the embryo and the development of different flavor precursors in SFC [31, 61, 63]. Although the *Acetobacter* genus is the most abundant in SFCs, in its place, Frateuria stood out in LDR, IDR, and HDR. This genus produces acetic acid from glucose and ethanol, and can oxidize lactate. Consequently, the relative abundance of these genera in LDR and, to a lesser extent, in HDR could also determine differences in flavors and odors found as a function of magnetic field density.

4.2.5. Effects in other microbial genera

Unlike other genera that commonly develop more abundantly in the anaerobic phase, the high abundance of four soil bacterial genera, such as *Stenotrophomonas*, *Luteibacter*, *Variovorax*, and *Bacillus*, was very notable in LDR, which shows more remarkable development of species at low field density. Most of these genera are related to the pectinolytic decomposition of the pulp, facilitating the aeration of the medium and the start of the aerobic phase [5 0– 54, 63]. Recently, this activity in the *Bacillus* genus has been related to flavor precursors and the formation of pyrazines [71, 72].

4.2.6. EMF conclusive evidence

There is evidence that EMF can condition changes in microbial metabolism (inducing the synthesis of different primary and secondary metabolites), such as those reported by Liao et al., [73] who demonstrated that the low–frequency magnetic field improved the performance of pigments of *Monascus purpureus* significantly reducing citrinin production and Alvarez et al., [74] who affirm

that the densities of the sinusoidal magnetic field of 5 to 20 mT in 4 to 12 h managed to increase the production of nisin by *Lactococcus lactis*. In this sense, it could be guessed that both the interaction and single effects of the OMF and the concentration of the inoculum could have a direct and indirect impact on the different autochthonous microbial species of the cocoa bean [60, 75], which could also occur, giving rise to favorable conditions in the fermentation process of the cocoa bean. These findings could be the slight notes of flavor fine found in CCN–51.

On the other hand, although a change in magnetic energy is insignificant compared to covalent bond energies, it has been seen that the magnetic field can or not change the energy levels in a biological system and its constituent molecules by changing the speed of biochemical reactions (especially those involving pairs of radicals) [58, 59, 76]. Thus, changes in the genetic expression of various microbial species induced by EMFs have also been shown, such as that reported by Wang et al. 2017 who found that ambient magnetic fields of 5 mT increase the expressions of genes related to signal transduction, cell motility and the activity of ammonium–oxidizing aerobic bacteria [77].

Since the metagenomic study was limited to the first 24 hours of fermentation and the optimal growth of the main genera in SFCs is established between 24 and 96 hours [15], the microbial population analysis found could have been underestimated. However, the first microorganisms to colonize can determine the course and progress of fermentation [47, 55, 60]. In this regard, the change observed in the cocoa bean fermentation could be an indirect effect of modifications in both the gene expression of the microbial species present and their metabolic activity.

Thus, in the coordinates obtained in the study, favorable conditions were generated for good fermentative performance and grain quality. Consequently, the appearance of undesirable microbial genera (*Pseudomonas*, *Mucor*) in HDR could lead to poor grain quality. In contrast, the microbial genera found in LDR and IDR could develop more favorable characteristics in the grain, conditioning better fermentative performance and sensory quality. Another hand, the genus *Cellulosimicrobium* found in LDR and IDR could be a contaminant obtained during the DNA extraction process as described in other research, as this genus is usually found in the soil [78].

On the other hand, although the process was optimized, the study coordinates were limited to the OMF emission range of the electromagnetic device, where stable emissions were obtained over time. However, results indicate that optimal values of cocoa bean quality could still be reached at densities below 5 mT. Therefore, before carrying out a process on a larger scale, evaluation of the lower OMF density ranges that fell outside the limits of this study should be considered.

5. Conclusions

This study proposes a new concept to improve fermentation performance and cocoa bean quality using electromagnetic fields and a new direction to explore the mechanism of magnetic field

influence on the cocoa bean fermentation process. In addition, the observed phenomena should also be explained in terms of new process parameters (*e.g.*, abiotic factors, microbial populations, volatile components, and kinetic variables). Nevertheless, despite the production costs required to control the large–scale cocoa bean fermentation process, the quality assurance of cocoa providing a stable market is promising. Thus, technological synergies will bring advances and future contributions to the science and industry of chocolate.

Author Contributions:

The authors contributed in the following manner to this research project. Conceptualization, Methodology, Validation, Formal analysis: T.M.G.A: Resources, writing – original draft; J.R.N: Resources, Investigation, supervision, writing – original draft & review; L.R.G: Investigation, Resources, writing – review; LSG: writing – review, visualization & editing; SW: Investigation, writing – a review. All authors have read and agreed to the published version of the manuscript.

Acknowledgments

The authors thank Octavio Cordova for his technical support in the OMF–device validation process.

Conflicts of Interest

The authors declare no conflict of interest

References

[1] M. A. Fadel, Z. A. Mohamed, M. A. Abdellateef, and A. A. Hosny, Effect of extremely low frequency of electromagnetic fields on some toxic species of cyanobacteria., *Int. J. New Horiz. s Phys.*, vol. 5, pp. 5–10, 2018, https://dx.doi.org/1018576/ijnhp/050102 .

[2] M. M. Movahedi, F. Nouri, A. Tavakoli Golpaygani, L. Ataee, S. Amani, and M. Taheri, Antibacterial Susceptibility Pattern of the Pseudomonas aeruginosa and Staphylococcus aureus after Exposure to Electromagnetic Waves Emitted from Mobile Phone Simulator., *J. Biomed. Phys. Eng.*, vol. 9, no. 6, pp. 637–646, Dec. 2019, https://dx.doi.org/1031661/jbpev0i0.1107 .

[3] L. Marynchenko, O. Nizhelska, A. Kurylyuk, V. Makara, and S. Naumenko, Observed effects of electromagnetic fields action on yeast and bacteria cells attached to surfaces, in *2020 IEEE 40th International Conference on Electronics and Nanotechnology (ELNANO)*, 2020, pp. 603–608, https://dx.doi.org/101109/ELNANO50318.2020.9088883.

[4] C. Guo, Y. Wang, and D. Luan, Non–thermal effects of microwave processing on inactivation of Clostridium Sporogenes inoculated in salmon fillets, *LWT*, vol. 133, p. 109861, 2020, https://doi.org/10.1016/j.lwt.2020.109861.

[5] M. Anaya, E. Gámez–Espinosa, O. Valdés, T. Guzmán, and S. Borrego, Effect of the oscillating magnetic field on airborne fungal., *Arch. Microbiol.*, vol. 203, no. 5, pp. 2139–2145, Jul. 2021, https://dx.doi.org/10.1007/s00203–021–02193–x

[6] Khokhlova, G., Abashina, T., Belova, N., Panchelyuga, V., Petrov, A., Abreu, F., & Vainshtein, M. Effects of combined magnetic fields on bacteria Rhodospirillum rubrum VKM B–1621, *Bioelectromagnetics*, vol. 39, no. 6, pp. 485–490, Sep. 2018, https://dx.doi.org/10.1002/bem.22130.

[7] A. Konopacka, R. Rakoczy, and M. Konopacki, The effect of rotating magnetic field on bioethanol production by yeast strain modified by ferrimagnetic nanoparticles, *J. Magn. Magn. Mater.*, vol. 473, pp. 176–183, 2019, https://doi.org/10.1016/j.jmmm.2018.10.053.

[8] Baraúna, R. A., Santos, A. V., Graças, D. A., Santos, D. M., Ghilardi Júnior, R., Pimenta, A., & Silva, A. Exposure to an extremely low–frequency electromagnetic field only slightly modifies the proteome of Chromobacterium violaceum ATCC 12472, *Genet. Mol. Biol.*, vol. 38, no. 2, pp. 227–230, May 2015, https://dx.doi.org/10.1590/S1415–4757382220140240.

[9] S.–S. I H, J. F A, Y. H H, and M. M E, Evaluation of Wi–Fi Radiation Effects on Antibiotic Susceptibility, Metabolic Activity and Biofilm Formation by Escherichia Coli 0157H7, Staphylococcus Aureus and Staphylococcus Epidermis., *J. Biomed. Phys. Eng.*, vol. 9, no. 5, pp.

579–586, https://dx.doi.org/10.31661/jbpe.v0i0.1106.

[10] S. H. Salmen and S. A. Alharbi, Impact of high frequency electromagnetic field on survival rate and the morphology of pathogenic bacteria, 2017. *in Journal of Animal & Plant Sciences.*, Issue 4, p1225–1230. http://www.thejaps.org.pk//24.pdf

[11] Kanematsu, H., Katsuragawa, T., Barry, D. M., Yokoi, K., Umeki, S., Miura, H., & Zimmerman, S. Biofilm formation behaviors formed by E. Coli under weak alternating electromagnetic fields, in *Advances in Ceramics for Environmental, Functional, Structural, and Energy Applications II*, 2019, pp. 195–210. ISBN 9781119631484

[12] E. Amado González, A. Álvarez Ovallos, and A. Quijano Parra, Electromagnetic Fields (0.04 to 0.39) mT effect on cellular growth cycles of Saccharomyce*S. cerevisiae* wine strains, *BISTUA Rev. la Fac. Ciencias Básicas*, vol. 17, no. 2 SE–Artículos, pp. 196–206, Nov. 2020, https://doi.org/10.24054/01204211.v2.n2.2019.249.

[13] S. Amani, M. Taheri, M. M. Movahedi, M. Mohebi, F. Nouri, and A. Mehdizadeh, Evaluation of Short–Term Exposure to 2.4 GHz Radiofrequency Radiation Emitted from Wi–Fi Routers on the Antimicrobial Susceptibility of Pseudomonas aeruginosa and Staphylococcus aureus., *Galen Med. J.*, vol. 9, p. e1580, 2020, https://doi.org/10.31661/gmj.v9i0.1580.

[14] H. L. Miñano, A. C. Silva, S. Souto, and E. J. Costa, Magnetic Fields in Food Processing Perspectives, Applications and Action Models, *Processes*, vol. 8, no. 7. 2020, https://doi.org/10.3390/pr8070814.

[15] L. De Vuyst and S. Weckx, *The cocoa bean fermentation process: from ecosystem analysis to starter culture development*, vol. 121, pp. 5–17, 2016, https://doi.org/10.1111/jam.13045.

[16] V. T. T. Ho, J. Zhao, and G. Fleet, The effect of lactic acid bacteria on cocoa bean fermentation, *Int. J. Food Microbiol.*, vol. 205, pp. 54–67, 2015, https://doi.org/10.1016/j.ijfoodmicro.2015.03.031

[17] P. Adler, L. J. Frey, A. Berger, C. J. Bolten, C. E. Hansen, and C. Wittmann, The key to acetate: metabolic fluxes of acetic acid bacteria under cocoa pulp fermentation–simulating conditions., *Appl. Environ. Microbiol.*, vol. 80, no. 15, pp. 4702–4716, Aug. 2014, https://doi.org/10.1128/AEM.01048–14.

[18] Crafack, M., Keul, H., Eskildsen, C. E., Petersen, M. A., Saerens, S., Blennow, A., & Nielsen, D. S. Impact of starter cultures and fermentation techniques on the volatile aroma and sensory profile of chocolate, *Food Res. Int.*, vol. 63, pp. 306–316, 2014, https://doi.org/10.1016/j.foodres.2014.04.032.

[19] Koné, M. K., Guéhi, S. T., Durand, N., Ban–Koffi, L., Berthiot, L., Tachon, A. F., & Montet, D. Contribution of predominant yeasts to the occurrence of aroma compounds during cocoa bean fermentation, *Food Res. Int.*, vol. 89, pp. 910–917, 2016, https://doi.org/10.1016/j.foodres.2016.04.010.

[20] Jaimez, R. E., Barragan, L., Fernández–Niño, M., Wessjohann, L. A., Cedeño–Garcia, G., Cantos, I. S., & Arteaga, F. *Theobroma cacao L*. cultivar CCN–51: a comprehensive review on origin, genetics, sensory properties, production dynamics, and physiological aspects., *PeerJ*, vol. 10, p. e12676, 2022, https://doi.org/10.7717/peerj.12676

[21] L. Quintana Fuentes, S. Gómez–Castelblanco, A. García Jerez, and N. Martinez, Perfil sensorial del Clon de cacao (*Theobroma cacao L*.) CCN51 (primera cosecha de 2015), vol. 13, May 2015, https://doi.org/10.24054/16927125.v1.n1.2015.1866

[22] Dulce, V. R., Anne, G., Manuel, K., Carlos, A. A., Jacobo, R. C., de Jesús, C. E. S., & Eugenia, L. C. Cocoa bean turning as a method for redirecting the aroma compound profile in artisanal cocoa fermentation, *Heliyon*, vol. 7, no. 8, p. e07694, 2021, https://doi.org/10.1016/j.heliyon.2021.e07694

[23] S. Streule, S. Freimüller Leischtfeld, M. Galler, and S. Miescher Schwenninger, Monitoring of cocoa post–harvest process practices on a small–farm level at five locations in Ecuador, *Heliyon*, vol. 8, no. 6, p. e09628, 2022, https://doi.org/10.1016/j.heliyon.2022.e09628 .

[24] I. J. C. Jiménez, I. G. T. Guncay, Ms. J. N. Q. Guerrero, and D. C. R. M. G. Batista, Presecado: Su efecto sobre la calidad sensorial del licor de cacao (*Theobroma cacao L*.)., *Rev. Científica Agroecosistemas*, vol. 6, no. 2 SE–Artículos, Sep. 2018, [Online]. Available: https://aes.ucf.edu.cu/index.php/aes/article/view/195

[25] M. A. Lazo Vélez and C. R. Vizcaíno Almeida, Effect of co–fermentation of probiotic microorganisms and fruit pulps in the cocoa beans of the ccn–51 variety, Universidad del Azuay, 2020. Sep. 2021, [Online]. Available: http://dspace.uazuay.edu.ec/handle/datos/10404

[26] J. H. Hu, L. S. St–Pierre, C. A. Buckner, R. M. Lafrenie, and M. A. Persinger, Growth of injected melanoma cells is suppressed by whole body exposure to specific spatial–temporal configurations of weak intensity magnetic fields., *Int. J. Radiat. Biol.*, vol. 86, no. 2, pp. 79–88, Feb. 2010, https://doi.org/10.3109/09553000903419932

[27] H. K. Kondaveeti, N. K. Kumaravelu, S. D. Vanambathina, S. E. Mathe, and S. Vappangi, A systematic literature review on prototyping with Arduino: Applications, challenges, advantages, and limitations, *Comput. Sci. Rev.*, vol. 40, p. 100364, 2021, https://doi.org/10.1016/j.cosrev.2021.100364

[28] M. E. Tardzenyuy, Z. Jianguo, T. Akyene, and M. P. Mbuwel, Improving cocoa beans value chain using a local convection dryer: A case study of Fako division Cameroon., *Sci. African*, vol. 8, p. e00343, 2020, https://doi.org/10.1016/j.sciaf.2020.e00343

[29] Y. B. Saunshi, M. V. S. Sandhya, N. K. Rastogi, and P. S. Murthy, Starter consortia for on–farm cocoa fermentation and their quality attributes, *Prep. Biochem. Biotechnol.*, vol. 50, no. 3, pp. 272–280, Mar. 2020, https://doi.org/10.1080/10826068.2019.1689508

[30] Sandhya, M. V. S., Yallappa, B. S., Varadaraj, M. C., Puranaik, J., Rao, L. J., Janardhan, P., & Murthy, P. S. Inoculum of the starter consortia and interactive metabolic process in enhancing quality of cocoa bean (*Theobroma cacao*) fermentation, *LWT – Food Sci. Technol.*, vol. 65, pp. 731–738, 2016, https://doi.org/10.1016/j.lwt.2015.09.002

[31] Rottiers, H., Tzompa Sosa, D. A., De Winne, A., Ruales, J., De Clippeleer, J., De Leersnyder, I., & Dewettinck, K. Dynamics of volatile compounds and flavor precursors during spontaneous fermentation of fine flavor Trinitario cocoa beans, *Eur. Food Res. Technol.*, vol. 245, no. 9, pp. 1917–1937, 2019, https://doi.org/10.1007/s00217–019–03307–y

[32] A. Kocira, S. Kocira, M. Świeca, U. Złotek, A. Jakubczyk, and K. Kapela, Effect of foliar application of a nitrophenolate–based biostimulant on the yield and quality of two bean cultivars, *Sci. Hortic. (Amsterdam).*, vol. 214, pp. 76–82, 2017, https://doi.org/10.1016/j.scienta.2016.11.021

[33] J. Kongor, E. O. Afoakwa, J. Takrama, A. Budu, and H. Mensah–Brown, Effects of Fermentation and Drying on the Fermentation Index and Cut Test of Pulp Pre–conditioned Ghanaian Cocoa (Theobroma cacao) Beans, *J. Food Sci. Eng.*, vol. 3, pp. 625–634, Nov. 2013, https://csirspace.foodresearchgh.site/handle/123456789/1340

[34] K. I. Tomlins, D. M. Baker, P. Daplyn, and D. Adomako, Effect of fermentation and drying practices on the chemical and physical profiles of Ghana cocoa, *Food Chem.*, vol. 46, no. 3, pp. 257–263, 1993, https://doi.org/10.1016/0308–8146(93)90116–W

[35] N. Taha, O. M., I. M. El–Metwally, and R. Darwesh, Impact of Drip and Gated Pipe Irrigation Systems, Irrigation Intervals on Yield, Productivity of Irrigation Water and Quality of Two Common Bean (Phaseolus vulgaris L) Cultivars in Heavy Clay Soil, *Egypt. J. Chem.*, vol. 163, pp. 5103–5116, Nov. 2020, https://doi.org/10.21608/ejchem.2020.49013.3001

[36] ISO, ISO 6658:2017 Sensory analysis — Methodology — General guidance, 2017.

[37] A. Christmann and S. Van Aelst, Robust estimation of Cronbach's alpha, *J. Multivar. Anal.*, vol. 97, no. 7, pp. 1660–1674, 2006, https://doi.org/10.1016/j.jmva.2005.05.012

[38] K. Illeghems, S. Weckx, and L. De Vuyst, Applying meta–pathway analyses through metagenomics to identify the functional properties of the major bacterial communities of a single spontaneous cocoa bean fermentation process sample, vol. 50, pp. 54–63, 2015, https://doi.org/10.1016/j.fm.2015.03.005

[39] De Bruyn, F., Zhang, S. J., Pothakos, V., Torres, J., Lambot, C., Moroni, A. V., & De Vuyst, L. Exploring the Impacts of Postharvest Processing on the Microbiota and Metabolite Profiles during Green Coffee Bean Production., *Appl. Environ. Microbiol.*, vol. 83, no. 1, Dec. 2016, https://doi.org/10.1128/AEM.02398–16

[40] A. Comasio, Novel Fermentation strategies and ingredients to produce innivative sourdoughs and breads, Vrije Universiteit Brussel, 2019.

[41] T. Strader, Clean–Up with Wizard ® SV for Gel and PCR. 2021.

[42] B. J. Callahan, P. J. McMurdie, M. J. Rosen, A. W. Han, A. J. A. Johnson, and S. P. Holmes, DADA2: High–resolution sample inference from Illumina amplicon data, *Nat. Methods*, vol. 13, no. 7, pp. 581–583, Jul. 2016, https://doi.org/10.1038/nmeth.3869

[43] Põlme, S., Abarenkov, K., Henrik Nilsson, R., Lindahl, B. D., Clemmensen, K. E., Kauserud, H., & Tedersoo, L. FungalTraits: a user–friendly traits database of fungi and fungus–like stramenopiles, *Fungal Divers.*, vol. 105, no. 1, pp. 1–16, 2020, https://doi.org/10.1007/s13225–020–00466–2

[44] Agyirifo, D. S., Wamalwa, M., Otwe, E. P., Galyuon, I., Runo, S., Takrama, J., & Ngeranwa, J. (2019) Metagenomics analysis of cocoa bean fermentation microbiome identifying species diversity and putative functional capabilities. Heliyon, 5(7). https://doi.org/10.1016/j.heliyon.2019.e02170

[45] T. M. Porter and M. Hajibabaei, Scaling up: A guide to high–throughput genomic approaches for biodiversity analysis, *Mol. Ecol.*, vol. 27, no. 2, pp. 313–338, Jan. 2018, https://doi.org/10.1111/mec.14478

[46] B. M., Pod breaking delay. Influence on the yields and quality of raw and roasted cocoa., *The Cafe Cacao*, vol. v. 31. 1987.

[47] G. G. Montgomery, D. C.; Peck, E. A.; Vining, Introducción al análisis de regresión lineal., 3ra edicio., México, 2006.

[48] M. J. Anderson and P. J. Whitcomb, Optimizing Processes Using Response Surface Methods for Design of Experiments, Second Edition, Second Edi. New York, 2016.

[49] Andrade, C.M.; Cogo, A.J.D.; Perez, V.H.; dos Santos, N.F.; Okorokova–Façanha, A.L.; Justo, O.R. & Façanha, A.R. Increases of bioethanol productivity by S. cerevisiae in unconventional bioreactor under ELF–magnetic field: New advances in the biophysical mechanism elucidation on yeasts. Renew. Energy 2021, 169, 836–842. https://doi.org/10.1016/j.renene.2021.01.074

[50] C. Z. Boeira, M. A. de C. Silvello, R. D. Remedi, A. C. P. Feltrin, L. O. Santos, and J. Garda–Buffon, Mitigation of nivalenol using alcoholic fermentation and magnetic field application, *Food Chem.*, vol. 340, p. 127935, 2021, https://doi.org/10.1016/j.foodchem.2020.127935.

[51] L. Lin, X. Wang, R. He, and H. Cui, Action mechanism of pulsed magnetic field against E. coli O157:H7 and its application in vegetable juice, *Food Control*, vol. 95, pp. 150–156, 2019, https://doi.org/10.1016/j.foodcont.2018.08.011.

[52] S. Nakasono, C. Laramee, H. Saiki, and K. J. McLeod, Effect of power–frequency magnetic fields on genome–scale gene expression in *Saccharomyces. cerevisiae*., *Radiat. Res.*, vol. 160, no. 1, pp. 25–37, Jul. 2003, https://doi.org/10.1667/rr3006

[53] L. Strasák, V. Vetterl, and J. Smarda, Effects of low–frequency magnetic fields on bacteria Escherichia coli., *Bioelectrochemistry*, vol. 55, no. 1–2, pp. 161–164, Jan. 2002, https://doi.org/10.1016/s1567–5394(01)00152–9

[54] J. Novák, L. Strasák, L. Fojt, I. Slaninová, and V. Vetterl, Effects of low–frequency magnetic fields on the viability of yeast *Saccharomyces cerevisiae*., *Bioelectrochemistry*, vol. 70, no. 1, pp. 115–121, Jan. 2007, https://doi.org/10.1016/j.bioelechem.2006.03.029

[55] V. Bayraktar, Magnetic field effect on yeast *Saccharomyces. cerevisiae* activity at grape must fermentation, *Biotechnol. Acta*, vol. 6, pp. 125–137, Feb. 2013, https://doi.org/10.15407/biotech6.01.125

[56] M. Gao, J. Zhang, and H. Feng, Extremely low frequency magnetic field effects on metabolite of *Aspergillus niger*, *Bioelectromagnetics*, vol. 32, no. 1, pp. 73–78, Jan. 2011, https://doi.org/10.1002/bem.20619

[57] Hamdouche, Y., Meile, J. C., Lebrun, M., Guehi, T., Boulanger, R., Teyssier, C., & Montet, D. Impact of turning, pod storage and fermentation time on microbial ecology and volatile composition of cocoa beans, *Food Res. Int.*, vol. 119, pp. 477–491, 2019, https://doi.org/10.1016/j.foodres.2019.01.001

[58] Díaz–Muñoz, C., Van de Voorde, D., Tuenter, E., Lemarcq, V., Van de Walle, D., Maio, J. P. S., & De Vuyst, L An in–depth multiphasic analysis of the chocolate production chain, from bean to bar, demonstrates the superiority of *Saccharomyces. cerevisiae* over Hanseniaspora opuntiae as

functional starter culture during cocoa fermentation, *Food Microbiol.*, vol. 109, p. 104115, Feb. 2023, https://doi.org/10.1016/j.fm.2022.104115

[59] T. Balogu and R. A. Onyeagba, Polyphenol and Microbial Profile of On–farm Cocoa Beans Fermented with Selected Microbial Consortia, *Appl. Food Biotechnol. 2017, 4 (4)229–240*, vol. 4, pp. 229–240, Oct. 2017, https://doi.org/10.22037/afb.v%vi%i.1684

[60] Almeida, O. G. G. D., Pinto, U. M., Matos, C. B., Frazilio, D. A., Braga, V. F., von Zeska–Kress, M. R., & De Martinis, E. C. P. Does Quorum Sensing play a role in microbial shifts along spontaneous fermentation of cocoa beans? An in silico perspective, *Food Res. Int.*, vol. 131, p. 109034, 2020, https://doi.org/10.1016/j.foodres.2020.109034

[61] J. Cevallos–Cevallos, L. Gysel, M. Maridueña–Zavala, and M. Molina–Miranda, *Time–Related Changes in Volatile Compounds during Fermentation of Bulk and Fine–Flavor Cocoa (Theobroma cacao) Beans*, vol 5, no. 2, Oct 2018, https://doi.org/10.1155/2018/175838

[62] Mota–Gutierrez, J., Botta, C., Ferrocino, I., Giordano, M., Bertolino, M., Dolci, P., & Cocolin, L. Dynamics and Biodiversity of Bacterial and Yeast Communities during Fermentation of Cocoa Beans, *Appl. Environ. Microbiol.*, vol. 84, no. 19, pp. e01164–18, Oct. 2018, https://doi.org/10.1128/AEM.01164–18

[63] Gutiérrez–Ríos, H. G., Suárez–Quiroz, M. L., Hernández–Estrada, Z. J., Castellanos–Onorio, O. P., Alonso–Villegas, R., Rayas–Duarte, P., & González–Rios, O. Yeasts as Producers of Flavor Precursors during Cocoa Bean Fermentation and Their Relevance as Starter Cultures: A Review, *Fermentation*, vol. 8, no. 7. 2022, https://doi.org/10.3390/fermentation8070331

[64] L. De Vuyst and F. Leroy, Functional role of yeasts, lactic acid bacteria and acetic acid bacteria in cocoa fermentation processes, *FEMS Microbiol. Rev.*, May 2020, https://doi.org/10.1093/femsre/fuaa014

[65] Z. Papalexandratou, N. Camu, G. Falony, and L. De Vuyst, Comparison of the bacterial species diversity of spontaneous cocoa bean fermentations carried out at selected farms in Ivory Coast and Brazil, *Food Microbiol.*, vol. 28, no. 5, pp. 964–973, 2011, https://doi.org/10.1016/j.fm.2011.01.010

[66] Papalexandratou, Z., Falony, G., Romanens, E., Jimenez, J. C., Amores, F., Daniel, H. M., & De Vuyst, L. Species Diversity, Community Dynamics, and Metabolite Kinetics of the Microbiota Associated with Traditional Ecuadorian Spontaneous Cocoa Bean Fermentations, *Appl. Environ. Microbiol.*, vol. 77, no. 21, pp. 7698 LP – 7714, Nov. 2011, https://doi.org/10.1128/AEM.05523–11

[67] G. Ozturk and G. M. Young, Food Evolution: The Impact of Society and Science on the Fermentation of Cocoa Beans., Compr. Rev. food Sci. food Saf., vol. 16, no. 3, pp. 431–455, May

2017, https://doi.org/10.1111/1541-4337.12264

[68] Sudarti, S. Bektiarso, S. H. B. Prastowo, T. Prihandono, Maryani, and R. D. Handayani, Optimizing lactobacillus growth in the fermentation process of artificial civet coffee using extremely– low frequency (ELF) magnetic field, *J. Phys. Conf. Ser.*, vol. 1465, no. 1, p. 12010, 2020, https://doi.org/10.1088/1742–6596/1465/1/012010

[69] S. Soumahoro, H. G. Ouattara, M. Droux, W. Nasser, S. L. Niamke, and S. Reverchon, Acetic acid bacteria (AAB) involved in cocoa fermentation from Ivory Coast: species diversity and performance in acetic acid production., *J. Food Sci. Technol.*, vol. 57, no. 5, pp. 1904–1916, May 2020, https://doi.org/10.1007/s13197–019–04226–2

[70] Z. Papalexandratou and L. De Vuyst, Assessment of the yeast species composition of cocoa bean fermentations in different cocoa–producing regions using denaturing gradient gel electrophoresis, vol. 11. 2011, https://doi.org/10.1111/j.1567–1364.2011.00747.x

[71] J. L. Serra, F. G. Moura, G. V. de M. Pereira, C. R. Soccol, H. Rogez, and S. Darnet, Determination of the microbial community in Amazonian cocoa bean fermentation by Illumina–based metagenomic sequencing, *LWT*, vol. 106, pp. 229–239, 2019, https://doi.org/10.1016/j.lwt.2019.02.038

[72] Assi–Clair, B. J., Koné, M. K., Kouamé, K., Lahon, M. C., Berthiot, L., Durand, N., & Guéhi, T. S. Effect of aroma potential of *Saccharomyces. cerevisiae* fermentation on the volatile profile of raw cocoa and sensory attributes of chocolate produced thereof, *Eur. Food Res. Technol.*, vol. 245, no. 7, pp. 1459–1471, 2019, https://doi.org/10.1007/s00217–018–3181–6 .

[73] Q. Liao, Y. Liu, J. Zhang, L. Li, and M. Gao, A low–frequency magnetic Field regulates Monascus pigments synthesis via reactive oxygen species in M. purpureus, *Process Biochem.*, vol. 86, pp. 16–24, 2019, https://doi.org/10.1016/j.procbio.2019.08.009

[74] D. C. Alvarez, V. H. Pérez, O. R. Justo, and R. M. Alegre, Effect of the extremely low frequency magnetic field on nisin production by Lactococcus lactis subsp. lactis using cheese whey permeate, *Process Biochem.*, vol. 41, no. 9, pp. 1967–1973, 2006, https://doi.org/10.1016/j.procbio.2006.04.009

[75] G. C. A. Chagas Junior, N. R. Ferreira, and A. S. Lopes, The microbiota diversity identified during the cocoa fermentation and the benefits of the starter cultures use: an overview, *Int. J. Food Sci. Technol.*, vol. 56, no. 2, pp. 544–552, Feb. 2021, https://doi.org/10.1111/ijfs.14740

[76] C. T. Rodgers and P. J. Hore, Chemical magnetoreception in birds: The radical pair mechanism, *Proc. Natl. Acad. Sci.*, vol. 106, no. 2, pp. 353–360, Jan. 2009,

https://doi.org/10.1073/pnas.0711968106

[77] Wang, Z., Liu, X., Ni, S. Q., Zhang, J., Zhang, X., Ahmad, H. A., & Gao, B. Weak magnetic field: A powerful strategy to enhance partial nitrification. *Water Res.*, vol. 120, pp. 190–198, Sep. 2017, https://doi.org/10.1016/j.watres.2017.04.058

[78] Salter, S. J., Cox, M. J., Turek, E. M., Calus, S. T., Cookson, W. O., Moffatt, M. F., & Walker, A. W. Reagent and laboratory contamination can critically impact sequence–based microbiome analyses, BMC Biol., vol. 12, no. 1, p. 87, 2014, https://doi.org/10.1186/s12915–014–0087–z

Suplementary material

Table S1. Analysis of variance (ANOVA) reduced for Central Composite Design (CCD CCF) Face–Centered Cube (α = 1) for fermentative yield (Y2) and bean quality (Y4).

Source	Fermentative yield Y2					Almond quality Y4				
	Sum of Squares	df	Mean Square	F–value	p–value	Sum of Squares	df	Mean Square	F–value	p–value
Model	4663.36	8	567.27	44.79	0.0001	16737.25	6	2789.54	97.10	0.0001
A–OMF density	1613.28	1	1512.25	119.41	0.0001	14724.43	1	14724.43	512.54	0.0001
B–Exposure time	68.76	1	71.82	5.67	0.0224	3.27	1	3.27	0.1137	0.7377
C–Inoculum concentration	104.13	1	136.08	10.74	0.0022	588.65	1	588.65	20.49	0.0001
AB	363.04	1	419.53	33.13	0.0001	–	–	–	–	–
AC	351.62	1	407.25	32.16	0.0001	–	–	–	–	–
A2	1140.70	1	1134.12	89.55	0.0001	613.88	1	613.88	21.37	0.0001
B2	178.39	1	175.79	13.88	0.0006	666.35	1	666.35	23.19	0.0001
C2	392.61	1	278.62	22.00	0.0001	264.37	1	264.37	9.20	0.0042

Y2: R^2 0.8766 Adjusted–R^2 0.8458; Predicted R^2 0.7790; Adeq Precision 18.6259; C.V. % 4.42
Y4: R^2 0.9597; Adjusted–R^2 0.9562; Predicted R^2 0.9458; Adeq Precision 29.0873; C.V. % 5.79
df= degree of freedom

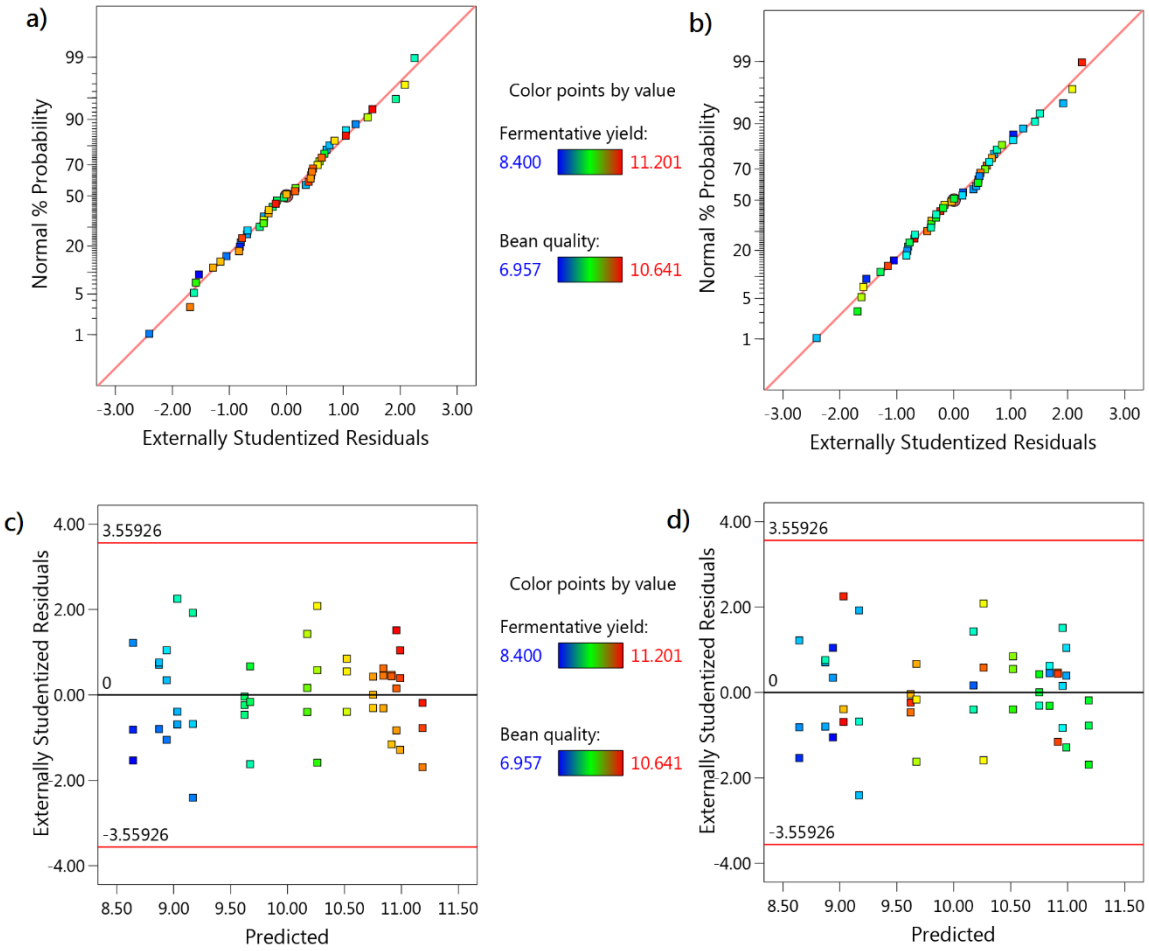

Figure S1. Diagnostics Plots: a.b) Normal Probability; c.d) Externally Studentized residuals

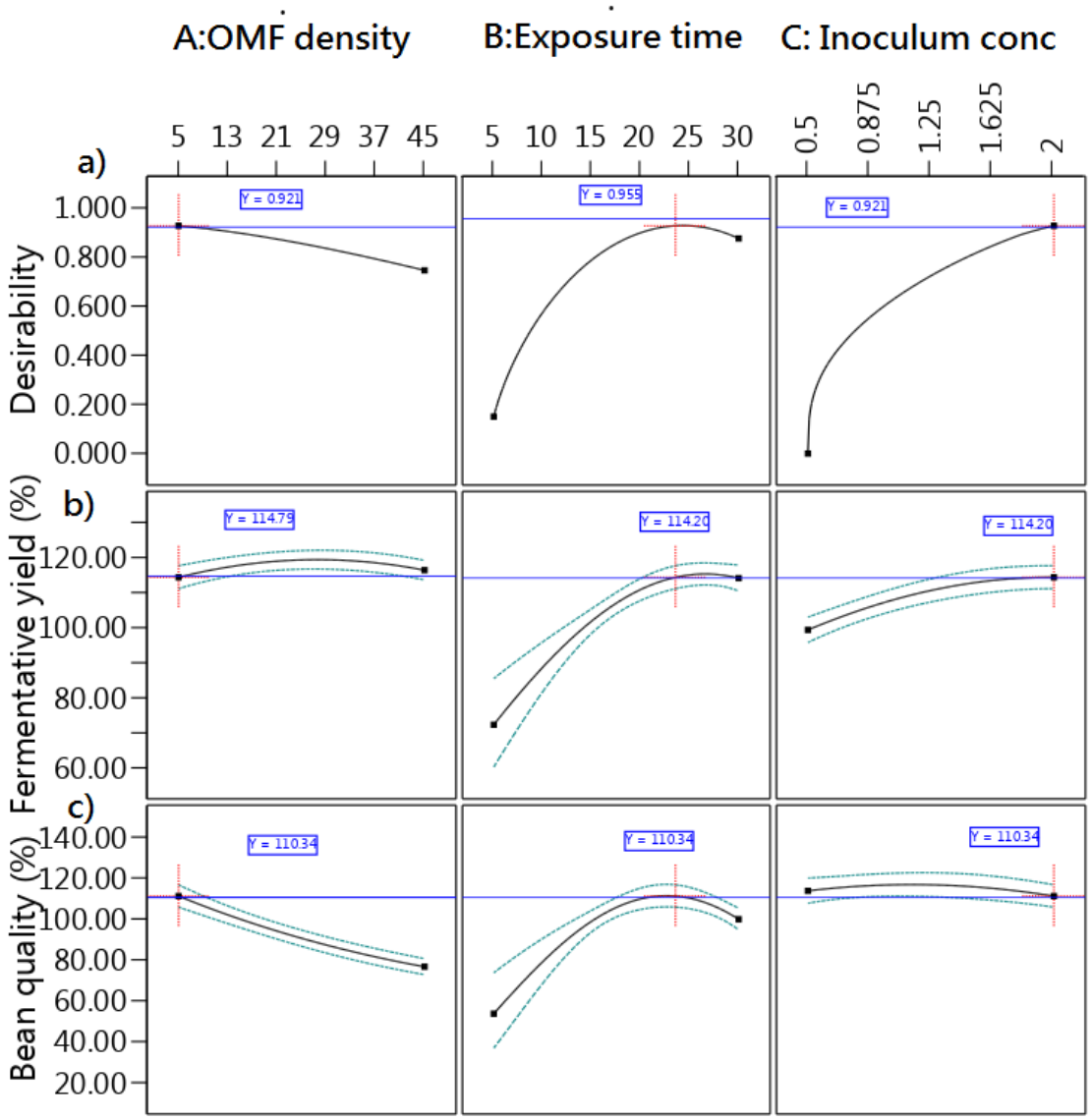

Figure S2. Numerical Optimization Graphs

Table S2. Confirmation matrix of theoretical and practical results

Analysis	Predicted Mean	Std Dev	n	SE Pred	95% PI low	Observed Mean	95% PI high
Fermentative yield	114.37	3.92	3	N/A	108.77	110.46	120.05
Bean quality	111.04	6.73	3	N/A	101.59	102.67	120.70

Chapter 4

Raman spectroscopic and sensory evaluation of cocoa liquor prepared with Ecuadorian cocoa beans treated with gamma irradiation or induced electromagnetic field fermentation

Tania María Guzmán Armenteros[1], Jenny Ruales[1], Cristina Cuesta[2], Juan Bravo[2], Marco Sinche[3], Edwin Vera[1], Edison Vera[1], Paul Vargas[3], Valerian Ciobota[4], Fernando Ortega[5], Gemma Montalvo[5], Andrés Proaño[6], Armando Echeverría[7], and Luis Ramos–Guerrero[8, 2*]

[1] Departamento de Ciencia de Alimentos y Bio–tecnología, Facultad de Ingeniería Química y Agroindustria, Escuela Politécnica Nacional (EPN), Quito 170525, Ecuador.; tania.guzman@epn.edu.ec; jenny.ruales@epn.edu.ec; edwin.vera@epn.edu.ec

[2] Agencia de Regulación y Control Fito y Zoosanitario, AGROCALIDAD, Av. Interoceánica km 14 ½, 170184 Tumbaco, Ecuador; maria.cuesta@agrocalidad.gob.ec; juanitob920@hotmail.com

[3] Departamento de Ciencias Nucleares, Facultad de Ingeniería Química y Agroindustria, Escuela Politécnica Nacional, Ladrón de Guevara E11–253, 170525 Quito, Ecuador; marco.sinche@epn.edu.ec; edison.vera@epn.edu.ec; paul.vargas@epn.edu.ec

[4]Rigaku Analytical Devices, Pasedagplatz 3–4, 13088 Berlin, Germany; valerian.ciobota@rigaku.com

[5] Department of Analytical Chemistry, Physical Chemistry and Chemical Engineering and University Institute of Research in Police Sciences (IUICP), University of Alcalá, Ctra. Madrid–Barcelona Km. 33.6, Alcalá de Henares (Madrid), 28871, Spain; fernando.ortega@uah.es; gemma.montalvo@uah.es

[6] Programa de Reactivación de Café y Cacao, Ministerio de Agricultura y Ganadería, Av. Eloy Alfaro y Av. Amazonas, Quito, Ecuador; e–mail@e–mail.com

[7] Facultad de Ciencias Técnicas, Universidad Internacional del Ecuador, Quito, Ecuador; e–mail@e–mail.com

[8] Centro de Investigación de Alimentos, CIAL, Universidad UTE, EC 170527, Quito, Ecuador;

luis.ramos@ute.edu.ec

* Corresponding author: luis.ramos@ute.edu.ec; Tel.: +593 0980548444

Abstract

Cocoa liquor is the primary precursor of the highly worldwide appreciated chocolate commodity. Its quality depends on several factors, like cocoa type, the fermentation process, and the control of the contaminants on the fermented beans. This study aims to evaluate if the induced magnetic field treatment during the fermentation process or the pathogen reduction with gamma irradiation after the fermentation affects the characteristics of cocoa liquor obtained from Ecuadorian cocoa beans. For this purpose, liquor samples from control (standard process), from beans treated with an induced magnetic field up to 80 mT, and from beans irradiated with doses up to 3 kGy were characterized through Raman spectroscopic analysis and sensorial evaluation. The most relevant bands of the cocoa liquor were assigned according to literature reports, spectroscopic data, and chemometrics. The spectra corresponding to different treatments and doses were visually very similar, but they could be discriminated using OPLS_DA. The most intense Raman signals were attributed to lipid components. At 1 kG, the sensory evaluation qualifies a marked tendency to unpleasant flavors, while at higher doses (3 kG) I highlight the presence of floral and fruit flavors, and intense aroma. Therefore, both treatments may exert an influence on cocoa beans and, therefore, on the cocoa liquor quality.

Keywords: chocolate; cocoa beans; cocoa liquor; Raman spectroscopy; magnetic field; fermentation

1. Introduction

The production of cocoa beans and the chocolate industry constitute an essential part of the economies of many countries [1]. Indeed, the demand for high–quality cocoa beans and their products shows a consistent rise year by year [2], with chocolate ranked as one of the most popular foods in the world [3]. Moreover, there is an increase in the consumer's interest in premium chocolates containing organic, single–origin, and fair–trade cocoa, as well as chocolates with high cocoa content [4]. Therefore, rapid growth in cocoa–related industries has been observed, which implies remarkable incomes for many countries [5].

Chocolate is composed of cocoa liquor, sweeteners, emulsifiers, and additional components that are held in suspension within cocoa butter or other substitute fat sources [6], and subjected to refining, conching, tempering, and standardization [7]. The cocoa fermentation process hugely influences the quality of chocolate; during this step, the beans go through chemical and physical transformations that define desired characteristics such as aroma and flavor [8]. Cocoa fermentation occurs due to the sequential microbial action of yeasts, lactic acid bacteria, and, eventually, acetic acid bacteria [9]. Each group of microorganisms produces specific compounds responsible for cocoa beans' sensory and organoleptic attributes. For instance, volatile organic compounds like fatty acetate esters and acid ethyl esters; are produced through the action of yeasts involved in reactions of the amino acid metabolism during fermentation. These compounds play a crucial role in creating the aromatic and

flavor profiles, often marked by fruity undertones, found in chocolate [10].

The application of electromagnetic fields can help improve the fermentation processes of different agricultural products [11,12], including cocoa beans [13]. It is considered a safe technology that does not generate toxic products and is not difficult to apply. Food processes induced by electromagnetic fields have shown effectivity in terms of bacteria activation, stimulation of their growth, production of metabolites, and improved sensory quality when compared to conventional treatments [14].

The electromagnetic fields utilized in food processing can be categorized into dynamic forms (pulsating and alternating fields) and static forms (like constant magnetic fields). Additionally, the classification can be based on the magnetic field's intensity in the given space, leading to uniform or non–uniform fields. The response of charges within the food matrix determines whether the magnetic field type is oscillating, pulsed, or static [14]. The intensity may fall under different ranges: less than 1 T (considered weak), 1 to 5 T (regarded as strong), or higher than 5 T (classified as ultra–strong) [15,16]. This variation depends on the interaction between the induced field and the organisms. The sought–after outcomes encompass stimulating the growth of beneficial microbes, enhancing their metabolic activity, and improving mycelium production, among other effects [17].

On the other hand, consuming chocolate with a high cocoa content has positive effects on health [18], such as lowering blood pressure, inhibiting platelet activation, improving endothelial function, and avoiding insulin resistance [19]. This fact is consistent with scientific evidence of the presence of phenolic compounds in chocolate, such as flavan–3–ols and derivatives, hydroxycinnamic acids, flavones, ellagitannins, hydroxybenzoic acids, and curcuminoids [20]. However, the presence of pathogens may overshadow these benefits, as in the case of aerobic microbes, spores from thermophilic acidophilus bacteria, and mesophilic aerobic bacteria reported in chocolate [21]. The conversion of fermented cocoa beans into chocolate requires thermal processing (roasting); However, some microbial structures, such as mold and bacterial spores, can persist and remain viable [22]. This underscores the importance of employing methods that prevent the growth of undesirable microorganisms.

For many years, gamma irradiation has been utilized to eradicate microbiological risks (including pathogenic and food spoilage microorganisms) in food products. This application has been demonstrated to effectively enhance food safety without undermining nutritional characteristics, consumer well–being, or sensory attributes [23,24]. In this technology, food products are exposed to the ionizing radiations emitted by Cobalt–60 or Cesium–137 radioisotopes, which have high energy and a penetration capacity of several feet [25,26]. Additional applications include the shelf–life extension in processed foods and meats, sprout inhibition in bulbs and tubers, ripening delay in fresh products, insect disinfecting in cereals, quarantine control in fruits, pathogen reduction in spices, parasite inactivation [27], and improving food mycotoxicological safety [28]. Food irradiation, also

known as ionization, exhibits exciting benefits such as the absence of chemical residues after the treatment; the avoidance of important temperature increases during the process; versatility since it can be applied to low and high moisture products as well as fresh or frozen food [29]; and ease regarding the operation of the radiators since the gamma rays are emitted in all directions, continuously, and at a predictable rate [30]. The process does not require much electric energy, and it is not a water–consuming method. On the other hand, gamma rays are unsuitable for some products, especially those in which quality properties are affected by the reduction of firmness, such as plums and pears [28, 31]. The dose sensitivity of a product depends on its composition because some macromolecules are more susceptible to radiation than others (lipids> carbohydrates>proteins). In this sense, radiation is widely recommended for fish, meat, and poultry. Contrary to fruits and vegetables, which are characterized by higher contents of carbohydrates that could experience hydrolysis reactions, foods with a high lipid content are susceptible to auto–oxidation [29, 32]. Therefore, the dose must be carefully selected depending on the nutritional profile of the product.

Food exposed to a proper irradiation dose for technical purposes is safe and nutritionally adequate [33]. The flavor and some nutritional properties could experience modifications, but these changes are, in general, less noticeable than those observed when applying conventional preserving treatments (cooking, canning, pickling, freezing, and drying) [28]. Additionally, food ionization could be more expensive than other methods, the availability of irradiation facilities is limited, and certain importing markets decline irradiated products [34]. However, unit costs can be lowered if larger volumes of product are subjected to this treatment and if irradiation facilities operate close to their maximum capacity. Also, many products have overcome trade barriers through gamma irradiation [35]. Many people still resist accepting irradiated food due to misconceptions about ionizing radiation. In these cases, consumer reliance on this technology could be acquired through education and scientific evidence [36]. All things considered, gamma treatments exhibit a more significant number of advantages than drawbacks. The key challenge of this food technology is to identify the dose at which desirable aspects are maximized and shortcomings are minimized.

Another significant aspect of consideration, aside from the controlled fermentation process and ensuring microbial safety, is that the quality of chocolate is inherently tied to both the quality of the raw materials and the various stages of manufacturing [37]. Chemical, physical, and sensory methods are used to analyze it. Safety, color, aroma, flow behavior, and texture are the principal quality parameters in chocolate [38]. Also, particle size distribution, viscosity, melting profile, and hardness [39]; sensory properties related to mouthfeel [40]; fat, protein, carbohydrates, water, and ash content [41] are quality attributes essayed in chocolates.

Chocolatiers require quick, efficient, and easy to apply techniques for quality control [42]. In this sense, spectroscopic tools are fast, simple, and inexpensive; they do not require much sample preparation and do not need reagents that later constitute chemical waste [43, 44]. Raman's

spectroscopy has a broad spectrum of potential applications in the food industry, as it enables the identification of various components within a food matrix as macromolecules (water, protein, carbohydrates, and fat), the migration of packaging material to the product, the presence of synthetic dyes and carotenoids, changes experienced during stages of manufacture at a structural or conformational level, and evaluation of counterfeits and microorganisms [45, 46]. The structure, type, conformation of the molecules, and crystallinity are some of the data acquired by examining the spectra generated from the dispersed light once the laser is in contact with the sample [47].

Raman's spectroscopy finds specific applications in assessing chocolate quality. For instance, it is used to analyze the crystallization behavior of cocoa butter by identifying distinctive spectral signatures corresponding to its various crystal polymorphs [48], especially the V polymorph responsible for textural properties such as glossiness, snap, and absence of fat boom since crystallization determines the chocolate's texture, stability, quality [49], and sensory properties. Raman spectroscopy has been reported to characterize the lipid fraction chemically and infer the presence of other fat sources in different types of dark, milk, and white chocolates [50]. Also, chocolate constituents have been mapped with Raman microspectroscopy [51]. Concerning the authentication of single–origin chocolates, it could be done based on the results from Raman spectroscopy; in fact, this technique has made possible the distinction between two Ecuadorian cocoa varieties [44]. Raman's technology, coupled with other techniques, can offer alternatives to evaluating the quality of chocolate.

This line of research extends to the field of innovation and differentiation in the chocolate industry, looking for unique flavors and profiles that differentiate their products. The application of magnetic fields or gamma radiation, if shown to have a controlled and positive effect on the quality of cocoa liquor, could potentially be used as a novel method to develop distinctive flavor profiles, improve product diversity, and captivate consumers most demanding consumers.

This study aims to assess whether the magnetic field induced during the fermentation process, or gamma radiation from fermented cocoa beans, correlates with changes in the quality of the resulting cocoa liquors. For this purpose, spectroscopic measurements were done on cocoa liquor samples from regularly fermented and non–irradiated beans (control), from beans irradiated with up to 3 kGy, and from beans exposed to an electromagnetic field system up to 80 mT during fermentation. The impact of gamma irradiation on the sensory profile was also analyzed through sensorial evaluation carried out for non–irradiated and irradiated samples.

2. Materials and Methods

2.1 Cocoa bean fermentation induced by magnetic fields

CCN–51 cocoa (*Theobroma cacao L.*) pods were sourced from local producers in Santo Domingo, Ecuador. Careful selection ensured that the pods were defect–free, undamaged, and uniformly orange, indicating optimal maturity. The cocoa beans were appropriately packed in polyethylene bags, followed by transportation and storage in a cold room maintained at temperatures between 7 and 12 °C. These conditions were maintained until the tests were conducted, which took place within a span of no more than 32 hours. The cocoa pods were washed and opened manually to obtain clean grains free of impurities or defects. In each trial, 3 kg of prepared cocoa beans ready for fermentation were positioned in 5 L plastic fermentation containers equipped with openings on the front and sides. The incubation setup (Heraeus, Model B 5042) was upheld at a consistent temperature of 37±0.5 °C and a relative humidity of 85±0.8% (Heraeus, Model B 5042). The fermentation was stopped after seven days, and the beans were dried in a forced–air rotary kiln (Roller, R610) at 60 °C for 4 hours and subsequently roasted.

A day after initiating the fermentation process, during the aerobic phase, the samples were exposed to a low–frequency magnetic field of intensities 0 (control), 5, 48, 62, and 80 mT. This exposure was accomplished using a Helmholtz prototype designed for generating electromagnetic emissions. The setup includes a validated Helmholtz coil with a surface area of 0.2 m^2, an alternating current generator, and a digital signal connection system to ensure the uniformity of the oscillating magnetic field (OMF) between the coils. For comprehensive information regarding the setup and operational procedures, reference can be made to a previous report [13]. All experiments were conducted in triplicate.

2.2. Gamma irradiation treatment of fermented cocoa beans

Cocoa beans from the National and CCN–51 varieties, which had undergone regular fermentation and drying, were stored at ambient temperature (18 °C). These beans were then exposed to ionization using a Co–60 panoramic irradiator (CIS bio International, France). The cocoa beans (1.3 kg) were packed in polystyrene trays covered with a plastic film, placed vertically, and irradiated at doses from 0.10 to 3.00 kGy in triplicate, according to the descriptions in Tables S1 and S2. Non–irradiated samples of each variety were used as controls of the experiment. The dosimetry was assessed by four Bruker BioS pin dosimeters placed in one of the triplicates at different tray positions, as shown in Figures S1 and S2. The exposed dosimeters were read in an Electron Paramagnetic Resonance Spectrometer (BrukerBiospin, e–scan, Canton, MA).

2.3. Cocoa liquor samples

The liquor samples were prepared from CCN–51 cocoa beans subjected to the induced magnetic field fermentation process using 0, 5, 48, 62, or 80 mT at 60 min, and from CCN–51 and National cocoa beans irradiated with doses of 0.10; 0.20; 0.30; 0.45; 0.60; 0.75; 1.00; 2.00 and 3.00 kGy. Sensory evaluation was performed as the only answer for Multivariate Analysis of data. Two hundred cocoa beans were toasted at 123 °C for 10 minutes in an oven (Memmert, UF30, Schwabach, Germany). The beans were manually peeled and pre–grinded (Foss, KN 295, Hillerod, Denmark) for 2 minutes at room temperature (25 °C). The grounded beans were refined (NCM, 502, New Taipei City, Taiwan) for 15 minutes. The obtained cocoa liquor was poured into molds, cooled at 15 °C, and stored in labeled plastic bags at 0 °C, once the liquor was solidified.

2.4 Raman spectra measurements of cocoa liquor samples

Raman analyses of cocoa liquor samples were conducted using a spectrometer (Rigaku Raman Technologies, Wilmington, MA, USA) equipped with a 1,064 nm Nd: YAG laser source and a Peltier–cooled InGaAs photodiode array. Temperature regulation was achieved by utilizing a cryogenically cooled Ge detector to maintain the samples' solid state. Measurement conditions were 490 mW, 1,000 ms of exposure, and 5 counts. The measurements were done randomly in different spots on the sample's surface, and each sample had 20 replicates. Before Raman measurements, a daily calibration method was carried out with a standard.

2.5 Sensorial evaluation of cocoa liquor from gamma–irradiated cocoa beans

Six trained panelists assessed the sensory profile of the liquors corresponding to the irradiated CCN–51 and National cocoa beans, by a quality rating method [38]. The following attributes were considered: floral, fruity, almondy or nutty, cocoa, acid, bitter, astringent, and earthy flavors, and aroma in tenseness. The parameters were rated in duplicate, with an intensity scale from 0 to 5 (0: absence; 1: very mild; 2: mild; 3: medium; 4: strong; and 5: very strong).

The sensorial evaluation was done similarly to the method followed by Papalexandratou, et al., 2011 in liquor samples, with some modifications [52]. A portion of the liquor was placed on the tongue's surface to identify and quantify the attributes of interest. The evaluators cleansed their palates with water to eliminate any lingering flavors. They then allowed a 5–minute interval before sampling the next specimen. The cocoa liquor was tasted in a solid–state, at room temperature. The average ambient conditions of the room where the assessment was performed were 25±2 °C and 56% relative humidity.

2.6 Multivariate data analysis of the Raman spectra of cocoa liquor

Raman's spectra were imported in bulk using a script (steps' sequence) in Origin v2021 9.8 (OriginLab Corporation, Northampton, MA, USA). The spectra were organized sequentially and then transposed to have the objects (observations, subjects, or items) in rows and the wavelengths (variables) in columns. Then, the required demographic, categorical, and qualitative variables were added to describe the different samples, groups, categories, or classes.

A few spectra were plotted randomly to identify the spectral zone corresponding to the region of interest (ROI). The rest of the ranges (without information) were removed from the data. The spectral region of interest (ROI) for all samples underwent a pre–processing sequence that is widely recognized and commonly employed in spectroscopy, as documented in previous studies. The sequence consisted of a baseline correction, SNV standardization (subtracting the arithmetic mean and dividing by the standard deviation), and soft smoothing (noise reduction) using the Savitzky–Golay method. Finally, the multivariate data analysis involved implementing orthogonal partial least squares regression with discriminant analysis (OPLS–DA) within the SIMCA software (Sartorius, Göttingen, Germany). This process was carried out following a methodology designed to achieve the highest degree of meaningful differentiation between samples.

3. Results and Discussion

3.1. Cocoa liquor Raman spectra

The average Raman spectra of 20 cocoa liquor samples prepared with the CCN–51 variety is depicted in Figure 1, and their frequency assignment is summarized in table 1.

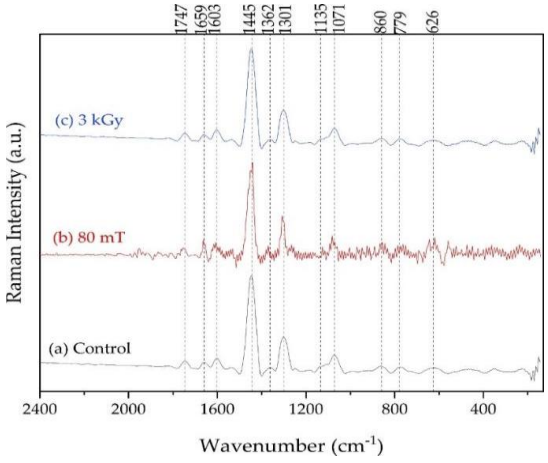

Figure 1. Average Raman spectrum of cocoa liquor from CCN 51 variety: (a) standard process (control); (b) induced magnetic field fermentation process (80 mT); (c) gamma irradiated process (3 kGy).

Table 1. Experimental frequencies (cm^{-1}) and assignment of the Raman spectra of Ecuadorian cocoa liquor (CCN–51 variety).

Experimental wavenumber (cm^{-1})	Intensity	Assignment vibrational modes	Proposed compound	Exact wave number (cm^{-1})	Reference
		Distortion of the skeletal structure of aromatic rings, substituent groups, and side chains	Native lignin	634	[1]
626	VW	–	Polygalacturonic (pectic) acid H–Pec	621	[20]
		C=C–C deformation	Theobromine	626	[2]
		OH out–of–plane deformation coupled with C=C ring stretching	Vitamin C	621	[29,30]
779	VW	Deformation of aromatic rings, substituent groups, and side chains involving O=C–C deformation	Native lignin	787	[1]
			Theobromine	777	[2, 3]
860	VW	(C6–C5–O5–C1–O1)	Polygalacturonic (pectic) acid H–Pec (a–glycosidic bonds in H–Pec)	853	[4]
		N=C–H deformation	Caffeine	850	[2]
		ν(C–C)	Cocoa butter	1000–1150	[5]
		ν(C–C)	Cocoa butter polymorphs form V	1063	[6]
		C–O stretchings ring modes	Cell Wall of *Valonia ventricosa* cellulose	1071	[7]
1071	M	ν(CO) + δ(OH)	Polygalacturonic (pectic) acid H–Pec	1079	[4]
		C–N symmetric stretching	Caffeine	1080	[2]
		Stretching of the C–O–C bond and bending of the C–O–H bond	Vitamin C	1081	[8,9]
		a mode of coniferaldehyde unit	Native lignin	1134	[1]
1135	sh	ν (COC) glycosidic bond, ring	Polygalacturonic (pectic) acid H–Pec	1145	[4]
		C–N stretching	Caffeine	1131	[2]

The main constituents of cocoa liquor are lipids, since around 44% of its precursor (cocoa beans) corresponds to this type of molecule [53]. Triacylglycerols account for around 98% of cocoa lipids, and their composition differs between geographical origins [54, 55]. Cocoa butter is formed mainly by three triacylglycerols (TAG): glycerol–1–palmitate–2–oleate–3–stearate (POS); glycerol–1,3–distearate–2–oleate (SOS), and glycerol–1,3–dipalmitate–2–oleate (POP) [56]. Palmitic (C16:0), oleic (C18:1), stearic (C18:0) [57, 58], and linoleic (C18:2) [59] acids are the main components of TAGs cocoa butter fatty acid profile. In this sense, the Raman spectra of the cocoa liquor should also mainly be represented by the spectral signals of those compounds. Indeed, the Raman spectra of cocoa liquor exhibit the more intense bands at 1,071, 1,301, and 1,445 cm^{-1}, which occur at similar wavelengths found in fatty acid moieties reported previously in the literature and correspond to the C–C stretching, C–H twisting, and scissoring deformation modes, respectively [60].

In agreement, Raman measures conducted in cocoa butter evidenced bands in polymorphs from V at 1,063 and 1,297 assigned to the stretching v(C–C), skeletal, and $\tau(CH_2)$ twisting modes, respectively

[48]. Also, Raman peaks in several TAGs: tripalmitin, trimyristin, trilaurin, triundecanin, and triacetin showed a strong band due to the CH2 scissoring vibration at 1,445 cm^{-1} [61,62]. Therefore, the mentioned bands of cocoa liquor can be assigned to fatty acid groups and alkaloid moieties of cocoa triacylglycerols.

Additionally, it should be noted that most of the Raman bands occurring in lipid materials are ascribed to the acyl chain, which is why fatty acids spectra are similar to TAGs spectra containing them [63]. Fatty acids share the assignations aforementioned related to TAGs, and the following bands have been reported: between 1,050 and 1,150 cm^{-1} correspond to ν(C–C) stretching, at 1,296 cm^{-1} for $\delta(CH_2)$ twisting, and between 1,400 and 1,500 cm^{-1} for $\delta(CH_3)$ or $\delta(CH_2)$ deformations [64]. Literature has indicated that monosaturated and unsaturated fatty acids show peaks occurring in the same wave numbers, with the difference that the latter has broader bands.

Other Raman signals occurring in the assessed cocoa liquor spectra related to the fatty acid fractions include the band at 1,664 cm^{-1}, which can be assigned to the stretching of the C=C double bonds, and the 1,747 cm^{-1} one to the elongation of C=O of the ester carbonyl stretching mode [60]. Both spectral features in the spectrum of cocoa liquor seem to be typical of unsaturated fatty components, particularly oleic acid moiety (1,659 and 1,744 cm^{-1}) [65,66]. Therefore, these bands could be attributed to oleic acid moiety from cocoa liquor TAG, but the presence of other TAGs cannot be ruled out because the signals reported previously for other TAGs are very close (1,743 cm^{-1} for tripalmitin, 1,742 for trimyristin and trilaurin) [67].

The previous assignation of the C=O and C=C double bonds agrees with another work in cocoa butter that depicted peaks at 1,745.4 and 1,733.8 cm^{-1}, representing crystallization forms III and IV, respectively, which correspond to the region described for stretching vibrations due to C=O bonds. Also, the C=C stretching region exhibits a band at 1,662.7 cm^{-1} associated to the presence of oleic acid and representative of form IV of cocoa butter at room temperature [68]. Also, by the Raman spectra of their corresponding monoacid triglycerides reported in the literature, which assignations of C=O stretching vibrations are at 1,720–1,750 cm^{-1}, C=C stretching vibrations at 1,600–1,680 cm^{-1}, CH2 or CH3 group scissoring deformations at 1,400–1,500 cm^{-1}, CH2 twisting at approx. 1,300 cm^{-1} and C–C stretching vibrations at 1,060–1,090 and 1,110–1,180 cm^{-1} region [63].

Most identified predominant Raman features in the cocoa liquor spectra correspond to fatty components. However, peaks from other compounds present in cocoa liquor may be current. Some signals previously assigned to the fatty fraction may overlap with others corresponding to lignin, cellulose, hemicellulose, pectins, phenolic compounds, and alkaloids present in cocoa liquor in lower amounts. In this regard, weak signals corresponding to lignin may occur in cocoa liquor Raman spectra; based on, low values of the ratio between lipid and lignin in the inner surface of the cocoa nibs have been found [44]. The lignin features observed in the spectra appear at 356, 456, 539, 626,

779, 1,135, 1,220, 1,301, 1,362, 1,445, 1,603, and 1,659 cm^{-1}. Consistently, bands at similar wavelengths in native lignin spectra have been identified at 357, 463, 537, 634, 787, 1,134, 1,216, 1,297, 1,454, 1,602 and 1,658 cm^{-1} [69].

Most of the strongest bands of cellulose may not be visible in cocoa liquor samples due to the overlap of more intense ones corresponding to other compounds; for instance, cellulose and hemicellulose reported bands are expected to overlap with those of monolignol units of lignin [70]. However, some weak signals appear in the spectra at 356, 456, 989, 1,071, 1,108, 1,250, 1,301, 1,362, and 1,445 cm^{-1}, which are similar to those reported by softwood–cellulose at 351, 458 (some heavy atom stretching), 1,073, and 1,298 cm^{-1} [71]. Another study of regenerated cellulose II showed bands at 352, 456, 1,115, and 1,307 cm^{-1} some nearby the mentioned in softwood–cellulose. Similar wavelengths of some bands occurred in cellulose I from the bacterial origin [72] and, in *Valonia ventricosa* cellulose, bands at 366 and 462 (assignation not reported), 997 and 1,071 (assigned to C–O stretching ring modes), 1,249 (assignation not reported), 1,293 (CH_2 twisting), 1,359 (C–H deformation), and 1,454 (O–H deformation) cm^{-1} were distinguished [73]. Hemicellulose has similar chemical bonds to cellulose; hence their bands could be overlapped [74,75].

Pectins are plant cell wall polysaccharides formed by D–galacturonic acid [76]. Polygalacturonic (pectic) acid H–Pec spectra depicted bands at 537 and 621, 775 (ring 'breezing'), 853 ((C6–C5–O5–C1–O1)), 990 (γ(COOH)dimers), 1,079 (ν(CO) + δ(OH)), 1,105 (ν(CC)(CO)), 1,145 (ν(COC) glycosidic bond, ring), 1,254 (δ(CH)), 1,740 (ν(C=O) COOH) [77]. Cocoa liquor spectra showed bands in similar locations to the previously reported at 539, 626, 779, 860, 989, 1,071, 1,108, 1,135, 1,250 and 1,747 cm^{-1}. In addition, potassium pectate (K–Pec) depicted similar bands, differing in only one band (νas (COO–) that was at 1,607 cm^{-1} instead of 1,740 cm^{-1}.

Regarding polyphenolic compounds, cocoa, and chocolate have great contents of procyanidin flavonoids, catechin, and epicatechin [78]. Cocoa liquor may depict some Raman features that support its presence and are discussed below based on occurring peaks reported in the literature. Distinct spectral bands have been documented for polyphenolic compounds, encompassing aromatic ring vibrations within the range of 1,300 to 1,600 cm^{-1}. These vibrations arise from the stretching of a semicircle of the ring, accompanied by contractions in the other parts. Additionally, CH bends are observed between 1,400 to 1,500 cm^{-1}, and C–C ring vibrations result from the stretching of two opposing benzene ring quadrants, while the remaining quadrants contract, within the range of 1,500 to 1,600 cm^{-1} [79,80]. Flavonoid spectra revealed notable bands within the 1,570 to 1,700 cm^{-1} range [81]. Specifically, the band identified at 1,603 cm^{-1} in the spectra might correspond to vibrations arising from the aromatic ring's ν (C=C) of polyphenolic compounds [82].

Methylxanthines are the most abundant alkaloids in cocoa, theobromine, caffeine, and theophylline; together with polyphenols, they are responsible for the characteristic bitter taste [83–85]. The

similarity of the molecular structure of alkaloids gives rise to a resemblance in their Raman features, mainly in the range of 900 to 3,200 cm^{-1} [86]. Representative bands associated with alkaloids that were observed in the cocoa liquor spectra will be discussed next, even though most of them might overlap. Theobromine spectra depicted bands at 460, 620, 777, 946, 1,298, 1,360, 1,594 and 1,660 cm^{-1} [87,88]. Similar bands with slight shifts that corroborate the presence of this alkaloid in the analyzed samples were observed at 456, 626, 779, 940, 1,301, 1,362, 1,603, and 1,659 cm^{-1}; they could be assigned to δ (pyrimidine ring) + δ(CNO) + δ(CH) [87], C=C–C deformation [65], O=C–C deformation, $\rho(CH_3)$, ν(C–N) + $\rho(CH_3)$, ν(C=N) + ν(C–N), ν(C=C) + ν(C–N) + $\delta(CH_3)$ and C=O asymmetric stretching [87,88]; respectively.

Consistently, a study made with cocoa beans and their extracts reported some of the mentioned Raman bands at 459, 620, 776, 1,296, and 1,594 cm^{-1} and suggested that they constitute useful information to distinguish theobromine from theophylline [65,88]. All bands above 1,000 cm^{-1} may be overlapped with more intense ones, like those reported above. Caffeine Raman spectra depict bands at 225, 850, 975, 1,080, 1,131, 1,188, 1,241, 1,600, 1,656, and 1,700 cm^{-1} [88], while the cocoa liquor spectra of our study shows similar bands with slight shifts; this corroborates the presence of the mentioned alkaloid in the analyzed samples. The spectral bands found at 225, 860, 1,071, 1,135, 1,250, and 1,699 cm^{-1}, which are common in both cocoa varieties, could be linked to specific molecular vibrations, namely N–C–N deformation, N=C–H deformation, C–N symmetric stretching, C–N stretching, C–N stretching, and C=N stretching [88]. Moreover, the signals identified at 1,178, 1,603, and 1,659 cm^{-1} might be attributed to stretching vibrations involving C–C, C=C, and asymmetric C=O bonds [88].

The presence of organic acids in Ecuadorian cocoa liquor has also been evidenced [89]. The identified spectral bands at 225, 860, 1,071, 1,135, 1,250, and 1,699 cm^{-1}, which are commonly observed in both cocoa varieties, can be associated with specific molecular vibrations: N–C–N deformation, N=C–H deformation, C–N symmetric stretching, C–N stretching, C–N stretching, and C=N stretching [88]. Additionally, the signals found at 1,178, 1,603, and 1,659 cm^{-1} are likely linked to stretching vibrations involving C–C, C=C, and asymmetric C=O bonds [88]. Citric acid features may be present in the evaluated cocoa liquor spectra of both varieties at 456, 626, 1,108, 1,071, 1,250, 1,362, and 1,445 cm^{-1}, and in CCN–51 at 989, 1,108, 1,659 cm^{-1}.

On the other hand, Figure 2 (a) shows the score's scatter 3D plot for the cocoa liquor produced using low–intensity magnetic field–induced fermentation. At first glance, the data were rather scattered, especially for the samples that received large magnetic field doses (Figure 2, front location in the front view, or right–hand location in the top view). Although the lab conditions were as controlled as possible during the processing of the cocoa liquor, such data dispersion is probably due to the many variables involved in this experimental (non–commercial) processing. Notwithstanding this, the figure visibly demonstrates distinct differentiation among the samples based on the specific

magnetic field treatments they were subjected to. It must be noticed that the points corresponding to the largest magnetic field doses tend to separate the most from each other. This would tell that those samples were very different in their Raman responses, that is, in their composition and possible properties.

Figure 2(b) shows the contribution plot for the t0 samples (lower part) regarding the t4 samples (upper part) shown in Figure 2(a). This plot remarks on the variables explaining why the t0 samples deviate from the t4 samples. The intensity of the deviation is shown as bars/lines. This way, the larger the bars/lines values (in the Y axis), the larger the variable importance, and the sign of the line–sequence (down = minus and up = plus) indicates in which direction the variables deviate. The variables colored orange are outside the 3 std dev limit range; that means they are even more important variables.

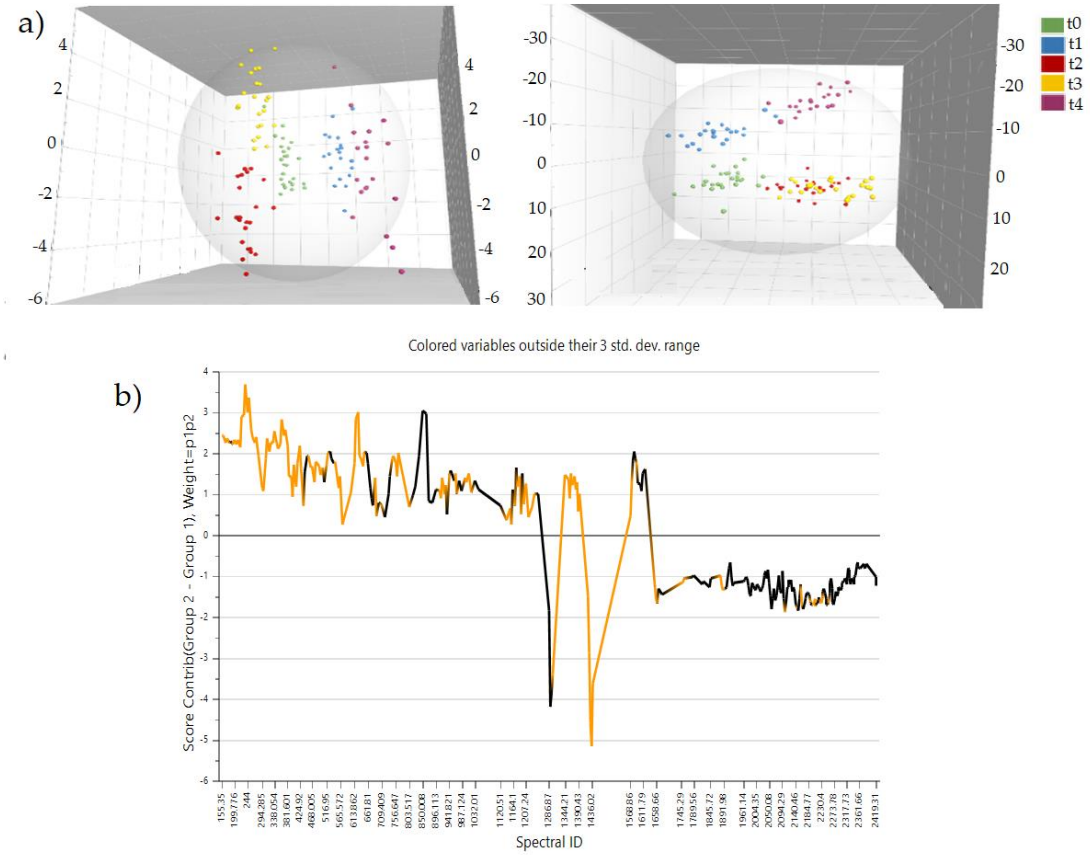

Figure 2. Chemometric analysis of the cocoa liquor produced using magnetic field–induced fermentation: (a) Front and top (right–wise rotated) views of the Scores Scatter 3D plot. The magnetic field is shown as t0 (0 mT), t1 (5 mT), t2 (48 mT), t3 (62 mT), and t4 (80 mT); (b) Contribution plot for the t0 samples (lower/positive side) regarding the t4 samples (upper/negative side). The orange–colored variables are outside the 3 Std Dev limit range.

The most important bands for the t0 samples were at 1,292 (related to the 0mT group), 1,297 (related to the $\tau(CH_2)$ of cocoa polymorphs [48]), 1,303, 1,431, 1,436, and 1,441 cm^{-1} (related to δCH_3) or $\delta(CH_2)$ of triolein and trilinolein reported at 1,440 [63]). The most important bands for the t4 were

at 225 (N–C–N deformation of caffeine), 231 (related to the 62mT group), 238, 244, 250, 363 (OH groups bending vibrations , out–of–plane γ(B) , γ(OH) of quercetin at 365 [92]), 620, 626 (C=C–C deformation of theobromine [65,88]), 739, 745, 751, 757, 768(O=C–C deformation of theophylline at 760 [88]), 850 (N=C–H deformation of caffeine [88]), 862, 1,344, 1,360 (ν(C=N) + ν(C–N) of theobromine [87]), 1,365, 1,370, 1,375, 1,380, 1,385, 1,390, 1,574, 1,579, 1,583, 1,588, 1,593 (C=C stretching of theobromine at 1,594 [65,88]), and 1,621 cm^{-1}.X

The most important bands for the non–irradiated samples were at 1,060 (related to the group), 1,065, 1,071 (related to ν(C–C) of cocoa butter polymorphs form V at 1,063 [46]), 1,098, 1,103 (ν(C–C) TAG triolein at 1,118 [72]), 1,124, 1,130 (ν(C–C) of cocoa butter [56]), 1,286, 1,291, 1,296, 1,301 (τ(CH_2) of cocoa butter polymorphs form V at 1,297 [46]), and 1,636.69 cm^{-1}. The most important bands for the 2.00 kGy irradiated samples were at 209 (related to the group), 248 (related to the group), 261, 324, 337, 350 (some heavy atom stretching of softwood–cellulose at 351[58]), 362, 437, 443, 449, 462 (δ(pyrimidine ring) + δ(CNO) + δ(CH) of theobromine at 460 [55]), 474, 486, 499, 523, 535 (OH groups bending vibrations, out–of–plane γ(B), γ(OH) of quercetin at 546 [91] also pectins), 548, 560, 608, 620 (C=C–C deformation of theobromine [52,59]), 632, 644, 656, 668, 680, 691, 738, 831, 842, 1,306 (τ(CH_2)of TAG triolein and trilinolein at 1,302 [72] and ν(C–N) + ρ(CH_3) of theobromine at 1,298 [55]), 1,311, 1,316, 1,337, and 1,357 (ν(C=N) + ν(C–N) of theobromine at 1,360 [55] cm^{-1}.

Figure 3(a) shows the score's scatter 3D plot for the cacao liquor produced after the irradiation of the CCN–51 samples of cocoa beans. The data was less scattered when compared to the set in Figure 2. The figure shows a good discrimination of the samples regarding the different irradiation doses they received, especially when the doses were higher.

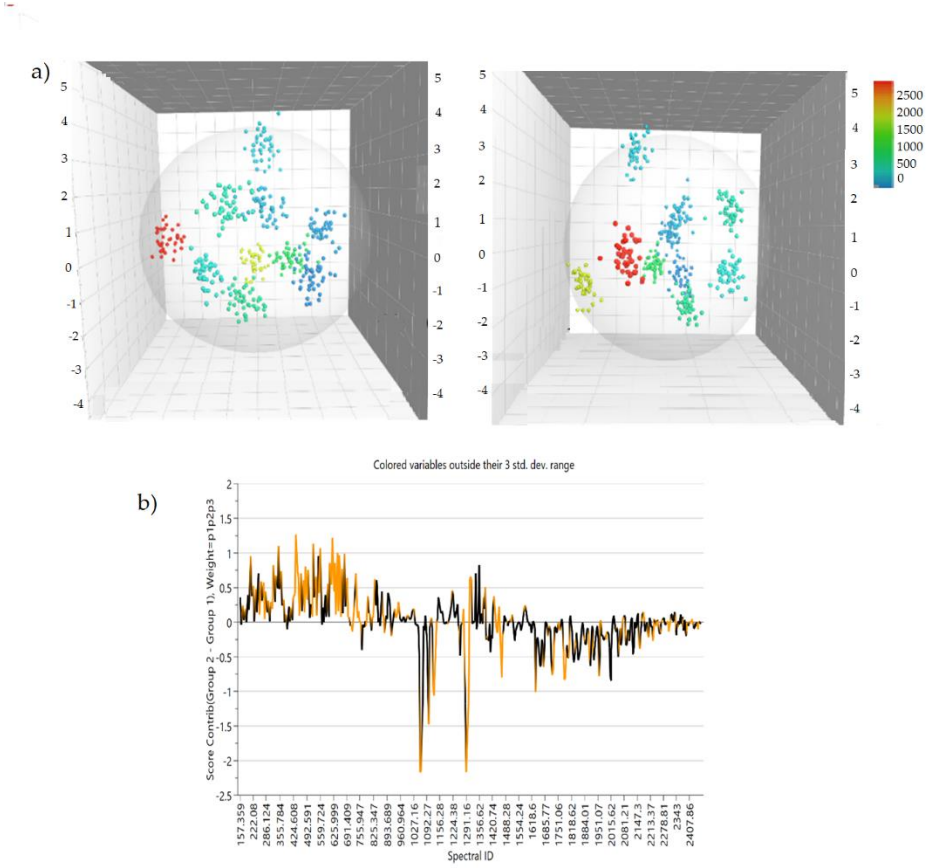

Figure 3. Chemometric analysis of the cocoa liquor produced after irradiating the CCN51 samples: (a) Front and right–rotated side views of the Scores Scatter 3D plot. The radiation doses were: 0.00, 0.10, 0.20, 0.30, 0.45, 0.60, 0.75, 1.00, 2.00, and 3.00 kGy; (b) contribution plot for the non–irradiated samples (lower/positive side) regarding the 2.00 kGy irradiated samples (upper/negative side). The orange–colored variables are outside the 3 StdDev limit range.

The front view (Figure 3(a), left) shows that the lower dose (darker blue) samples remained rather close to each other, which would indicate that those samples were less different from each other. This, in turn, would imply that their Raman responses were still similar at the macroscale, which suggests that their composition and possibly, their properties were also somehow similar at the macroscale. On the other hand, the two largest doses (yellow and red in Figure 3(b)) were completely separated from the rest of the samples and from each other. This tells us that these samples were very different in their Raman responses, both in their composition and in their properties. Figure 3(b) shows the contribution plot for the non–irradiated samples (lower part) regarding the 2.00 kGy irradiated samples (upper part), shown as the darkest blue and yellow dots in Figure 3, respectively. This plot remarks on the variables explaining why the non–irradiated samples deviate from the 2.00 kGy irradiated samples.

3.2. Sensorial attributes of cocoa liquor from gamma irradiated cocoa beans

The averages of the evaluated attributes in cocoa liquor prepared from irradiated beans of CCN–51

and National varieties are presented in Table S3 and Figure 4.

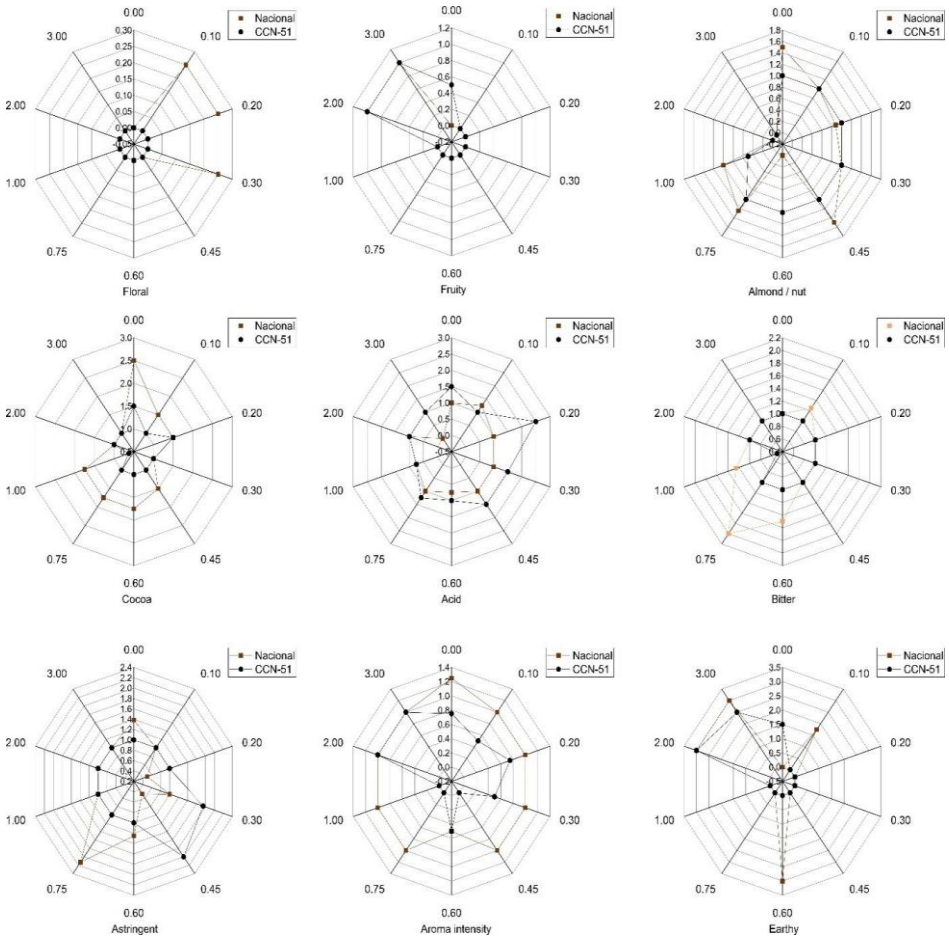

Figure 4. Sensory attributes of cocoa liquor from gamma–irradiated cocoa beans. The scales of the attributes are based on the intensity that has been generated after the treatments. Radiation treatments are represented on the radial axis in Gy, 0 corresponds to the control (non–irradiated).

Several odor–active compounds enable humans to perceive the characteristic chocolate flavor [93]. Cocoa presents basic flavors like acid, bitter, astringent, sweet, and salty, and specific flavors like cocoa, floral, nutty, and fruity. Chocolates appreciate and look for attributes such as floral, cocoa, sweet, and nutty since they give chocolate special notes [94].

The sensory attributes of fruity, almondy or nutty flavors, bitter and astringent flavors, and the aroma of tenseness exhibited a very mild intensity in the CCN–51 control sample. Additionally, the floral attribute was absent, while cocoa, acid, and earthy flavors showed a mild intensity. On the other hand, the National liquor control sample exhibited a medium intensity in the cocoa attribute and a mild intensity in the almondy or nutty flavor. Also, the fruity and floral attributes were absent, whereas the acid, bitter, and astringent flavors, and the aroma of tenseness showed a very mild intensity. The National variety demonstrated higher values regarding the almondy, cocoa, and astringent flavors, and the aroma's intensity.

The cocoa flavor depends on the genotype and on the preharvest (farming practices, environmental

conditions) and postharvest processing of the beans, stages in which specific aroma arises [83]. Concerning genotype, the bulk cocoa variety, CCN–51, devoid of the typical flavors and aromas of the fine varieties [95], while the National one, a fine variety, is known to have a distinctive sensory profile with floral and aromatic notes [83]. Different authors have highlighted its unique organoleptic quality [96].

Interestingly, the evaluated attributes in both cocoa varieties exhibited several changes in the irradiated samples. The very mild fruity attribute in the CCN–51 increased at 2.00 and 3.00 kGy. Therefore, it is inferred that radiation could enhance compounds responsible for the perception of this attribute, which is found in fine varieties but present in minimal quantities in CCN–51. For example, β–myrcene and β–cis–ocimene are compounds attributed to fruity flavor and floral aroma, respectively. β–myrcene (5.70 ± 1.00 %) and β–cis–ocimene (5.20 ± 0.70 %) are present in the pulp of the fine cocoa variety SCA6, whereas CCN–51 has less than 0.30% of these terpenes [95]. Other volatile compounds that have been found in CCN–51 are 2,3–butanediol, which is related to aroma, and acetophenone and 1–phenyl–2–ethanol that are linked to fruity and floral notes [97]. The fruity and floral attributes associated with the National cocoa variety were enhanced with the irradiation, since it made them more evident to the senses. This may be akin to the enhancement in ethyl ethanoate (fruit fragrance) in rice wine achieved with the increase in radiation dose [98].

Almondy flavor in CCN–51 was maintained with irradiation at doses up to 0.75 kGy, while at higher doses, it experienced a progressive decrease. In the National variety, this flavor decreased non–uniformly with ionization at different doses, except at 0.45 kGy, in which the initial value was maintained. There was a complete loss of the almondy attribute at 2.00 and 3.00 kGy in both varieties. Concerning the cocoa attribute in CCN–51, it diminished at all doses except at 0.20 kGy, in which the mild intensity remained similar to the control, while the greatest loss occurred at 1.00 kGy. In the National samples, this attribute decreased too, and the lowest values were found at 0.30, 2.00, and 3.00 kGy. Pyrazines, aldehydes, and esters are related to the nutty, cocoa aroma, and fruity flavors, respectively in cocoa and chocolate. Several aroma–active compounds in a cocoa liquor study identified tetramethylpyrazine, benzaldehyde, and 3,5–diethyl–2–methylpyrazine that confer nutty, almondy, and cocoa aromas; respectively [96]. Thus, an influence of radiation on the compounds responsible for the aforementioned attributes is inferred.

The findings demonstrated alterations in attribute intensity corresponding to the administered doses, mirroring the diverse impacts of radiation doses (ranging from 2.5 to 10.0 kGy) on irradiated salted and fermented anchovy sauce. The study concluded an increment in furan and alcohol content at the essayed doses, an increase in the concentration of aldehydes, esters, ketones, and S–containing compounds only at doses up to 7.5 kGy, and a reduction at higher ones. They suggested the radiolysis reactions of functional groups induced by the radiation at 10 kGy [99].

The mild acid taste of CCN–51 was maintained at 0.30 and 0.45 kGy, while it decreased at 0.60 kGy and higher doses. The largest reduction of this attribute occurred at 0.75 kGy, and an increase was observed at 0.20 kGy. The acid taste of the National variety is lower; this behavior was maintained at almost all the irradiation doses. This attribute increased at 0.10 kGy, decreased at 0.60 and 1.00, and was completely lost at 3.00 kGy. Acids generated during the fermentation process of cocoa, including lactic and acetic acids, contribute to acidic flavor notes, which are recognized as characteristic sensory attributes [95, 100]. Based on experimental data, it can be deduced that gamma irradiation could decrease the acidity of both varieties at 1.00 kGy and larger doses, to a greater extent in the CCN–51 variety. The increase in acidity could be due to the degradation of large fat molecules caused by the radiation, followed by the production of smaller ones, including free fatty acids [101]. On the other hand, the reduction in acidity might be a consequence of the hydrolytic decomposition of the acid groups produced by gamma rays [102, 103].

The behavior of bitterness and astringency attributes could be explained by changes in the content of antioxidants that may affect the sensory profile of cocoa liquor prepared from irradiated beans. Since plants and plant materials use their antioxidant system as a defense mechanism from the stress caused by the products of oxidative reactions, such as the free radicals released through gamma irradiation [104].

The mild bitter taste determined in the CCN–51 control sample was maintained at the different treatments and decreased solely at 1.00 kGy. In contrast, in the National variety, it increased at 0.10, 0.60, 0.75, and 1.00 kGy. The most remarkable increment was at 0.75 kGy, which may suggest that radiation also interacts with the compounds attributed to bitter taste. The presence of methylxanthines, namely theobromine and caffeine, provides the bitter taste consumers perceive in Amazonian cocoa and chocolate [105]. Indeed, alkaloids, flavonoid content, antioxidant activity, and phenolic compounds have increased in gamma–irradiated seeds [106, 107]. Besides, a correlation between total polyphenol content and bitter flavor has been established [108]. This may explain the increasing bitter taste in cocoa liquor obtained from irradiated beans. Conversely, a study of gamma–irradiated monsoon coffee suggested an increasing degradation of chlorogenic acid with the dose [109], which may explain the reduction of the bitter taste in the evaluated cocoa liquors.

The astringency in CCN–51 only changed at 0.30 and 0.45 kGy, doses at which the attribute increased. In the National variety, it decreased in all the treatments, except at 0.75 kGy. The reduction in the cocoa bean's astringency could improve its palatability, since an increase in bitterness, astringency, and acidity (due to an inappropriate fermentation) could negatively affect the cocoa flavor and other attributes [94]. The aroma intensity in CCN–51 was completely lost when doses of 0.45, 0.75, and 1.00 kGy were used, but it increased at 2.00 and 3.00 kGy. Unlike what was observed in the bulk variety, the aroma decreased in all the radiation treatments with the National variety, with a maximum reduction of 0.60 kGy.

Other authors have also found a difference in the flavor profile in irradiated samples. A study of dried scallions exposed separately to three irradiation sources and subsequently assessed by electronic sensing (e–nose and e–tongue) concluded that the irradiation treatments affected the amounts of the identified volatile compounds. A notable increase associated with the aroma profile was found at 4 and 7 kGy, while the perception of taste attributes increased at the last dose (7 kGy) for samples irradiated in an e–beam and with gamma rays. There was a detectable change in the volatile compound profile during gamma–ray treatment [110]. Kakdugi samples prepared with red pepper powder ionized with gamma rays at doses of 0 (control), 3, 5, and 7 kGy were grouped into four different clusters after e–nose analysis at the beginning of the fermentation process. This could have been due to the influence of radiation on its odor molecules [111]. Grapes subjected to gamma irradiation at 0.67, 1.30, 2.00, and 2.70 kGy exhibited an increment in anthocyanin concentrations at the higher doses, contrary to the maintained flavonoids and flavonols. The concentrations of aroma compounds associated with fruity and floral notes showed an increase at the first three doses [112].

The increase in the perception of aroma attributes may be explained by the influence of radiation in compound bonds. Since bounded glucosides in grapevine are identified as odorless in contrast with free volatile compounds [112, 113]. Besides, a study on irradiated nutmeg concluded that glycosides responsible for aroma in nutmeg were broken down by irradiation, resulting in an enhancement in the content of volatile compounds [112, 114].

Both cocoa varieties showed a rancid flavor in the samples irradiated at 1.00 kGy, and it was more intense at 2.00 and 3.00 kGy. This could be attributed to the interaction of the triacylglycerol fatty acids with gamma rays; in particular, unsaturated fatty acids are susceptible to radiation, and they generate products that contribute to rancidity [115]. A dependence on the type and content of unsaturated fatty acids has been reported [116,117].

4. Conclusions

To the best of our knowledge, this study is the first to assess the influence of an induced magnetic field during cocoa bean fermentation on the constituents of the liquor obtained from them and the influence of the ionization of fermented cocoa beans with gamma rays on the flavor constituents of the liquor. Raman's spectroscopy enables the identification of compounds that are present in cocoa liquor. Raman's bands were attributed to lipid and lignocellulosic compounds, pectin, flavonoids, theobromine, and organic acids. Also, the irradiation dose, the electric field intensity, and the cocoa variety can be discriminated using chemometric tools. Therefore, the potential application of this spectroscopic tool to identify and evaluate irradiated foods, products exposed to induced magnetic fields during fermentation, and chocolate products have been demonstrated. Cocoa constituents exhibited interactions with gamma rays that may be translated into changes in the sensory profile of the resulting cocoa liquors, which are perceptible to human senses. In this regard, sensory attributes

exhibited variable behaviors depending on the dose, and in some of them, a marked tendency (i.e. rancid) was observed at 1 kGy and higher doses. All in all, radiation an influence on cocoa bean constituents and compounds responsible for sensory attributes in cocoa liquor prepared with irradiated National and CCN–51 cocoa beans. The determination of a dose that provides the irradiation benefits and preserves the cocoa's nutritional and flavor attributes should be pursued in future research.

Regarding the induced magnetic field in cocoa fermentation, further experiments are needed to find out and explain the variables responsible for the data dispersion, which would help to improve the cocoa liquor processing.

Supplementary Materials: Figure S1: Schematic representation of the dosimeter at four positions in the plastic trays, identification of the maximum and minimum dose and DUR calculus at each irradiation treatment; Figure S2: Location of 4 dosimeters at A, B, C, and D position in the plastic tray containing cocoa beans in each treatment; table S1: Time treatment, dose, dosimeter readings, and Dose Uniformity Rates (DUR) of irradiated Nacional cocoa beans; table S2: Time treatment, dose, dosimeter readings, and Dose Uniformity Rates (DUR) of irradiated CCN–51 cocoa beans and table S3: Averages of the evaluated attributes in cocoa liquor obtained from fermented and dried beans irradiated at different doses for varieties CCN–51 and National.

Author Contributions: For research articles with several authors, a short paragraph specifying their individual contributions must be provided. The following statements should be used Conceptualization, T.M.G.–A. and L.R; methodology, C.C, and J.R; software, J.B; validation, M.S, E.V., and E.V; formal analysis, P.V.; investigation, V.C.; resources, F.O.; data curation, G.M.; writing—original draft preparation, A.P; writing—review and editing, A.E; visualization, L.R; supervision, G.M; project administration, A.P; funding acquisition, A.E. All authors have read and agreed to the published version of the manuscript. Please turn to the CRediT taxonomy for the term explanation. Authorship must be limited to those who have contributed substantially to the work reported.

Acknowledgments: To Programa de Reactivación de Café y Cacao of Ministerio de Agricultura y Ganadería (Ecuador) for providing the samples for the study. To the Centro de Investigación de Alimentos, CIAL of the Universidad UTE (Ecuador), and Escuela Politécnica Nacional (Ecuador) for the academic and technical support provided to this project. Octavio Cordova for his technical support in the OMF–device validation process.

Conflicts of Interest: Declare conflicts of interest or state The authors declare no conflict of interest.

References

1. Sarbu, I. & Csutak, O. The Microbiology of Cocoa Fermentation. In *Caffeinated and Cocoa Based Beverages: Volume 8. The Science of Beverages*; Grumezescu, A.M., Holban, A.M., Eds.; Elsevier, **2019**; pp. 423–446 ISBN 9780128158647

2. Beg, M.S.; Ahmad, S.; Jan, K. & Bashir, K. Status, Supply Chain and Processing of Cocoa – A Review. *Trends Food Sci. Technol.* **2017**, *66*, 108–116, https://doi.org/10.1016/j.tifs.2017.06.007

3. Gunaratne, T.M.; Gonzalez Viejo, C.; Fuentes, S.; Torrico, D.D.; Gunaratne, N.M.; Ashman, H. & Dunshea, F.R. Development of Emotion Lexicons to Describe Chocolate Using the Check–All–That–Apply (CATA) Methodology across Asian and Western Groups. *Food Res. Int.* **2019**, *115*, 526–534.

4. Sepúlveda, W.S.; Maza, M.T.; Uldemolins, P.; Cantos–Zambrano, E.G. & Ureta, I. Linking Dark Chocolate Product Attributes, Consumer Preferences, and Consumer Utility: Impact of Quality Labels, Cocoa Content, Chocolate Origin, and Price. **2021**, *34*, 518–537, https://doi.org/10.1080/08974438.2021.1908924

5. Le Gresley, A. & Peron, J.M.R. A Semi–Automatic Approach to the Characterization of Dark Chocolate by Nuclear Magnetic Resonance and Multivariate Analysis. *Food Chem.* **2019**, *275*, 385–389, https://doi.org/10.1016/j.foodchem.2018.09.089

6. Toker, O.S.; Pirouzian, H.R.; Palabiyik, I. & Konar, N. Chocolate Flow Behavior: Composition and Process Effects. *https://doi.org/10.1080/10408398.2021.1993782* **2021**, https://doi.org/10.1080/10408398.2021.1993782

7. Mahunu, G.K.; Afoakwah, N.A.; Mariod, A.A.; Hudu, A.R. & Tahir, H.E. Fermentation of Cocoa Bean. *African Fermented Food Prod. New Trends* **2022**, 473–485, https://doi.org/10.1007/978–3–030–82902–5_31/COVER

8. Almeida, O.G.G.; Pinto, U.M.; Matos, C.B.; Frazilio, D.A.; Braga, V.F.; von Zeska–Kress, M.R. & De Martinis, E.C.P. Does Quorum Sensing Play a Role in Microbial Shifts along Spontaneous Fermentation of Cocoa Beans? An in Silico Perspective. *Food Res. Int.* **2020**, *131*, 109034, https://doi.org/10.1016/J.FOODRES.2020.109034

9. Gutiérrez–Ríos, H.G.; Suárez–Quiroz, M.L.; Hernández–Estrada, Z.J.; Castellanos–Onorio, O.P.; Alonso–Villegas, R.; Rayas–Duarte, P.; Cano–Sarmiento, C.; Figueroa–Hernández, C.Y. & González–Rios, O. Yeasts as Producers of Flavor Precursors during Cocoa Bean Fermentation and Their Relevance as Starter Cultures: A Review. *Ferment. 2022, Vol. 8, Page 331* **2022**, *8*, 331, https://doi.org/10.3390/FERMENTATION8070331

10. Guo, L.; Azam, S.M.R.; Guo, Y.; Liu, D. & Ma, H. Germicidal Efficacy of the Pulsed Magnetic Field against Pathogens and Spoilage Microorganisms in Food Processing: An Overview. *Food Control* **2022**, *136*, 108496, https://doi.org/10.1016/J.FOODCONT.2021.108496

11. Guo, L.; Guo, Y.; Wu, P.; Liu, S.; Gu, C.; Yolandani; Wu, M.; Ma, H. & He, R. Enhancement of Polypeptide Yield Derived from Rapeseed Meal with Low–Intensity Alternating Magnetic Field. *Foods 2022, Vol. 11, Page 2952* **2022**, *11*, 2952, https://doi.org/10.3390/FOODS11192952

12. Guzmán–Armenteros, T.M.; Ramos–Guerrero, L.A.; Guerra, L.S.; Weckx, S. & Ruales, J. Optimization of Cacao Beans Fermentation by Native Species and Electromagnetic Fields. *Heliyon* **2023**, *9*, e15065, https://doi.org/10.1016/J.HELIYON.2023.E15065

13. Abinaya, S.; Panghal, A.; Roopa, H.; Chhikara, N.; Kumari, A. & Gehlot, R. Utilization of Magnetic Fields in Food Industry. In *Novel Technologies in Food Science*; Chhikara Navnidhi, Panghal Anil, Chaudhary Gaurav, Eds.; John Wiley & Sons, Ltd: Hoboken, **2023**; pp. 171–233 ISBN 9781119776376.

14. Li, W.; Ma, H.; He, R.; Ren, X. & Zhou, C. Prospects and Application of Ultrasound and Magnetic Fields in the Fermentation of Rare Edible Fungi. *Ultrason. Sonochem.* **2021**, *76*, 105613, https://doi.org/10.1016/J.ULTSONCH.2021.105613

15. Shuo, T.; Yumeng, Y.; Leilei, Y.; Yanhui, H.; Chao, Y.; Hua, Y.; Yuan, X.; Zhaoqian, J.; Cuicui, H. & Hongyan, Z. Static Magnetic Field Induces Abnormality of Glucose Metabolism in Rats' Brain and Results in Anxiety–like Behavior. *J. Chem. Neuroanat.* **2021**, *113*, 101923, https://doi.org/10.1016/J.JCHEMNEU.2021.101923

16. Rosen, A.D. Mechanism of Action of Moderate–Intensity Static Magnetic Fields on Biological Systems. *Cell Biochem. Biophys.* **2003**, *39*, 163–173, https://doi.org/10.1385/CBB:39:2:163

17. Del Rio, D.; Rodriguez–Mateos, A.; Spencer, J.P.E.; Tognolini, M.; Borges, G. & Crozier, A. Dietary (Poly)Phenolics in Human Health: Structures, Bioavailability, and Evidence of Protective Effects against Chronic Diseases. *Antioxidants Redox Signal.* **2013**, *18*, 1818–1892. https://doi.org/10.1089/ars.2012.4581

18. Martini, S.; Conte, A. & Tagliazucchi, D. Comprehensive Evaluation of Phenolic Profile in Dark Chocolate and Dark Chocolate Enriched with Sakura Green Tea Leaves or Turmeric Powder. *Food Res. Int.* **2018**, *112*, 1–16, https://doi.org/10.1016/j.foodres.2018.06.020

19. Żyżelewicz, D.; Bojczuk, M.; Budryn, G.; Zduńczyk, Z.; Juśkiewicz, J.; Jurgoński, A. & Oracz, J. Influence of Diet Based on Bread Supplemented with Raw and Roasted Cocoa Bean Extracts on Physiological Indices of Laboratory Rats. *Food Res. Int.* **2018**, *112*, 209–216,

https://doi.org/10.1016/j.foodres.2018.06.039

20. Van Der Velpen, V.; Wolkers–Rooijackers, J.C.M.; Zwietering, M. & Nout, M.J.R. Microbiota Dynamics and Diversity at Different Stages of Industrial Processing of Cocoa Beans into Cocoa Powder. **2016**, https://doi.org/10.1128/AEM.07691–11

21. Inamura, P.Y.; Uehara, V.B.; Teixeira, C.A.H.M. & del Mastro, N.L. Mediate Gamma Radiation Effects on Some Packaged Food Items. *Radiat. Phys. Chem.* **2012**, *81*, 1144–1146, https://doi.org/10.1016/j.radphyschem.2012.01.022

22. Fernandes, Â.; Barreira, J.C.M.; Günaydi, T.; Alkan, H.; Antonio, A.L.; Oliveira, M.B.P.P.; Martins, A. & Ferreira, I.C.F.R. Effect of Gamma Irradiation and Extended Storage on Selected Chemical Constituents and Antioxidant Activities of Sliced Mushroom. *Food Control* **2017**, *72*, 328–337, https://doi.org/10.1016/j.foodcont.2016.04.044 .

23. Farkas, J.; Ehlermann, D.A.E. & Mohácsi–Farkas, C. Food Technologies: Food Irradiation. In *Encyclopedia of Food Safety*; Elsevier, **2014**; Vol. 3, pp. 178–186 ISBN 9780123786128.

24. Bashir, K.; Aggarwal, M. Physicochemical, Structural and Functional Properties of Native and Irradiated Starch: A Review. *J. Food Sci. Technol.* **2019**, *56*, 513–523. https://doi.org/10.1007/s13197–018–3530–2

25. Dileep Sean, Y. & Manasa, K. Irradiation in Food Processing: A Review. *J. Pharmacogn. Phytochem.* **2018**, 905–912. https://www.phytojournal.com/special–issue?year=2018&vol=7&issue=1S&ArticleId=3244

26. Calado, T.; Venâncio, A. & Abrunhosa, L. Irradiation for Mold and Mycotoxin Control: A Review. *Compr. Rev. Food Sci. Food Saf.* **2014**, *13*, 1049–1061, https://doi.org/10.1111/1541–337.12095 .

27. Prakash, A. What Is the Benefit of Irradiation Compared to Other Methods of Food Preservation? In *Genetically Modified and Irradiated Food*; Elsevier, **2020**; pp. 217–231, https://doi.org/10.1016/B978–0–12–817240–7.00013–9

28. Hallman, G.J. Process Control in Phytosanitary Irradiation of Fresh Fruits and Vegetables as a Model for Other Phytosanitary Treatment Processes. *Food Control* **2017**, *72*, 372–377, https://doi.org/10.1016/j.foodcont.2016.02.010

29. Stefanova, R.; Vasilev, N. V. & Spassov, S.L. Irradiation of Food, Current Legislation Framework, and Detection of Irradiated Foods. *Food Anal. Methods* **2010**, *3*, 225–252, https://doi.org/10.1007/s12161–009–9118–8

30. Stewart, E.M. Food Irradiation Chemistry. In *Food Irradiation: Principles and Applications*; Molins, R.A., Ed.; John Wiley & Sons Inc: Toronto, **2001**; pp. 37–76 ISBN ISBN 0–471–35634–4 C.

31. World Health Organization. *High–Dose Irradiation: Wholesomeness of Food Iradiatied with Doses above 10 KGy;* Geneva, 1999; ISBN 9789241208901

32. Zhao, L. & Wang, S. Developing Treatment Protocols for Disinfesting Pine Wood Product Using Radio Frequency Energy. *Eur. J. Wood Wood Prod.* **2018**, *76*, 191–200, https://doi.org/10.1007/s00107–017–1189–4

33. Ferrier, P. Irradiation as a Quarantine Treatment. *Food Policy* **2010**, *35*, 548–555, https://doi.org/10.1016/j.foodpol.2010.06.001

34. Maherani, B.; Hossain, F.; Criado, P.; Ben–Fadhel, Y.; Salmieri, S. & Lacroix, M. World Market Development and Consumer Acceptance of Irradiation Technology. *Foods* **2016**, *5*, 79, https://doi.org/10.3390/foods5040079

35. Braga, S.C.G.N.; Oliveira, L.F.; Hashimoto, J.C.; Gama, M.R.; Efraim, P.; Poppi, R.J. & Augusto, F. Study of Volatile Profile in Cocoa Nibs, Cocoa Liquor and Chocolate on Production Process Using GC × GC–QMS. *Microchem. J.* **2018**, *141*, 353–361, https://doi.org/10.1016/j.microc.2018.05.042 .

36. Toker, O.S.; Palabiyik, I. & Konar, N. Chocolate Quality and Conching. *Trends Food Sci. Technol.* **2019**, *91*, 446–453, https://doi.org/10.1016/j.tifs.2019.07.047

37. Hinneh, M.; Abotsi, E.E.; Van de Walle, D.; Tzompa–Sosa, D.A.; De Winne, A.; Simonis, J.; Messens, K.; Van Durme, J.; Afoakwa, E.O. & De Cooman, L. Pod Storage with Roasting: A Tool to Diversifying the Flavor Profiles of Dark Chocolates Produced from 'Bulk' Cocoa Beans? (Part II: Quality and Sensory Profiling of Chocolates). *Food Res. Int.* **2020**, *132*, 109116, https://doi.org/10.1016/j.foodres.2020.109116

38. Silva, R. D. C. D. S. N. D., Minim, V. P. R., Carneiro, J. D. D. S., Nascimento, M., Della Lucia, S. M., & Minim, L. A. Quantitative sensory description using the Optimized Descriptive Profile: Comparison with conventional and alternative methods for evaluation of chocolate. Food Quality and Preference. **2013**, 30(2), 169–179. https://doi.org/10.1016/j.foodqual.2013.05.011

39. Suzuki, R.M.; Montanher, P.F.; Visentainer, J.V.; de Souza, N.E. Composição Centesimal e Quantificação de Ácidos Graxos Nas Cinco Maiores Marcas de Chocolates Do Brasil. *Cienc. e Tecnol. Aliment.* **2011**, *31*, 541–546, https://doi.org/10.1590/S0101–20612011000200040

40. Stohner, J.; Zucchetti, B.; Deuber, F.; Hobi, F.; Lukas, B. & Suter, M. *Newfood*. 2012, pp. 21–28.

41. Nunes, C.A. Vibrational Spectroscopy and Chemometrics to Assess Authenticity, Adulteration and Intrinsic Quality Parameters of Edible Oils and Fats. *Food Res. Int.* **2014**, *60*, 255–261. https://doi.org/10.1016/j.foodres.2013.08.041

42. Vargas Jentzsch, P.; Ciobotă, V.; Salinas, W.; Kampe, B.; Aponte, P.M.; Rösch, P.; Popp, J. & Ramos, L.A. Distinction of Ecuadorian Varieties of Fermented Cocoa Beans Using Raman Spectroscopy. *Food Chem.* **2016**, *211*, 274–280, https://doi.org/10.1016/j.foodchem.2016.05.017

43. Li, Y.S. & Church, J.S. Raman Spectroscopy in the Analysis of Food and Pharmaceutical Nanomaterials. *J. Food Drug Anal.* **2014**, *22*, 29–48, https://doi.org/10.1016/j.jfda.2014.01.003

44. Yaseen, T.; Sun, D.W. & Cheng, J.H. Raman Imaging for Food Quality and Safety Evaluation: Fundamentals and Applications. *Trends Food Sci. Technol.* **2017**, *62*, 177–189, https://doi.org/10.1016/j.tifs.2017.01.012

45. Celedón, A. & Aguilera, J.M. Applications of Microprobe Raman Spectroscopy in Food Science. *Food Sci. Technol. Int.* **2002**, *8*, 101–108, https://doi.org/10.1106/108201302024208

46. Bresson, S.; Rousseau, D.; Ghosh, S.; Marssi, M. El. & Faivre, V. Raman Spectroscopy of the Polymorphic Forms and Liquid State of Cocoa Butter. *Eur. J. Lipid Sci. Technol.* **2011**, *113*, 992–1004, https://doi.org/10.1002/ejlt.201100088

47. Sonwai, S.; Podchong, P. & Rousseau, D. Crystallization Kinetics of Cocoa Butter in the Presence of Sorbitan Esters. *Food Chem.* **2017**, *214*, 497–506, https://doi.org/10.1016/j.foodchem.2016.07.092

48. De Oliveira, L.N. & De Jesus Coelho Castro, R.; De Oliveira, M.A.L.; De Oliveira, L.F.C. Lipid Characterization of White, Dark, and Milk Chocolates by FT–Raman Spectroscopy and Capillary Zone Electrophoresis. *J. AOAC Int.* **2015**, *98*, 1598–1607, https://doi.org/10.5740/jaoacint.15–083

49. Kiumarsi, M.; Majchrzak, D.; Jäger, H.; Song, J.; Lieleg, O. & Shahbazi, M. Comparative Study of Instrumental Properties and Sensory Profiling of Low–Calorie Chocolate Containing Hydrophobically Modified Inulin. Part II: Proton Mobility, Topological, Tribological and Dynamic Sensory Properties. *Food Hydrocoll.* **2021**, *110*, 106144, https://doi.org/10.1016/J.FOODHYD.2020.106144

50. Agarwal, U.P.; Ralph, S.A. & Atalla, H. FT Raman Spectroscopic Study of Softwood Lignin.

In Proceedings of the 9th International Symposium on Wood and Pulping Chemistry; Montreal, **1997**; pp. 8–1, https://www.fpl.fs.usda.gov/documnts/pdf1997/agarw97c.pdf

51. Synytsya, A.; Čopíková, J.; Matějka, P. & Machovič, V. Fourier Transform Raman and Infrared Spectroscopy of Pectins. *Carbohydr. Polym.* **2003**, *54*, 97–106, https://doi.org/10.1016/S0144–617(03)00158–9 .

52. Gunasekaran, S.; Sankari, G. & Ponnusamy, S. Vibrational Spectral Investigation on Xanthine and Its Derivatives—Theophylline, Caffeine and Theobromine. *Spectrochim. Acta Part A Mol. Biomol. Spectrosc.* **2005**, *61*, 117–127, https://doi.org/10.1016/J.SAA.2004.03.030

53. Jehlička, J.; Vítek, P. & Edwards, H.G.M. Raman Spectra of Organic Acids Obtained Using a Portable Instrument at −5 °C in a Mountain Area at 2000 m above Sea Level. *J. Raman Spectrosc.* **2009**, n/a–n/a, https://doi.org/10.1002/jrs.2450

54. Yohannan Panicker, C.; Tresa Varghese, H. & Philip, D. FT–IR, FT–Raman and SERS Spectra of Vitamin C. *Spectrochim. Acta – Part A Mol. Biomol. Spectrosc.* **2006**, *65*, 802–804, https://doi.org/10.1016/j.saa.2005.12.044

55. Edwards, H.G.M.; Munshi, T. & Anstis, M. Raman Spectroscopic Characterisations and Analytical Discrimination between Caffeine and Demethylated Analogues of Pharmaceutical Relevance. *Spectrochim. Acta – Part A Mol. Biomol. Spectrosc.* **2005**, *61*, 1453–1459, https://doi.org/10.1016/j.saa.2004.10.022 .

56. Bresson, S.; Lecuelle, A.; Bougrioua, F.; El Hadri, M.; Baeten, V.; Courty, M.; Pilard, S.; Rigaud, S. & Faivre, V. Comparative Structural and Vibrational Investigations between Cocoa Butter (CB) and Cocoa Butter Equivalent (CBE) by ESI/MALDI–HRMS, XRD, DSC, MIR and Raman Spectroscopy. *Food Chem.* **2021**, *363*, 130319, https://doi.org/10.1016/J.FOODCHEM.2021.130319 .

57. Blackwell, J.; Vasko, P.D. & Koenig, J.L. Infrared and Raman Spectra of the Cellulose from the Cell Wall of Valonia Ventricosa. *J. Appl. Phys.* **1970**, *41*, 4375–4379, https://doi.org/10.1063/1.1658470

58. Agarwal, U.P. An Overview of Raman Spectroscopy as Applied to Lignocellulosic Materials. In *Advances in lignocellulosics characterization*; **1999**; pp. 201–225. https://www.fpl.fs.usda.gov/documnts/pdf1999/agarw99a.pdf

59. Edwards, H.G.M.; Villar, S.E.J.; De Oliveira, L.F.C. & Le Hyaric, M. Analytical Raman Spectroscopic Study of Cacao Seeds and Their Chemical Extracts. *Anal. Chim. Acta* **2005**, *538*, 175–180, https://doi.org/10.1016/j.aca.2005.02.039

60. Kobayashi, M. Crystallization and Polymorphism of Fats and Fatty Acids. In *Vibrational spectroscopic aspects of polymorphism and phase transition of fats and fatty acids*; Garty, N.., Sato, K., Eds.; Marcel Dekker: New York, **1988**. https://doi.org/10.1021/j100281a062

61. Bresson, S.; El Marssi, M. & Khelifa, B. Raman Spectroscopy Investigation of Various Saturated Monoacid Triglycerides. *Chem. Phys. Lipids* **2005**, *134*, 119–129, https://doi.org/10.1016/j.chemphyslip.2004.12.009

62. Mazurek, S.; Fecka, I.; Węglińska, M. & Szostak, R. Quantification of Active Ingredients in Potentilla Tormentilla by Raman and Infrared Spectroscopy. *Talanta* **2018**, *189*, 308–314, https://doi.org/10.1016/J.TALANTA.2018.07.012

63. Torres–Moreno, M.; Torrescasana, E.; Salas–Salvadó, J. & Blanch, C. Nutritional Composition and Fatty Acids Profile in Cocoa Beans and Chocolates with Different Geographical Origin and Processing Conditions. *Food Chem.* **2015**, *166*, 125–132, https://doi.org/10.1016/j.foodchem.2014.05.141

64. Lipp, M. & Anklam, E. Review of Cocoa Butter and Alternative Fats for Use in Chocolate—Part A. Compositional Data. *Food Chem.* **1998**, *62*, 73–97, https://doi.org/10.1016/S0308–8146(97)00160–X

65. Sirbu, D.; Corno, M.; Ullrich, M.S. & Kuhnert, N. Characterization of Triacylglycerols in Unfermented Cocoa Beans by HPLC–ESI Mass Spectrometry. *Food Chem.* **2018**, *254*, 232–240, https://doi.org/10.1016/j.foodchem.2018.01.194 .

66. Asep, E.K.; Jinap, S.; Jahurul, M.H.A.; Zaidul, I.S.M. & Singh, H. Effects of Polar Cosolvents on Cocoa Butter Extraction Using Supercritical Carbon Dioxide. *Innov. Food Sci. Emerg. Technol.* **2013**, *20*, 152–160, https://doi.org/10.1016/j.ifset.2013.06.010

67. Bresson, S.; Rousseau, D.; Ghosh, S.; El Marssi, M. & Faivre, V. Raman Spectroscopy of the Polymorphic Forms and Liquid State of Cocoa Butter. *Eur. J. Lipid Sci. Technol.* **2011**, *113*, 992–1004, https://doi.org/10.1002/ejlt.201100088

68. Ghazani, S.M. & Marangoni, A.G. Molecular Origins of Polymorphism in Cocoa Butter. **2021**, *12*, 567–590, https://doi.org/10.1146/ANNUREV–FOOD–070620–022551

69. Saldaña, M.D.A.; Mohamed, R.S. & Mazzafera, P. Extraction of Cocoa Butter from Brazilian Cocoa Beans Using Supercritical CO2 and Ethane. *Fluid Phase Equilib.* **2002**, *194–197*, 885–894, https://doi.org/10.1016/S0378–3812(01)00719–1

70. Mohamed, I.O. Enzymatic Synthesis of Cocoa Butter Equivalent from Olive Oil and Palmitic–

Stearic Fatty Acid Mixture. *Appl. Biochem. Biotechnol.* **2015**, *175*, 757–769, https://doi.org/10.1007/S12010–014–1312–5/METRICS

71. Jahurul, M.H.A.; Zaidul, I.S.M.; Norulaini, N.A.N.; Sahena, F.; Jinap, S.; Azmir, J.; Sharif, K.M. & Mohd Omar, A.K. Cocoa Butter Fats and Possibilities of Substitution in Food Products Concerning Cocoa Varieties, Alternative Sources, Extraction Methods, Composition, and Characteristics. *J. Food Eng.* **2013**, *117*, 467–476, https://doi.org/10.1016/j.jfoodeng.2012.09.024

72. Czamara, K.; Majzner, K.; Pacia, M.Z.; Kochan, K.; Kaczor, A. & Baranska, M. Raman Spectroscopy of Lipids: A Review. *J. Raman Spectrosc.* **2015**, *46*, 4–20, https://doi.org/10.1002/jrs.4607

73. De Gelder, J.; De Gussem, K.; Vandenabeele, P. & Moens, L. Reference Database of Raman Spectra of Biological Molecules. *J. Raman Spectrosc.* **2007**, *38*, 1133–1147, https://doi.org/10.1002/jrs.1734

74. Yang, D. & Ying, Y. Applications of Raman Spectroscopy in Agricultural Products and Food Analysis: A Review. *Appl. Spectrosc. Rev.* **2011**, *46*, 539–560. https://doi.org/10.1080/05704928.2011.593216

75. Bresson, S.; El Marssi, M. & Khelifa, B. Conformational Influences of the Polymorphic Forms on the CO and C–H Stretching Modes of Five Saturated Monoacid Triglycerides Studied by Raman Spectroscopy at Various Temperatures. *Vib. Spectrosc.* **2006**, *40*, 263–269, https://doi.org/10.1016/j.vibspec.2005.11.001

76. Castro–Alayo, E.M.; Torrejón–Valqui, L.; Cayo–Colca, I.S. & Cárdenas–Toro, F.P. Evaluation of the Miscibility of Novel Cocoa Butter Equivalents by Raman Mapping and Multivariate Curve Resolution–Alternating Least Squares. *Foods* **2021**, *10*, 3101, https://doi.org/10.3390/FOODS10123101/S1

77. Agarwal, U.P.; McSweeny, J.D. & Ralph, S.A. FT–Raman Investigation of Milled–Wood Lignins: Softwood, Hardwood, and Chemically Modified Black Spruce Lignins. *J. Wood Chem. Technol.* **2011**, *31*, 324–344, https://doi.org/10.1080/02773813.2011.562338

78. Schenzel, K. & Fischer, S. NIR FT Raman Spectroscopy – A Rapid Analytical Tool for Detecting the Transformation of Cellulose Polymorphs. *Cellulose* **2001**, *8*, 49–57, https://doi.org/10.1023/A:1016616920539

79. Agarwal, U.P. & Ralph, S.A. FT–Raman Spectroscopy of Wood: Identifying Contributions of Lignin and Carbohydrate Polymers in the Spectrum of Black Spruce (Picea Mariana). *Appl. Spectrosc.* **1997**, *51*, 1648–1655, https://doi.org/10.1366/0003702971939316

80. Agarwal, U.P. Raman Imaging to Investigate Ultrastructure and Composition of Plant Cell Walls: Distribution of Lignin and Cellulose in Black Spruce Wood (Picea Mariana). *Planta* **2006**, *224*, 1141–1153, https://doi.org/10.1007/S00425–006–0295–Z/METRICS

81. Yapo, B.M. Pectic Substances: From Simple Pectic Polysaccharides to Complex Pectins – A New Hypothetical Model. *Carbohydr. Polym.* **2011**, *86*, 373–385.

82. Gottumukkala, R.V.S.S.; Nadimpalli, N.; Sukala, K. & Subbaraju, G. V. Determination of Catechin and Epicatechin Content in Chocolates by High–Performance Liquid Chromatography. *Int. Sch. Res. Not.* **2014**, *2014*, 1–5, https://doi.org/10.1155/2014/628196

83. Colthup, N.; Daly, L. & Wiberley, S. Introduction to Infrared and Raman Spectroscopy; Academic Press: San Diego, **1990**; ISBN 9780080917405.

84. Bicchieri, M.; Monti, M.; Piantanida, G. & Sodo, A. Non–Destructive Spectroscopic Investigation on Historic Yemenite Scriptorial Fragments: Evidence of Different Degradation and Recipes for Iron Tannic Inks. *Anal. Bioanal. Chem.* **2013**, *405*, 2713–2721, https://doi.org/10.1007/S00216–012–6681–4/METRICS

85. Pompeu, D.R.; Larondelle, Y.; Rogez, H.; Abbas, O.; Pierna, J.A.F. & Baeten, V. Characterization and Discrimination of Phenolic Compounds Using Fourier Transform Raman Spectroscopy and Chemometric Tools. *Biotechnol. Agron. Soc. Environ.* **2018**, *22*, 13–28, https://doi.org/10.25518/1780–4507.16270

86. Aprotosoaie, A.C.; Luca, S.V. & Miron, A. Flavor Chemistry of Cocoa and Cocoa Products–An Overview. *Compr. Rev. Food Sci. Food Saf.* **2016**, *15*, 73–91, https://doi.org/10.1111/1541–4337.12180

87. Tuenter, E.; Delbaere, C.; De Winne, A.; Bijttebier, S.; Custers, D.; Foubert, K.; Van Durme, J.; Messens, K.; Dewettinck, K. & Pieters, L. Non–Volatile and Volatile Composition of West African Bulk and Ecuadorian Fine–Flavor Cocoa Liquor and Chocolate. *Food Res. Int.* **2020**, *130*, 108943, https://doi.org/10.1016/j.foodres.2019.108943

88. Tuenter, E.; Foubert, K. & Pieters, L. Mood Components in Cocoa and Chocolate: The Mood Pyramid. *Planta Med.* **2018**, *84*, 839–844, https://doi.org/10.1055/A–0588–5534

89. Xia, J.; Wang, D.; Liang, P.; Zhang, D.; Du, X.; Ni, D. & Yu, Z. Vibrational (FT–IR, Raman) Analysis of Tea Catechins Based on Both Theoretical Calculations and Experiments. *Biophys. Chem.* **2020**, *256*, 106282, https://doi.org/10.1016/J.BPC.2019.106282

90. Luna, F.; Crouzillat, D.; Cirou, L. & Bucheli, P. Chemical Composition and Flavor of

Ecuadorian Cocoa Liquor. *J. Agric. Food Chem.* **2002**, *50*, 3527–3532, https://doi.org/10.1021/jf0116597

91. Hanuza, J.; Godlewska, P.; Kucharska, E.; Ptak, M.; Kopacz, M.; Mączka, M.; Hermanowicz, K. & Macalik, L. Molecular Structure and Vibrational Spectra of Quercetin and Quercetin–5'–Sulfonic Acid. *Vib. Spectrosc.* **2017**, *88*, 94–105, https://doi.org/10.1016/J.VIBSPEC.2016.11.007

92. Counet, C.; Callemien, D.; Ouwerx, C. & Collin, S. Use of Gas Chromatography–Olfactometry to Identify Key Odorant Compounds in Dark Chocolate. Comparison of Samples before and after Conching. *J. Agric. Food Chem.* **2002**, *50*, 2385–2391, https://doi.org/10.1021/jf0114177 .

93. Ziegleder, G. Flavour Development in Cocoa and Chocolate. In *Industrial chocolate manufacture and use*; Beckett, S.T., Ed.; Blackwell Publishing Ltd.: York, **2009**; pp. 169–191 ISBN 978–1–405–13949–6.

94. Crafack, M.; Keul, H.; Eskildsen, C.E.; Petersen, M.A.; Saerens, S.; Blennow, A.; Skovmand–Larsen, M.; Swiegers, J.H.; Petersen, G.B. & Heimdal, H. Impact of Starter Cultures and Fermentation Techniques on the Volatile Aroma and Sensory Profile of Chocolate. *Food Res. Int.* **2014**, *63*, 306–316, https://doi.org/10.1016/j.foodres.2014.04.032

95. Vera Chang, J.F.; Vallejo Torres, C.; Párraga Morán, D.E.; Macías Véliz, J.; Ramos Remache, R. & Morales Rodríguez, W. Aributos físicos–químicos y sensoriales de las almendras de quince clones de cacao nacional (*Theobroma Cacao L.*) en el Ecuador. *Cienc. y Tecnol.* **2014**, *7*, 21–34, https://doi.org/10.18779/cyt. v7i2.99

96. Kadow, D.; Bohlmann, J.; Phillips, W. & Lieberei, R. Identification of Main Fine or Flavour Components in Two Genotypes of the Cocoa Tree (*Theobroma Cacao L.*). *J. Appl. Bot. Food Qual.* **2013**, *86*, 90–98, https://doi.org/10.5073/JABFQ.2013.086.013

97. Despreaux, D. Le Cacaoyer et La Cacaoculture. In *Cacao et chocolates production, utilisation, caracteristiques;* J. Pontillon, Ed.; Technique et Documentation Lavoisier: Paris, **1998**; pp. 44–93. ISBN: 2743001747

98. Kongor, J.E.; Hinneh, M.; de Walle, D. Van; Afoakwa, E.O.; Boeckx, P. & Dewettinck, K. Factors Influencing Quality Variation in Cocoa (Theobroma Cacao) Bean Flavour Profile – A Review. *Food Res. Int.* **2016**, *82*, 44–52. https://doi.org/10.1016/j.foodres.2016.01.012

99. Liu, M.; Liu, J.; He, C.; Song, H.; Liu, Y.; Zhang, Y.; Wang, Y.; Guo, J.; Yang, H. & Su, X. Characterization and Comparison of Key Aroma–Active Compounds of Cocoa Liquors from Five Different Areas. *Int. J. Food Prop.* **2017**, *20*, 2396–2408, https://doi.org/10.1080/10942912.2016.1238929

100. Criollo Nuñez, J.; Ramirez–Toro, C.; Bolivar, G.; Sandoval A., A.P. & Lozano Tovar, M.D. Effect of Microencapsulated Inoculum of Pichia Kudriavzevii on the Fermentation and Sensory Quality of Cacao CCN51 Genotype. *J. Sci. Food Agric.* **2023**, *103*, 2425–2435, https://doi.org/10.1002/JSFA.12433

101. Chang, A.C. The Effects of Gamma Irradiation on Rice Wine Maturation. *Food Chem.* **2003**, *83*, 323–327, https://doi.org/10.1016/S0308–8146(03)00050–5

102. Frauendorfer, F. & Schieberle, P. Changes in Key Aroma Compounds of Criollo Cocoa Beans During Roasting. *J. Agric. Food Chem.* **2008**, *56*, 10244–10251, https://doi.org/10.1021/jf802098f

103. Kim, J.H.; Ahn, H.J.; Yook, H.S.; Kim, K.S.; Rhee, M.S.; Ryu, G.H. & Byun, M.W. Color, Flavor, and Sensory Characteristics of Gamma–Irradiated Salted and Fermented Anchovy Sauce. *Radiat. Phys. Chem.* **2004**, *69*, 179–187, https://doi.org/10.1016/S0969–806X(03)00400–6

104. Krähmer, A.; Engel, A.; Kadow, D.; Ali, N.; Umaharan, P.; Kroh, L.W. & Schulz, H. Fast and Neat – Determination of Biochemical Quality Parameters in Cocoa Using near Infrared Spectroscopy. *Food Chem.* **2015**, *181*, 152–159, https://doi.org/10.1016/j.foodchem.2015.02.084

105. Zhang, Z. shan; Xie, Q. F. & Che, L. ming Effects of Gamma Irradiation on Aflatoxin B1 Levels in Soybean and on the Properties of Soybean and Soybean Oil. *Appl. Radiat. Isot.* **2018**, *139*, 224–230, https://doi.org/10.1016/j.apradiso.2018.05.003

106. Youssef, A.M.; Samra, S.E. & Ahmed, A.I. Effect of Gamma Irradiation on the Texture, Acidity and Catalytic Activity of Silica–Aluminium and Silica–Magnesia Catalysts. *Int. J. Radiat. Appl. Instrumentation. Part* **1991**, *38*, 313–316, https://doi.org/10.1016/1359–0197(91)90099–N

107. Samra, S.E.; Youssef, A.M. & Ahmed, A.I. Effect of Gamma Irradiation on the Surface and Catalytic Prop. INIS. *Bull. Soc. Chim. Fr.* **1990**, *127*. RN:22008092

108. Júnior, P.C.G.; dos Santos, V.B.; Lopes, A.S.; de Souza, J.P.I.; Pina, J.R.S.; Chagas Júnior, G.C.A. & Marinho, P.S.B. Determination of Theobromine and Caffeine in Fermented and Unfermented Amazonian Cocoa (*Theobroma Cacao L.*) Beans Using Square Wave Voltammetry after Chromatographic Separation. *Food Control* **2020**, *108*, 106887, https://doi.org/10.1016/J.FOODCONT.2019.106887

109. Mohajer, S.; Mat Taha, R. & Lay, M.M.; Khorasani Esmaeili, A.; Khalili, M. Stimulatory Effects of Gamma Irradiation on Phytochemical Properties, Mitotic Behaviour, and Nutritional Composition of Sainfoin (Onobrychis Viciifolia Scop.). *ScientificWorldJournal.* **2014**, *2014*, https://doi.org/10.1155/2014/854093

110. Aly, A.A.; Maraei, R.W.; Sharafeldin, R.G. & Safwat, G. Yield Traits of Red Radish Seeds Obtained from Plants Produced from γ–Irradiated Seeds and Their Oil Characteristics. *Gesunde Pflanz.* **2023**, 1–11, https://doi.org/10.1007/S10343–023–00859–8/FIGURES/3

111. Barrientos, L.D.P.; Oquendo, J.D.T.; Garzón, M.A.G. & Álvarez, O.L.M. Effect of the Solar Drying Process on the Sensory and Chemical Quality of Cocoa (*Theobroma Cacao L.*) Cultivated in Antioquia, Colombia. *Food Res. Int.* **2019**, *115*, 259–267, https://doi.org/10.1016/j.foodres.2018.08.084

112. Hussain, P.R.; Chatterjee, S.; Variyar, P.S.; Sharma, A.; Dar, M.A. & Wani, A.M. Bioactive Compounds and Antioxidant Activity of Gamma Irradiated Sun Dried Apricots (*Prunus Armeniaca L.*). *J. Food Compos. Anal.* **2013**, *30*, 59–66, https://doi.org/10.1016/J.JFCA.2013.02.001

113. Chung, N.; Ramakrishnan, S.R. & Kwon, J.H. Experimental Validation and Evaluation of Electronic Sensing Techniques for Rapid Discrimination of Electron–Beam, γ–Ray, and X–Ray Irradiated Dried Green Onions (Allium Fistulosum). *J. Food Sci. Technol.* **2019**, *56*, 5454–5464, https://doi.org/10.1007/S13197–019–04016–W/METRICS

114. Lee, J.H.; Lee, K.–T. & Kim, M.R. Effect of Gamma–Irradiated Red Pepper Powder on the Chemical and Volatile Characteristics of Kakdugi, a Korean Traditional Fermented Radish Kimchi. *J. Food Sci.* **2005**, *70*, c441–c447, https://doi.org/10.1111/J.1365–2621. 2005.TB11466.X

115. Mihaljević Žulj, M.; Bandić, L.M.; Bujak, I.T.; Puhelek, I.; Jeromel, A. & Mihaljević, B. Gamma Irradiation as Pre–Fermentative Method for Improving Wine Quality. *LWT* **2019**, *101*, 175–182, https://doi.org/10.1016/J.LWT.2018.11.016

116. Kiani, D.; Borzouei, A.; Ramezanpour, S.; Soltanloo, H. & Saadati, S. Application of Gamma Irradiation on Morphological, Biochemical, and Molecular Aspects of Wheat (*Triticum Aestivum L.*) under Different Seed Moisture Contents. *Sci. Reports 2022 121* **2022**, *12*, 1–10, https://doi.org/10.1038/s41598–022–14949–6

117. Ananthakumar, A.; Variyar, P.S. & Sharma, A. Estimation of Aroma Glycosides of Nutmeg and Their Changes during Radiation Processing. *J. Chromatogr. A* **2006**, *1108*, 252–257, https://doi.org/10.1016/j.chroma.2006.01.009

118. Garrido, J.; Borges, F. Wine and Grape Polyphenols – A Chemical Perspective. *Food Res. Int.* **2013**, *54*, 1844–1858, https://doi.org/10.1016/J.FOODRES.2013.08.002

119. Ehlermann, D.A.E. Safety of Food and Beverages: Safety of Irradiated Foods. In *Encyclopedia of Food Safety*; Elsevier, **2014**; Vol. 3, pp. 447–452 ISBN 9780123786128.

120. Kanatt, S.R.; Paul, P.; D'Souza, S.F. & Thomas, P. Effect of gamma irradiation on the lipid peroxidation in chicken, lamb and buffalo meat during chilled storage. *J. Food Saf.* **1997**, *17*, 283–294, https://doi.org/10.1111/j.1745–4565.1997.tb00195.x

121. Dini, H.; Fallah, A.A.; Bonyadian, M.; Abbasvali, M. & Soleimani, M. Effect of Edible Composite Film Based on Chitosan and Cumin Essential Oil–Loaded Nanoemulsion Combined with Low–Dose Gamma Irradiation on Microbiological Safety and Quality of Beef Loins during Refrigerated Storage. *Int. J. Biol. Macromol*. **2020**, 164, 1501–1509, https://doi.org/10.1016/J.IJBIOMAC.2020.07.215

Supplementary Material

Table S1. Time treatment, dose, dosimeter readings, and Dose Uniformity Rates (DUR) of irradiated Nacional cocoa beans.

Variety	EPR Holder used	Irradiation time (h)	Dose (kGy)	A (kGy)			B (kGy)			C (kGy)			D (kGy)			DUR
				Dosimeter Read. 1	Dosimeter Read. 2	Mean	Dosimeter Read. 1	Dosimeter Read. 2	Mean	Dosimeter Read. 1	Dosimeter Read. 2	Mean	Dosimeter Read. 1	Dosimeter Read. 2	Mean	
Nacional	PX063	1.22	0.10	0.10	0.10	0.10	0.11	0.11	0.11	0.11	0.11	0.11	0.09	0.09	0.09	1.22
	PX063	2.43	0.20	0.21	0.21	0.21	0.23	0.23	0.23	0.22	0.22	0.22	0.18	0.18	0.18	1.28
	PX063	3.65	0.30	0.32	0.32	0.32	0.34	0.34	0.34	0.33	0.33	0.33	0.27	0.27	0.27	1.26
	PX063	5.48	0.45	0,40	0.40	0.40	0.46	0.46	0.46	0.44	0.44	0.44	0.37	0.37	0.37	1.24
	PX063	7.30	0.60	0.63	0.63	0.63	0.67	0.67	0.67	0.65	0.65	0.65	0.53	0.53	0.53	1.26
	PX063	9.12	0.75	0.69	0.69	0.69	0.79	0.79	0.79	0.80	0.80	0.80	0.61	0.61	0.61	1.31
	PX063	12.13	1.00	1.07	1.07	1.07	1.14	1.14	1.14	1.07	1.07	1.07	0.92	0.92	0.92	1.24
	PL	24.67	2.00	2.47	2.46	2.47	2.81	2.79	2.80	2.57	2.56	2.57	2.21	2.21	2.21	1.27
	PH0156	36.93	3.00	–	–	–	3.05	3.02	3.04	2.92	2.93	2.93	–	–	–	1.22
	PL	36.93	3.00	2.75	2.76	2.76	–	–	–	–	–	–	2.49	2.47	2.48	

Table S2. Time treatment, dose, dosimeter readings, and Dose Uniformity Rates (DUR) of irradiated CCN–51 cocoa beans.

Variety	EPR	Irradiation time (h)	Dose (kGy)	A (kGy)			B (kGy)			C (kGy)			D (kGy)			DUR
	Holder used			Dosimeter Mean 1	Dosimeter Read. 2	Mean	Dosimeter Read. 1	Dosimeter Read 2	Mean	Dosimeter Read. 1	Dosimeter Read. 2	Mean	Dosimeter Read. 1	Dosimeter Read. 2	Mean	
CCN–51	PX063	1.22	0.10	0.11	0.11	0.11	0.12	0.12	0.12	0.12	0.12	0.12	0.09	0.09	0.09	1.33
	PX063	2.43	0.20	0.24	0.24	0.24	0.29	0.29	0.29	0.29	0.29	0.29	0.22	0.22	0.22	1.32
	PX063	3.58	0.30	0.26	0.32	0.29	0.32	0.32	0.32	0.30	0.30	0.30	0.24	0.24	0.24	1.33
	PX063	5.47	0.45	0.48	0.48	0.48	0.54	0.54	0.54	0.52	0.52	0.52	0.41	0.41	0.41	1.32
	PX063	7.28	0.60	0.65	0.65	0.65	0.68	0.68	0.68	0.63	0.63	0.63	0.51	0.51	0.51	1.33
	PX063	9.12	0.75	0.72	0.72	0.72	0.81	0.81	0.81	0.80	0.80	0.80	0.59	0.59	0.59	1.37
	PX063	12.15	1.00	1.07	1.07	1.07	1.23	1.23	1.23	1.21	1.21	1.21	0.94	0.94	0.94	1.31
	PL	24.67	2.00	2.42	2.42	2.42	2.81	2.84	2.83	2.67	2.63	2.65	2.15	2.16	2.16	1.31
	PH0156	36.85	3.00	2.93	2.93	2.93	3.18	3.20	3.19	3.29	3.37	3.33	–	–	–	1.17
	PL	36.85	3.00	–	–	–	–	–	–	–	–	–	2.84	2.84	2.84	

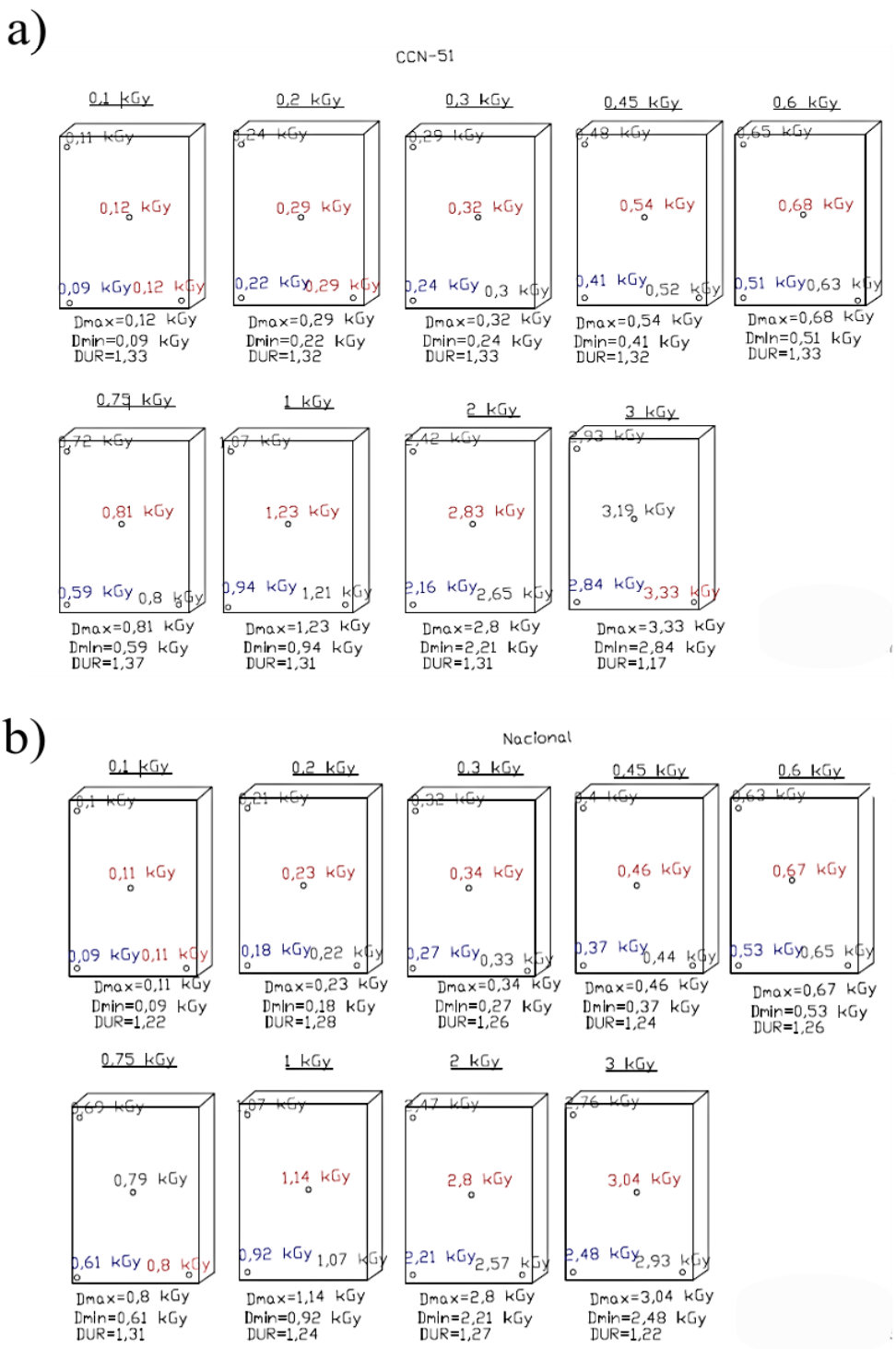

Figure S1. Schematic representation of the dosimeter at four positions in the plastic trays, identification of the maximum and minimum dose and DUR calculus at each irradiation treatment

Figure S2. Location of 4 dosimeters at A, B, C, and D position in the plastic tray containing cocoa beans in each treatment

Chapter 5

Electromagnetic field effects on microbial growth in cocoa fermentation: a controlled experimental approach using established growth models

Tania María Guzmán–Armenteros[1*], José Villacís–Chiriboga[1], Luis Santiago Guerra[1,2] and Jenny Ruales[1]

1 Departamento de Ciencia de Alimentos y Biotecnología (DECAB), Escuela Politécnica Nacional (EPN), Quito, Ecuador; tania.guzman@epn.edu.ec , jose.villacis@epn.edu.ec , jenny.ruales@epn.edu.ec

2 Universidad Central del Ecuador (UCE), Facultad de Ciencias Médicas, Carrera de Medicina, Campus El Dorado, Quito, Ecuador, lsguerrap@uce.edu.ec

*Corresponding author: tania.guzman@epn.edu.ec , taniamariaguzman@gmail.com

Abstract:

The objective of this research was to assess the impact of oscillating magnetic fields (OMF) on the growth kinetics of the core microbial communities in Collections Castro Naranjal (CCN–51) cocoa beans. The data were obtained by three different models: Gompertz, Baranyi, and Logistic. The cocoa beans were subjected to different OMF strengths ranging from 0 mT to 80 mT for one hour using the Helmholtz coil electromagnetic device. The viable microbial populations of yeast (Y), lactic acid bacteria (LAB), and acetic acid bacteria (AAB) were quantified using the colony–forming unit (CFU) counting method. The logistic model appropriately described the growth of LAB and Y under magnetic field exposure. Whereas, the Baranyi model was suitable for describing AAB growth. The microbial populations in cocoa beans exposed to magnetic fields showed lower (maximum specific growth rate (μ_{max}), values than untreated controls. Microbial populations in cocoa beans exposed to magnetic fields showed lower values (maximum specific growth rate (N_{max})) than untreated controls. The AABs exhibited the highest average growth rate value (N=7.25 Log CFU/g) at 5 mT, while the Ys exhibited the lowest average growth rate value (N=2.86 Log CFU/g) at 80 mT.

Keywords: kinetic models, cocoa fermentation, electromagnetic field, microbial growth

1. Introduction

Kinetic growth studies of microorganisms are crucial for understanding and optimizing fermentation and other biological processes. These studies provide insights into growth patterns, metabolic activities, population dynamics, nutrient utilization, and product formation [1 – 4]. They are

especially important for applications in the fermentation process, i.e., bioremediation [1], biodegradation of pollutants [2, 3], and biogas production [4]. Kinetic information on specific growth rates, lag phases, biomass yields, and substrate consumption rates under different environmental conditions help construct mathematical models that optimize and predict bioprocess outcomes [5]. In the food industry, selection of appropriate models depends on the characteristics of the microorganism and the food matrix, and their accuracy should be validated with experimental data [6, 7]. Comparative analysis of different mathematical models has shown that specific models are suitable for different types of microorganisms and food matrices [6, 8].

Logistic, Baranyi, and Gompertz models are widely used in the analysis of microbial kinetics. The logistic model is used to describe microbial population growth by considering initial density, time, growth rate, and final density. On the other hand, the Baranyi model considers dynamic conditions and encompasses lag, exponential, and stationary phases of microbial growth [9, 10]. The Gompertz model is suitable for microorganisms with longer lag phases and slower growth rates, since it assumes an exponential decline in growth rate over time [9]. Recent investigations have proposed modifications to these models and have carried out significant tests on their parameters to improve their understanding and application in studies of microbial growth [11].

Cocoa fermentation is a multifaceted process guided by the metabolic actions of diverse microorganisms, encompassing yeasts, lactic acid bacteria, and acetic acid bacteria. These microorganisms break down sugars and other compounds in the cocoa pulp, resulting in the formation of flavor and aroma compounds that significantly influence the quality of the final cocoa product [12 – 15]. However, the growth kinetics of cocoa bean fermentation microorganisms do not conform to conventional models, mainly due to the need for improved process control and the complexity of the microbial communities involved [16, 17].

In cocoa fermentation systems, the microbial community may exhibit dominance of a limited number of several major taxa within a complex network. Fitting kinetic models in fermentation involves determining an optimal time frame and sampling frequency to consider each group of microorganisms as an individual population [17]. Several approaches have been utilized, including models that integrate substrate utilization, microbial growth, metabolite production, and transport processes [16]. However, the choice of the model also depends on the specific fermentation system and the microorganisms being studied. These approaches have proven effective in fitting kinetic models and advancing fermentation research.

Recent studies have explored various techniques to speed up fermentation, improve the quality and intensity of flavor, and aroma of cocoa beans. These techniques such as pulp preconditioning [18], aeration [19], started culture [20], acetic and lactic reagents [21], enzymes [22], ohmic heating [23], and extremely low–frequency electromagnetic fields (ELF–EMF) [24] have improved the overall

quality of the beans, offering new development opportunities in the chocolate industry.

The potential influence of extremely low–frequency (50–60 Hz) electromagnetic fields ELF–EMF on microbial fermentation processes is remarkable. The findings indicate that electromagnetic fields can affect microbial growth and metabolic activity, which could affect the production of fermentation products [25, 26]. Understanding the effects of electromagnetic fields is particularly crucial in cocoa bean fermentation, as it improves the sensory and nutritional properties of cocoa beans by precisely controlling fermentation conditions [24, 27]. This understanding also opens avenues for enhancing the production of flavor precursors, antioxidants, and other bioactive compounds from cocoa beans.

This study aims to empirically demonstrate the impact of electromagnetic fields on microbial growth, particularly in the context of cocoa bean fermentation, using controlled conditions and established models. The results will enhance our understanding of this relationship and provide insights to optimize cocoa bean fermentation, ultimately improving cocoa quality and flavor development. Thus, this research not only advances scientific knowledge on ELF–EMF effects but also holds practical significance for enhancing fermentation processes and benefiting the chocolate industry.

2. Materials and Methods

2.1. The cocoa beans processing

The research methodology encompassed the selection and preparation of cocoa pods exposed to various electromagnetic field densities and two different fermentation scenarios: controlled conditions with meticulous temperature and humidity regulation, and uncontrolled conditions lacking environmental regulation. Controlled conditions included sterilization, inoculation with a starter culture, and continuous monitoring of fermentation parameters, while uncontrolled conditions omitted these procedures. This experimental design made it easy to examine and juxtapose the impacts of EMF and fermentation conditions on growth kinetics.

2.1.1. Selection and Preparation of Cocoa Pods:

The CCN–51 variety cocoa pods, obtained from local producers in the province of Santo Domingo, Ecuador, and the absence of pest–related damage or defects. The selected pods were packed in polyethylene bags and refrigerated at temperatures between 7–12 °C. The maximum storage time before the experiment was limited to 32 hours [24].

2.1.2. Controlled Fermentation Conditions (CFC):

In a controlled fermentation setup, each cocoa pod underwent sanitization by being immersed in a

sodium hypochlorite solution with a concentration of 200 ppm for a duration of 5 minutes. After this, the cocoa beans were aseptically extracted and placed in plastic containers with lateral and ventral openings, in an amount of 3 kg per experimental unit. The beans were inoculated with a previously obtained natural starter culture (section 2.2). The containers were placed in a fermentation chamber (Bauuman CFT, Valencia) with a controlled temperature (37 °C ± 0.5) and humidity (85% ± 0.8) for 84 hours, with periodic shifts every 24 hours. Experimental conditions were regularly monitored following established protocols [24, 28].

2.1.3. Uncontrolled fermentation conditions (UFC):

Cocoa beans were obtained from the pods without any prior chemical treatment for uncontrolled fermentation conditions. Similar to the controlled conditions, the beans were placed in plastic containers at 3 kg per unit. No inoculation with a starter culture was performed. The containers were placed in an isolated, cool place, free of pests and insects, but without environmental control [24].

2.2 Preparation of natural starter culture.

To acquire a natural inoculum of CCN–51 cocoa pulp, the beans were initially manually de–pulped, resulting in a semi–liquid mucilage subjected to controlled fermentation for eight hours at 37 °C [28]. This suspension was subjected to different electromagnetic field density treatments for one hour, followed by inoculation via spraying, according to the experimental design detailed in section 2.5.

2.3. Electromagnetic field (EMF) system

Helmholtz's coils were employed to produce an electromagnetic field according to the method described by Hu [29]. The system comprised two circular coils with a radius of 0.205 m, connected in series and powered by a variable voltage source operating at 60 Hz, generating a magnetic field density ranging from 1 to 120 mT. During the magnetic field treatment, the samples were positioned between the coils. A Hall effect Tesla meter (SS49E) measured the magnetic fields, regulated through a specialized electronic board (Arduino nano) to obtain a digital signal transmitted to a computer [30]. The v9.0 interface of the Laboratory Virtual Instrument Engineering Workbench (LabVIEW) software was used for data output Software, and the Comsol Multiphysics Software v12 to model the magnetic field lines between the coils (see Figure 1).

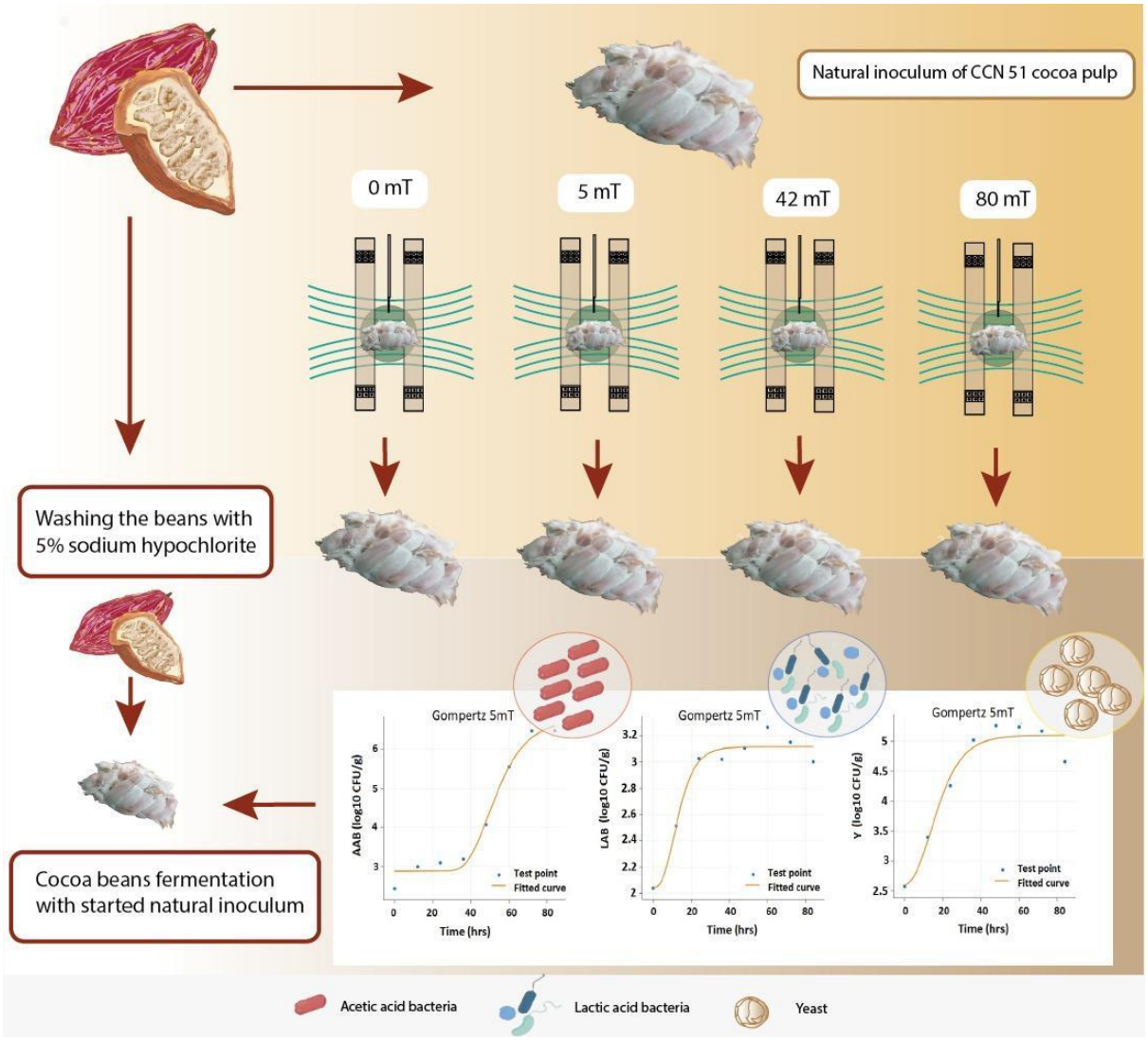

Figure 1. Influence of oscillating magnetic fields (OMF) by Helmholtz coil electromagnetic device, on the microbial growth kinetics of cocoa beans, CCN–51. OMF intensities ranging from 0 mT to 80 mT for one hour. Viable populations of lactic acid bacteria (LAB), acetic acid bacteria (AAB), and yeasts (Y) determined quantitatively as a function of time

2.3. Electromagnetic treatment

Each natural inoculum was placed at the center of the Helmholtz coils and exposed to varying intensities of OMF, as per the experimental design (section 2.5). The OMF densities used in the experiment were 0mT, 5mT, 42mT, and 80mT [24] (Table 1). In the fermentation conditions, two types of exposure were distinguished and carried out according to the experimental design: exposure to the beans (EB) and exposure to the culture (EC). The samples were positioned as closely to the center of both rings as feasible, ensuring a suitable separation between them. All interventions were closely observed and randomly arranged

2.4. Evaluation procedure

2.4.1 Microbial concentrations

The viable bacteria and yeast in cocoa bean samples and their growth were monitored every 12 hours using the colony–forming unit (CFU) method [31]. The samples of fermented cocoa beans were diluted in peptone water, homogenized, and then subjected to serial dilution, aiming for a maximum of 150 to 200 colonies per plate. Following that, diluted samples were distributed onto specific agar media. These included malt extract agar (MEA, Oxoid, Thermo Fisher Scientific) for yeast, De Man, Rogosa, and Sharpe (MRS, Oxoid, Thermo Fisher Scientific) agar for lactic acid bacteria, and mannitol yeast extract agar (MYP, Oxoid, Thermo Fisher Scientific) for acetic acid bacteria [19, 28]. The plates were incubated at optimal temperatures for yeast growth (24°C) and lactic and acetic acid bacteria growth (30°C) [32]. A digital colony counter (Isolab brand) was used to determine the number of colonies on each plate. The N values for each sample were calculated using equation 1 [31].

$$N = Log\left(\frac{\sum_{n=i}^{j} Ci}{Vi \times p \times d}\right) \quad (1)$$

Where n represents the number of replicas, i indicates the subset of n, j signifies the total number of replicas, Ci represents the total count of colonies in each replicate, V denotes the volume of the inoculum, p stands for the count of plates, and d refers to the minor dilution utilized to determine the colony–forming units (CFU) of microbial groups present in cocoa beans.

2.4.2 Kinetics models

Three mathematical models, namely Gompertz [33], Baranyi [34], and Logistic Models [35], were employed to analyze the microbial growth curves during fermentation. The non–linear regression analysis was employed to estimate the model parameters, and subsequently, the model equations (2–5) were fitted to the experimental data.

2.4.2.1 Gompertz kinetic model

The Gompertz model's parameters have significant biological implications. The maximum growth rate (k) is the slope of the curve at the inflection point, while the maximum population density represents the upper asymptote of the curve. The initial population density (No) is the curve's lower asymptote [9]. The Gompertz model assumes that the growth rate decreases exponentially as the population approaches the environment's carrying capacity. This model is commonly utilized to

describe bacterial population growth [33].

$$N_{(t)} = N_0 * exp\left[-exp\left(\mu e^{\left(\frac{1}{N_0}\right)}(t - t_{lag})\right)\right] \quad (2)$$

where N(t) is the population size at time t, No is the initial population size, μ is the maximum specific growth rate, t_lag is the lag time, and e is the base of the natural logarithm (2)

2.4.2.2. Baranyi kinetic model

The Baranyi model assumes that bacterial growth occurs in two stages: a lag phase and an exponential phase, with the latter characterized by constant growth. The Baranyi kinetic model's parameters include the lag phase duration (λ) when bacteria adapt to a new environment and initiate growth. The maximum growth rate (μ_{max}) is the maximum bacterial growth rate during the exponential phase. The shoulder duration (δ) is when bacteria reach their full growth rate after the lag phase. The final cell concentration (Nf) is the maximum cell concentration achieved at the end of the exponential phase [34]. The model also accounts for a stationary phase in which growth slows due to nutrient depletion or waste accumulation [9, 34].

$$N_{(t)} = N_0 + \frac{\lambda}{\alpha} * ln\left[\frac{\left(e^{(\alpha(\mu_{max}-\lambda)t)}\right) + \left(e^{(-\alpha*\lambda*t)}\right)}{2}\right] \quad (3)$$

Where: N(t) is the bacterial population at time t, No is the initial bacterial population, λ is the lag phase duration, μ_{max} is the maximum specific growth rate, α is the mean growth rate during the exponential phase, given by $\alpha = (\mu_{max} - \lambda) / N_{max}$, where N_{max} is the carrying capacity of the system [35, 36].

2.4.2.3. Logistic kinetic model

The Logistic model generates two essential parameters, the intrinsic growth rate (r) and the carrying capacity (N), which characterize population growth dynamics [37]. The intrinsic growth rate signifies the highest growth rate achievable in an unrestricted environment, while the carrying capacity indicates the maximum population size that the environment can support. Rooted in the assumption that population growth is proportionate to the present population size and constrained by the environment's carrying capacity, the logistic model finds wide application in describing population growth over time within the realms of population biology and ecology [9, 37].

$$N_{(t)} = N_0 * \left(1 + e^{(-rt)}\right)^N \quad (4)$$

Where: N(t) is the population size at time t, No is the initial population size, N is the growth rate

constant, r is the maximum population size, also known as the carrying capacity

The kinetic Lag Logistic model is a modification that incorporates a lag phase, during which the microorganisms adapt to the environment, followed by an exponential growth phase that slows down as the available resources are depleted [9, 36, 37]. This model has been applied in various fields, including food microbiology and environmental science, to study the growth of microorganisms under different conditions [37].

$$N_{(t)} = N_0 + \frac{(N_{max} - N_0)}{\left(1 + exp\ exp\left(\frac{(lag - t)}{\lambda}\right)\right)} \quad (5)$$

Where N(t) is the number of microorganisms at time t, N_0 is the initial number of microorganisms, N_{max} is the maximum number of microorganisms that the environment can support, lag is the lag time, and λ is a parameter that determines the steepness of the growth curve.

2.5. Statistic procedure

2.5.1. Experimental design

The adjustment of growth models, Gompertz, Baranyi, and Logistic, was analyzed using Logistic Regression Design (LRD) design in the Design Expert v 13 (Stat–Ease) software from historical data. The analysis considered four factors: OMF Density (0, 5, 42, and 80 mT), exposure type (exposure to beans and exposure to culture), exposure time (30 and 60 min), and operating conditions (uncontrolled and controlled fermentation conditions) [38]. The response variable used was a binary variable: level 1 represented Model Fit Success (MFS), while level 0 indicated Model Fit Failure (MFF) (Table S1a and b) in supplementary material).

The growth parameters and metrics, including μ_{max} (maximum specific growth rate), N (maximum population density), lag (lag phase duration), RMSE (Root Mean Square Error), AIC (Akaike Information Criterion), and BIC (Bayesian Information Criterion), The response variables were assessed utilizing analysis of variance (ANOVA) applied to historical data, with statistical significance ($p < 0.05$) serving as the criterion for identifying meaningful differences among the factors. Additionally, a post hoc analysis employing the Shefé method was conducted to further examine these differences [39]. The factors considered in the analysis were OMS density, with levels set at 0 mT, 5 mT, 42 mT, and 80 mT, and model type, with levels set as Gompertz, Baranyi, and Logistic (Table S2 a, and b in supplementary material).

2.5.2. Models fit

The fermentation process was mathematically modeled using online Micro Risk Lab predictive microbiology statistical software [40]. Various metrics were used in the same software to assess the fit and accuracy of the model predictions. Gompertz, Baranyi, and logistic equations were used to model microbial growth under different experimental conditions [9]. It was assumed that these models effectively captured the growth dynamics of diverse microbial species from distinct microbial categories under uniform conditions [9, 17]. For the fit of the kinetic models, the first 84 hours of fermentation microbial growth were considered, taking samples every twelve hours and considering each group's growth as a single population [16, 17].

The experimental data were utilized to fit the model equations and estimate their kinetic parameters. The quality of fit was evaluated using AIC and BIC calculations. AIC was computed using the formula AIC = –2 log(L) + 2p, with L indicating the likelihood function and p representing the number of model parameters employed. Similarly, BIC was determined as BIC = –2 log(L) + p log(n), where n stands for the sample size [39]. Additionally, the accuracy was assessed through RMSE, which measures the differences between predicted and actual values. This metric quantifies the effect size as the standardized mean difference between the two distributions [39].

3. Results and Discussion

3.1 The logistic model exhibited the best fit for LAB and Y and Baranyi model to AAC

The logistic model demonstrated its suitability to describe the growth of lactic acid bacteria (LAB) and yeasts (Y) under controlled fermentation conditions (CFC). On the other hand, the Baranyi model better represented the growth of acetic acid bacteria (AAB), as shown in Figures 2a, b, and c. ANOVA analysis of LAB, AAC, and Y metrics also reveals statistically significant differences between treatments and controls of the different microbial groups (Table S3). The evaluation of the model was based on three metrics: RMSE, AIC, BIC. In all cases, the logistic model exhibited the lowest values for these metrics, indicating a better fit. Specifically, at a magnetic field strength of 5 mT, the logistic model showed the best fit for LAB growth (Figures 2c and 3g), as evidenced by the lowest values of the RMSE, AIC, and BIC metrics, while the logistic model's worst fit was observed in the non–magnetic control group under the same CFC (Figures 2c and 4g) [40]. For yeast growth under the same CFC, the best–fit results for all models were obtained at 80 mT, while the highest fit values were obtained at 42 mT (Figures 2g, h, i; 5i and 6i).

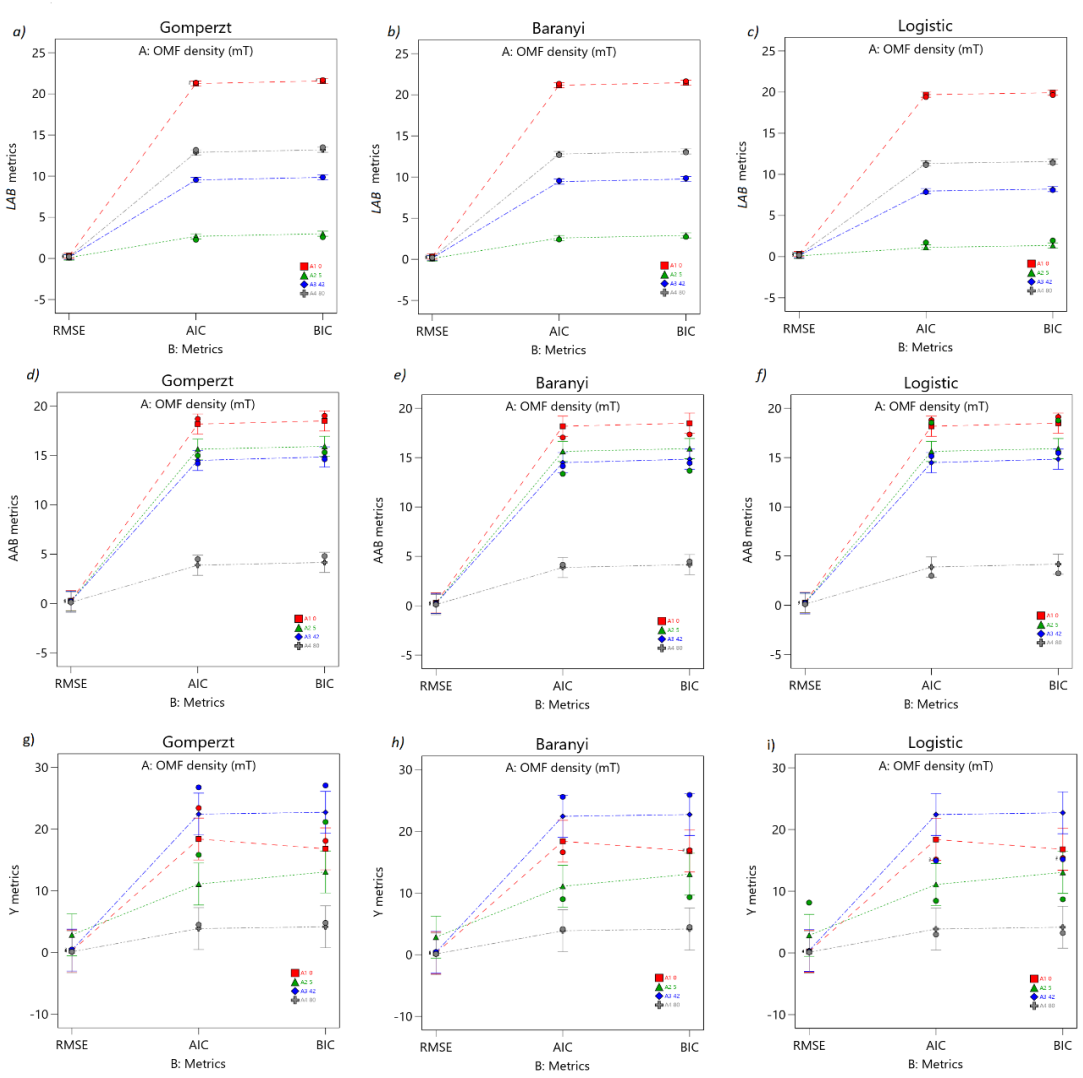

Figure 2. ANOVA Interaction plots. responses of LAB (a) Gomperzt model, (b) Baranyi model, and (c) Logistic model; AAB (e) Gomperzt model, (f) Baranyi model, and (g) Logistic model; and Y (h) Gomperzt model, (i) Baranyi model, and (j) Logistic model. The nominal factor, Metrics (RMSE, AIC, and BIC), was presented continuously, while the nominal OMF density factor (A) was displayed discretely as separate lines: A1 (0 mT) represented by a red line, A2 (5mT) represented by a green line, A3 (42 mT) represented by a blue line, and A4 (80mT) represented by a gray line. The I–Beam symbols depict the 95% least significant difference (LSD) interval for the plotted points. The dots on the plots indicated the values of the response variable around the mean, while the midpoint of the bar represented the mean value. Overlapping bar lines between levels indicated $p>0.05$, while the absence of overlap indicated $p<0.05$.

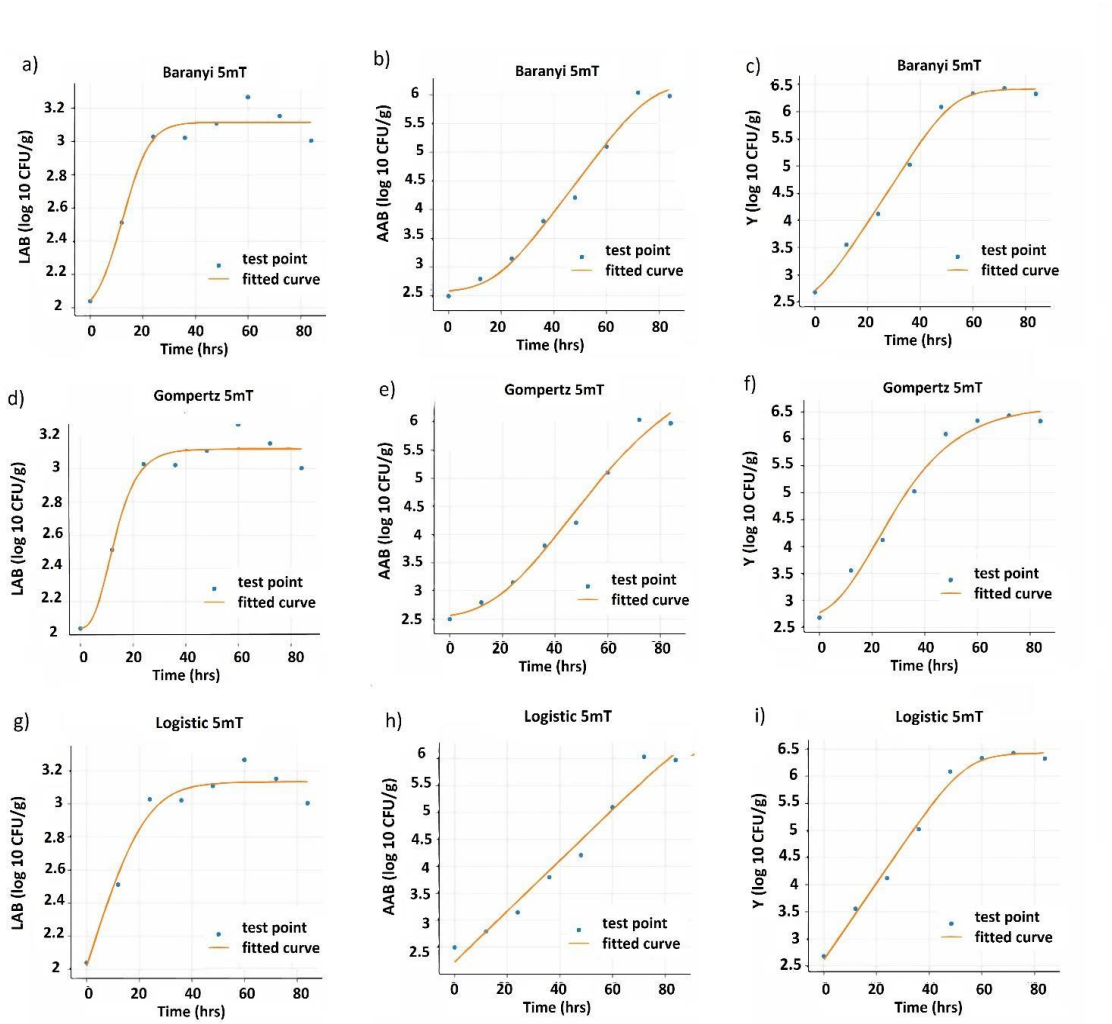

Figure 3. Growth curves of the model for the different microbial groups at 5mT. Baranyi model: (a) AAB, (b) LAB, and (c) Y. Gomperzt model: (d) AAB, (f) LAB, and (g) Y. Logistics model: (h) AAB, (i) LAB, and (j) Y.

Regarding AAB, the Baranyi model provided the best fit for its growth in CFC (Figures 2e) at 0 mT (Figure 4b), 5 mT (Figure 3b), and 42 mT (Figure 6b). However, at 80 mT, the logistic model displayed the best fit (Figures 2e and 5h). The highest growth adjustment for AAB was observed at 80 mT, while the lowest was observed in the control group. In all cases, there were significant differences ($p < 0.05$) between the treatments and controls based on AIC and BIC metrics. The RMSE metric showed significant differences only between the control group and the treatment group in yeast growth in CFC (Figure 2b).

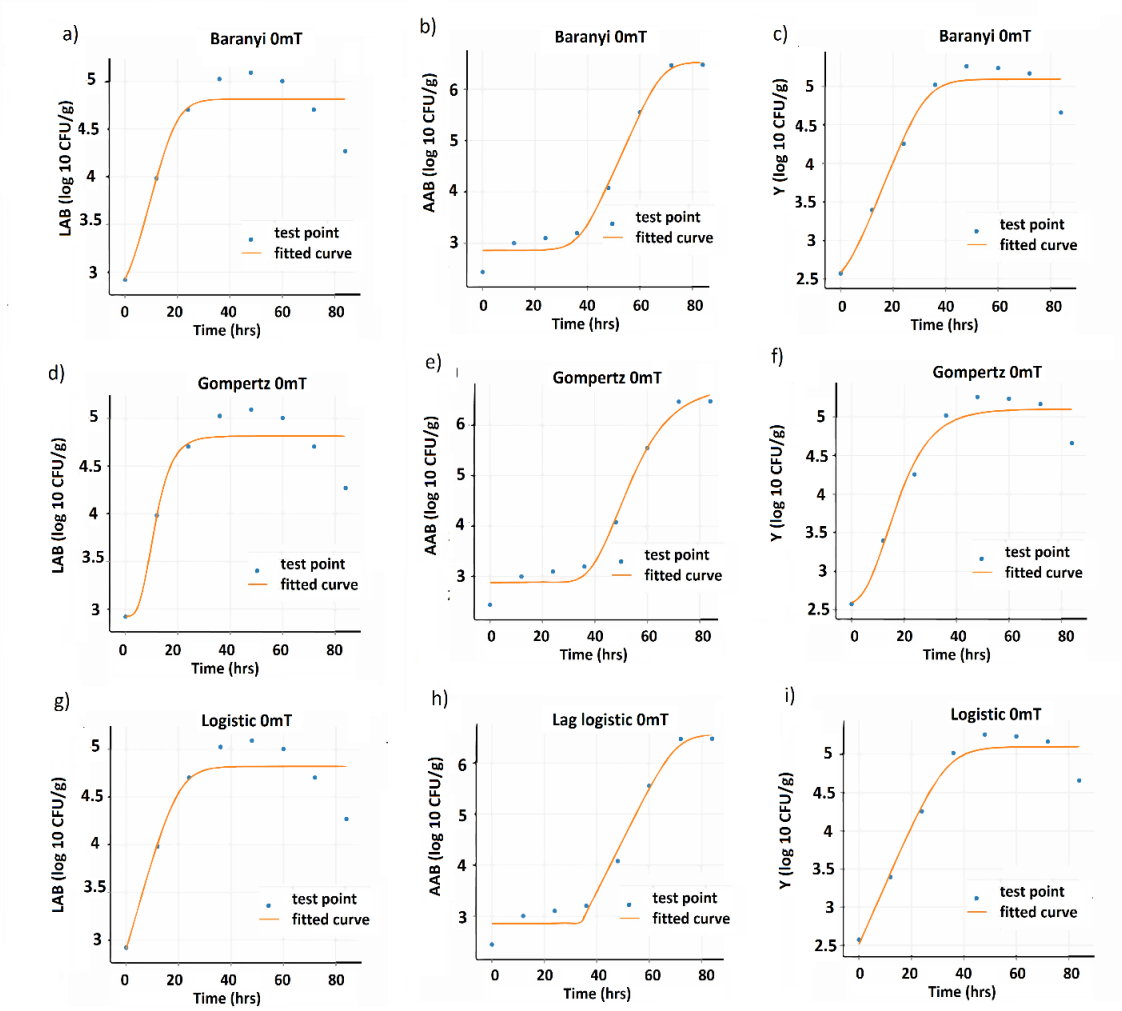

Figure 4. Growth curves of the model for the different microbial groups at 0mT. Baranyi model: (a) AAB, (b) LAB, and (c) Y. Gomperzt model: (d) AAB, (f) LAB, and (g) Y. Logistics model: (h) AAB, (i) LAB, and (j) Y.

Interestingly, the logistic model effectively captured the growth dynamics of most microbial groups in CFCs, indicating that this model effectively captured the CFC growth dynamics. Similarly, Noboa et al. (2021) [41] provide valuable information on the optimization of bioethanol production from cocoa mucilaginous residues. The application of the integrated logistic model allowed to determine the maximum specific growth rate (μ_{max}) of *Saccharomyces. cerevisiae*, which was estimated at 0.39 h. This logistic model was a suitable option to describe the growth dynamics of the microorganism under the given fermentation conditions. Consistently, at a magnetic field strength of 80 mT, the logistic model also showed the best fit for AAB growth. This indicates a change in AAB growth behavior at higher magnetic field strengths, which requires a different model for a more accurate representation.

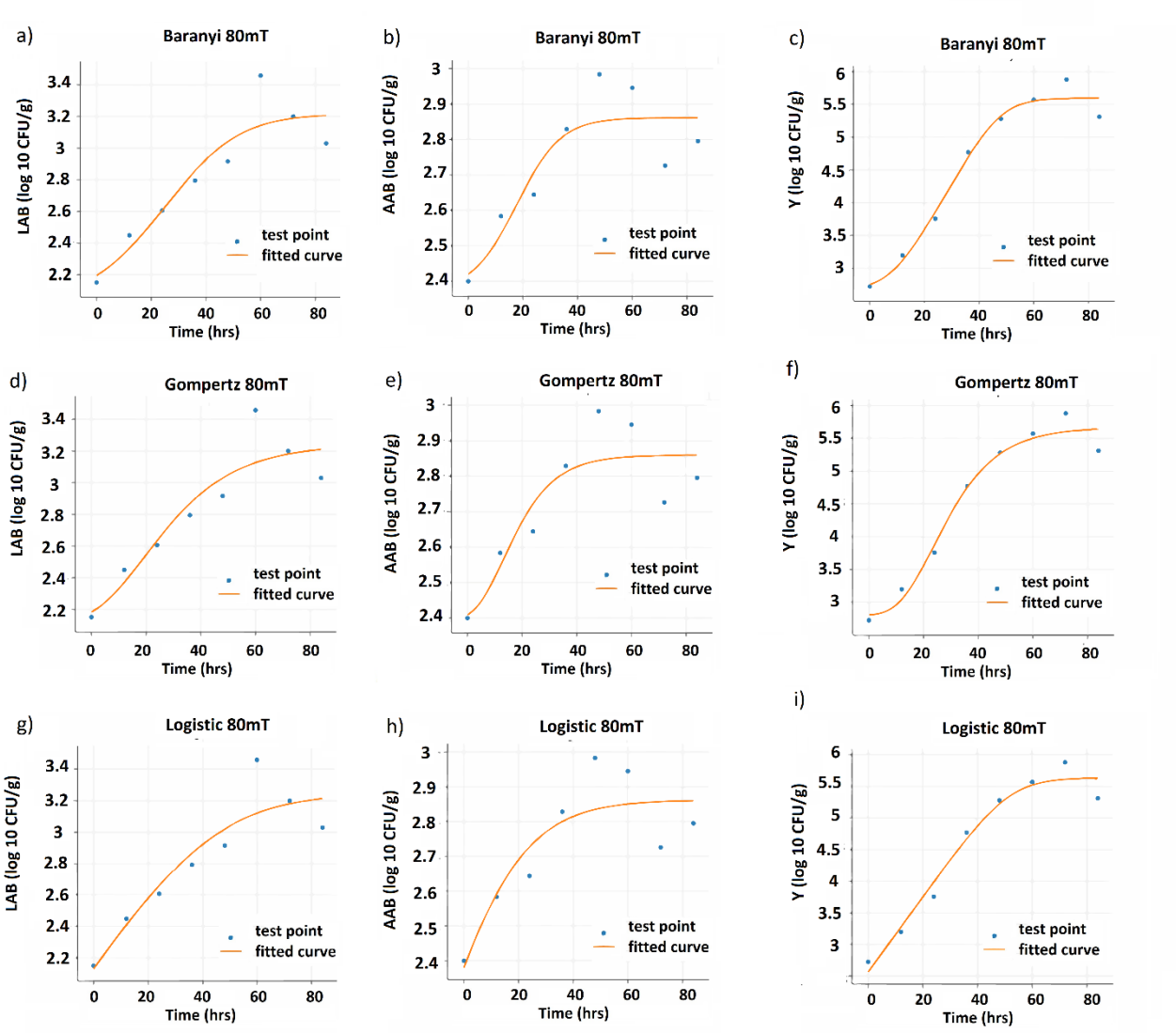

Figure 5. Growth curves of the model for the different microbial groups at 80mT. Baranyi model: (a) AAB, (b) LAB, and (c) Y. Gomperzt model: (d) AAB, (f) LAB, and (g) Y. Logistics model: (h) AAB, (i) LAB, and (j) Y

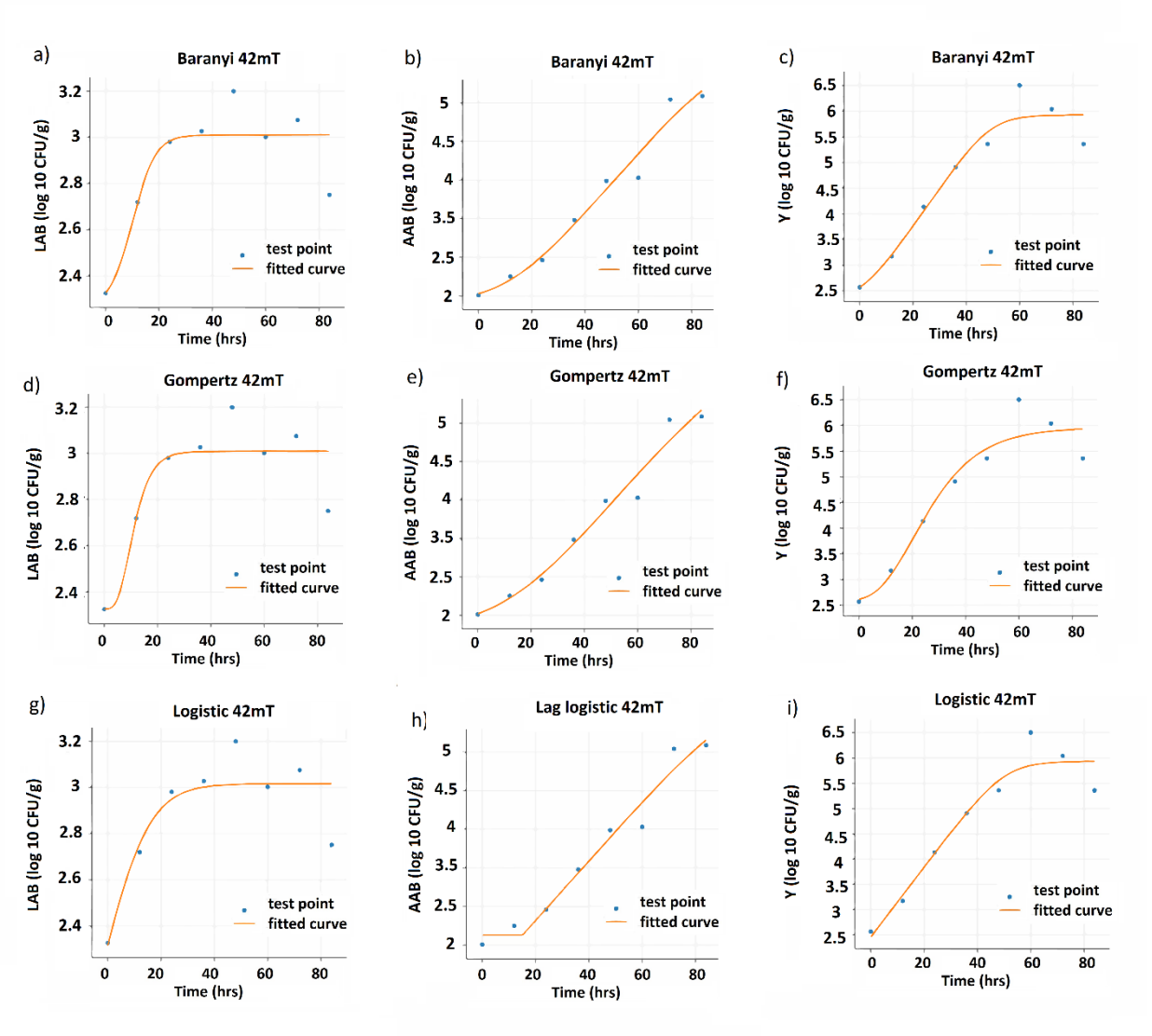

Figure 6. Growth curves of the model for the different microbial groups at 42mT. Baranyi model: (a) AAB, (b) LAB, and (c) Y. Gomperzt model: (d) AAB, (f) LAB, and (g) Y. Logistics model: (h) AAB, (i) LAB, and (j) Y

Regarding AAB growth, the Baranyi model provided the best fit with magnetic field strengths of 0 mT, 5 mT, and 42 mT. This is consistent with the rapid growth of this microbial group in the exponential phase, and suggests that Baranyi's model was able to capture these growth dynamics well in CFCs and EMFs.

Fujikawa et al. (2005) (2006) [42, 43], compared the newly developed logistic model and the Baranyi model to predict the microbial growth in foods. The first study revealed that the logistic model provides more accurate predictions of the constant growth rate of E. coli and Salmonella and lag time compared to the Baranyi model [42]. The second finding of the Baranyi model exhibited the smallest error in cell number estimation. In contrast, the logistic model demonstrated the smallest error in estimating the constant rate and lag period. In the case of dynamic temperature conditions, the logistic model successfully predicted bacterial growth, whereas the Baranyi model tended to overestimate it significantly. These results suggest that the logistic model accurately describes bacterial growth

curves in bagged mashed potatoes [42]. These investigations support that each model has its own strengths and weaknesses, and selecting an appropriate model depends on the specific application and the microbial growth pattern under investigation.

Supporting the results of this study, the works of Mitchell et al. (2004) [44] and Mazaheri and Shojaosadati, (2013) [45] provide further support for the importance of accurate modeling in understanding microbial growth dynamics. The authors also emphasized the importance of modeling microbial growth and substrate utilization in wastewater treatment processes. Taken together, several investigations have highlighted the need to select appropriate models that are adapted to the specific fermentative system to obtain reliable predictions. Consistently, the variability in growth patterns between different microbial species and the need to consider specific models adapted to their characteristics is evidenced in this study.

However, it should be noted that the worst fit of the logistic model was observed in the control group without magnetic treatment. This further emphasizes the influence of magnetic treatment on microbial growth dynamics and highlights the potential of magnetic fields to modulate microbial behavior. It also suggests that the increase in magnetic treatment could have influenced the microbial growth behavior of AABs resulting in a deviation from the Baranyi model predictions. These findings highlight the importance of considering external factors, such as magnetic treatment, which can potentially impact microbial growth and affect model performance.

The results obtained in this study also corroborate the findings of different authors that indicate that variations in the densities of magnetic fields can significantly affect the rates and patterns of microbial growth [25, 26]. The interaction between magnetic fields and charged particles, such as ions and charged molecules, has been shown to influence key cellular processes [25, 46 –49]. Magnetic fields can modulate enzyme activity, ion transport, and signal transduction, which are essential for microbial growth and metabolism [25, 47]. Furthermore, changes in membrane permeability and potential induced by magnetic fields can affect nutrient uptake and energy production in microorganisms [46, 48]. Also, alterations in the orientation and movement of cellular components [25, 47], such as proteins and organelles [48], due to magnetic fields can affect their functionality and cellular processes in general [46, 49].

Aligning with findings from previous research, it is evident that distinct models exhibit both advantages and limitations. The choice of the most suitable model relies on the particular application and the microbial growth pattern being studied. Moreover, it is crucial to underscore that external variables like magnetic treatment and process control play a pivotal role in shaping the dynamics of microbial growth and the model's suitability.

3.2 CEC influence on model's fit

The analysis of the experimental data showed that the fit of the kinetic models was not affected by the time and type of exposure examined. This observation was supported by the results presented in table S4. However, it was found that when the Controlled Fermentation Conditions (CEC) were applied, there was a probability exceeding 95% of successfully adjusting the growth models (MFS) (Figure 7a, b, and c). These findings suggest that the probability of achieving a successful model fit increases under different combinations of operating conditions. Thus, implementation of CEC had a significant ($p<0.05$) impact on improving the fit of the growth models to the experimental data, as illustrated in Figure 7 and Table S4.

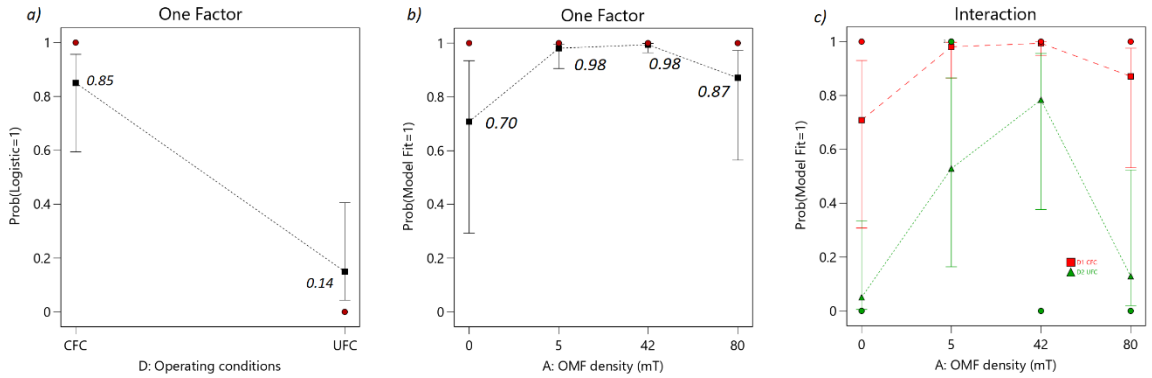

Figure 7. Logistic probability plots. Binary variable with level 1 denoting Model Fit Success (MFS) and level 0 representing Model Fit Failure (MFF). Two factors were considered in the analysis: a) Operating conditions, with levels of UFC and CFC, b) OMF density, with levels of 0 mT, 5 mT, 42 mT, and 80 mT, c) Interactions.

The above findings highlight the importance of kinetic models for understanding fermentation processes under controlled conditions. Studies have shown that specific environmental factors, like humidity, temperature, and starter cultures, significantly influence the dynamics of solid–state (SSF) fermentation. Particularly in cocoa bean fermentation, these factors play a crucial role in affecting microbial growth and fermentation performance [16, 45, 50].

Findings from previous studies by Hamidi–Esfahani et al. (2019) [50], He et al. (2019) [51], Calvo et al. (2021) [52], and Rahardjo et al. (2022) [53] collectively highlight the importance of environmental factors in microbial growth and fermentation processes. In the current study, the implementation of CEC had a significant impact in improving the fit of the growth models to the experimental data.

The study by Rahardjo et al. (2022) [53] showed that controlled fermentation emerged as the most effective method to achieve shorter fermentation times and improve grain quality. This technique not only influenced microbial succession, but also had a significant impact on growth patterns. The

probability of successfully fitting the growth models increased to more than 80 % when CEC was applied, indicating that the implementation of controlled fermentation conditions improved the fit of the growth models to the experimental data.

Similarly, the study by Hamidi–Esfahani et al. (2019) [50] demonstrated that temperature and humidity were influential factors in microbial growth. On the other hand, Calvo et al. (2021) [52] highlighted the role of pH and temperature regulation in the control of microbial succession during cocoa fermentation. In the current study, regulated temperature and humidity improved the fit of the growth models. This suggests that the controlled environmental conditions provided by CEC contributed to a more accurate representation of microbial growth dynamics. These factors probably influenced the growth models, contributing to a better fit to the experimental data.

Additionally, moisture content is known to influence microbial growth and fermentation processes, and maintaining optimal moisture conditions is crucial to achieving desired results. He et al. (2019) [51] emphasized the importance of moisture content regulation in solid–state fermentation (SSF). The implementation of CEC involved careful control of moisture content, which has played an important role in improving the fit of growth models.

Furthermore, our findings are also consistent with the significant impact of starter cultures on microbial growth in fermentation processes. Rahardjo et al. (2022) [53] also found that the inoculation of starter cultures in cocoa fermentation reduced fermentation time and maintained bean quality. This indicates that the presence of specific microbial strains in the form of starter cultures may influence the growth dynamics of cocoa fermentation.

The use of starter cultures can potentially alter the microbial composition and succession patterns, thus influencing the growth behavior of the different microbial species involved in cocoa fermentation [12 – 15]. In addition, the presence of starter cultures can introduce specific metabolic pathways and interactions between microbial populations, which can determine changes in the fit of mathematical models that accurately represent growth dynamics.

The dynamics of microbial communities in cocoa fermentation are closely linked to process parameters and the initial microorganisms responsible for initiating the transformation of cocoa beans. The interplay of these fermentations, can positively impact the quality of cocoa beans. These observations highlight the intricate influence of multiple parameters on microbial growth kinetics during cocoa fermentation, underscoring the complex nature of microbial physiology and its interactions with the surrounding environment.

3.3. OMF density increases MFS probability and induces changes in growth parameters

Table S4 revealed a significant ($p<0.05$) influence of OMF density on the fit of the kinetic models. Furthermore, Figure 7b displayed the variation in the probability of attaining a successful model fit across different OMF density levels, exhibiting a progressive pattern until reaching 80 mT. However, at 80 mT, a decline in the probability of SMF was observed, while continuing to outperform the control group (Figure 7b).

The maximum specific growth rate (μ_{max}) of lactic acid bacteria (LAB) in the untreated control ranged from 0.23 to 0.35 h^{-1}, which was significantly higher ($p<0.05$) than the other treatments (Figures 4a, d, g, and 8a). The μ_{max} values for the treatments were as follows: 5mT ranged from 0.15 to 0.22 h^{-1} 42mT ranged from 0.13 to 0.25 h^{-1}, and 80mT ranged from 0.23 to 0.35 h^{-1} (Figures, 3, 5 and 6; sub a, d, g). Among these treatments, the lowest range of μ_{max} values was observed in the 80 mT treatment (Figure 8a).

Similar statistically significant differences ($p<0.05$) between the controls and treatments were found for AAB and Y. As shown in Figure 8a, AAB exhibited μ_{max} values ranging from 0.24 to 0.30 h^{-1} in the untreated control, 0.09 to 0.14 h^{-1} in the 5mT treatment, 0.10 to 0.14 h^{-1} in the 42mT treatment, and 0.04 to 0.13 h^{-1} in the 80mT treatment (Figures 3, 4, 5 and 6 sub b, e, h). For Y, the μ_{max} values ranged from 0.18 to 0.24 h^{-1} in the untreated control, 0.13 to 0.20 h^{-1} in the 5mT treatment, 0.16 to 0.21 h^{-1} in the 42mT treatment, and 0.23 to 0.35 h^{-1} in the 80mT treatment (Figures 3, 4, 5, 6 sub c, f, i and 8a).

Significant differences between the control and treatment groups were observed primarily in the lag phase for LAB and AAB (Figures 3, 4, 5, 6 sub a b, d, e, g, h, and 8a). In the case of LAB, the longest lag phase was observed in the 80mT treatment, ranging from 13 to 38 hours, with statistically significant differences compared to the control and other treatments (0mT: lag phase 1.24 to 2.59 hours, 5mT: lag phase 3.25 to 5.08 hours, 42mT: lag phase 1.24 to 7.31 hours (Figure 8b).

For AAB, the longest lag phase was observed in the control group, ranging from 15 to 37.8 hours, and showed statistically significant differences compared to the other treatments (Figure 8b). On the other hand, the shortest lag phase was observed in the 80mT treatment, ranging from 4.53 to 14.59 hours, with significant differences compared to the control and other treatments (5mT: lag phase 2.31 to 18.33 hours, 42mT: lag phase 2.91 to 10.95 hours) (Figure 8b).

Among all treatments and microbial groups, AABs exhibited the highest average growth rate value at 5 mT (N = 7.25 Log CFU/g), as shown in Figure 8c (Figure 3 b, e, h). Conversely, AAB and Y at 80 mT had the lowest mean value of maximum growth rate, with AAB at 80 mT (N = 2.80 Log CFU/g) and Y at 80 mT (N = 2.86 Log CFU/g), showing a significant difference ($p < 0.05$) compared

to the control and other treatments (Figure 8c and 5 b, c, e, f, h, i). The control group of LAB displayed the highest growth rate within its group (N = 4.87 Log CFU/g) compared to the other treatments, including 5mT (N = 3.2 Log CFU/g), 45mT (N = 3.01 Log CFU/g), and 80mT (N = 3.23 Log CFU/g), as illustrated in Figure 8c.

Previous studies have reported a range of μ_{max} values for yeast between 0.07 and 0.53 h^{-1}, LAB between 0.06 and 0.36 h^{-1}, and AAB between 0.414 and 0.49 h^{-1}. The reported results align more closely with the findings observed in the control groups of the current study and stand in contrast to the outcomes observed in the magnetic treatment group [24, 36, 47, 54–56]. Consistent with previous studies, cocoa bean fermentation is characterized by initial microbial counts ranging from approximately 3 to 7 log CFU g^{-1} for yeast, 4 to 5 and 8 to 9 log CFU g^{-1} for lactic acid bacteria (LAB), and 3 to 4 and 6 to 7 log CFU g^{-1} for acetic acid bacteria (AAB). These counts gradually decline throughout the fermentation process, ultimately reaching final levels of approximately 2 to 3 log CFU g^{-1} for yeast, 1.5 log CFU g^{-1} for LAB, and 0 log CFU g^{-1} for AAB [47, 55, 56].

In the present study, the final counts attained by different microbial groups were not considered for the model fitting; however, the growth profiles exhibited a notable initial population and rapid growth of both yeast and LAB, while AAB proliferation occurred concurrently but at a slower pace. These observations align with the counts reported in previous studies on heap fermentation of cocoa beans from Ghana as well [55, 56].

The observed distinctions between the treatment groups and control groups were notable, and upon analyzing the kinetic parameters, it became evident that EMF had a discernible influence on the fermentation process. Consequently, these findings align with prior studies that emphasize the effects of magnetic fields on the growth of bacteria and yeasts.

While some studies have reported stimulating effects of EMF on certain microbial species, the presence of magnetic fields has also been shown to have inhibitory effects on cell growth. These studies suggest that exposure to magnetic fields can modulate the growth and metabolic activity of various microorganisms. Masod et al. (2018) (2020) [47, 57] conducted an investigation to assess the impact of various types of exposure to weak magnetic fields on bacterial growth. The studies focused on comparing the relative changes in bacterial growth after the removal of magnetic fields. Bacteria were cultivated on a single glass surface in both liquid and solid media, under different weak magnetic field conditions. The findings revealed that the growth pattern of bacteria was influenced differently by distinct magnetic fields, depending on the specific bacterial strain. Notably, the weak magnetic field was observed to impede the growth rate even after the removal of the magnetic field. According to the research findings, electromagnetic fields (EMF) have the ability to potentially affect the rate of bacterial growth, and other kinetic parameters.

The results from the present investigation are in line with prior studies that have examined the effects of magnetic fields on microbial growth and metabolic processes. For instance, in a study by Konopacka et al. (2019) [58], the impact of a rotating magnetic field (RMF) on bioethanol production was explored. The researchers found that the RMF stimulation led to increased growth and metabolic activity of S. cerevisiae, consequently enhancing ethanol production and overall process efficiency. These findings coincide with the outcomes of the current research, wherein exposure to magnetic fields was found to exert a notable impact on the specific growth rate (μ_{max}) of lactic acid bacteria (LAB) and acetic acid bacteria (AAB). Notably, the μ_{max} values for LAB and AAB were comparatively lower in the treatment groups than in the control, with the most diminished values observed in the 80 mT treatment condition.

Konopacki et al. (2019) [59] also studied the effects of RMF on different bacterial strains and found strain–specific responses. The present study observed similar strain–specific effects, with increased cell growth in Gram–positive bacteria and inhibition in *E. coli* and *K. oxytoca* strains. Kohno et al. (2000) [60] explored the effects of static magnetic fields on bacterial growth and found that the strength of the EMF influenced the growth rate and maximum growth number of specific bacterial species. This is consistent with the current study's findings, which showed that the lag phase and μ_{max} values varied depending on the magnetic field strength and microbial group.

Furthermore, Sudarti (2020) [27] demonstrated the impact of extremely low–frequency (ELF) magnetic fields on lactobacillus growth, similar to the current study's findings on LAB. Zhao et al. (2020) [61] investigated the effects of static magnetic fields on biogas production and observed significant increases in gas and methane volumes, as well as changes in microbial community composition. These findings align with the current study's observations on the growth rates of LAB and AAB and indicate that magnetic fields can influence microbial growth and metabolic processes. Additionally, Ciecholewska et al. (2022) [62] found that exposure to a rotating magnetic field reduced the number of viable bacterial cells within biofilms, which is consistent with the current study's results on the lag phase and growth rates of LAB and AAB.

In a broader context, the findings also align with previous studies by Novák et al. (2007) [63] who observed a similar inhibitory effect on the growth of *S. cerevisiae* when manipulating the magnetic field parameters with Bm = 10 mT, f = 50 Hz, and 24 min exposure. Similarly, Potenza et al. (2004) [64], indicated a detrimental impact of 300 mT static magnetic fields (SMF) on *E. coli* cell growth. These findings emphasize that exposure to magnetic fields can affect microbial growth characteristics.

In summary, an increase in magnetic field strength was associated with a decrease in the maximum growth rate, a longer delay phase, and lower μ_{max} (maximum specific growth rate) values for these microbial groups. The mechanism behind the change in the growth rate of microorganisms under

weak magnetic fields is not fully understood, but research suggests that it may involve perturbation of ion transport in the nutrient broth and bacterial cell dynamics, thus affecting the mobility and absorption of nutrients in the cells and therefore their duplication rate [25, 48, 49, 57].

The observed disparities in kinetic parameters between experimental treatments and control groups suggest that factors beyond nutrient depletion and toxic metabolite accumulation, which are commonly known to affect batch fermentations, may be influencing microbial growth during the fermentation of the cocoa bean. Consequently, the impact of EMF on the fermentation process is becoming evident based on the analysis of kinetic parameters.

3.4 Magnetic fields can affect the cocoa beans' fermentative processes

Expanding upon prior research carried out by the authors [24], the current study aims to build upon the optimization of the fermentation process for CCN–51 cocoa beans. This optimization involves the utilization of native species and electromagnetic fields (CEM) to enhance both yield and quality. The research employed response surface methodology to fine–tune variables such as magnetic field density (D), exposure time (T), and inoculum concentration (IC), resulting in the creation of two second–order models. These models effectively accounted for 88.39% and 92.51% of the variations in yield and grain quality, respectively.

The study's results unequivocally showed that exposure to CEM had a significant impact on both the yield and quality of CCN–51 cocoa beans. Particularly noteworthy was the combination of optimal parameters: 5 mT (D), 22.5 min (T), and 1.6% (CI), which resulted in remarkable improvements. These enhancements included a staggering 110% increase in yield and a substantial 120% enhancement in grain quality compared to the control group.

Further insights were gained through metagenomic analysis, revealing shifts in microbial communities at lower to moderate field densities (5–42 mT). These shifts positively influenced the aroma profile of the cocoa beans, culminating in higher yields and the emergence of floral, fruity, and nutty flavors. Conversely, the study highlighted that field densities of 80 mT led to diminished yields and undesirable flavor notes characterized by acidity and bitterness.

In a similar vein, Sudarti et al. (2022) [25] conducted an investigation into the effects of extremely low frequency (ELF) magnetic fields on the fermentation process of dried cocoa beans. The study encompassed the analysis of various parameters, including moisture content, alcohol content, and pH. The outcomes of the research demonstrated that the fermentation process of dried cocoa beans can indeed be impacted by exposure to ELF magnetic fields. Intriguingly, the samples subjected to a magnetic field density (MFD) of 0.2 mT for a duration of 5 minutes displayed the most substantial bacterial growth. These findings strongly suggest that the utilization of ELF magnetic fields as an

alternative approach could potentially augment the fermentation process of dried cocoa beans.

Both studies deliver evidence suggesting that exposure to ELF–ELF magnetic fields impact the fermentation process of dried cocoa beans. These findings highlight the need for further research to validate and expand upon these observations, and to identify the optimal conditions for utilizing ELF EMF in cocoa bean fermentation. Furthermore, these studies offer valuable insights into the potential advantages of magnetic field exposure during the fermentation process of cocoa beans. Continued investigation in this field has the potential to contribute to the development of innovative techniques aimed at optimizing cocoa bean fermentation, thereby enhancing product quality and yield in the cocoa industry.

4. Conclusions

The models used in this study provide valuable information on the dynamics of microbial populations during cocoa bean fermentation. These models may not fully capture the complex intricacies associated with microbial interactions and the many variables influencing the fermentation process, i.e., environmental factors. Furthermore, the effectiveness of these models can be affected by the quality and availability of the data used for their development and validation. In addition, it is important to recognize that laboratory–scale fermentation may not fully represent the conditions and variations observed in actual on–farm fermentation, which may further exacerbate the limitations described above.

However, through these models, the potential influence of exposure to magnetic fields on the growth characteristics of microorganisms in cocoa beans, as evidenced by the observed changes in various kinetic parameters, might be demonstrated. This highlights the importance of investigating the effects of magnetic field exposure on microbial growth during cocoa fermentation in different environments. Furthermore, these findings shed light on the growth kinetics of microbial groups in cocoa beans under different magnetic field strengths and emphasize the importance of selecting appropriate models to assess growth kinetics in this context.

Author Contributions:

The authors contributed in the following manner to this research project. Conceptualization, Methodology, Validation, Formal analysis: T.M.G.A: Resources, writing – original draft; J.R: Resources, Investigation, supervision, writing – original draft & review, J.C.–V: review, visualization & editing, LSG: writing – review, visualization & editing. All authors have read and agreed to the published version of the manuscript.

Acknowledgments

The authors wish to express their sincerest gratitude to Octavio Córdova, Betty Fortis and Javier Paladines for their invaluable collaboration in preparing the article. Their experience, knowledge, and dedication contributed greatly to the quality and depth of the content. We acknowledge your great effort and sincerely appreciate your valuable input and support throughout the methodological process. Their contributions have been instrumental in shaping the article and enhancing its overall value.

Conflicts of Interest

The authors declare no conflict of interest.

References

[1] Wang, X. H., Yang, L., Ren, Y. X., Chen, N., Xiao, Q., Cui, S., & Li, D. (2019). Nitrogen removal by heterotrophic nitrifying bacterium *Pseudomonas putida* YH and its kinetic characteristics. *Huan Jing ke Xue Huanjing Kexue*, 40(4), 1892–1899. https://doi.org/10.13227/j.hjkx.201809044

[3] Ray, M., Kumar, V., & Banerjee, C. (2022). Kinetic modelling, production optimization, functional characterization and phyto–toxicity evaluation of biosurfactant derived from crude oil biodegrading Pseudomonas sp. IITISM 19. *Journal of Environmental Chemical Engineering*, 10(2), 107190.https://doi.org/10.1016/j.jece.2022.107190

[4] Ferreira, T. F., Santos, P. A., Paula, A. V., de Castro, H. F., & Andrade, G. S. (2021). Biogas generation by hybrid treatment of dairy wastewater with lipolytic whole cell preparations and anaerobic sludge. *Biochemical Engineering Journal*, 169, 107965. https://doi.org/10.1016/j.bej.2021.107965

[5] Hamedi, H., Mohammadzadeh, O., Rasouli, S., & Zendehboudi, S. (2021). A critical review of biomass kinetics and membrane filtration models for membrane bioreactor systems. *Journal of Environmental Chemical Engineering*, 9(6), 106406. https://doi.org/10.1016/j.jece.2021.106406

[6] Stavropoulou, E., & Bezirtzoglou, E. (2019). Predictive modeling of microbial behavior in food. *Foods*, 8(12), 654. https://doi.org/10.3390/foods8120654

[7] Bolívar, A., Garrote Achou, C., Tarlak, F., Cantalejo, M. J., Costa, J. C. C. P., & Pérez–Rodríguez, F. (2023). Modeling the Growth of Six *Listeria monocytogenes* Strains in Smoked Salmon Pâté. *Foods*, 12(6), 1123. https://doi.org/10.3390/foods12061123

[8] Andrade–Velasques, A., Domínguez–Cañedo, L., & Melgar–Lalanne, G. (2021). Growth kinetic model, antioxidant and hypoglycemic effects at different temperatures of potential probiotic Lactobacillus spp. *Revista Mexicana de Ingeniería Química*, 20(1), 37–49. https://doi.org/10.24275/rmiq/Alim1425

[9] G. uye Skinner, J. W. Larkin, and E. J. Rhodehamel, (1994). Mathematical modeling of microbial growth: a review. *Journal of food safety*, 14(3), 175–217. https://doi.org/10.1111/j.1745–4565.1994.tb00594.x

[10] Nguimkeu, P. (2014). A simple selection test between the Gompertz and Logistic growth models. *Technological Forecasting and Social Change*. 88, 98–105. https://doi.org/10.1016/j.techfore.2014.06.017

[11] Murunga, S.and Were, F. (2019). Predicting Microbial Growth in Anaerobic Digester Using Gompertz and Logistic Models. *IRE Journals*, 3(4), 198–205. ISSN: 2456–8880.

[12] Díaz-Muñoz, C., & De Vuyst, L. (2022). Functional yeast starter cultures for cocoa fermentation. *Journal of Applied Microbiology*, 133(1), 39–66. https://doi.org/10.1111/jam.15312

[13] Korcari, D., Fanton, A., Ricci, G., Rabitti, N. S., Laureati, M., Hogenboom, J., & Fortina, M. G. (2023). Fine Cocoa Fermentation with Selected Lactic Acid Bacteria: Fermentation Performance and Impact on Chocolate Composition and Sensory Properties. *Foods*, 12(2), 340. https://doi.org/10.3390/foods12020340

[14] Castro–Alayo, E. M., Idrogo–Vásquez, G., Siche, R., & Cardenas–Toro, F. P. (2019). Formation of aromatic compounds precursors during fermentation of Criollo and Forastero cocoa. *Heliyon*, 5(1). https://doi.org/10.1016/j.heliyon.2019.e01157

[15] Díaz–Muñoz, C., Van de Voorde, D., Comasio, A., Verce, M., Hernandez, C. E., Weckx, S., & De Vuyst, L. (2021). Curing of cocoa beans: fine–scale monitoring of the starter cultures applied and metabolomics of the fermentation and drying steps. *Frontiers in Microbiology*, 11, 616875. https://www.frontiersin.org/articles/10.3389/fmicb.2020.616875

[16] Moreno–Zambrano, M., Ullrich, M. S., & Hütt, M. T. (2022). Exploring cocoa bean fermentation mechanisms by kinetic modelling. *Royal Society Open Science*, 9(2), 210274. https://doi.org/10.1098/rsos.210274

[17] Nazaruddin, R., Seng, L. K., Hassan, O., & Said, M. (2006). Effect of pulp preconditioning on the content of polyphenols in cocoa beans (*Theobroma cacao*) during fermentation. *Industrial Crops and Products*, 24(1), 87–94. https://doi.org/10.1098/rsos.180964

[18] R. Nazaruddin, L. K. Seng, O. Hassan, and M. Said, Effect of pulp preconditioning on the content of polyphenols in cocoa beans (Theobroma Cacao) during fermentation, *Ind. Crops Prod.*, vol. 24, no. 1, pp. 87–94, 2006, https://doi.org/10.1016/j.indcrop.2006.03.013

[19] Hamdouche, Y., Meile, J. C., Lebrun, M., Guehi, T., Boulanger, R., Teyssier, C., & Montet, D. (2019). Impact of turning, pod storage and fermentation time on microbial ecology and volatile composition of cocoa beans. *Food Research International*, 119, 477–491. https://doi.org/10.1016/j.foodres.2019.01.001

[20] Fleet, G. H., & Zhao, J. (2018). Unravelling the contribution of lactic acid bacteria and acetic acid bacteria to cocoa fermentation using inoculated organisms. *International Journal of Food Microbiology*, 279, 43–56. https://doi.org/10.1016/j.ijfoodmicro.2018.04.040

[21] Evina, V. J. E., De Taeye, C., Niemenak, N., Youmbi, E., & Collin, S. (2016). Influence of acetic and lactic acids on cocoa flavan–3–ol degradation through fermentation–like incubations. *LWT–Food Science and Technology*, 68, 514–522. https://doi.org/10.1016/j.lwt.2015.12.047

[22] Ganda–Putra, G. P., Wrasiati, L. P., & Wartini, N. M. (2010). Fermentation Process of Cocoa Based on Optimum Condition of Pulp PectinDepolymerization by Endogenous Pectolityc Enzymes. Pelita Perkebunan. *Coffee and Cocoa Research Journal*. 26(2), 122–132 https://doi.org/10.22302/iccri.jur.pelitaperkebunan.v26i2.130

[23] Koffi, A. S., Sampson, G. O., Ouattara, H. G., Bruneau, D., Konan, K., & Diby, K. A. (2018). Analysis of the performance of a newly designed fermenter built in local materials for improvement of cocoa fermentation, in Ivory Coast. *Journal of Applied Biosciences*, 129, 13108–13117. https://doi.org/10.4314/jab.v129i1.13

[24] Guzmán–Armenteros, T. M., Ramos–Guerrero, L. A., Guerra, L. S., & Ruales, J. (2023). Optimization of cacao beans fermentation by native species and electromagnetic fields. Heliyon, 9(4), e15065. http://dx.doi.org/10.2139/ssrn.4364538

[25] Wei, Y., & Wang, X. (2022). Biological effects of rotating magnetic field: A review from 1969 to 2021. 178, 103–115 *Progress in Biophysics and Molecular Biology*. https://doi.org/10.1016/j.pbiomolbio.2022.12.006

[26] Miñano, H. L. A., Silva, A. C. D. S., Souto, S., & Costa, E. J. X. (2020). Magnetic fields in food processing perspectives, applications and action models. *Processes*, 8(7), 814. https://doi.org/10.3390/pr8070814

[27] Bektiarso, S., Prastowo, S. H. B., Prihandono, T., & Handayani, R. D. (2020, February). Optimizing lactobacillus growth in the fermentation process of artificial civet coffee using extremely–low frequency (ELF) magnetic field. In *Journal of Physics*: Conference Series (Vol. 1465, No. 1, p. 012010). *IOP Publishing*. https://doi.org/10.1088/1742–6596/1465/1/012010

[28] Camu, N., De Winter, T., Verbrugghe, K., Cleenwerck, I., Vandamme, P., Takrama, J. S., ... & De Vuyst, L. (2007). Dynamics and biodiversity of populations of lactic acid bacteria and acetic acid bacteria involved in spontaneous heap fermentation of cocoa beans in Ghana. *Applied and environmental microbiology*, 73(6), 1809–1824. https://doi.org/10.1128/AEM.02189–06

[29] Pierre, L. S., Buckner, C. A., Lafrenie, R. M., & Persinger, M. A. (2010). Growth of injected melanoma cells is suppressed by whole body exposure to specific spatial–temporal configurations of weak intensity magnetic fields. *International journal of radiation biology*, 86(2), 79–88. https://doi.org/10.3109/09553000903419932

[30] Kondaveeti, H. K., Kumaravelu, N. K., Vanambathina, S. D., Mathe, S. E., & Vappangi, S. (2021). A systematic literature review on prototyping with Arduino: Applications, challenges, advantages, and limitations. Computer Science Review, 40, 100364. https://doi.org/10.1016/j.cosrev.2021.100364

[31] ISO, ISO 6658:2017 Sensory analysis — Methodology — General guidance, 2017.

[32] Lefeber, T., Gobert, W., Vrancken, G., Camu, N., & De Vuyst, L. (2011). Dynamics and species diversity of communities of lactic acid bacteria and acetic acid bacteria during spontaneous cocoa bean fermentation in vessels. Food microbiology, 28(3), 457–464. https://doi.org/10.1016/j.fm.2010.10.010

[33] Gompertz, B. (1825). XXIV. On the nature of the function expressive of the law of human mortality, and on a new mode of determining the value of life contingencies. In a letter to Francis Baily, Esq. FRS &c. Philosophical transactions of the Royal Society of London, (115), 513–583. https://doi.org/10.1098/rstl.1825.0026

[34] Baranyi, J., & Roberts, T. A. (1994). A dynamic approach to predicting bacterial growth in food. International journal of food microbiology, 23(3–4), 277–294. https://doi.org/10.1016/0168–1605(94)90157–0

[35] Pearl, R., & Reed, L. J. (1920). On the rate of growth of the population of the United States since 1790 and its mathematical representation. Proceedings of the national academy of sciences, 6(6), 275–288. https://doi.org/10.1073/pnas.6.6.275

[36] Peleg, M., Corradini, M. G., & Normand, M. D. (2007). The logistic (Verhulst) model for sigmoid microbial growth curves revisited. *Food research international*, 40(7), 808–818. https://doi.org/10.1016/j.foodres.2007.01.012

[37] Wachenheim, D. E., Patterson, J. A., & Ladisch, M. R. (2003). Analysis of the logistic function model: derivation and applications specific to batch cultured microorganisms. *Bioresource Technology*, 86(2), 157–164. https://doi.org/10.1016/s0960–8524(02)00149–9

[38] Montgomery, D. C., & Peck, E. A. (2001). Introduction to Linear Regression Analysis (3a ed.). John Wiley & Sons.

[39] Sen, S., & Bradshaw, L. (2017). Comparison of relative fit indices for diagnostic model selection. *Applied psychological measurement*, 41(6), 422–438. https://doi.org/10.1177/0146621617695521

[40] Liu, Y., Wang, X., Liu, B., Yuan, S., Qin, X., & Dong, Q. (2021). Microrisk Lab: An online

freeware for predictive microbiology. Foodborne Pathogens and Disease, 18(8), 607–615. https://doi.org/10.1089/fpd.2020.2919

[41] Delgado–Noboa, J., Bernal, T., Soler, J., & Peña, J. Á. (2021). Kinetic modeling of batch bioethanol production from CCN–51 Cocoa Mucilage. *Journal of the Taiwan Institute of Chemical Engineers*, 128, 169–175. https://doi.org/10.1016/j.jtice.2021.08.040

[43] Fujikawa, H., Yano, K., & Morozumi, S. (2006). Model comparison for *Escherichia coli* growth in pouched food. *Shokuhin Eiseigaku Zasshi*, 47(3), 115–118. https://doi.org/10.3358/shokueishi.47.115

[44] Mitchell, D. A., von Meien, O. F., Krieger, N., & Dalsenter, F. D. H. (2004). A review of recent developments in modeling of microbial growth kinetics and intraparticle phenomena in solid–state fermentation. *Biochemical Engineering Journal*, 17(1), 15–26. https://doi.org/10.1016/S1369–703X(03)00120–7

[45] Mazaheri, D., & Shojaosadati, S. A. (2013). Mathematical models for microbial kinetics in solid–state fermentation: a review. *Iranian Journal of Biotechnology*, 11(3), 156–167. https://doi.org/10.5812/ijb.9426

[46] Woroszyło, M., Ciecholewska–Juśko, D., Junka, A., Pruss, A., Kwiatkowski, P., Wardach, M., & Fijałkowski, K. (2021). The impact of intraspecies variability on growth rate and cellular metabolic activity of bacteria exposed to rotating magnetic field. Pathogens, 10(11), 1427. https://doi.org/10.3390/pathogens10111427

[47] Masood, S., Saleem, I., Smith, D., & Chu, W. K. (2020). Growth pattern of magnetic field–treated bacteria. Current Microbiology, 77(2), 194–203. https://doi.org/10.1007/s00284–019–01820–7

[48] Shoda, M., Nakamura, K., Tsuchiya, K., Okuno, K., Ano, T. (1999). Bacterial Growth under Strong Magnetic Field. In: Bersani, F. (eds) Electricity and Magnetism in Biology and Medicine. Springer, Boston, MA. https://doi.org/10.1007/978–1–4615–4867–6_47

[49] Peplow, M. (2004) Magnetic field benefits bacteria. *Nature*, 1476–4687. https://doi.org/10.1038/news041122–13

[50] Hamidi–Esfahani, Z., Shojaosadati, S. A., & Rinzema, A. (2004). Modelling of simultaneous effect of moisture and temperature on A. niger growth in solid–state fermentation. *Biochemical Engineering Journal*, 21(3), 265–272. https://doi.org/10.1016/j.bej.2004.07.007

[51] He, Q., Peng, H., Sheng, M., Hu, S., Qiu, J., & Gu, J. (2019). Humidity control strategies for

solid–state fermentation: Capillary water supply by water–retention materials and negative–pressure auto–controlled irrigation. *Frontiers in Bioengineering and Biotechnology*, 7, 263. https://www.frontiersin.org/articles/10.3389/fbioe.2019.00263

[52] Calvo, A. M., Botina, B. L., García, M. C., Cardona, W. A., Montenegro, A. C., & Criollo, J. (2021). Dynamics of cocoa fermentation and its effect on quality. Scientific reports, 11(1), 16746. https://doi.org/10.1038/s41598–021–95703–2

[53] Rahardjo, Y. P., Rahardja, S., Dalapati, A., Amalia, A. F., Purwaningsih, H., & Syamsu, K. (2022). A literature review on cocoa fermentation techniques to shorten fermentation time. In IOP Conference Series: *Earth and Environmental Science* 974(1), 012111. IOP Publishing. https://doi.org/10.1088/1755–1315/974/1/012111

[54] Camu, N., González, A., De Winter, T., Van Schoor, A., De Bruyne, K., Vandamme, P, & De Vuyst, L. (2008). Influence of turning and environmental contamination on the dynamics of populations of lactic acid and acetic acid bacteria involved in spontaneous cocoa bean heap fermentation in Ghana. *Applied and Environmental Microbiology*, 74(1), 86–98. https://doi.org/10.1128/AEM.01512–07

[55] Papalexandratou, Z., Vrancken, G., De Bruyne, K., Vandamme, P., & De Vuyst, L. (2011). Spontaneous organic cocoa bean box fermentations in Brazil are characterized by a restricted species diversity of lactic acid bacteria and acetic acid bacteria. *Food Microbiology*, 28(7), 1326–1338. https://doi.org/10.1016/j.fm.2011.06.003

[56] Ardhana, M. M., & Fleet, G. H. (2003). The microbial ecology of cocoa bean fermentations in Indonesia. International journal of food microbiology, 86(1–2), 87–99. https://doi.org/10.1016/s0168–1605(03)00081–3

[57] Masood, S. (2017). Effect of weak magnetic field on bacterial growth. Biophysical Reviews and Letters, 12(04), 177–186. https://doi.org/10.1142/S1793048017500102

[58] Konopacka, A., Rakoczy, R., & Konopacki, M. (2019). The effect of rotating magnetic field on bioethanol production by yeast strain modified by ferrimagnetic nanoparticles. *Journal of Magnetism and Magnetic Materials*, 473, 176–183. https://doi.org/10.1016/j.jmmm.2018.10.053

[59] Konopacki, M., & Rakoczy, R. (2019). The analysis of rotating magnetic field as a trigger of Gram–positive and Gram–negative bacteria growth. *Biochemical Engineering Journal*, 141, 259–267. https://doi.org/10.1016/j.bej.2018.10.026

[60] Kohno, M., Yamazaki, M., Kimura, I., & Wada, M. (2000). Effect of static magnetic fields on bacteria: *Streptococcus mutans*, *Staphylococcus aureus*, and *Escherichia coli*. *Pathophysiology*, 7(2),

143–148. https://doi.org/10.1016/s0928–4680(00)00042–0

[61] Zhao, B., Sha, H., Li, J., Cao, S., Wang, G., & Yang, Y. (2020). Static magnetic field enhanced methane production via stimulating the growth and composition of microbial community. *Journal of Cleaner Production*, 271, 122664. https://doi.org/10.1016/j.jclepro.2020.122664

[62] Ciecholewska–Juśko, D., Żywicka, A., Junka, A., Woroszyło, M., Wardach, M., Chodaczek, G., & Fijałkowski, K. (2022). The effects of rotating magnetic field and antiseptic on in vitro pathogenic biofilm and its milieu. *Scientific Reports*, 12(1), 8836. https://doi.org/10.1038/s41598–022–12840–y

[63] Novák, J., Strašák, L., Fojt, L., Slaninová, I., & Vetterl, V. (2007). Effects of low–frequency magnetic fields on the viability of yeast *Saccharomyces cerevisiae*. *Bioelectrochemistry*, 70(1), 115–121. https://doi.org/10.1016/j.bioelechem.2006.03.029

[64] Potenza, L., Ubaldi, L., De Sanctis, R., De Bellis, R., Cucchiarini, L., & Dachà, M. (2004). Effects of a static magnetic field on cell growth and gene expression in *Escherichia coli*. Mutation Research/Genetic *Toxicology and Environmental Mutagenesis*, 561(1), 53–62. https://doi.org/10.1016/j.mrgentox.2004.03.009 .

Chapter 6

Cocoa Mucilage as a Novel Culture Medium: Unveiling its Potential for Microbial Growth and Biotechnological Applications

Tania María Guzmán–Armenteros[1]*, Luis Santiago Guerra[2], and Jenny Ruales[1]

[1] Departamento de Ciencia de Alimentos y Biotecnología (DECAB), Escuela Politécnica Nacional (EPN), Quito, Ecuador; tania.guzman@epn.edu.ec, jenny.ruales@epn.edu.ec

[2]Universidad Central del Ecuador (UCE), Facultad de Ciencias Médicas, Carrera de Medicina, Campus El Dorado, Quito, Ecuador, lsguerrap@uce.edu.ec

*Corresponding author: tania.guzman@epn.edu.ec, taniamariaguzman@gmail.com

Abstract

The cocoa mucilage is typically disposed of during processing, yet its abundant content of organic compounds, polysaccharides, and nutrients renders it valuable for various applications. This scientific article investigates the suitability of cocoa mucilage as an alternative culture medium for *Lactobacillus plantarum*, *Saccharomyces. cerevisiae*, and *Aspergillus niger*, aiming to provide a viable alternative to traditional media. Through a mixed–design approach, the powdered mucilage, peptone, and yeast extract ingredients were optimized using the recovery rates of each microorganism as the response variable. The optimal formulation of the medium, consisting of 49.6% mucilage, 30% yeast extract, and 20.9% peptone, resulted in remarkable microbial recovery rates. *L. plantarum* achieved an outstanding recovery rate of 98.18%, while *S. cerevisiae* and *A. niger* exhibited recovery rates of 90.57% and 89.90%, respectively. Notably, these recovery rates surpassed those obtained using conventional culture mediums. Thus, cocoa mucilage emerges as an effective component for formulating a natural culture medium that facilitates the growth of yeasts, lactic acid bacteria, and fungi. The YPM medium demonstrated enhanced growth, particularly for yeasts and lactic acid bacteria, with recovery rates exceeding 90%. Conversely, *A. niger* displayed a relatively lower recovery rate. These findings emphasize the potential of cocoa mucilage as a valuable resource for preparing natural culture media that promote the growth of yeasts, lactic acid bacteria, and fungi, offering promising prospects for various applications in microbiology and biotechnology.

Keywords: cocoa mucilage, culture medium, bacteria, yeasts, fungi, mix design, microbial growth.

1. Introduction

Cocoa mucilage, a gelatinous substance that surrounds cocoa beans, has drawn attention as a promising candidate for industrial applications. Despite being traditionally discarded during cocoa processing, this by–product has aroused interest due to its rich composition of organic compounds, polysaccharides, and nutrients [1–3]. These characteristics make cocoa mucilage a sustainable and valuable alternative for various biotechnological applications.

Recently, the use of cocoa mucilage residues as a substrate for the production of biofuels [2], bioethanol [3, 4], and high–value chemical products [5, 6] has been highlighted. In addition, numerous studies have shown its ability to promote microbial growth and activity. Research has also shown that cocoa mucilage favors the proliferation of cellulolytic microorganisms, leading to increased production of cellulase enzymes [7, 8].

Furthermore, cocoa mucilage has potential applications in the food industry. Its water–retaining and satiety–increasing properties [9], as well as its ability to decrease nutrient absorption time [9, 10], make it an intriguing ingredient to incorporate into various food products. Various fermentation processes for wines [11] and alcoholic beverages [12], as well as the preparation of juices [13], soft drinks [14], and jellies [15], have used cocoa mucilage in their formulation. Ongoing research in this area aims to harness the potential of cocoa mucilage as a food ingredient, offering unique flavors and nutritional benefits in the development of new food products.

The composition of cocoa mucilage also plays a fundamental role in its potential as a culture medium [4]. It contains various carbohydrates, including glucose, fructose, and galactose, which serve as carbon sources for microbial metabolism [10–14]. In addition, cocoa mucilage is devoid of alkaloids and toxic substances and is enriched with phenolic compounds, organic acids, vitamins, and minerals [16, 18]. These bioactive components stimulate the growth of beneficial microorganisms, in particular lactic acid bacteria, which are crucial for fermentation processes in the food industry. However, more research is needed to fully explore the biotechnological potential of cocoa mucilage, which promises the development of environmentally friendly and sustainable processes within the cocoa industry.

Three microbial species commonly isolated from cocoa mucilage stand out displaying remarkable applications in various industries: *Saccharomyces cerevisiae*, a versatile yeast, is indispensable in alcohol production due to its exceptional fermentation abilities. It efficiently converts sugars into alcohol through anaerobic respiration, making it ideal for large–scale fermentation processes [4, 5, 19]. Besides alcoholic beverages, *S. cerevisiae* contributes to biofuel production by synthesizing ethanol as a renewable alternative to fossil fuels [5, 19, 20]. It also holds the potential for producing high–value compounds in biotechnology [19]. *Lactobacillus plantarum*, lactic acid bacteria (LAB),

exhibits probiotic properties that benefit human health and plays a crucial role in vitamin production [21–24], offering economic and safe options for various applications in the food and nutraceutical industries. *A. niger*, a filamentous fungus, excels at producing commercially valuable compounds like citric acid and enzymes used in various industries [25, 26]. It shows promise as a host organism for the production of proteins and secondary metabolites, further enhancing its significance in pharmaceutical and biotechnological fields [25–27].

The remarkable technological potential exhibited by these microorganisms underscores their integral role in the biotechnological landscape. Unlocking your full capabilities and driving transformational change across multiple industries requires continued focus on research and development efforts. To this end, this study aims to investigate the growth potential of *S. cerevisiae*, *Lactobacillus plantarum*, and *Aspergillus niger* in an innovative medium composed of cocoa mucilage and compare their growth rate with that observed in conventional growth media.

Using mucilage, this technique moves away from conventional culture media ingredients to minimize the waste of cocoa by–products while supporting microbial growth. This underscores its remarkable potential to find applications in biotechnology, promote microbial cultivation practices, and protect the environment.

By exploring the growth dynamics of these microorganisms in cocoa mucilage, light is shed on the viability and efficacy of this new growth medium. These research efforts hold great promise in terms of providing cost–effective and sustainable solutions. The unique composition of cocoa mucilage presents an exciting opportunity to discover a new pathway for the cultivation of these microorganisms, which could revolutionize their industrial applications.

2. Methodology

2.1. Experimental procedure

2.1.1 Obtaining cocoa mucilage powder (CMP)

The cocoa mucilage exudate (CME) was obtained from the liquid mucilage of the CCN–51 cocoa variety, sourced from local producers in the Santo Domingo de los Tsáchilas province. After 18 hours of cocoa bean harvesting, the removal of the mucilaginous pulp surrounding the seeds takes place. This process involves the enzymatic action of pectin, which leads to the liquefaction of the pulp and the subsequent separation of the mucilage from the beans. The drained mucilage then transforms into cocoa mucilage exudate (CME) [28]. This step is crucial in cocoa processing, as it helps to eliminate the pulp and extract the desired mucilage. The collection process involved using sterile stainless–steel containers with a capacity of 10 L, and it was carried out at a temperature of 25 ºC. Multiple

collections were conducted over up to three days of fermentation, resulting in a total volume of 20 L of liquid mucilage. Once collected, the liquid mucilage was stored at 4 °C until further processing.

To preserve the properties of the mucilage, the CME was subjected to spray drying with a 15% efficiency. The spray drying process involved a controlled flow rate of 0.1 to 0.5 L per minute. This process was continued until 1.96 kg of powdered mucilage was obtained. The cocoa mucilage powder (CMP) obtained from the spray drying process was stored at 25 °C until it was ready for use [29].

2.1.2. Culture medium

2.1.2.1. Culture medium formulation

The culture medium employed in this study was prepared using commercially available components, and cocoa mucilage powder (CMP) obtained as described in subchapter 2.1.1; yeast extract (YE), peptone (PEP), and agar–agar (AA) purchased from Oxoid brand, Thermo Fisher Scientific. The formulation of the culture medium was meticulously established using a mixture design methodology, as elucidated in subchapter 2.2.1 and outlined comprehensively in Table 1. It is noteworthy that the agar–agar served the specific role of solidifying the medium and was maintained at a constant concentration of 2.5%(v/v).

To ensure optimal conditions for microbial growth, the pH of each formulation was carefully adjusted to achieve neutral values. The procedure included the initial measurement of pH, in the media suspended in distilled water, with the gradual addition of an acid (HCl) or base (NaOH) while monitoring the pH, until reaching the target pH (neutral). This adjustment was crucial in creating a favorable environment for the microorganisms to thrive and exhibit their growth potential. By standardizing the pH in the different formulations, any variation in microbial growth rates could only be attributed to the specific ingredients and their concentrations, and not to this factor (pH), allowing a full evaluation of the efficacy of the culture medium.

Tabla 1. Mix design components

		Labels				central tendency measures	
Factors	Variables	Minimum	Maximum	minor code	high code	mean	Sd
A	CMP	40	50	+0 ↔ 40	+0.5 ↔ 50	43.63	3.83
B	YE	5	15	+0 ↔ 5	+0.5 ↔ 15	8.02	3.67
C	PEP	5	15	+0 ↔ 5	+0.5 ↔ 15	8.25	3.63

CMP: Cocoa Mucilage Powder; YE: Yeast Extract; PEP: peptone

2.1.2.2. Culture medium preparation

To create optimal growth environments for the various microbial groups under investigation, specific agar media were meticulously prepared according to the guidelines provided by the manufacturer [30]. The main objective was to tailor the nutrient compositions of the media to support the growth of each target microorganism. For the cultivation of *L. plantarum*, Man Rogosa Sharpe Agar (MRS) was the medium of choice, while Malt Yeast Extract Agar (MYA) was selected to suit the growth of the S. cerevisiae. To promote *A. niger* growth, Sabouraud Dextrose Agar (SDA) was used as a suitable growth medium. All media used were Oxoid brand, and Thermo Fisher Scientific.

The agar medium preparation procedure was methodical and aimed at ensuring the creation of an environment conducive to microbial growth. The process began with the meticulous dissolution of the agar powder in distilled water. Special attention was paid to this step to ensure complete dissolution. The mixture then went through a critical autoclaving phase. This sterilization step was essential to eradicate any possible contaminants, thus safeguarding the purity and integrity of the agar medium [30,31].

After successful sterilization, the agar medium was carefully poured into sterile Petri dishes. This step required precision to avoid any unintentional contamination that could jeopardize the subsequent microbial culture. Once poured, the medium was allowed to solidify naturally within the Petri dishes. This solidification process was instrumental in creating the proper foundation for microbial growth [30,31]. The methodology took a comprehensive approach to ensure that the unique nutritional requirements of each microbial group were met through custom agar media. The rigorous preparation process, including dissolution, sterilization, and solidification, was instrumental in establishing a controlled, uncontaminated environment conducive to the successful cultivation of target microorganisms [30–31].

2.1.3. Microbial cultivation

2.1.3.1 Preparation of the inoculum

Cell suspensions of three different microbial strains, namely Saccharomyces cerevisiae, Lactobacillus plantarum, and Aspergillus niger, were prepared for enumeration. These strains were chosen based on their relevance to cocoa bean fermentation, the main focus of the study. Pure cultures were obtained through meticulous isolation procedures and maintained under controlled conditions to ensure purity and microbial viability, consistent with standard pre–culture techniques [30–32]. A small volume of each microorganism was inoculated in Lysogenic Broth (LB medium, Oxoid) which provides the necessary nutrients and conditions for the growth of all microbial groups under study.

Once inoculated, each culture is incubated under controlled room temperature conditions (*L. plantarum* 35ºC at 24h; *S. cerevisiae* 30ºC at 48h, and *A. niger* 25ºC at 72h)

The preparation of the cell suspensions involved several critical steps to ensure the accuracy and reliability of the subsequent microbial enumeration process. Each pure culture was first grown under optimal growth conditions, allowing them to reach a suitable population size. These populations were then meticulously diluted to achieve a range of cell concentrations that would be possible to count. The target concentration for each microbial strain was set at 1000 colony–forming units (CFU) per milliliter, a concentration that balances the need for precision against practical feasibility [30,31].

To create the necessary dilutions for an accurate count, serial dilution techniques were employed. This involved transferring precise aliquots of the cell suspensions to separate tubes containing sterile diluents, such as distilled water or buffered peptone solution supplied by Merck. Through the use of diluents, the concentration of microbial cells was systematically reduced in a controlled manner, resulting in dilutions of 1:10, 1:100, and 1:1000. These dilutions have been specifically designed to cover a wide range of microbial concentrations, allowing for accurate quantification of microbial load. Serial dilution facilitated accurate counting, ensuring that the counting process is within the range of the counting chamber or slides used for microscopic analysis. (avoiding overcrowding of the cells), which could lead to miscounts [31].

2.1.3.2 Inoculation and Incubation.

With a sterile pipette, a known volume of 0.1 mL of each dilution was transferred to agar plates containing the previously described media. For yeast and fungi, the inoculum was spread evenly over the surface of the agar plates using a sterile spreader to ensure adequate distribution [30–32]. For the LAB, the bilayer planting technique was used. In a pipette, a 0.1mL aliquot of the liquid bacterial culture was gently dispensed onto the surface of the solid agar base layer. The liquid culture was carefully spread to ensure even distribution across a significant area of the agar surface. Subsequently, the liquid culture was allowed to be absorbed into the agar base layer by leaving the plate undisturbed for a few minutes, facilitating the immobilization of the bacteria within the agar.

A second layer of molten agar, maintained at a temperature of approximately 45–50 °C to avoid thermal damage to the bacteria, was then poured onto the plate, ensuring uniform coverage over the immobilized bacteria. Upon solidification, the resulting plate established a bilayer system where the bacteria were embedded within the solid agar base layer, while the second layer served as an overlay [31, 32].

To prevent contamination, the Petri dishes were securely sealed with parafilm. Subsequently, the agar plates were placed in an incubator set at the optimal temperature for the growth of each

microorganism. Lactobacillus plantarum was inoculated on MRS agar and incubated at a temperature range of 30–35 °C for 2–3 days. *S. cerevisiae*, on the other hand, was inoculated on MYA agar and incubated at a temperature range of 20–25 °C for 2–3 days. For the growth of *Aspergillus niger*, the fungus was inoculated on SDA agar and incubated at a temperature range of 20–25 °C for a slightly longer duration of 3–7 days. These specific incubation conditions were chosen to ensure optimal growth and development of each microorganism in their respective culture media [32].

2.2 Statistical procedure

2.2.1 Experimental design

A standard simplex lattice mix design was employed specifically for the selected simplex–lattice (q, m) design. This design involved q components, with q being equal to 3 in this case, allowing for the fitting of a statistical model of order m. The design points encompassed all possible combinations of elements or mixtures, with the proportions represented by xi ranging from 0 to 1 and taking m + 1 values. The specific values of xi were 0, 1/m, 2/m, ..., and m/m, corresponding to the proportions in which the components of the mixture participated (x1, x2, ..., xq) [33].

The specific design points used were as follows: (x1, x2, x3) = (1, 0, 0); (0, 1, 0); (0, 0, 1); (1/2, 1/2, 0); (1/2, 0, 1/2); and (0, 1/2, 1/2). These design points represented the three pure mixtures and the three binary mixtures, providing a comprehensive range of combinations for the experimental investigation. By utilizing this design, the study aimed to explore the effects of different mixture compositions on the observed outcomes, enabling a thorough analysis of the variables under investigation [33].

The primary objective of implementing this design was to further refine the mathematical models by systematically varying the concentrations of the mixtures to assess the impact of these factors on the growth of microorganisms. This allowed for a more in–depth evaluation of the efficacy of cocoa mucilage as a natural culture medium for microbial development (Table 2).

Table 2. Experimental runs and mixture design results

Random runs	Blocks	Runs	CMP	YE	PEP
3	Block 1	1	50	5	5
21	Block 1	2	50	5	5
11	Block 1	3	43.33	8.33	8.33
19	Block 1	4	40	5	15
2	Block 1	5	40	5	15
12	Block 1	6	40	15	5
7	Block 1	7	41.66	6.66	11.66
10	Block 1	8	46.66	6.66	6.66
9	Block 1	9	40	5	15
18	Block 1	10	40	15	5
13	Block 1	11	40	15	5
8	Block 2	12	50	5	5
17	Block 2	13	40	10	10
15	Block 2	14	45	5	10
1	Block 2	15	45	10	5
4	Block 2	16	40	10	10
16	Block 2	17	45	5	10
5	Block 2	18	45	5	10
20	Block 2	19	41.66	11.66	6.66
14	Block 2	20	45	10	5
6	Block 2	21	50	5	5

CMP: Cocoa Mucilage; Powder YE: Yeast Extract; PEP: peptone

To increase the size of the experiment, the design was replicated, resulting in a total of 21 mixtures. The formulation consisted of three main ingredients, which together represented sixty percent of the total weight (Figure 1 and Table 1): cocoa mucilage powder (CMP), yeast extract (YE), and peptone (PEP). The objective was to investigate the effects of these components on the growth rates of the study microorganisms. The experimental results obtained from the mixture design were adjusted to a quadratic model, represented by the following equation:

$$E_{(y)} = \beta_1 * x_1 + \beta_2 * x_2 + \beta_3 * x_3 + \beta_{12} * x_1 * x_2 + \beta_{13} * x_1 * x_3 + \beta_{23} * x_2 * x_3 \quad (1)$$

2.1.1 Model response variables

The experimental design included the measurement of the recovery rates of three different microbial species: *L. plantarum*, *S. cerevisiae*, and *A. niger*. These recovery rates were selected as the main response variables of interest, reflecting the growth and development of the microorganisms under investigation (Figure 1 and Table 3).

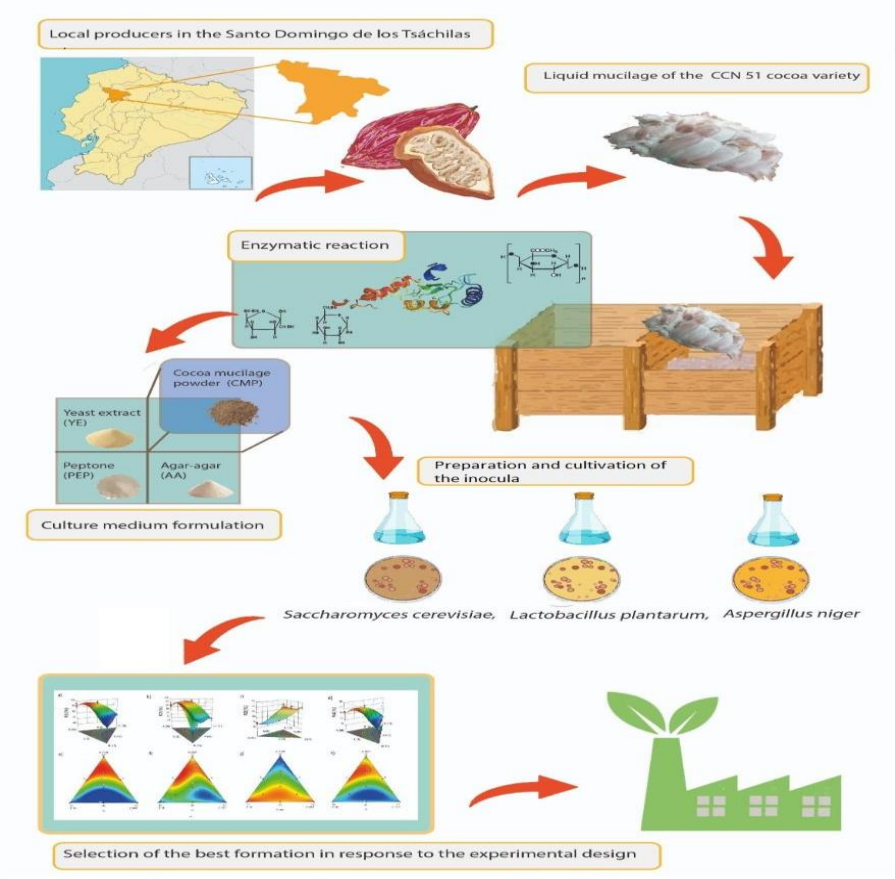

Figure 1. Schematic drawing of the experimental procedure for the evaluation of the culture medium.

To ensure robust and reliable results within the region of the workspace where maximum microbial growth values are achieved, a total of 21 experimental runs were conducted. This complete experimental setup allowed for thorough exploration and analysis of the variables influencing the recovery rates of the microbial groups. The increased number of experimental runs contributed to enhanced reliability and statistical robustness in the evaluation of microbial growth outcomes.

To enhance the precision and reliability of the experimental results, the allocation of runs in this study was randomized. The values of the blocks, which represented different concentrations of the mixtures used, were determined within the defined study area. This approach, as outlined in Table 2, ensured comprehensive coverage of the experimental space and minimized the potential influence of confounding factors.

Table 3. Microbial recovery rates in the formulations

Runs	CEP	YE	PEP	R1(%)	R2(%)	R3(%)	R4(%)
1	50	5	5	88.74	86.72	72.42	82.627
2	50	5	5	91.91	91.9	75.53	86.447
3	43.33	8.33	8.33	73.35	83.78	84.64	80.590
4	40	5	15	71.03	70.55	87.77	76.450
5	40	5	15	72.52	70.31	88.58	77.137
6	40	15	5	71.25	70.61	90.6	77.487
7	41.66	6.66	11.66	70.9	72.71	86.43	76.680
8	46.66	6.66	6.66	96.22	94.77	77	89.330
9	40	5	15	70.16	73.73	90.15	78.013
10	40	15	5	70.28	70.96	88.95	76.730
11	40	15	5	70.25	73.27	89.99	77.837
12	50	5	5	95.56	92.55	74.33	87.480
13	40	10	10	70.37	89.56	85.56	81.830
14	45	5	10	97.07	98.06	76.03	90.387
15	45	10	5	98.41	98.7	78.13	91.747
16	40	10	10	74.93	77.44	89.67	80.680
17	45	5	10	95.52	96.68	78.53	90.243
18	45	5	10	94.81	93.95	75.28	88.013
19	41.66	11.66	6.66	72.87	77.56	90.36	80.263
20	45	10	5	97.12	99.02	77.68	91.273
21	50	5	5	90.89	89.09	74.98	84.987

CMP: Cocoa Mucilage; Powder YE: Yeast Extract; PEP: peptone; R1: *S. cerevisiae* rate; R2: *L. plantarum* rate; R3: *A. niger* rate; R4: Total rate.

2.2.2. Optimization procedure

2.2.2.1. Numerical and graphical optimization

Numerical and graphical optimization was performed with Expert v13 software (Stat–Ease). The objective of the optimization process was to maximize the recovery rates of the four microorganisms by adjusting the proportions of the three ingredients within the specified study range [34, 35]. To achieve the maximum objective, the desirability of each response was determined using the following criteria formulas:

$$d_i = 0, \qquad Y_i \leq Low_i \tag{2}$$

$$d_i = \left[\frac{Y_i - Low_i}{High_i - Low_i}\right]^{wt_i}, \qquad Low_i < Y_i < High_i \tag{3}$$

$$d_i = 1, \qquad Y_i \geq High_i \tag{4}$$

Where d1 = 0 represents the minimum desirability and di = 1 represents the maximum desirability.

In the desirability objective function D(X), each response can be assigned an importance relative to the other responses. The optimization was carried out on the original scale and assigned a maximum importance of 5 advantages (+++++) to the proposed objective to adjust the desirability function. Where importance (ri) varies from the least important (+) value of 1 to the most important (+++++) value of 5 [34, 35]. If varying degrees of importance are assigned to the different responses, the objective function is:

$$D = \left(d_1^{r_1} * d_1^{r_2} * \ldots * d_1^{r_n}\right)^{\frac{1}{\sum r_1}} = \left(\prod_{i=1}^{n} d_i^{r_1}\right)^{\frac{1}{\sum r_1}} \tag{5}$$

During the graphical optimization of the four responses, the goal was to identify regions where the requirements and critical properties were met simultaneously. This was achieved by overlaying the contours of the critical responses on a contour plot. By doing so, the optimal compromise, or sweet spot, could be selected.

2.2.1.2 Confirmation analysis

The models obtained from each response were used to provide predictions and interval estimates at the optimization point. During confirmation, the model's prediction interval was compared to the average of a follow–up sample. If the average of the samples is within the prediction interval, the model is confirmed. Confirmation was made at the most convenient numerical optimization point [34].

To confirm that the model can predict the actual results in the optimal configuration determined from

the numerical analysis, seven confirmation runs were performed. The average of those runs is compared to the prediction interval. Smaller intervals indicate good precision in the estimates, and the default value for the prediction interval (L) is 95% = (1–0.05) *100%.

2.2.3. Effect size assessment

To evaluate the effectiveness of the formulated mixtures, the effect size was calculated using Cohen's d (d: 0.2 small; d: 0.5 medium; d: 0.8 large) based on the microbial growth rates [35]. The growth rates achieved in the Yeast–extract Peptone Mucilage (YPM) agar were compared to those obtained in traditional media commonly used for the respective microbial groups.

For *L. plantarum*, the growth rates in the YPM medium were compared to those in Man Rogosa Sharpe (MRS) agar. Yeast growth rates in the YPM medium were compared to those in Malt Extract Yeast Extract Glucose Agar (MYA), while fungal growth rates in the YPM medium were compared to those in Sabouraud Dextrose Agar (SDA). All culture media were from Merck, Co. Ltd.

To ensure the reliability and reproducibility of the results, all experiments were conducted in triplicate under identical conditions, using the same concentrations of components and microbial groups. This approach minimized the potential influence of confounding factors and allowed for a robust comparison between the YPM medium and traditional media for each microbial group.

2.3 Analytical determinations

2.3.1 Determination of the total microbial population

To estimate the total number of *L. plantarum* in the suspension, the turbidimetric method relying on the McFarland standard was employed. By comparing the turbidity of the bacterial suspension to the turbidity of a well–defined McFarland standard through a standard curve [36], the total number of *L. plantarum* present could be determined. The McFarland density standards were verified using a digital spectrophotometer (Perkin Elmer LAMBDA 1050) with a 1 cm light path at 625 nm. Subsequently, the total number of cells per microliter (Ns) was obtained.

The determination of total yeasts and fungi (spores) was accomplished by direct counting using a Neubauer chamber [37]. The total number of cells per microliter (Ns) of each suspension was calculated from the number of cells counted in the counting area, using the following equation (6) to convert the count to the number of cells per microliter.

$$Ns = \frac{Ct}{A * Cd * Df} \quad (6)$$

Where N is the number of cells per microliter, Ct is the number of cells counted, A is the counted area, Cd is the chamber depth, and Df is the dilution factor

2.3.2 Determination of Colony–Forming Units (CFU)

Colony–forming units (CFU) were determined using microbial culture techniques in this study. For *S. cerevisiae* and *A. niger*, as well as *L. plantarum*, the serial dilution method described in ISO 6887–1 [31] was employed. Microbial suspensions with known concentrations were cultured using different formulations of the Yeast Extract Peptone Mucilage (YPM) agar, as well as traditional media such as MRS agar, MYA agar, and SDA.

The microbial cultures were inoculated and incubated according to the procedures outlined in Chapter 2.1.3.2. Following incubation, the total cell growth (Nv) values were determined using equation 7 [31]. These techniques allowed for the quantification of microbial growth and provided valuable data for comparing the effectiveness of the YPM medium with traditional media in supporting the growth of *L. plantarum*, *S. cerevisiae*, and *A. niger*.

$$Nv = \left(\frac{\frac{1}{n} \sum_{i=1}^{n} (C)_i}{V * p * d} \right) * 100 \quad (7)$$

Where n: replicas; i: the subset of n; j: a total of replicas; C: the total number of colonies; V: Inoculum volume; p: number of plates counted; and d: minor dilution.

2.3.3 Recovery rates

The recovery rate (Rx) for each microbial group was determined by evaluating the Nv (number of viable cells) within each group relative to the total number of microorganisms in the corresponding microbial suspension, indicated as Ns. To calculate recovery rates for *L. plantarum*, *S. cerevisiae*, and *A. niger*, Equation 8 was used, which provides specific formulas for each microbial group [38]. The total recovery rate (RR) was calculated as the average of the recovery rates for each microbial group, as expressed in Equation 9.

In the context of the mixture design, the recovery rates obtained for each microbial group (Rx) and the total recovery rate (RR) were considered response variables. These response variables served as

crucial indicators to assess the efficacy of the formulated medium. Additionally, parallel evaluations were performed using traditional media to compare the recovery rates obtained on the optimized media. This analysis aimed to determine the size of the effect, thus providing information on optimized media for promoting microbial growth and recovery.

$$R(x) = \left(\frac{\frac{1}{n} \sum_{i=1}^{n} (Nv)_i}{\frac{1}{n} \sum_{i=1}^{n} (Ns)_i} \right) * 100 \quad (8)$$

Where x is the microbial group, i: replicas, n: a total of replicas, Nv: the number of viable cells per milliliter, and Ns: the total number of cells per milliliter in suspension.

$$RR = \frac{1}{3} \sum R(x) \quad (9)$$

Where R is the recovery rate and x is the microbial group.

3. Results

3.1. Analysis of the obtained models

Table 3 presents the recovery rates obtained for each microorganism through different mixtures. Among these mixtures, formulations 8, 12, 14, 15, and 20 demonstrated the highest recovery rate of *S. cerevisiae*, reaching 96.65%. Similarly, formulations 8, 14, 17, and 20 exhibited the highest recovery rate of *L. plantarum*, with a value of 97.44%. In addition, it was found that the recovery rate of *A. niger* was higher in formulations 6, 9, and 19. However, this microorganism exhibited the lowest recovery rates. These findings indicate cocoa mucilage's effectiveness in promoting the growth and recovery of the study microorganisms.

The mixture design analysis yielded four significant models (Table 4) that effectively describe the relationship between recovery rates of different microorganisms (R1: *S. cerevisiae*, R2: *L. plantarum*, R3: *A. niger*, and R4: total) and the proportions of various ingredients (A: mucilage, B: yeast extract, C: peptone). These models exhibited a statistically significant influence ($p<0.05$) on the studied variables, with a confidence level of 95%. Specifically, the mixtures of mucilage/yeast extract (AB) and mucilage/peptone (AC) were consistently identified as significant terms ($p<0.05$) in all models.

Furthermore, in the R2 model, the yeast extract/peptone (BC) mixture also demonstrated significance ($p<0.05$). Moreover, for the recovery rates of R3 and R4, the combination of all three components (ABC) in the mixture was found to be significant ($p<0.05$) (Table 4). These results emphasize the

importance of the specific ingredient combinations that influence the recovery rates of different microorganisms, highlighting the significance of optimizing the proportions of mucilage, yeast extract, and peptone in promoting microbial recovery.

Table 4 ANOVA and fit statistics results of mixture design.

Models	Sig.term p<0.05	Lack of fit (p)	F–value	p– value	R^2 Ajusted	R^2 Predicted	CV (%)	Adeq Precision
Model R1	AB, AC	0.56	84.43	<0.00	0.97	0.93	2.14	22.48
Model R2	AB, AC, BC	0.19	15.57	<0.00	0.82	0.65	4.32	11.59
Model R3	AB, AC ABC	0.98	52.14	<0.00	0.94	0.88	1.86	17.59
Model R4	AB, AC ABC	0.39	57.39	<0.00	0.92	0.81	1.51	16.68

*Model terms with p–values below 0.05 are considered statistically significant, indicating their importance in the model. Non–significant terms are removed, resulting in reduced models. The equations of these reduced models are expressed as functions of the coded terms. The lack of fit of the models is non–significant when compared to the pure error, suggesting that the models adequately fit the data. The Predicted R^2 is in reasonable agreement with the Adjusted R^2 i.e. the difference is less than 0.2

The lack of fit tests conducted on the four models revealed non–significant results ($p > 0.05$), indicating that these models adequately capture the variation observed between replicates without disregarding data due to random error (Table 4). The predicted and fitted coefficients of determination (R^2) for each model exceeded 0.5, and the predicted R^2 values closely aligned with the fitted R^2 values, differing by less than 0.2 [33, 34]. Hence, these models provide a reliable framework for exploring the design space (Table 4). Each mathematical model effectively represents the expected change in the response variable per unit change in the corresponding variable, while maintaining the other variables constant [34].

3.2. Microbial species' recovery rate

Figure 2 (a and e) displays the recovery rate of *S. cerevisiae.* The contour plots and response surface generated from the models reveal a clear pattern, indicating that an increase in mucilage concentration corresponds to a higher recovery rate of *S. cerevisiae*, as evidenced by the prominent red areas in the plots. The observed positive relationship between mucilage concentration and the yeast recovery rate can primarily be attributed to the significant mixtures of mucilage/peptone and mucilage/yeast extract, as indicated by the statistical analysis (Table 4). Conversely, when the concentration of mucilage in the mixtures decreases, there is a marked decrease in the recovery rate of *S. cerevisiae.*

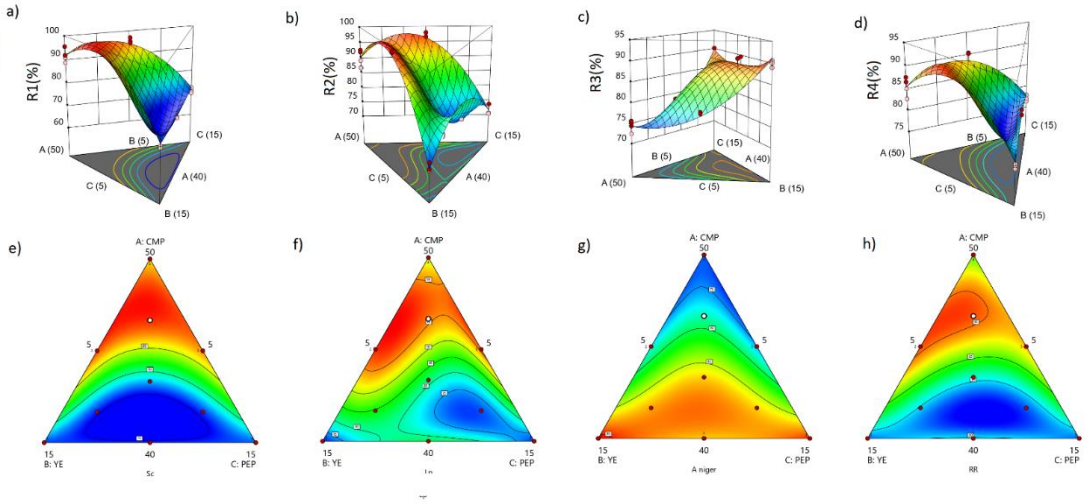

Figure 2 Response surface and contour of recovery rate. (a) R1: S. cerevisiae R2; (b) L plantarum; (c) R3: A. niger and (d) R4: RR

The contour plot and response surface analysis (Figures 2 b and f) reveal a similar pattern in the recovery rate of *L. plantarum* compared to *S. cerevisiae*. Increasing the concentration of cocoa mucilage in the mixture leads to a noticeable improvement in the recovery rate of *L. plantarum*. Furthermore, evidence suggests that decreasing the proportion of yeast extract while simultaneously increasing the mucilage concentration significantly enhances the recovery rate of *L. plantarum*.

However, a distinct crest is observed in the response surface plot for *L. plantarum*, indicating a potential limit to the beneficial effects of mucilage concentration on its recovery rate. This suggests that there may be an optimal range of mucilage concentration that yields the desired effect for *L. plantarum* (Figures 2 b and f).

In contrast to *S. cerevisiae* and *L. plantarum*, the recovery rate of *A. niger* exhibited a distinct response to variations in mucilage, yeast extract, and peptone concentrations in the mixtures (Figure 2 c, g). Specifically, as the mucilage concentration increases, the recovery rate of *A. niger* decreases. Conversely, an increase in the proportions of yeast extract and peptone in the mixtures resulted in an improvement in the recovery rate of *A. niger*.

The graphical representation suggests that optimizing the recovery rate of *A. niger* requires targeting specific values beyond designated limits, where maximum recovery rates can be achieved. To maximize the recovery rate of *A. niger*, adjustments to the proportions of the design can be made.

The study findings underline the importance of strategic manipulation of formulation components to optimize the recovery rate of *L. plantarum*, *S. cerevisiae*, and *A. niger*. Increasing the mucilage concentration while reducing the proportions of yeast extract and peptone is predicted to have a positive impact on the growth and recovery of bacteria and yeast in the given context. Furthermore, the results emphasize the importance of lower concentrations of mucilage and high concentrations

of yeast extract and peptone to achieve optimal recovery of the fungus.

These findings provide valuable information to optimize the recovery process of these microbial species and underscore the crucial role of cocoa mucilage in recovery and growth promotion.

3.2.1 Total recovery rate

The observations presented in Figures 2 d and h provide valuable insights into the behavior of the total recovery rate and its relation to the mucilage concentration. It becomes apparent that as the mucilage concentration increases significantly, there is a noticeable upward trend in the total recovery rate. This finding strongly suggests that higher concentrations of mucilage have the potential to contribute to improved recovery rates, which in turn opens up the possibility of reducing the proportions of yeast extract and peptone in the formulation while still achieving desirable recovery results.

The implications of these findings are significant. By carefully manipulating the mucilage concentration, it becomes feasible to optimize the full recovery rates of the microbial groups under investigation. This observation serves as compelling evidence that the inclusion of mucilage in the culture medium plays a crucial role in enhancing the recovery rates of these microorganisms.

3.3 Optimization Results

3.3.1. Overlapping areas

The visualization of the superimposed graph in Figure 3 (f) reveals the optimization process of the four response variables. Within this context, an area with an optimal formulation characterized by specific coordinates where the maximum recovery rates of all microbial groups are obtained is identified.

Analysis of the specific coordinates of the optimal formulation indicated as X1: A, X2: B, and X3:C reveals that the optimal formulation consists of 44.53% mucilage (A), 9.05% yeast extract (B), and 6.40% peptone (C). It is noteworthy that within these coordinates, the four response variables that represent recovery rates (R1, R2, R3, and R4) reach their highest values (Figure 3a–e).

The recovery rates achieved by the optimized formulation are remarkable for S. cerevisiae, with a recovery rate of 87.60%, while L. plantarum demonstrates a recovery rate of 96.09%, and A. niger presents a recovery rate of 82.70%. Taking all microbial groups into account, the overall recovery rate reaches 87.40% (Figure 3f).

These compelling results provide strong evidence for the efficacy of the optimized formulation. The achievement of maximum recovery rates for all microbial groups within the identified coordinates emphasizes the success of the optimization process and its possible practical applications. These findings underscore the crucial role that mucilage, yeast extract, and peptone play in promoting the growth and recovery of *L. plantarum, S. cerevisiae,* and *A. niger*, as well as the efficiency of the overall process.

Table 5 Prediction results

Responses	Predicted Mean	Standard Deviation	Standard Error	Number of runs	Lower Limit **LI**	Observed Mean	Upper limit. **LS**
R1	87.607	1.771	1.680	7	83.920	88.160	91.316
R2	94.280	3.700	2.357	7	89.187	91.191	99.372
R3	82.705	1.537	1.111	7	80.303	81.742	85.103
R4	87.399	1.252	1.187	7	84.788	87.897	90.018

3.3.2 Evaluation at the Point of Optimization

The evaluation of the experimental formulation at the point of optimization, as presented in Table 5, highlights the robustness of the model's predictions. With a confidence level of 95%, the average observations of each confirmation experiment align closely with the prediction interval of the confirmation node. This alignment demonstrates the accuracy and reliability of the model's predictions at the specified coordinates, as depicted in Figure 3.

The successful validation of the model's predictions through confirmatory experiments reinforces the practicality and effectiveness of the optimized formulation. The confirmed predictions support the suitability and reproducibility of the identified formulation coordinates, which involve specific ratios of mucilage, yeast extract, and peptone. These findings assure that the optimized formulation can consistently yield the desired outcomes and provide a reliable foundation for further experimentation and practical applications.

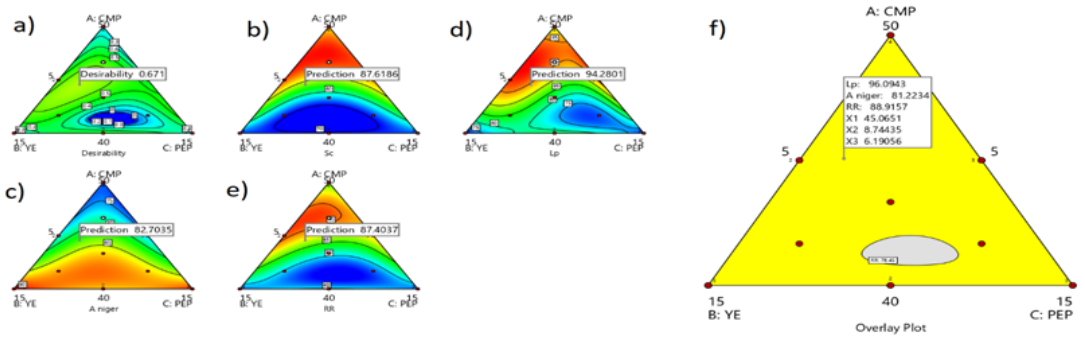

Figure 3 Overlapping and numerical optimization graphs. (a) The contour plot of maximum desirability. Contour plots for each response are shown separately: (b) for R1, (c) for R2, (d) for R3, and (e) for R4, with optimal points marked; (f) Overlaid graph represented by different regions indicating maximum (yellow areas) and minimum (grey areas). The optimum values of the ingredients and the four recovery rates are shown as a flag planted.

3.4. Effect size assessment

Effect size analysis, as presented in Table 6, sheds light on the impact of optimized YPM medium compared to traditional culture media on microbial growth. When examining the growth values of *S. cerevisiae* and *L. plantarum* in the traditional media (MRS, MYA, and SDA) versus the YPM medium, it should be noted that the traditional media generally exhibited higher growth values. However, these growth differences were found to not be statistically significant ($p > 0.05$) for both *S. cerevisiae* and *L. plantarum*. The analysis of the size of the effect, expressed through the d–Cohen values, also indicate that the magnitude of these differences is relatively low (0.2) for both microbial groups. Dispersion of data for YMP medium suggests a broader range of underlying factors or influences that contribute to variation in microbial growth.

Table 6. Effect size: Cohen's t and d test

M.O	R (%)	YPM (UFC/g)	MRS (UFC/g)	MYA (UFC/g)	SDA (UFC/g)	**d–Cohen**	**p**
S. cerevisiae	88.160	7.68±5.95 [a]	–	8.73±0.62 [a]	–	0.2	0.649
L plantarum	91.191	7.74±6.08 [a]	8.84±0.62 [a]	–	–	0.2	0.642
A. niger	81.742	7.31±1.46[a]	–	–	9.16±0.68[b]	1.6	0.001

MRS: Man Rogosa Sharpe Agar; MYA: Malt Yeast Extract Agar; SDA: Sabouraud Dextrose Agar; YPM: Yeast–extract Peptone Mucilage. Statistical differences expressed in superscript letters are determined in rows.

On the contrary, a significant difference ($p<0.05$) was observed in the fungal growth values between the YPM medium and the SDA medium. The effect size analysis, represented by a Cohen d value greater than 0.8, underscores a substantial effect size. This means that the disparities in fungal growth between these two media are considerable, with the YPM medium showing a clear disadvantage.

Although traditional media may exhibit slightly higher growth values for *S. cerevisiae* and *L. plantarum*, the lack of statistical significance and relatively low effect sizes suggest that the optimized YPM medium remains a viable alternative. Furthermore, the significant disparity in fungal growth between YPM medium and SDA medium underscores the importance of optimizing the formulation to promote optimal fungal growth. These findings contribute to a more profound understanding of the differential effects of the YPM medium on various microbial groups and emphasize the need for further research and refinement to improve its overall performance.

4. Discussion

A mixed design was employed to assess the collective behavior of various factors impacting microbial recovery rates, shedding light on the individual contributions of each factor. Notably, an increase in mucilage concentration exhibited a profound influence on the recovery rates of S. cerevisiae, *L. plantarum*, and *A. niger*, resulting in substantial improvements. This scientific discussion explores the underlying mechanisms driving these observations and their broader implications.

4.1 Cocoa mucilage acts as a catalyst for microbial growth.

Microbial behavior within mixtures is influenced by their distinct nutritional preferences and the specific components present. Cocoa mucilage, rich in glucose, fructose, vitamins, nitrogen, and trace elements, optimally supports the growth of microorganisms such as S. cerevisiae, L. plantarum, and *A. niger* by fulfilling their metabolic demands [4, 11, 18]. Prior studies confirm these observations, showing similar microbial growth patterns when altering mucilage concentrations [39–41].

Delgado–Noboa et al. (2021) emphasize the positive correlation between higher sugar concentrations and increased microbial growth in cocoa mucilage [41–44]. Sugars, especially glucose, and fructose, are critical carbon sources for microorganisms. Manipulating mucilage concentrations consistently yielded similar effects on microbial growth, affirming the importance of sugars [42–45]. Microorganisms have specific metabolic capacities for utilizing cocoa mucilage's nutritional components. S. cerevisiae, a prominent cocoa yeast, efficiently converts glucose and fructose into alcohol and flavor compounds [41].

De Vuyst et al. (2020) highlight S. cerevisiae and *L. plantarum's* efficient metabolism of glucose and fructose in cocoa mucilage, indicating their preference for these carbon sources [42–44]. Lactic acid bacteria like *L. plantarum* utilize these sugars to generate lactic acid, contributing to fermentation acidity [41, 42]. For fungi such as *A. niger*, glucose, and fructose are pivotal for growth and enzymatic activities, inducing conidial germination [46, 47].

4.2. S. cerevisiae and L. plantarum rely on higher concentrations of pure mucilage for optimal growth.

The study's findings highlight the significance of specific nutrient concentrations in supporting the growth of yeasts in mucilage. Particularly, higher concentrations of pure, unmixed mucilage are shown to nurture yeast growth effectively. This parallels the reliance of both yeasts and LAB on increased sugar concentrations, particularly glucose, and fructose, for their growth and metabolic activities. *S. cerevisiae*, renowned for its adeptness in fermenting sugars, exemplifies this, utilizing glycolysis to break down glucose and fructose, generating energy in the form of ATP and precursor molecules crucial for organic compound synthesis [41–45].

The importance of glucose and fructose to *S. cerevisiae* and *L. plantarum* during cocoa fermentation is consistently underscored, as these sugars are pivotal for their growth and metabolism. Intriguingly, the utilization of glucose and fructose from mucilage unfolds in a dynamic manner [41]. Glucose is swiftly consumed within the initial 48 to 72 hours of fermentation, followed by the prominence of fructose utilization after approximately 120 hours [41–43]. This preferential glucose uptake by yeasts that can convert sucrose shapes the microbial process and life cycle dynamics over time. These findings emphasize the positive impact of mucilage on these microorganisms and their functions, unveiling the intricate interplay of nutrients in the cocoa fermentation process.

4.2 High levels of PEP and YE are essential for optimal growth of A. niger.

The results indicate that by increasing the mucilage concentration, YE and PEP can potentially be reduced without compromising the RR. However, the recovery of *A. niger* depends more on high concentrations of PEP and YE for optimal growth. The study's findings suggest that an increase in cocoa mucilage concentration could lead to a reduction in the requirements for yeast extract (YE) and peptone (PEP) without compromising microbial recovery. However, optimal growth of *A. niger* appears to depend more on higher concentrations of PEP and YE.

Traditionally, yeast extract and peptone have been used to meet the nutritional needs of microorganisms [41,42,46–49]. In the designed formulation, it compensates for the low nitrogen content of the mucilage, making it a suitable culture medium for *S. cerevisiae*, *L. plantarum*, and *A. niger*.

Yeast extract and peptone, derived from yeast cells and animal tissues respectively, effectively assimilate nitrogenous compounds, amino acids, and peptides, fulfilling microorganisms' nitrogen requirements [50]. This strategy enhances nitrogen source utilization, stimulating the multiplication of yeasts, LAB, and fungi essential for enzyme, coenzyme, nucleic acid, vitamin, and cellular

component synthesis [50–53]. The greater dependence of *A. niger* on nitrogen sources for growth compared to *S. cerevisiae* and *L. plantarum* is attributed to factors such as its expansive filamentous structures enabling efficient nutrient uptake, metabolic versatility in utilizing diverse nitrogen sources, and nitrogen's critical role in fungal growth processes [46–48]. In contrast, unicellular yeasts and bacteria depend on mechanisms like diffusion or active transport for nutrient acquisition, which might limit their nitrogen uptake efficiency compared to fungi [50].

4.4. A. niger shows limited growth at high concentrations of mucilage.

Fungi's susceptibility to osmotic stress significantly impacts their growth inhibition in concentrated sugar solutions, setting them apart from yeasts and lactic acid bacteria (LABs) [69–74]. This distinction arises from multiple factors, encompassing the distinctive structural and physiological attributes of fungal membranes, the repercussions of osmotic imbalances on cellular water equilibrium, and the differential adaptations of yeasts and LABs to osmotic stress.

Primarily, fungal membranes, enriched with ergosterol, exhibit higher vulnerability to osmotic stress compared to yeasts and LABs [70]. The composition and structure of ergosterol–rich membranes confer increased fluidity and permeability, rendering them more susceptible to damage under osmotic stress [72–74]. In contrast, yeast and LAB membranes' composition imparts greater stability and resistance against osmotic imbalances. Furthermore, the presence of concentrated sugar solutions, like those in mucilage, can trigger osmotic imbalance affecting cellular water content. Fungal cells, facing such solutions, encounter a net water loss due to higher osmotic pressure externally. This loss leads to cell dehydration, significantly impairing fungal growth and viability, and disrupting water uptake and retention.

In contrast, yeasts and LABs have evolved robust osmoregulation mechanisms to endure osmotic stress and flourish in high–sugar environments. Yeasts utilize high–affinity sugar transporters and osmotic stress–responsive signaling pathways, adapting to high–sugar conditions [70, 71]. LABs showcase resilient membrane integrity and defensive mechanisms safeguarding against osmotic stress–induced harm [70]. Initial studies on yeast *S. cerevisiae's* molecular regulation against osmotic pressure revealed MAP kinase and the high osmolarity glycerol (HOG) pathway's pivotal roles in cellular responses [72–74]. The Aspergillus genus' response mechanisms to osmotic stress differ, revolving around TcsB–type histidine kinase homologues, with some exceptions like *A. niger* [72–74].

4.5. The effect size indicates that YPM medium is comparable to its traditional counterparts.

The YPM medium demonstrates comparable growth potential to traditional media for *S. cerevisiae*

and *L. plantarum*, as indicated by non–significant differences in growth values. The effect size analysis further supports this, suggesting minimal practical differences. The optimized composition of YPM, including nutrient composition and growth–promoting factors, makes it a viable alternative for yeast and LAB cultures.

However, contrasting results were observed in fungal growth between YPM and SDA media. A significant difference in fungal growth values was noted, indicating a substantial impact of the medium type on fungal growth. This was reinforced by a large effect size (Cohen's d > 0.8), underlining the significant disparities in fungal growth between the two media.

These disparities emphasize the necessity for ongoing optimization of YPM media, especially to better accommodate the requirements of fungi. While YPM medium holds promise for yeast and LAB cultures, further adjustments are needed, potentially involving ingredient modifications, pH adjustments, and tailored growth factors to better suit the specific needs of fungal growth.

4.6. Future contributions of the YPM medium.

The unique composition and properties of mucilage offer several advantages for microbial growth and metabolism. The findings highlight the untapped potential of cocoa mucilage as a versatile substrate for the microbial culture of different microbial species (Figure 4). Microorganisms grown in the cocoa mucilage–based medium could exhibit new metabolic capabilities that target various industrial processes, enhancing their role in advancing biotechnological innovations.

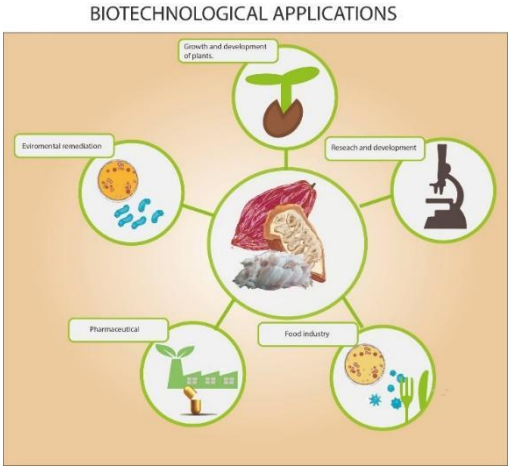

Figure 1. Biotechnological applications of cacao mucilage medium

4.6.1 Production of Bioactive Compounds

The cocoa mucilage–based culture medium offers an attractive substrate for the production of bioactive compounds with pharmaceutical, nutraceutical, and cosmeceutical applications.

Microorganisms grown in this medium could acquire metabolic capacities to biosynthesize various secondary metabolites, such as antimicrobial agents, antioxidants, enzymes, and polyphenols. Research has demonstrated the ability of cocoa–associated microorganisms to produce bioactive compounds, including antimicrobial peptides and enzymes, with industrial relevance. Harnessing the potential of cocoa mucilage as a culture medium can contribute to the sustainable production of valuable bioactive compounds [1–4, 56–59].

4.6.2. Biodegradation and environmental remediation

The organic compounds present in cocoa mucilage make it an ideal substrate for the biodegradation of recalcitrant pollutants and environmental remediation. Microorganisms grown in the cocoa mucilage–based medium may also exhibit enhanced biodegradation capabilities, targeting various contaminants such as hydrocarbons, pesticides, and textile dyes. The unique combination of sugars, organic acids, and phenolic compounds in cocoa mucilage provides a favorable environment for the growth of pollutant–degrading microorganisms, which would facilitate detoxification and remediation in contaminated environments.

4.6.3. Bioprocessing and Industrial Applications

The application of culture media based on cocoa mucilage extends to the bioprocessing and industrial sectors. Different microorganisms grown in this medium can efficiently improve the conversion of sugars into desired products, contributing to sustainable and ecological manufacturing processes. The polysaccharides present in cocoa mucilage can serve as a potential source of biopolymers, with applications in packaging materials and biomedical products [5–12, 60–63].

4.6.5 Agriculture and Plant Growth Promotion

Cocoa mucilage–based media also have the potential for agriculture and plant growth promotion. Being that, organic compounds and growth factors can stimulate the growth and development of beneficial microorganisms. This medium could also improve the development of plant growth–promoting bacteria and mycorrhizal fungi. In this way, agricultural practices can improve the availability of nutrients, improve the soil structure, promoting interactions between plants and microorganisms, which leads to greater productivity and sustainability of crops [50–60].

Biotechnological applications of a cocoa mucilage–based microbial culture medium span a wide range of industries, including pharmaceuticals, environmental remediation, bioprocessing, and agriculture. Harnessing the untapped potential of cocoa mucilage can drive innovation in biotechnology, opening new avenues for sustainable practices.

4.7. Final considerations

A limitation of this study is that it focused solely on the design of the experimental space and specific microbial cultures. Future research should consider exploring other regions beyond the experimental design space, evaluating other microbial cultures from various sources, and identifying key growth factors, to refine culture media formulations. Furthermore, with the identification of potential growth strategies based on specific nutritional needs, even higher recovery rates could be achieved in different microbial species.

5. Conclusions

By combining rigorous statistical analysis, meticulous experimental design, and accurate predictions, this study provides a robust framework for optimizing YPM microbial culture medium formulation. The influence of the mucilage concentration on the microbial recovery rates, reveals the importance of the contributions of this ingredient to the recovery rate of different microbial species. The mechanisms underlying this observation could involve protective, adhesive, and nutritive properties of the mucilage, which together enhance the recovery efficiency of the microorganisms.

These findings open the doors to various biotechnological applications, which extend beyond the scope of this study and offer promising avenues for future research and practical applications in various biotechnological fields.

References

1. Balladares, C., Chóez–Guaranda, I., García, J., Sosa, D., Pérez, S., González, J. E. & Manzano, P. (2016). Physicochemical characterization of *Theobroma cacao L*. sweatings in Ecuadorian coast. *Emirates Journal of Food and Agriculture*, 28(10), 741–745. https://doi.org/10.9755/ejfa.2016–02–187

2. Mendoza–Meneses, C. J., Feregrino–Pérez, A. A., & Gutiérrez–Antonio, C. (2021). Potential Use of Industrial Cocoa Waste in Biofuel Production. *Journal of Chemistry*, 1–11. https://doi.org/10.1155/2021/3388067

3. Roini, C., Limatahu, N. A., & Hartati, T. M. (2019, May). Characterization of cocoa pulp (*Theobroma cacao L*) from South Halmahera as an alternative feedstock for bioethanol production. In *IOP Conference Series: Earth and Environmental Science*, 276(1): 012038). IOP Publishing. https://doi.org/10.1088/1755–1315/276/1/012038

4. Soares, T. F., & Oliveira, M. B. P. (2022). Cocoa by–products: characterization of bioactive compounds and beneficial health effects. *Molecules*, 27(5), 1625.https://doi.org/10.3390/molecules27051625

5. Delgado–Noboa, J., Bernal, T., Soler, J., & Peña, J. Á. (2021). Kinetic modeling of batch bioethanol production from CCN–51 Cocoa Mucilage. Journal of the Taiwan Institute of Chemical Engineers, 128, 169–175. https://doi.org/10.1016/j.jtice.2021.08.040

6. Ayala, H., Kaiser, D., Pavón, S., Molina, E., Siguenza, J., Bertau, M., & Lapo, B. (2022). Valorization of cocoa's mucilage waste to ethanol and subsequent direct catalytic conversion into ethylene. *Journal of Chemical Technology & Biotechnology*, 97(8), 2171–2178. https://doi.org/10.1002/jctb.7095

7. Saavedra–Sanabria, O. L., Durán, D., Cabezas, J., Hernández, I., Blanco–Tirado, C., & Combariza, M. Y. (2021). Cellulose biosynthesis using simple sugars available in residual cacao mucilage exudate. Carbohydrate Polymers, 274, 118645. https://doi.org/10.1016/j.carbpol.2021.118645

8. Akpo, A. S. M., Alain, Y. A., Théodore, D. N. D., Gabaze, G. A. A., Julien, C. K., Robert, G. J., ... & Rajeshwar, T. D. (2020). Valorization of the Mucilage Juice of Cocoa Beans for the Production of a Biopesticide based on Bacillus thuringiensis var. kurstaki HD–1. Int. J. Curr. *Microbiol. App. Sci*, 9(11), 3600–3610. https://doi.org/10.20546/ijcmas.2020.911.431

9. Endraiyani, V., Ludescher, R. D., Di, R., & Karwe, M. V. (2017). Total phenolics and antioxidant capacity of cocoa pulp: Processing and storage study. *Journal of Food Processing*

and Preservation, 41(4), e13029. https://doi.org/10.1111/jfpp.13029

10. Martínez, R., Torres, P., Meneses, M. A., Figueroa, J. G., Pérez–Álvarez, J. A., & Viuda–Martos, M. (2012). Chemical, technological and in vitro antioxidant properties of cocoa (*Theobroma cacao L.*) co-products. *Food Research International* 49 (1): 39–45.https://doi.org/10.1016/j.foodres.2012.08.005

11. Tịnh, N. T. T., An, N. T., Hòa, H. T. T., & Tươi, N. T. (2016). A study of wine fermentation from mucilage of cocoa beans (*Theobroma cacao L.*). *Dalat University Journal of Science*, 6(3), 387–397. https://doi.org/10.37569/DalatUniversity.6.3.83

12. Puerari, C., Magalhães, K. T., & Schwan, R. F. (2012). New cocoa pulp–based kefir beverages: Microbiological, chemical composition and sensory analysis. *Food Research International*, 48(2), 634–640. https://doi.org/10.1016/j.foodres.2012.06.005

13. Afolabi, M. O., Ibitoye, W. O., & Agbaje, A. F. (2015). Evaluation of nutritional and sensory properties of cocoa pulp beverage supplemented with pineapple juice. *Journal of Food Research*, 4(6), 58. : http://dx.doi.org/10.5539/jfr.v4n6p58

14. Lu, F., Rodriguez–Garcia, J., Van Damme, I., Westwood, N. J., Shaw, L., Robinson, J. S., & Charalampopoulos, D. (2018). Valorisation strategies for cocoa pod husk and its fractions. *Current Opinion in Green and Sustainable Chemistry*, 14, 80–88. https://doi.org/10.1016/j.cogsc.2018.07.007

15. Anvoh, K. Y. B., Bi, A. Z., & Gnakri, D. (2009). Production and characterization of juice from mucilage of cocoa beans and its transformation into marmalade. *Pakistan Journal of Nutrition*, 8(2), 129–133. https://doi.org/10.3923/pjn.2009.129.133

16. Jayeola, C. O., Adebowale, B. A., Yahaya, L. E., Ogunwolu, S. O., & Olubamiwa, O. Chapter 18. Production of bioactive compounds from waste. In: *Therapeutic, Probiotic, and Unconventional Foods* (eds. A.M. Grumezescu and A.M. Holban). http://www.sciencedirect.com/science/article/pii/B9780128146255000170

17. Figueroa, K. H. N., García, N. V. M., & Vega, R. C. (2020). Cocoa By-products. In: Campos–Vega, R., Oomah, B. D., & Vergara–Castañeda, H. A. (eds.) Food wastes and by–products: Nutraceutical and Health Potential. John Wiley & Sons, 373–411. ISBN 9781119534105

18. Vizcaino-Almeida, C. R., Guajardo-Flores, D., Caroca-Cáceres, R., Serna-Saldívar, S. O., Briones-García, M., & Lazo-Vélez, M. A. (2022). Non-conventional fermentation at laboratory scale of cocoa beans: Using probiotic microorganisms and substitution of mucilage by fruit pulps. *International Journal of Food Science & Technology*, 57(7), 4307–4315.

https://doi.org/10.1111/ijfs.15757

19. Parapouli, M., Vasileiadis, A., Afendra, A. S., & Hatziloukas, E. (2020). *Saccharomyces cerevisiae* and its industrial applications. *AIMS microbiology*, 6(1), 1. 1.https://doi.org/10.3934/microbiol.2020001

20. Swaraz, A. M., Satter, M. A., Rahman, M. M., Asad, M. A., Khan, I., & Amin, M. Z. (2019). Bioethanol production potential in Bangladesh from wild date palm (Phoenix sylvestris Roxb.): *An experimental proof. Industrial Crops and Products*, 139, 111507. https://doi.org/10.1016/j.indcrop.2019.111507

21. Al–Tawaha, R., & Meng, C. (2018). Potential benefits of Lactobacillus plantarum as probiotic and its advantages in human health and industrial applications: *A review. Adv. Environ. Biol*, 12, 16–27. https://doi.org/10.22587/aeb.2018.12.1.4

22. Arena, M. P., Fiocco, D., Massa, S., Capozzi, V., Russo, P., & Spano, G. (2014). Lactobacillus plantarum as a strategy for an in situ production of vitamin B2. *Journal of Food and Nutritional Disorders*, 1(4), S1–004. http://dx.doi.org/10.4172/2324–9323.S1–004

23. Bunčić, S., Paunović, L. J., Teodorović, V., Radišić, D., Vojinović, G., Smiljanić, D., & Baltić, M. (1993). Effects of gluconodeltalactone and *Lactobacillus plantarum* on the production of histamine and tyramine in fermented sausages. *International Journal of Food Microbiology*, 17(4), 303–309. https://doi.org/10.1016/0168–1605(93)90200–Z

24. Alan, Y., Topalcengiz, Z., & Dığrak, M. (2018). Biogenic amine and fermentation metabolite production assessments of *Lactobacillus plantarum* isolates for naturally fermented pickles. *LWT*, 98, 322–328. https://doi.org/10.1016/j.lwt.2018.08.067

25. Dienye, B. N., Ahaotu, I., Agwa, O. K., & Odu, N. N. (2018). Citric acid production potential of *Aspergillus niger* using Chrysophyllum albidum peel. *Advances in Bioscience and Biotechnology*, 9(04), 190–203. https://doi.org/10.4236/abb.2018.94013

26. Hannan, A., Bajwa, R., & Latif, Z. (2009). Status of Aspergillus niger strains for pectinases production potential. *Pak. J. Phytopathol*, 21(1), 77–82. ISSN: 1019–763X

27. Conesa, A., van den Hondel, C. A., & Punt, P. J. (2000). Studies on the production of fungal peroxidases in Aspergillus niger. *Applied and environmental microbiology*, 66(7), 3016–3023. https://doi.org/10.1128/AEM.66.7.3016–3023.2000

28. Vergara–Mendoza, M., Martínez, G. R., Blanco–Tirado, C., & Combariza, M. Y. (2022). Mass Balance and Compositional Analysis of Biomass Outputs from Cacao Fruits. *Molecules*,

27(12), 3717. https://doi.org/10.3390/molecules27123717

29. Cervantes–Martínez, C. V., Medina–Torres, L., González–Laredo, R. F., Calderas, F., Sánchez–Olivares, G., Herrera–Valencia, E. E., & Rodriguez–Ramirez, J. (2014). Study of spray drying of the Aloe vera mucilage (Aloe vera barbadensis Miller) as a function of its rheological properties. *LWT–Food Science and Technology*, 55(2), 426–435. https://doi.org/10.1016/j.lwt.2013.09.026

30. Weenk, G. H. (1992). Microbiological assessment of culture media: comparison and statistical evaluation of methods. *International journal of food microbiology*, 17(2), 159–181. https://doi.org/10.1016/0168–1605(92)90113–H

31. ISO 6887–1; Microbiology of the Food Chain—Preparation of Test Samples, Initial Suspension and Decimal Dilutions for Microbiological Examination—Part 1: General Rules for the Preparation of the Initial Suspension and Decimal Dilutions. ISO: Geneva, Switzerland, 2017. Available online: https://www.iso.org/standard/63335.html (accessed on 5 January 2023).

32. Bonnet, M., Lagier, J. C., Raoult, D., & Khelaifia, S. (2020). Bacterial culture through selective and non–selective conditions: the evolution of culture media in clinical microbiology. *New microbes and new infections*, 34, 100622. https://doi.org/10.1016/j.nmni.2019.100622

33. Cornell, J. A. (1973). Experiments with mixtures: a review. Technometrics, 15(3), 437–455. https://doi.org/10.1080/00401706.1973.10489071

34. Gunst, R. F. (1996). Response surface methodology: process and product optimization using designed experiments. https://doi.org/10.1080/00401706.1996.10484509

35. Maher, J. M., Markey, J. C., & Ebert–May, D. (2013). The other half of the story: effect size analysis in quantitative research. *CBE—Life Sciences Education*, 12(3), 345–351. https://doi.org/10.1080/00401706.1996.10484509

36. Sutton, S. (2011). Measurement of microbial cells by optical density. Journal of Validation technology, 17(1), 46–49. https://citeseerx.ist.psu.edu/document?repid=rep1&type=pdf&doi=f66c948bb74c7f67724a95506441cdd35033e825

37. Wang, R., Lorantfy, B., Fusco, S., Olsson, L., & Franzén, C. J. (2021). Analysis of methods for quantifying yeast cell concentration in complex lignocellulosic fermentation processes. *Scientific Reports*, 11(1), 11293. https://doi.org/10.1038/s41598–021–90703–8 .

38. Downey, A. S., Da Silva, S. M., Olson, N. D., Filliben, J. J., & Morrow, J. B. (2012). Impact of processing method on recovery of bacteria from wipes used in biological surface sampling. *Applied and environmental microbiology*, 78(16), 5872–5881. https://doi.org/10.1128/AEM.00873–12

39. Vizcaino-Almeida, C. R., Guajardo-Flores, D., Caroca-Cáceres, R., Serna-Saldívar, S. O., Briones-García, M., & Lazo-Vélez, M. A. (2022). Non-conventional fermentation at laboratory scale of cocoa beans: Using probiotic microorganisms and substitution of mucilage by fruit pulps. *International Journal of Food Science & Technology*, 57(7), 4307–4315. https://doi.org/10.1111/ijfs.15757

40. Saavedra–Sanabria, O. L., Durán, D., Cabezas, J., Hernández, I., Blanco–Tirado, C., & Combariza, M. Y. (2021). Cellulose biosynthesis using simple sugars available in residual cacao mucilage exudate. *Carbohydrate Polymers*, 274, 118645. https://doi.org/10.1016/j.carbpol.2021.118645

41. De Vuyst, L., & Leroy, F. (2020). Functional role of yeasts, lactic acid bacteria and acetic acid bacteria in cocoa fermentation processes. *FEMS Microbiology Reviews*, 44(4), 432–453. https://doi.org/10.1093/femsre/fuaa014

42. Pereira, G. V. D. M., Miguel, M. G. D. C. P., Ramos, C. L., & Schwan, R. F. (2012). Microbiological and physicochemical characterization of small–scale cocoa fermentations and screening of yeast and bacterial strains to develop a defined starter culture. *Applied and environmental microbiology*, 78(15), 5395–5405. https://doi.org/10.1128/AEM.01144–12

43. Lefeber, T., Janssens, M., Camu, N., & Vuyst, L. D. (2010). Kinetic Analysis of Strains of Lactic Acid Bacteria and Acetic Acid Bacteria in Cocoa Pulp Simulation Media toward Development of a Starter Culture for Cocoa Bean Fermentation. *Applied and Environmental Microbiology*, 76(23), 7708–7716. https://doi.org/10.1128/AEM.01206–10

44. Ardhana, M. M., & Fleet, G. H. (2003). The microbial ecology of cocoa bean fermentations in Indonesia. *International journal of food microbiology*, 86(1–2), 87–99..https://doi.org/10.1016/S0168–1605(03)00081–3

45. Pereira, G. V. D. M., Miguel, M. G. D. C. P., Ramos, C. L., & Schwan, R. F. (2012). Microbiological and physicochemical characterization of small–scale cocoa fermentations and screening of yeast and bacterial strains to develop a defined starter culture. *Applied and environmental microbiology*, 78(15), 5395–5405. https://doi.org/10.1128/AEM.01144–12

46. Hamad, H., Alma, M., Ismael, H., & Göçeri, A. The effect of some sugars on the growth of

Aspergillus niger. KSÜ Doğa Bilimleri Dergisi, 2014, vol. 17, no 4, p. 7–11.https://doi.org/10.18016/ksujns.28479

47. Ijadpanahsaravi, M., Punt, M., Wösten, H. A., & Teertstra, W. R. (2021). Minimal nutrient requirements for induction of germination of Aspergillus niger conidia. *Fungal biology*, 125(3), 231–238. https://doi.org/10.1016/j.funbio.2020.11.004

48. Laothanachareon, T., Bruinsma, L., Nijsse, B., Schonewille, T., Antonio, J., P., V. A., & Schaap, P. J. (2021). Global Transcriptional Response of *Aspergillus niger* to Blocked Active Citrate Export through Deletion of the Exporter Gene. Journal of Fungi, 7(6), 409. https://doi.org/10.3390/jof7060409

49. Fries, N. (1948). The nutrition of fungi from the aspect of growth factor requirements. Transactions of the British Mycological Society, 30, 118–134. https://doi.org/10.1016/S0007–1536(48)80041–0

50. Koim–Puchowska, B., Kłosowski, G., Dróżdż–Afelt, J. M., Mikulski, D., & Zielińska, A. (2021). Influence of the Medium Composition and the Culture Conditions on Surfactin Biosynthesis by a Native Bacillus subtilis natto BS19 Strain. *Molecules*, 26(10). https://doi.org/10.3390/molecules26102985

51. Davami, F., Eghbalpour, F., Nematollahi, L., Barkhordari, F., & Mahboudi, F. (2015). Effects of Peptone Supplementation in Different Culture Media on Growth, Metabolic Pathway and Productivity of CHO DG44 Cells; a New Insight into Amino Acid Profiles. *Iranian Biomedical Journal*, 19(4), 194–205. https://doi.org/10.7508/ibj.2015.04.002

52. Seesuriyachan, P., Kuntiya, A., Hanmoungjai, P., & Techapun, C. (2011). Exopolysaccharide production by Lactobacillus confusus TISTR 1498 using coconut water as an alternative carbon source: the effect of peptone, yeast extract and beef extract. *Songklanakarin Journal of Science & Technology*, 33(4). http://cmuir.cmu.ac.th/jspui/handle/6653943832/50384

53. Champagne, C. P., Gomes da Cruz, A., & Daga, M. (2018). Strategies to improve the functionality of probiotics in supplements and foods. *Current Opinion in Food Science*, 22, 160–166. https://doi.org/10.1016/j.cofs.2018.04.008

54. Guirlanda, C. P., da Silva, G. G., & Takahashi, J. A. (2021). Cocoa honey: Agro–industrial waste or underutilized cocoa by–product? *Future Foods*, *4*, 100061. https://doi.org/10.1016/j.fufo.2021.100061

55. Perli, T., Wronska, A. K., Ortiz-Merino, R. A., Pronk, J. T., & Daran, J. M. (2020). Vitamin requirements and biosynthesis in *Saccharomyces cerevisiae*. Yeast, 37(4), 283–304.

https://doi.org/10.1002/yea.3461

56. Gutiérrez–Macías, P., Mirón–Mérida, V. A., Rodríguez–Nava, C. O., & Barragán–Huerta, B. E. (2021). Cocoa: Beyond chocolate, a promising material for potential value–added products. In Valorization of Agri–Food Wastes and By–Products (pp. 267–288). *Academic Press*. https://doi.org/10.1016/B978–0–12–824044–1.00038–6

57. Kim–Ngoc, V. T., Cong–Hau, N., Bui–Phuc, T., & Thang, N. (2022). Quality Assessment During the Fermentation of Cocoa Beans: Effects of Partial Mucilage Removal. *Journal of Applied Sciences and Environmental Management*, 26(8), 1369–1374. https://doi.org/10.4314/jasem.v26i8.8

58. Silva, E. N. D., Ramos, D. D. C., Menezes, L. M., Souza, A. O. D., & Lannes, S. C. D. S. (2014). Nutritional value and antioxidant capacity of cocoa honey (*Theobroma cacao L.*). *Food Science and Technology*, 34, 755–759. https://doi.org/10.1590/1678–457X.6447

59. Evers, M. S., Morge, C., Sparrow, C., Gobert, A., Vichi, S., & Alexandre, H. (2023). Thiamine and Biotin: Relevance in the Production of Volatile and Non–Volatile Compounds during *Saccharomyces. cerevisiae* Alcoholic Fermentation in Synthetic Grape Must. *Foods*, *12*(5), 972. https://doi.org/10.3390/foods12050972

60. Ruiz–Barba, J. L., & Jimenez–Diaz, R. (1995). Availability of essential B–group vitamins to Lactobacillus plantarum in green olive fermentation brines. *Applied and environmental microbiology*, 61(4), 1294–1297. https://doi.org/10.1128/aem.61.4.1294–1297.1995

61. Anvoh, K. Y. B., Bi, A. Z., & Gnakri, D. (2009). Production and characterization of juice from mucilage of cocoa beans and its transformation into marmalade. *Pakistan Journal of Nutrition*, 8(2), 129–133. https://doi.org10.3923/pjn.2009.129.133

62. Martínez, R., Torres, P., Meneses, M., Figueroa, J., Pérez–Álvarez, J., & Viuda–Martos, M. (2012). Chemical, technological and in vitro antioxidant properties of cocoa (*Theobroma cacao L.*) co–products. Food Research International, 49(1), 39–45. https://doi.org/10.1016/j.foodres.2012.08.005

63. Canadell, D., González, A., Casado, C., & Ariño, J. (2015). Functional interactions between potassium and phosphate homeostasis in *Saccharomyces. cerevisiae*. Molecular *Microbiology*, 95(3), 555–572. https://doi.org/10.1111/mmi.12886

64. Kahm, M., Navarrete, C., Llopis–Torregrosa, V., Herrera, R., Barreto, L., Yenush, L., & Kschischo, M. (2012). Potassium starvation in yeast: mechanisms of homeostasis revealed by mathematical modeling. *PLoS computational biology*, 8(6), e1002548.

https://doi.org/10.1371/journal.pcbi.1002548

65. Ribeiro–Filho, N., Linforth, R., Bora, N., Powell, C. D., & Fisk, I. D. (2022). The role of inorganic–phosphate, potassium and magnesium in yeast–flavour formation. *Food Research International*, 162, 112044. https://doi.org/10.1016/j.foodres.2022.112044

66. Saeed A, H., & Salam A, I. (2013). Current limitations and challenges with lactic acid bacteria: a review. *Food and Nutrition Sciences*, 2013. https://doi.org/10.4236/fns.2013.411A010

67. Goksen, G., Demir, D., Dhama, K., Kumar, M., Shao, P., Xie, F., & Lorenzo, J. M. (2023). Mucilage polysaccharide as a plant secretion: Potential trends in food and biomedical applications. *International Journal of Biological Macromolecules*, 123146. https://doi.org/10.1016/j.ijbiomac.2023.123146

68. Nikolaou, E., Agrafioti, I., Stumpf, M., Quinn, J., Stansfield, I., & Brown, A. J. (2009). Phylogenetic diversity of stress signalling pathways in fungi. *BMC Evolutionary Biology*, 9, 1–18. https://doi.org/10.1186/1471–2148–9–44

69. Gadd, G. M., Chalmers, K., & Reed, R. H. (1987). The role of trehalose in dehydration resistance of Saccharomyces cerevisiae. *FEMS Microbiology Letters*, 48(1–2), 249–254. https://doi.org/10.1111/j.1574–6968.1987.tb02551.x

70. Le Marrec, C. (2011). Responses of lactic acid bacteria to osmotic stress. In Stress responses of lactic acid bacteria (pp. 67–90). Boston, MA: Springer US. https://doi.org/10.1007/978–0–387–92771–8_4

71. Blomberg, A., & Adler, L. (1992). Physiology of osmotolerance in fungi. *Advances in microbial physiology*, 33, 145–212. https://doi.org/10.1016/S0065–2911(08)60217–9

72. Duran, R., Cary, J. W., & Calvo, A. M. (2010). Role of the osmotic stress regulatory pathway in morphogenesis and secondary metabolism in filamentous fungi. *Toxins*, 2(4), 367–381. https://doi.org/10.3390/toxins2040367

73. Hernández–Téllez, C. N., Rodríguez–Córdova, F. J., Rosas–Burgos, E. C., Cortez–Rocha, M. O., Burgos–Hernández, A., Lizardi–Mendoza, J., & Plascencia–Jatomea, M. (2017). Activity of chitosan–lysozyme nanoparticles on the growth, membrane integrity, and β–1, 3–glucanase production by *Aspergillus parasiticus*. *Biotech*, 7, 1–13. https://doi.org/10.1007/s13205–017–0913–4

74. Beever, R. E. (1983). Osmotic sensitivity of fungal variants resistant to dicarboximide fungicides. *Transactions of the British Mycological Society*, 80(2), 327–331.

https://doi.org/10.1016/S0007–1536(83)80017–5

Chapter 7

Discussion and concluding remarks

1. Discussion

The investigation revealed that electromagnetic fields (EMFs) had a significant impact on multiple factors related to cocoa bean fermentation. Beyond the obvious effects on pH, humidity, and temperature, the EMF exposure resulted in notable changes in the size, color, and fermentation rates of the cocoa beans.

The cited studies by Camu et al. (2008) [1] and Saputro et al. (2022) [2] support the notion that weight loss in cocoa bean fermentation primarily stems from water loss and organic matter degradation. The fermentation process's rate, duration, color, texture, and flavor alterations are impacted by cocoa bean type, fermentation method, and environmental conditions. Specific microbial communities, particularly lactic acid bacteria, influence fermentation rate and temperature elevation, as shown by Camu et al. (2018) [3]. Microorganisms and enzymes have been recognized by various authors for softening pulp, reducing bean size, and shaping cocoa's characteristic flavor [4, 5]. Notably, the use of lactic acid bacteria as starter cultures yields higher fermentation indices and darker bean colors, significantly affecting cocoa quality [6]. Initial 48 to 72 hours of fermentation exhibit the most intense microbial activity, elevating temperatures and producing organic acids like acetic and lactic acid, which contribute to bean changes and flavor enhancement [7, 8]. These findings highlight the intricate relationship between electromagnetic fields, fermentation processes, and microbial activity. It's evident that the effects of electromagnetic fields on fermentation rates are mediated by microbial community dynamics. Consequently, changes in the growth of microbial communities could also influence the impact of EMF on these rates.

The study's outcomes emphasize that the density of the applied oscillating magnetic field (OMF) profoundly impacted fermentation quality and efficiency, with optimal OMF conditions leading to notable improvements. Both response variables exhibited quadratic behavior in relation to changes in OMF density, aligning with Anaya et al. [9], who noted similar behavior in fungal species' colony diameter under OMF exposure. The obtained results concerning sensory quality enhancement and performance augmentation of cocoa beans through electromagnetic field (EMF) modulation during fermentation are consistent with previous research exploring diverse EMF–affected processes. Examples include Andrade et al. [10] observing increased bioethanol production by S. cerevisiae under rotating magnetic fields, Boeira et al. [11] reporting reduced nivalenol in S. cerevisiae fermentation, Lin et al. [12] showing pulsed magnetic fields' efficacy against E. coli O157:H7, and Nakasono et al. [13] observing no impact on yeast cultures under specific OMF exposure. The higher microbial diversity in the low–density region (LDR) and lower diversity in the high–density region

(HDR) after 24 hours might be attributed to EMF effects on microorganisms, corroborated by studies showing EMFs' stimulation or inhibition of microbial growth. Strašák et al. [14], Novák et al. [15], Bayraktar et al. [16], and Gao et al. [17] demonstrated varying effects of OMF exposure on microbial species, thus influencing microbial population dynamics in diverse ecosystems.

The study's kinetic variables revealed accelerated yeast and LAB growth, while AAB proliferation was comparatively slower. These findings are in line with previous research showing the varied effects of magnetic fields on microbial species, suggesting that such exposure can indeed modulate microbial growth and metabolic activity. This aligns with studies by Masood et al. (2018) [18] and Masood et al. (2020) [19] which indicated the potential of magnetic fields to influence bacterial growth patterns even after the field's removal, echoing the current study's findings and prior research on magnetic field impacts. Research by Konopacka et al. (2019) [20], Novák et al. [15], and Potenza et al. [23] demonstrated species–specific responses, growth rate influences, and inhibitory effects of magnetic fields on diverse microbial types, underscoring the potential for magnetic fields to impact microbial growth dynamics. Overall, the study found that stronger magnetic fields were associated with reduced maximum growth rates, extended delay phases, and lower μmax values across microbial groups. Although the exact mechanism remains incompletely understood, it could involve disruptions in ion transport, nutrient absorption, and bacterial cell dynamics [18, 20–26]. The observed differences in kinetic parameters between experimental and control groups suggest factors beyond nutrient depletion and toxic metabolite accumulation may influence microbial growth during cocoa bean fermentation, revealing the apparent influence of electromagnetic fields on the fermentation process through kinetic analysis.

Metagenomic analysis unveiled the impact of magnetic field densities on microbial communities during dried cocoa bean fermentation. Lower to moderate field densities (5–42 mT) yielded positively altered microbial communities that enhanced aroma profiles, resulting in elevated yields with floral, fruity, and nutty flavors. Conversely, a higher field density (80 mT) led to lower yields and unfavorable acidity and bitterness notes. Consistent with these findings, in solid–state cocoa fermentation (SCFs), enterobacterial species drove pectinolytic cocoa pulp degradation and citric acid assimilation, while Tatumella correlated with desirable flavor compounds. Pseudomonas presence correlated with undesirable chocolate odors, while lactic acid bacteria (LAB), particularly Weissella and Lactobacillus, impacted flavor and color development. Acetic acid bacteria (AAB), especially Acetobacter, contributed to SCF by converting ethanol and lactic acid. Electromagnetic fields (EMFs) have been shown to influence microbial metabolism, resulting in diverse metabolite synthesis. EMFs' interaction with inoculum concentration influences cocoa bean microbial species, favoring fermentation conditions and desirable CCN–51 flavor notes. While the energy change from EMFs may be small compared to covalent bond energies, it can still impact biological system energy levels and reactions, especially involving radical pairs [27–39].

Cocoa bean fermentation involves intricate interactions among microbial populations, including yeasts, lactic acid bacteria (LAB), and acetic acid bacteria (AAB), influenced by factors like bean variety and fermentation conditions. Magnetic field usage during fermentation affects these microorganisms' proliferation and dynamics, with treatments at 5 mT and 42 mT showing significant yeast and AAB growth within 48 to 120 hours. Studies on S. cerevisiae align, showing low–frequency magnetic fields stimulate microbial growth. However, rotating magnetic fields (RMF) exposure has been found to decrease yeast cell numbers and inhibit metabolic activity, while 80 mT magnetic treatment in cocoa fermentation exhibited lower LAB and AAB concentrations, hinting at suppressive effects. Despite this, recent research highlights magnetic fields' potential to enhance cocoa fermentation, improving pH, fermentable sugar content, and quality, indicating their profound impact on microbial metabolism. Magnetic field exposure alters microbial dynamics, influencing pH, acetic acid, ethanol production, and fermentable sugar content, potentially enhancing chocolate's sensory characteristics. Finding optimal magnetic field parameters for specific fermentation processes and microorganisms, alongside evaluating their lasting chocolate quality effects, necessitates further investigation [16, 27, 40–43, 49–51].

The study primarily focuses on Raman bands stemming from lipid materials, particularly fatty acids and triacylglycerols (TAGs), present in cocoa liquor spectra. These bands result from acyl chain vibrations, C=O stretching, and C=C double bond stretching, revealing characteristics like ν(C–C), δ(CH2) twisting, and δ(CH3) or δ(CH2) strains in various fatty acids. Specific Raman signals linked to unsaturated fat components, such as oleic acid, are also identified. The presence of other compounds in cocoa liquor, including lignin, cellulose, hemicellulose, pectin, phenolic compounds, and alkaloids, might contribute to observed peaks, leading to overlaps and potential challenges in interpretation. Despite these complexities, Raman spectroscopy shows potential in assessing cocoa beans exposed to magnetic fields during fermentation and chocolate products, offering insights into processing and further warranting exploration for improved cocoa liquor analysis [52–65].

In the CCN–51 cocoa variety, higher irradiation doses lead to increased fruity attributes, indicating heightened compounds responsible for fruity flavor, while β–myrcene and β–cis–ocimene terpenes were augmented, resembling those found in fine cacao types. National Cocoa variety showcased improved fruit and floral attributes post–irradiation, akin to rice wine's fragrance enhancement with higher radiation doses. However, both varieties exhibited diminishing almond flavor as irradiation doses increased, along with a decrease in the cocoa attribute. These alterations are influenced by radiation's impact on pyrazines, aldehydes, and esters that contribute to cocoa and chocolate's nutty, cocoa aroma and flavor. Radiation also affects compounds tied to fruity, floral, rancid, and earthy aromas [57–60]. Notably, the acidity of both varieties decreased with higher doses, while bitterness and astringency experienced varied responses. Aroma intensity and quality were influenced by radiation, potentially affecting antioxidants, glucosides, and volatile compound content. Irradiation's

effect on unsaturated fatty acids might contribute to rancidity. These changes are linked to interactions with compounds like methylxanthines, alkaloids, flavonoids, and chlorogenic acid, as well as potential breakdown of fat molecules and hydrolytic acid group degradation [66–78].

2. Conclusions and future perspectives of electromagnetic fields in cocoa bean fermentation

The future potential of electromagnetic fields in cocoa bean fermentation extends beyond current applications in the cocoa industry. While current research emphasizes the beneficial impacts of magnetic fields on cocoa fermentation, there's room for diverse and innovative exploration to transform this critical processing stage. Customizing electromagnetic field parameters to target specific microbial communities offers opportunities to optimize flavor, reduce fermentation time, and enhance cocoa quality. Integration with emerging technologies like AI and machine learning could enable real–time monitoring and adaptive control, aided by sensor networks and data analytics for process optimization.

Additionally, exploring magnetic fields' influence on post–fermentation steps like drying and roasting may improve efficiency and flavor stability, benefiting cocoa constituents. Investigating waste recovery and environmental impact potential underscores the potential for ecological and efficient practices. Amid climate change and market challenges, electromagnetic fields offer resilience, supporting consistent yields and stable supply chains. In conclusion, interdisciplinary collaboration and innovative approaches can maximize the impact of electromagnetic fields in cocoa fermentation, revolutionizing cocoa processing and ensuring a thriving cocoa sector for the future

References

1. Camu, N., De Winter, T., Addo, S. K., Takrama, J. F., Bernaert, H., De Vuyst, L., & Vuyst, L. D. (2018). Fermentation of cocoa beans: influence of microbial activities and polyphenol concentrations on the flavour of chocolate. Journal of the Science of Food and Agriculture, 98(5), 1754–1763. https://doi.org/10.1002/jsfa.8642 .

2. Saputro, D., Priambodo, D., Pahlawan, M., & Masithoh, R. (2022). Classification of cocoa beans based on fermentation level using PLS–DA combined with Visible Near–infrared (VIS–NIR) spectroscopy. In 2nd International Conference on Smart and Innovative Agriculture (ICoSIA 2021) (pp. 100–106). Atlantis Press. https://doi.org/10.2991/absr.k.220305.015 .

3. Camu, N., De Winter, T., Addo, S. K., Takrama, J. F., Bernaert, H., De Vuyst, L., & Vuyst, L. D. (2018). Fermentation of cocoa beans: influence of microbial activities and polyphenol concentrations on the flavour of chocolate. Journal of the Science of Food and Agriculture, 98(5), 1754–1763. https://doi.org/10.1002/jsfa.8642 .

4. De Vuyst, L., & Weckx, S. (2016). The cocoa bean fermentation process: from ecosystem analysis to starter culture development. *Journal of Applied Microbiology*, 121(1), 5–17.https://doi.org/10.1111/jam.13045

5. Guerra, L. S., Cevallos–Cevallos, J. M., Weckx, S., & Ruales, J. (2022). Traditional fermented foods from ecuador: A Review with a Focus on Microbial Diversity. *Foods*, 11(13), 1854.https://doi.org/10.3390/foods11131854 .

6. Guehi, T. S., Dadie, A. T., Koffi, K. P., Dabonne, S., Ban-Koffi, L., Kedjebo, K. D., & Nemlin, G. J. (2010). Performance of different fermentation methods and the effect of their duration on the quality of raw cocoa beans. *International journal of food science & technology*, 45(12), 2508–2514.https://doi.org/10.1111/j.1365–2621.2010.02424.x

7. Afoakwa, E. O., Kongor, J. E., Takrama, J. F., & Budu, A. S. (2012). Changes in acidification, sugars, and mineral composition of cocoa pulp during fermentation of pulp pre–conditioned cocoa (Theobroma cacao) beans. *International Journal of Food Science & Technology*, 47(12), 2510–2517. https://doi.org/10.1111/j.1365–2621.2012.03125.x

8. Cortez, D., Quispe–Sanchez, L., Mestanza, M., Oliva–Cruz, M., Yoplac, I., Torres, C., & Chavez, S. G. (2023). Changes in bioactive compounds during fermentation of cocoa (*Theobroma cacao*) harvested in Amazonas–Peru. *Current Research in Food Science*, 6, 100494. https://doi.org/10.1016/j.crfs.2023.100494 .

9. Anaya, M., Gámez–Espinosa, E., Valdés, O., Guzmán, T., & Borrego, S. (2021). Effect of the

oscillating magnetic field on airborne fungal. *Archives of Microbiology*, 203, 2139–2145. https://doi.org/10.1007/s00203–021–02193–x

10. de Andrade, C. M., Cogo, A. J., Perez, V. H., dos Santos, N. F., Okorokova–Façanha, A. L., Justo, O. R., & Façanha, A. R. (2021). Increases of bioethanol productivity by S. cerevisiae in unconventional bioreactor under ELF–magnetic field: New advances in the biophysical mechanism elucidation on yeasts. Renewable Energy, 169, 836–842. https://doi.org/10.1016/j.renene.2021.01.074

11. Boeira, C. Z., de Carvalho Silvello, M. A., Remedi, R. D., Feltrin, A. C. P., Santos, L. O., & Garda–Buffon, J. (2021). Mitigation of nivalenol using alcoholic fermentation and magnetic field application. *Food Chemistry*, 340, 127935. https://doi.org/10.1016/j.foodchem.2020.127935.

12. Lin, L., Wang, X., He, R., & Cui, H. (2019). Action mechanism of pulsed magnetic field against E. coli O157: H7 and its application in vegetable juice. *Food Control*, 95, 150–156. https://doi.org/10.1016/j.foodcont.2018.08.011 .

13. Nakasono, S., Laramee, C., Saiki, H., & McLeod, K. J. (2003). Effect of power–frequency magnetic fields on genome–scale gene expression in *Saccharomyces cerevisiae*. Radiation research, 160(1), 25–37. https://doi.org/10.1667/rr3006

14. Strašák, L., Vetterl, V., & Šmarda, J. (2002). Effects of low–frequency magnetic fields on bacteria *Escherichia coli*. *Bioelectrochemistry*, 55(1–2), 161–164. https://doi.org/10.1016/s1567–5394(01)00152–9

15. Novák, J., Strašák, L., Fojt, L., Slaninová, I., & Vetterl, V. (2007). Effects of low–frequency magnetic fields on the viability of yeast *Saccharomyces cerevisiae*. *Bioelectrochemistry*, 70(1), 115–121. https://doi.org/10.1016/j.bioelechem.2006.03.029

16. Bayraktar, V. N. (2013). Magnetic field effect on yeast Saccharomyces cereviisiiae activity at grape must fermentation. *Biotechnologia Acta*, 6(1), 125–137. https://doi.org/10.15407/biotech6.01.125

17. Gao, M., Zhang, J., & Feng, H. (2011). Extremely low frequency magnetic field effects on metabolite of *Aspergillus niger*. *Bioelectromagnetics*, 32(1), 73–78. https://doi.org/110.1002/bem.20619

18. Masood, S. (2017). Effect of weak magnetic field on bacterial growth. *Biophysical Reviews and Letters*, 12(04), 177–186. https://doi.org/10.1142/S1793048017500102

19. Masood, S., Saleem, I., Smith, D., & Chu, W. K. (2020). Growth pattern of magnetic field–treated bacteria. *Current Microbiology*, 77(2), 194–203. https://doi.org/10.1007/s00284–019–01820–7 .

20. Bektiarso, S., Prastowo, S. H. B., Prihandono, T., & Handayani, R. D. (2020, February). Optimizing lactobacillus growth in the fermentation process of artificial civet coffee using extremely–low frequency (ELF) magnetic field. In *Journal of Physics: Conference Series* (Vol. 1465, No. 1, p. 012010). IOP Publishing. https://doi.org/10.1016/j.jmmm.2018.10.053.

21. Sudarti, S. Bektiarso, S. H. B. Prastowo, T. Prihandono, Maryani, and R. D. Handayani, Optimizing lactobacillus growth in the fermentation process of artificial civet coffee using extremely– low frequency (ELF) magnetic field, J. Phys. Conf. Ser., vol. 1465, no. 1, p. 12010, 2020, https://doi.org/10.1088/1742–6596/1465/1/012010 .

22. Zhao, B., Sha, H., Li, J., Cao, S., Wang, G., & Yang, Y. (2020). Static magnetic field enhanced methane production via stimulating the growth and composition of microbial community. *Journal of Cleaner Production*, 271, 122664. https://doi.org/10.1016/j.jclepro.2020.122664 .

23. Potenza, L., Ubaldi, L., De Sanctis, R., De Bellis, R., Cucchiarini, L., & Dachà, M. (2004). Effects of a static magnetic field on cell growth and gene expression in *Escherichia coli*. *Mutation Research/Genetic Toxicology and Environmental Mutagenesis*, 561(1–2), 53–62. https://doi.org/10.1016/j.mrgentox.2004.03.009.

24. Wei, Y., & Wang, X. (2022). Biological effects of rotating magnetic field: A review from 1969 to 2021. Progress in Biophysics and Molecular Biology. https://doi.org/10.1016/j.pbiomolbio.2022.12.006

25. Shoda, M., Nakamura, K., Tsuchiya, K., Okuno, K., & Ano, T. (1999). Bacterial growth under strong magnetic field. *Electricity and Magnetism in Biology and Medicine*, 215–217. https://doi.org/10.1007/978–1–4615–4867–6_47 .

26. Peplow, M. Magnetic field benefits bacteria. Nature (2004). https://doi.org/10.1038/news041122–13

27. Guzmán–Armenteros, T. M., Ramos–Guerrero, L. A., Guerra, L. S., & Ruales, J. (2023). Optimization of cacao beans fermentation by native species and electromagnetic fields. Heliyon, 9(4) e15065. http://dx.doi.org/10.2139/ssrn.4364538

28. Balogu, T. V., & Onyeagba, A. R. (2017). Polyphenol and microbial profile of on–farm cocoa beans fermented with selected microbial consortia. *Applied Food Biotechnology*, 4(4), 229–240. http://dx.doi.org/10.22037/afb.v%vi%i.16845

29. Agyirifo, D. S., Wamalwa, M., Otwe, E. P., Galyuon, I., Runo, S., Takrama, J., & Ngeranwa, J. (2019) Metagenomics analysis of cocoa bean fermentation microbiome identifying species diversity and putative functional capabilities. Heliyon, 5(7). https://doi.org/10.1016/j.heliyon.2019.e02170

30. Korcari, D., Fanton, A., Ricci, G., Rabitti, N. S., Laureati, M., Hogenboom, J., & Fortina, M. G. (2023). Fine Cocoa Fermentation with Selected Lactic Acid Bacteria: Fermentation Performance and Impact on Chocolate Composition and Sensory Properties. *Foods*, 12(2), 340. https://doi.org/10.3390/foods12020340 .

31. Zhao, J., & Fleet, G. (2015). The effect of lactic acid bacteria on cocoa bean fermentation. *International Journal of food microbiology*, 205, 54–67. https://doi.org/10.1016/j.ijfoodmicro.2015.03.031

32. Adler, P., Frey, L. J., Berger, A., Bolten, C. J., Hansen, C. E., & Wittmann, C. (2014). The key to acetate: metabolic fluxes of acetic acid bacteria under cocoa pulp fermentation–simulating conditions. *Applied and Environmental Microbiology*, 80(15), 4702–4716. https://doi.org/10.1128/AEM.01048–14 .

33. Crafack, M., Keul, H., Eskildsen, C. E., Petersen, M. A., Saerens, S., Blennow, A., ... & Nielsen, D. S. (2014). Impact of starter cultures and fermentation techniques on the volatile aroma and sensory profile of chocolate. *Food Research International*, 63, 306–316. https://doi.org/10.1016/j.foodres.2014.04.032

34. Koné, M. K., Guéhi, S. T., Durand, N., Ban–Koffi, L., Berthiot, L., Tachon, A. F., & Montet, D. (2016). Contribution of predominant yeasts to the occurrence of aroma compounds during cocoa bean fermentation. Food Research International, 89, 910–917. https://doi.org/10.1016/j.foodres.2016.04.010 .

35. Jaimez, R. E., Barragan, L., Fernández–Niño, M., Wessjohann, L. A., Cedeño–Garcia, G., Cantos, I. S., & Arteaga, F. (2022). Theobroma cacao L. cultivar CCN 51: a comprehensive review on origin, genetics, sensory properties, production dynamics, and physiological aspects. PeerJ, 10, e12676. https://doi.org/10.7717/peerj.12676 .

36. Quintana, L., Gómez, S., García, A., & Martínez, N. (2015). Perfil sensorial del Clon de cacao (Theobroma cacao L.) CCN51 (primera cosecha de 2015). @ limentech, Ciencia y Tecnología Alimentaria, 13(1). https://doi.org/10.24054/16927125.v1.n1.2015.1866 .

37. Dulce, V. R., Anne, G., Manuel, K., Carlos, A. A., Jacobo, R. C., de Jesús, C. E. S., & Eugenia, L. C. (2021). Cocoa bean turning as a method for redirecting the aroma compound profile in

artisanal cocoa fermentation. *Heliyon*, 7(8). https://doi.org/10.1016/j.heliyon.2021.e07694 .

38. Streule, S., Leischtfeld, S. F., Galler, M., & Schwenninger, S. M. (2022). Monitoring of cocoa post–harvest process practices on a small–farm level at five locations in Ecuador. *Heliyon*, 8(6). https://doi.org/10.1016/j.heliyon.2022.e09628.

39. Liao, Q., Liu, Y., Zhang, J., Li, L., & Gao, M. (2019). A low–frequency magnetic field regulates Monascus pigments synthesis via reactive oxygen species in *M. purpureus*. *Process Biochemistry*, 86, 16–24. https://doi.org/10.1016/j.procbio.2019.08.009.

40. Alvarez, D. C., Pérez, V. H., Justo, O. R., & Alegre, R. M. (2006). Effect of the extremely low frequency magnetic field on nisin production by Lactococcus lactis subsp. lactis using cheese whey permeate. *Process biochemistry*, 41(9), 1967–1973. https://doi.org/10.1016/j.procbio.2006.04.009 .

41. Chagas Junior, G. C. A., Ferreira, N. R., & Lopes, A. S. (2021). The microbiota diversity identified during the cocoa fermentation and the benefits of the starter cultures use: An overview. *International Journal of Food Science & Technology*, 56(2), 544–552. https://doi.org/10.1111/ijfs.14740 .

42. Konopacka, A., Rakoczy, R., & Konopacki, M. (2019). The effect of rotating magnetic field on bioethanol production by yeast strain modified by ferrimagnetic nanoparticles. Journal of Magnetism and Magnetic Materials, 473, 176–183. https://doi.org/10.1016/j.jmmm.2018.10.053 .

43. Bubanja, I. N., Lončarević, B., Lješević, M., Beškoski, V., Gojgić–Cvijović, G., Velikić, Z., & Stanisavljev, D. (2019). The influence of low–frequency magnetic field regions on the Saccharomyces. cerevisiae respiration and growth. Chemical Engineering and Processing–Process Intensification, 143, 107593. https://doi.org/10.1016/j.cep.2019.107593

44. De Andrade, C. M., Cogo, A. J., Perez, V. H., dos Santos, N. F., Okorokova–Façanha, A. L., Justo, O. R., & Façanha, A. R. (2021). Increases of bioethanol productivity by S. cerevisiae in unconventional bioreactor under ELF–magnetic field: *New advances in the biophysical mechanism elucidation on yeasts. Renewable Energy*, 169, 836–842.https://doi.org/10.1016/j.renene.2021.01.074

45. Zieliński, M., Dębowski, M., & Kazimierowicz, J. (2021). The Effect of Static Magnetic Field on Methanogenesis in the Anaerobic Digestion of Municipal Sewage Sludge. Energies, 14(3), 590.https://doi.org/10.3390/en14030590 .

46. Zaidi, N. S., Sohaili, J., Muda, K., & Sillanpää, M. (2014). Magnetic field application and its

potential in water and wastewater treatment systems. Separation & Purification Reviews, 43(3), 206–240.https://doi.org/10.3390/en14030590

47. Ma, S., Liu, H., Hou, J., & Zhang, J. (2023). External static magnetic field potentiates the reduction of antibiotic resistance genes during swine manure composting. Journal of Hazardous Materials, 448, 130882. https://doi.org/10.1016/j.jhazmat.2023.130882 .

48. Hu, B., Leng, J., Quan, J., Zhang, K., Wu, P., Zhao, H., & Zhao, J. (2022). Impact of static magnetic field on electron transport and microbial community shifts in the nitritation sequencing batch reactor. Journal of Environmental Chemical Engineering, 10(6), 108774.https://doi.org/10.1016/j.jece.2022.108774

49. Lyu, W., Song, Q., Shi, J., Wang, H., Wang, B., & Hu, X. (2021). Weak magnetic field affected microbial communities and function in the A/O/A sequencing batch reactors for enhanced aerobic granulation. Separation and Purification Technology, 266, 118537. https://doi.org/10.1016/j.seppur.2021.118537 .

50. Rakoczy, R., Konopacki, M., & Fijałkowski, K. (2016). The influence of a ferrofluid in the presence of an external rotating magnetic field on the growth rate and cell metabolic activity of a wine yeast strain. Biochemical Engineering Journal, 109, 43–50.https://doi.org/10.1016/j.bej.2016.01.002

51. Bayraktar, V. N. (2013). Magnetic field effect on yeast *Saccharomyces cerevisiae* activity at grape must fermentation. Biotechnologia Acta, 6(1), 125–137. http://nbuv.gov.ua/UJRN/biot_2013_6_1_15

52. Sudarti, S., Hariyati, Y., Sari, A. B. T., Sumardi, S., & Muldayani, W. (2022). Fermentation Process of Dry Cocoa Beans through Extremely Low Frequency (ELF) Magnetic Field Exposure. Journal Penelitian Pendidikan IPA, 8(2), 584–591.https://doi.org/10.29303/jppipa.v8i2.1356

53. Czamara, K., Majzner, K., Pacia, M. Z., Kochan, K., Kaczor, A., & Baranska, M. (2015). Raman spectroscopy of lipids: a review. *Journal of Raman spectroscopy*, 46(1), 4–20. https://doi.org/10.1002/jrs.4607 .

54. De Gelder, J., De Gussem, K., Vandenabeele, P., & Moens, L. (2007). Reference database of Raman spectra of biological molecules. Journal of Raman Spectroscopy: An International Journal for Original Work in all Aspects of Raman Spectroscopy, Including Higher Order Processes, and also Brillouin and Rayleigh Scattering, 38(9), 1133–1147. https://doi.org/10.1002/jrs.1734 .

55. Bresson, S., Lecuelle, A., Bougrioua, F., El Hadri, M., Baeten, V., Courty, M., & Faivre, V. (2021). Comparative structural and vibrational investigations between cocoa butter (CB) and cocoa butter equivalent (CBE) by ESI/MALDI–HRMS, XRD, DSC, MIR and Raman spectroscopy. *Food Chemistry*, 363, 130319. https://doi.org/10.1016/J.FOODCHEM.2021.130319 .

56. Edwards, H. G., Villar, S. E. J., de Oliveira, L. F. C., & Le Hyaric, M. (2005). Analytical Raman spectroscopic study of cacao seeds and their chemical extracts. *Analytica Chimica Acta*, 538(1–2), 175–180. https://doi.org/10.1016/j.aca.2005.02.039

57. Yang, D., & Ying, Y. (2011). Applications of Raman spectroscopy in agricultural products and food analysis: A review. *Applied Spectroscopy Reviews*, 46(7), 539–560. https://doi.org/10.1080/05704928.2011.593216

58. Bresson, S., El Marssi, M., & Khelifa, B. (2006). Conformational influences of the polymorphic forms on the CO and C–H stretching modes of five saturated monoacid triglycerides studied by Raman spectroscopy at various temperatures. *Vibrational spectroscopy*, 40(2), 263–269. https://doi.org/10.1016/j.vibspec.2005.11.001

59. Castro–Alayo, E. M., Torrejón–Valqui, L., Cayo–Colca, I. S., & Cárdenas–Toro, F. P. (2021). Evaluation of the miscibility of novel cocoa butter equivalents by Raman mapping and multivariate curve resolution–alternating least squares. *Foods*, 10(12), 3101.https://doi.org/10.3390/FOODS10123101/S1 .

60. Jentzsch, P. V., Ciobotă, V., Salinas, W., Kampe, B., Aponte, P. M., Rösch, P., ... & Ramos, L. A. (2016). Distinction of Ecuadorian varieties of fermented cocoa beans using Raman spectroscopy. Food chemistry, 211, 274–280. https://doi.org/10.1016/j.foodchem.2016.05.017 .

61. Agarwal, U. P., Ralph, S. A., & Atalla, R. H. (1997, June). FT Raman spectroscopic study of softwood lignin. In Proceedings of 9th international symposium on wood and pulping chemistry (ISWPC), Montreal (pp. 8–1). https://www.fpl.fs.usda.gov/documnts/pdf1997/agarw97c.pdf

62. Schenzel, K., & Fischer, S. (2001). NIR FT Raman spectroscopy–a rapid analytical tool for detecting the transformation of cellulose polymorphs. Cellulose, 8, 49–57. https://doi.org/10.1023/A:1016616920539 .

63. Mazurek, S., Fecka, I., Węglińska, M., & Szostak, R. (2018). Quantification of active ingredients in Potentilla tormentilla by Raman and infrared spectroscopy. Talanta, 189, 308–

314. https://doi.org/10.1016/J.TALANTA.2018.07.012 .

64. Agarwal, U. P., & Ralph, S. A. (1997). FT–Raman spectroscopy of wood: identifying contributions of lignin and carbohydrate polymers in the spectrum of black spruce (Picea mariana). Applied spectroscopy, 51(11), 1648–1655. https://doi.org/10.1366/0003702971939316 .

65. Agarwal, U. P. (2006). Raman imaging to investigate ultrastructure and composition of plant cell walls: distribution of lignin and cellulose in black spruce wood (*Picea mariana*). *Planta*, 224(5), 1141–1153. https://doi.org/10.1007/S00425–006–0295–Z/METRICS .

66. Kadow, D., Bohlmann, J., Phillips, W., & Lieberei, R. (2013). Identification of main fine flavour components in two genotypes of the cocoa tree (*Theobroma cacao L.*). Journal of *Applied Botany and Food Quality*, 86(1). https://doi.org/10.5073/JABFQ.2013.086.013 .

67. Criollo Nuñez, J.; Ramirez–Toro, C.; Bolivar, G.; Sandoval A., A.P.; Lozano Tovar, M.D. Effect of Microencapsulated Inoc–ulum of Pichia Kudriavzevii on the Fermentation and Sensory Quality of Cacao CCN51 Genotype. *J. Sci. Food Agric.* 2023, 103, 2425–2435, https://doi.org/10.1002/JSFA.12433 .

68. Chang, A.C. (2003). The Effects of Gamma Irradiation on Rice Wine Maturation. *Food Chem*, 83, 323–327, https://doi.org/10.1016/S0308–8146(03)00050–5

69. Zhang, Z. S., Xie, Q. F., & Che, L. M. (2018). Effects of gamma irradiation on aflatoxin B1 levels in soybean and on the properties of soybean and soybean oil. *Applied radiation and isotopes*, 139, 224–230. https://doi.org/10.1016/j.apradiso.2018.05.003 .

70. Youssef, A. M., Samra, S. E., & Ahmed, A. I. (1991). Effect of gamma irradiation on the texture, acidity and catalytic activity of silica–aluminium and silica–magnesia catalysts. *International Journal of Radiation Applications and Instrumentation. Part C. Radiation Physics and Chemistry*, 38(3), 313–316. https://doi.org/10.1016/1359–0197(91)90099–N .

71. Júnior, P. C. G., dos Santos, V. B., Lopes, A. S., de Souza, J. P. I., Pina, J. R. S., Júnior, G. C. A. C., & Marinho, P. S. B. (2020). Determination of theobromine and caffeine in fermented and unfermented Amazonian cocoa (Theobroma cacao L.) beans using square wave voltammetry after chromatographic separation. *Food Control*, 108, 106887. https://doi.org/10.1016/J.FOODCONT.2019.106887 .

72. Mohajer, S., Mat Taha, R., Lay, M. M., Khorasani Esmaeili, A., & Khalili, M. (2014). Stimulatory effects of gamma irradiation on phytochemical properties, mitotic behaviour, and nutritional composition of sainfoin (Onobrychis viciifolia Scop.). *The Scientific World Journal*,

2014. https://doi.org/10.1155/2014/854093 .

73. Aly, A.A.; Maraei, R.W.; Sharafeldin, R.G. and Safwat, G. Yield Traits of Red Radish Seeds Obtained from Plants Produced from γ–Irradiated Seeds and Their Oil Characteristics. *Gesunde Pflanz*. 2023, 1–11, https://doi.org/10.1007/S10343–023–00859–8/FIGURES/3 .

74. Barrientos, L. D. P., Oquendo, J. D. T., Garzón, M. A. G., & Álvarez, O. L. M. (2019). Effect of the solar drying process on the sensory and chemical quality of cocoa (*Theobroma cacao L.*) cultivated in Antioquia, Colombia. *Food research international*, 115, 259–267. https://doi.org/10.1016/j.foodres.2018.08.084 .

75. Hussain, P. R., Chatterjee, S., Variyar, P. S., Sharma, A., Dar, M. A., & Wani, A. M. (2013). Bioactive compounds and antioxidant activity of gamma irradiated sun dried apricots (Prunus armeniaca L.). *Journal of Food Composition and analysis*, 30(2), 59–66. https://doi.org/10.1016/J.JFCA.2013.02.00

76. Lee, J. H., Lee, K. T., & Kim, M. R. (2005). Effect of gamma-irradiated red pepper powder on the chemical and volatile characteristics of kakdugi, a Korean traditional fermented radish kimchi. Journal of food science, 70(7), c441–c447. https://doi.org/10.1111/J.1365–2621.2005.TB11466.X .

77. Žulj, M. M., Bandić, L. M., Bujak, I. T., Puhelek, I., Jeromel, A., & Mihaljević, B. (2019). Gamma irradiation as pre–fermentative method for improving wine quality. Lwt, 101, 175–182. https://doi.org/10.1016/J.LWT.2018.11.016 .

78. Ehlermann, D.A.E. (2014). Safety of Food and Beverages: Safety of Irradiated Foods. In *Encyclopedia of Food Safety*; *Elsevier*. 3, 447–452. ISBN 9780123786128.